GEOLOGY AND GEOCHEMISTRY OF THE SANGSTER LAKE AND LARRYS RIVER PLUTONS, GUYSBOROUGH COUNTY, NOVA SCOTIA

by

George. A. O'Reilly

Submitted in partial fulfillment of the requirements

for the degree of Master of Science

at

Dalhousie University

Halifax, Nova Scotia

September, 1988

DALHOUSIE UNIVERSITY

DEPARTMENT OF GEOLOGY

The undersigned hereby certify that they have read and recommended to the Faculty of Graduate Studies for acceptance a thesis entitled " The Geology and Geochemistry of the Sangster Lake and Larrys River Plutons, Guysborough County, Nova Scotia. "

by George A. O'Reilly

in partial fulfillment of the requirements for the degree of Master of Science.

Dated September, 1988

External Examiner

Research Supervisor

Examining Committee

DALHOUSIE UNIVERSITY

DATE September, 1988

AUTHOR George A. O'Reilly

TITLE " The Geology and Geochemistry of the Sangster Lake and Larrys River Plutons, Guysborough County, Nova Scotia "

Department or School Department of Geology, Dalhousie University

Degree M.Sc. Convocation Fall Year 1988

Permission is herewith granted to Dalhousie University to circulate and to have copied for non-commercial purposes, at its discretion, the above title upon the request of individuals or institutions.

TABLE OF CONTENTS

TABLE OF CONTENTS cont'd Page

TABLE OF CONTENTS cont'd Page

TABLE OF CONTENTS cont'd Page

TABLE OF CONTENTS cont'd Page

TABLE OF CONTENTS cont'd

LIST OF FIGURES

LIST OF PLATES

LIST OF PLATES cont'd

LIST OF PLATES cont'd

LIST OF TABLES

LIST OF TABLES cont'd

ABSTRACT

The Sangster Lake and Larrys River Plutons are small (<36 km^2), strongly peraluminous granitoids which intrude, at 375Ma, the Cambro-Ordovician Meguma Group metasedimentary rocks in the eastern Meguma Zone. Thermal metamorphic mineral assemblages related to emplacement of the plutons post-date regional metamorphic mineral assemblages in the adjacent metasediments. A deformation fabric related to a dextral east-west trending shear zone (363Ma) overprints both plutons, in particular, the Sangster Lake Pluton. Within the Sangster Lake Pluton the juxtaposition of concentric dome-like structures with large blocks of metasediment trapped around the peripheries suggest that the pluton is exposed at its uppermost roof zone.

The plutons consist predominantly of textural varieties of monzogranite, varying from megacrystic and biotite-rich to equigranular and muscovite-rich. The monzogranites are intruded by much smaller minor intrusions and dykes of leucomonzogranite, leucogranite and pegmatite. One of these intrusions, the Beans Lake Leucomonzogranite, has extensively metasomatized contact zones with sheeted quartz vein zones and associated greisens.

The Sangster Lake Pluton has an airborne gamma-ray spectrometric response that is anomalous in equivalent uranium (eU) and the equivalent uranium/equivalent thorium ratio (eU/eTh). The Larrys River Pluton has an average response, typical of most of the granitoids of the Meguma Zone. Within the Sangster Lake Pluton the increase of airborne gamma-ray spectrometric response correlates well with areas that display features indicative of increasing intensity of post-crystallization hydrothermal alteration. For example, there was widespread albitization of plagioclase and development of secondary muscovite, apatite, Cl-apatite and Fe-U-phosphate. The alteration occurs in two modes: (a) pervasive, widespread replacement of the primary minerals throughout much of the eastern portion of the pluton; and (b) fracture-controlled intense alteration restricted to contact zones of late-stage, highly evolved intrusions.

Whole-rock geochemistry indicates that the hydrothermally altered

areas are characterized by an increase of the Na_2O/K_2O ratio, and an increase in P_2O_5 levels. There is also a general enrichment in such elements as U, Sn, Rb, Li, F, Be and B and decrease of Sr, Th, Ba, TiO_2 and CaO. The geochemical trends are a result of a combination of magmatic and postmagmatic processes with the latter being most important in the enrichment of U within the rocks. Levels of rare earth elements (REE) and $\delta^{18}O$ are comparable to levels reported from other Meguma Zone granitoids and are consistent with interaction of the rocks with a fluid phase at some time during their evolution. A smooth and continuous decreasing trend of REE with decreasing Zr, Th, TiO_2 and P_2O_5 is interpreted to be the result of fluid-melt interaction. Therefore, the extremely low REE levels in the hydrothermally altered rocks is inherited from the original, unaltered rock and the REE-rich accessory minerals were unaffected by the alteration.

The coincidence of textural, mineralogical and geochemical characteristics indicative of hydrothermal alteration in these rocks with increasing gamma-ray radiometric response demonstrates that such surveys can detect plutons that have undergone similar processes. The association of post-magmatic alteration with granophile element mineralization is well established; thus radiometric surveys can be a useful exploration tool for mineralization other than uranium.

ACKNOWLEDGEMENTS

Financial support for this thesis was provided by the Nova Scotia Department of Mines and Energy under the Canada-Nova Scotia Cooperative Minerals Program 1981-1984. Additional funding was provided through a NSERC operating grant to Dr. G. K. Muecke.

I am most grateful to my thesis supervisor, Dr. Gunter Muecke for his guidance, advice and patience without which this thesis could not have been completed. Drs. A. K. Chatterjee and D. B. Clarke also provided invaluable supervision throughout the project.

I have benefitted by numerous collaborations and discussions with a host of "experts" in peraluminous granites. I thank K. L. Ford of the G.S.C. for his explanations on the systematics and interpretation of airborne gamma-ray spectrometric surveys. The South Mountain Batholith mapping crew (SMEEBS), M. A. MacDonald, M. C. Corey, L. J. Ham, R. J. Horne, have discussed the geology of this significant granitic terrain with me on many occasions. Dr. D. J. Kontak kindly "opened the doors" to his extensive collection of reprints of pertinent papers on granite petrogenesis.

The thesis was reviewed by Drs. D. Pollock and R. A. Jamieson. I thank them for their comments and constructive criticisms.

Technical support was provided by the following to whom I am very grateful. S. Parikh (Dalhousie) helped with chemical analyses. R McKay (Dalhousie) and H. DeSusan (U.N.B.) assisted with electron microprobe and scanning electron microscope analyses respectively. Drafting support was provided by J. Campbell, P. Belliveau, C.

Phillips, W. Kaizer and E. Limpert. C. Murphy and R. Morrison provided photographic services.

Last but not least I would like to thank Diane, for doing more than her share of housework, Katie, for forgiving her absentee father and Lasa, for many missed walks at her beloved Shubie Park. Their moral support was necessary during the hectic, final stages of the thesis.

CHAPTER 1

INTRODUCTION

1.1 STUDY AREA LOCATION AND PHYSIOGRAPHY

The southern mainland of Nova Scotia is intruded by numerous peraluminous granitic bodies that vary in size from batholithic proportions down to small plutons and plugs. Since the early 1970's, they have been the focus of in-depth geological, petrological and geochemical studies. One of these intrusive suites, the South Mountain Batholith, is the largest granitic body in the Appalachians. This batholith and its smaller satellite bodies are rapidly becoming one of the most intensely studied peraluminous granitic terrains in the world.

In the eastern region of mainland Nova Scotia a number of smaller granitic plutons occur which have only been mapped on a reconnaissance level, even though some have excellent outcrop exposure (Fig. 1-1). An airborne gamma-ray spectrometric survey of this region by the Geological Survey of Canada in 1980 showed interesting variations in radiometric response over certain granitoids. One such body, the Sangster Lake Pluton of Guysborough County, displays anomalous expressions of equivalent uranium (eU) and the equivalent uranium/equivalent thorium ratio (eU/eTh). The Larrys River Pluton, found adjacent to the Sangster Lake Pluton, has an airborne spectrometric signature very similar to that over much of the peraluminous granitic rocks of the mainland. The combination of excellent outcrop exposure, and close

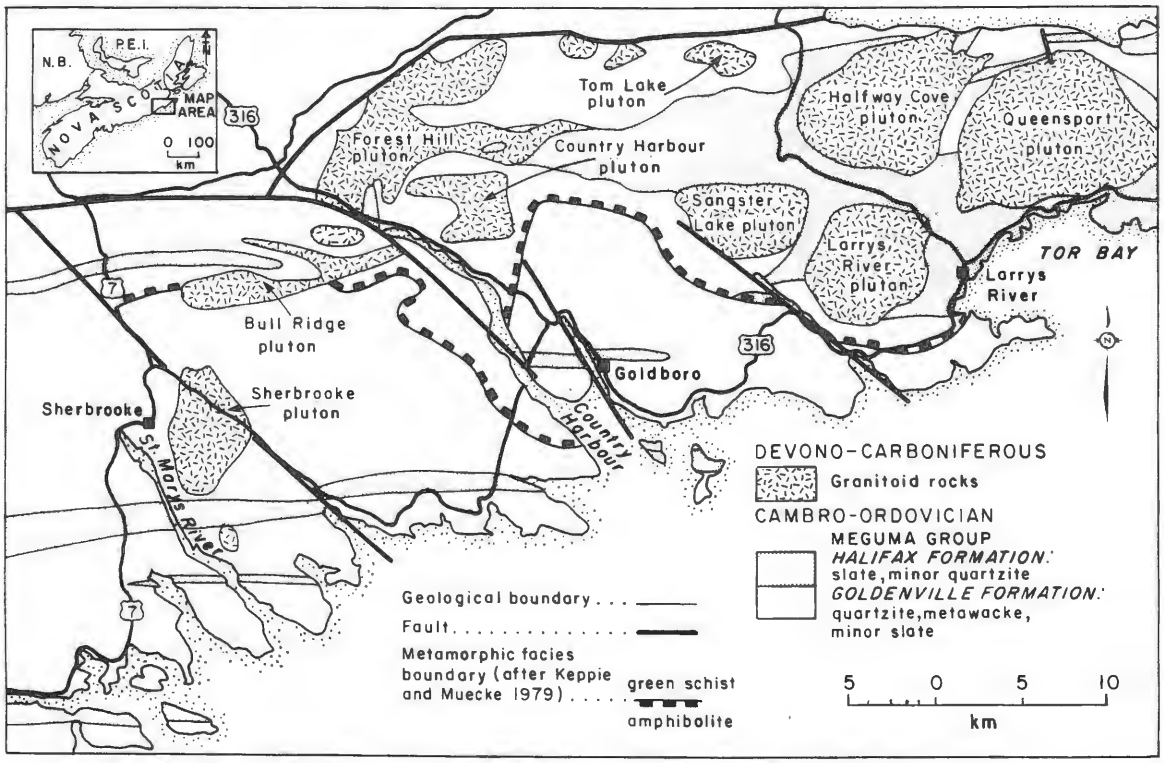

Figure 1-1 Generalized geological map of the eastern Meguma Zone giving names of the various granitic plutons.

juxtaposition of these two plutons, provides an opportunity to study the causes of the radiometric contrast between them.

Both plutons are dominated by boulder fields, bedrock barrens and rolling to hummocky topography. Two types of barrens predominate: (A) bedrock ledges of 60-90% outcrop form most high areas of both plutons and; (B) rolling ablationary boulder fields of glacial origin with little or no outcrop occur in most low-lying areas. Much of the eastern and southern portion of the Larrys River Pluton is dominated by the ablation glacial till.

Access to the area is excellent around the peripheries of the plutons by paved provincial highways. The interior portion of both plutons is accessed with difficulty by traverses over very rough terrain. This factor proved to be a definite hindrance in mapping.

1.2 PURPOSES OF THE THESIS

The purposes of this thesis are to:

1. produce a geological map of the Sangster Lake and Larrys River Plutons to define the textural and compositional variations and areal extent of granitic phases;
2. study the contact relations of the granitic rocks with the Meguma Group country rocks;
3. compare the observed geological and petrological relations with the recorded airborne gamma-ray spectrometric responses in the anomalous Sangster Lake and average Larrys River Plutons;

4. examine in detail the major and trace element geochemical trends associated with pluton emplacement, magmatic differentiation and deuteric and/or post-crystallization alterations;
5. determine whether a correlation exists between geochemical trends and the observed variations in radiometric responses, using both whole-rock and mineral geochemistry;
6. formulate conclusions on the petrogenesis of the plutons;
7. discuss the economic potential of the plutons and the feasibility of using airborne radiometric surveys to define plutons of economic interest;
8. recommend further studies.

1.3 METHODOLOGY

The Nova Scotia Department of Mines and Energy and the Canada Department of Energy Mines and Resources were involved in a Cooperative Minerals Program from 1981-1984. Part of this program was a multidisciplinary study of an area of eastern mainland Nova Scotia. This study was entitled the Meguma Project and involved mapping and detailed structural and metamorphic studies of the Meguma Group metasedimentary rocks. These rocks host significant auriferous mineral deposits and one of the main aims of this study was to understand the metallogeny of these occurrences.

The project area included several granitic plutons. Time limitation and Meguma Project personnel shortage resulted in an agreement between the Nova Scotia Department of Mines and Energy and the Dalhousie Geology Department to have four of these plutons (Sangster Lake,

Larrys River, Halfway Cove and Queensport Plutons; Fig. 1-1) mapped as two masters level graduate theses. The Nova Scotia Department of Mines and Energy provided field and analytical support for the projects.

During the 1983 field season the Sangster Lake and Larrys River Plutons were mapped and samples of the various rock types were collected for petrographic and whole-rock geochemical studies. The barren physiography of this area subjects outcrops to extremes of weather conditions and thus deep mechanical and chemical weathering, especially in coarse-grained rocks. Lack of fresh road cut outcrops resulted in a problem of obtaining fresh samples. A program of helicopter-assisted drilling and blasting was necessary, but even then one rock, the megacrystic biotite monzogranite, proved so deeply weathered that several attempts were necessary to obtain fresh samples.

1.4 PREVIOUS WORK

The Sangster Lake and Larrys River Plutons have never been mapped on other than a reconnaissance level. Fletcher and Faribault (1887) included these plutons in a geological survey of Nova Scotia. Their work in the Meguma Zone concentrated on the gold-bearing metasedimentary rocks of the Meguma Group. There was no attempt to separate the granitic rocks into their various facies, although any known granite-hosted mineral deposits were indicated.

Schiller (1961) and Stevenson (1964) mapped the geology of NTS sheets 11F/5 and 11F/6 respectively. These map sheets include the northern portion of both the Sangster Lake and Larrys River Plutons, but again, the granitic rocks were not subdivided. Schiller (1959)

described the metamorphic petrology of a succession of aluminous metasedimentary rocks of the Halifax Formation that forms the northern contact of both the Sangster Lake and Larrys River Plutons. His study did not involve the granitic rocks to a significant extent.

Ford and Ballantyne (1983) published the results of reconnaissance lithogeochemistry of the granitic plutons of the eastern Meguma Zone. Their objective was to follow up a federal government, airborne gamma-ray spectrometric survey of this area that shows interesting radio-element distribution patterns associated with some of the granitic rocks. Their study confirmed the observed airborne variations, and indicated that interesting geochemical trends were associated with the plutons displaying anomalous radioelement signatures. It was the preliminary work of Ford and Ballantyne (1983) that laid the groundwork and provided the impetus for my selection of this project for further study.

CHAPTER 2

GEOLOGICAL SETTING OF THE MEGUMA ZONE

2.1 INTRODUCTION

Mainland Nova Scotia south of the Cobequid-Chedabucto Fault Zone is underlain mainly by rocks of Cambrian to Triassic age (Fig. 2-1). This region was named the Meguma Zone by Williams (1978). The Meguma Zone consists predominantly of Cambrian to Early Devonian metasedimentary rocks intruded by a suite of Devono-Carboniferous peraluminous granitic rocks. Overlying these Early to Middle Paleozoic rocks are sequences of sedimentary and volcanic rocks of Carboniferous and Triassic age. The regional geology of the Meguma Zone is described in detail by Taylor (1967; 1969) and Schenk (1971), and is summarized by Keppie (1977).

2.2 METASEDIMENTARY ROCKS

The metasedimentary sequence within the Meguma Zone consists predominantly of the Meguma Group of Cambro-Ordovician age. This Group represents the oldest known rocks of the Meguma Zone and consists of the Goldenville Formation and conformably overlying Halifax Formation. The Goldenville Formation is predominantly wacke and quartzite and lesser amounts of slate and calcareous horizons. The Halifax Formation, on the other hand, consists predominantly of slates of various colors and lesser amounts of wacke, quartzite and calcareous horizons (Taylor, 1969; O'Brien, 1985a). The Goldenville Formation has no

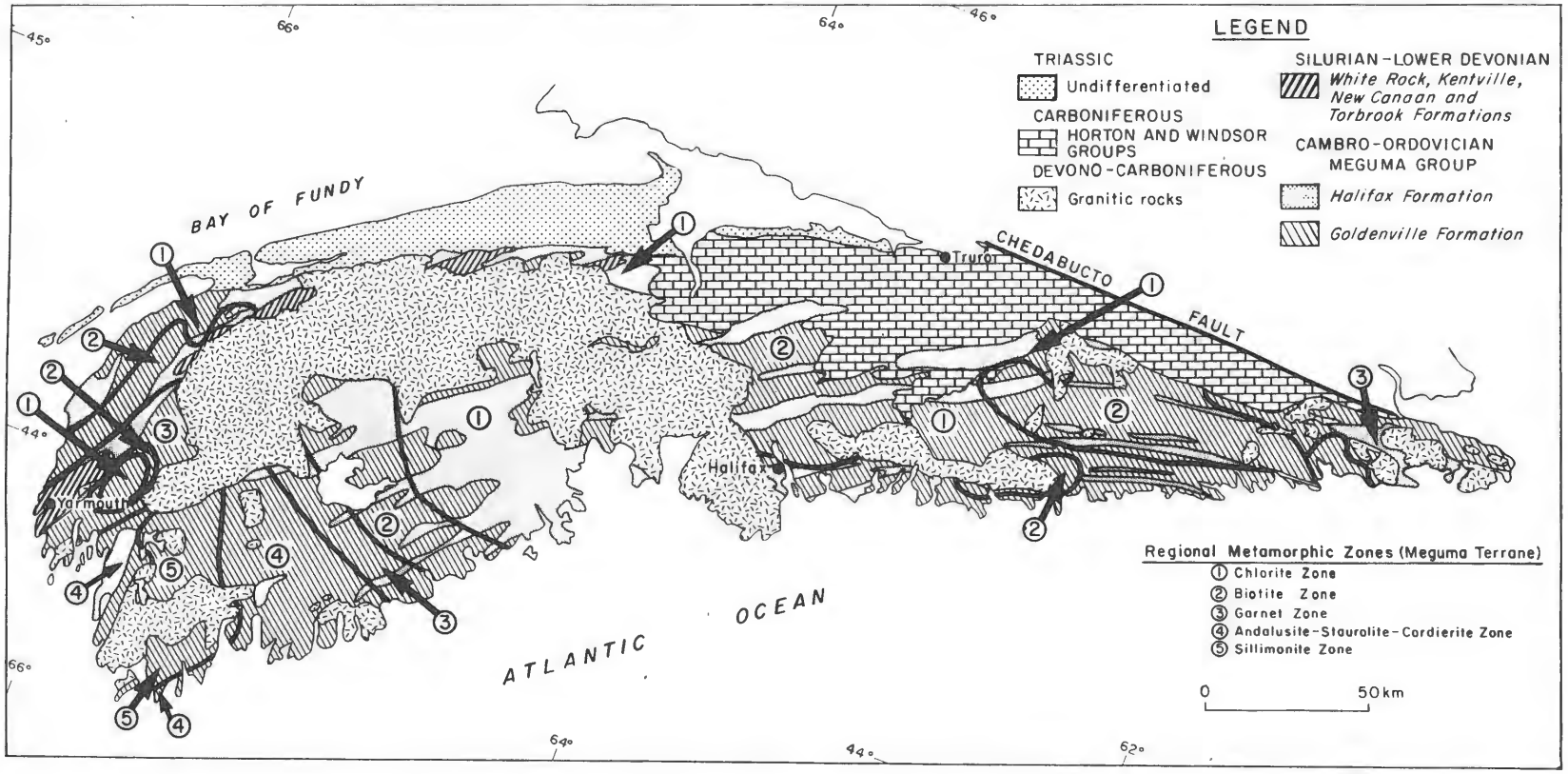

Figure 2-1 Geological map of the Meguma Zone, mainland Nova Scotia showing the regional metamorphic zones (Keppie and Muecke, 1979).

exposed base, but is estimated to be at least 6 km thick. The Halifax Formation varies in thickness throughout the Meguma Zone, but averages approximately 3 km (Taylor, 1969; O'Brien, 1985a). In the western and southwestern regions of the Meguma Zone the Halifax Formation is overlain successively by rocks of the White Rock, Kentville, New Canaan and Torbrook Formations (Taylor, 1969; Smitheringale, 1973). Formational contacts are generally conformable.

The White Rock Formation consists predominantly of dark slates and basic metavolcanic rocks of alkaline affinity (Sarkar, 1978) in the southwestern portion of the Meguma Zone near Yarmouth. Quartzite, slate, conglomerate and much less volcanic material comprise this Formation toward the northeast (Taylor, 1967; Lane, 1975). The White Rock Formation is approximately 5 km thick in the Yarmouth area but thins drastically toward the northeast mainly because of a decreasing amount of volcanic material.

The White Rock Formation is conformably overlain by black fossiliferous slates and limestones of the Kentville Formation. In turn, the Kentville Formation is overlain conformably by the diverse, but thin, assemblage (300 m) of slate, quartzite, limestone and acid volcanics of the New Canaan Formation. The youngest pre-granitic rocks of the Meguma Zone belong to the richly fossiliferous Torbrook Formation. This Formation conformably overlies the New Canaan Formation and consists of slates, sandstones and limestones.

Schenk (1971) interpreted this metasedimentary pile as a continuous sequence of deep-water turbidites (Meguma Group) and alkaline volcanics and sediments (White Rock Formation) shoaling upwards into a

more shallow-water environment siltstones, quartz sandstones and limestones (Kentville, New Canaan and Torbrook Formations). Based on paleontological evidence summarized by Keppie (1977), the metasedimentary rocks of the Meguma Zone range in age from Cambro-Ordovician (Meguma Group) to Lower Devonian (Torbrook Formation).

The source region for the sediments is not known with certainty, but Schenk (1983) and Schenk and Lane (1982) present sedimentological and paleocurrent data to indicate deposition occurred from the southeast from a quartz-rich gneissic and predominantly granodioritic continent of Precambrian age. They postulate the northwestern African continent as a possible source region.

Clarke and Halliday (1985) presented Sm/Nd data indicating the metasediments have a mean crustal residence age of 1773 ± 95 Ma. They suggested the Saharan Shield granites and Ben Bousera granulites of northwest Africa as possible sources for the sediments. They do concede that their data are not conclusive and that other similar Precambrian cratonic areas need consideration and examination.

The metasedimentary rocks of the Meguma Zone were deformed into tight, upright, northeast-trending folds by the Acadian Orogeny in the Lower Devonian (Fyson, 1966). The onset of greenschist to amphibolite facies regional metamorphism accompanied the middle to late stages of this deformational event (Taylor and Schiller, 1966 and Keppie and Muecke, 1979). The regional metamorphic grade throughout the Meguma Zone is variable and ranges from chlorite and biotite grade in the central region up to andalusite-staurolite-cordierite grade and sillimanite grade towards the east and the southwest (Fig. 2-1). The

various features of structural geology associated with the deformation and associated regional metamorphism of these units are described and discussed by Fyson (1966), Taylor and Schiller (1966), Keppie (1983, 1984) and O'Brien (1983, 1985b).

The regional metamorphic event associated with the Acadian Orogeny has been dated radiometrically by $^{40}Ar/^{39}Ar$ and indicates a minimum age of 390-405 Ma for time of initiation of this event in Nova Scotia (Muecke et al., in press).

2.3 GRANITIC ROCKS

The Meguma Zone metasedimentary rocks are intruded by a suite of peraluminous granitic rocks (Fig. 2-1). The largest of these massifs, the South Mountain Batholith, crops out over approximately 10,000 km^2 (McKenzie and Clarke, 1975). A number of smaller granitic batholiths and plutons intrude throughout the rest of the Meguma Zone. Many authors have mapped and studied the geology, phase distribution, petrology and geochemistry of many of these peraluminous granites (e.g. Wright, 1931; Smith, 1974; McKenzie and Clarke, 1975; Coolen, 1974; Charest, 1976; O'Reilly, 1976; Albuquerque, 1977; MacDonald and Clarke, 1985). A summary of these studies is given in Clarke and Muecke (1985).

Field relations indicate the granitic rocks are post-tectonic and have superimposed a thermal metamorphic aureole, that grades up to hornblende-hornfels facies, on the regional metamorphic assemblages in the metasediments. Throughout the Meguma Zone the long axis of many of the granitic bodies, including the South Mountain Batholith, parallels

the trend of the regional structures associated with the Acadian Orogeny. However, on a more local scale the contacts are clearly discordant and in most instances truncate the Acadian regional tectonic fabrics.

Previous workers established the intrusive sequence of the granitic rocks from oldest to youngest as biotite granodiorite, biotite monzogranite, two-mica monzogranite, smaller intrusions and dykes of leucomonzogranite, porphyry, leucogranite and aplite. Smith (1974) noted that the major units of the South Mountain Batholith in the area immediately west of Halifax (biotite granodiorite, quartz monzonite and muscovite-biotite monzogranite) all have gradational relations. McKenzie and Clarke (1975) reported that, in the central part of the batholith, biotite granodiorite is intruded by two-mica monzogranite and that both of these are intruded by minor, highly differentiated intrusions. More recent work in the same area shows that, although such contact relationships occur, the areas of granodiorite have a gradational relationship with monzogranites of a similar coarse-grained megacrystic texture (Corey, 1986; Ham and Horne, 1986; MacDonald and Horne, 1986).

Within many of the granites textural and compositional variations can commonly only be delineated by very detailed mapping. Charest (1976) found such variations most common in the New Ross-Vaughan area of the central region of the South Mountain Batholith. He concluded that the variations are related to late-stage metasomatic and pneumatolytic alteration concentrated in this more differentiated and higher level of the batholith.

Approximately 80-90% of the granitic rock exposed at the surface in the Meguma Zone consists of two units: biotite granodiorite and biotite monzogranite. The granodiorite is grey to light grey, coarse-grained and generally megacrystic. This granodiorite commonly contains abundant metasedimentary xenoliths in various stages of digestion. The abundance of xenoliths often bears no relationship to distance from known areas of country rock. The monzogranites are quite variable in texture and composition. Color can range from pink to grey to white and textures from medium to coarse-grained and massive to megacrystic. Biotite and muscovite occur in most of the monzogranites, but their ratio can be variable. Muscovite shows evidence of formation by magmatic, late magmatic and post-magmatic processes. The granodiorite and monzogranites commonly contain zircon, apatite, opaques, cordierite, andalusite, garnet and tourmaline as accessory minerals. An interesting characteristic of the Meguma Zone granites is their peraluminous nature which results in the appearance of the various aluminosilicates in the trace and minor phase mineralogy (e.g. Clarke et al. 1976; Allan and Clarke, 1981; MacDonald, 1981; Maillet and Clarke, 1985).

Many small intrusions of muscovite-bearing monzogranite, leucomonzogranite and leucogranite intrude both the granodiorite and monzogranites. These plutons are often alaskitic in texture, but must be classed as leucomonzogranite on their mineralogy (Charest, 1976 p. 29). Pegmatite dykes and pods, both zoned and massive, are often found spatially and probably genetically associated with these muscovite-bearing rocks (O'Reilly et al., 1982).

McKenzie and Clarke (1975) and Muecke and Clarke (1981) present petrological and geochemical evidence to show that the South Mountain Batholith is an autointruded, comagmatic suite that differentiated in-situ from a parent magma derived, at least in part, by partial melting of lower crust. Biotite granodiorite was first to crystallize, but with biotite and plagioclase fractionation the magma became monzo-granitic in composition. The more differentiated monzogranite plutons then intruded the granodiorite. Further fractional crystallization resulted in saturation and exsolution of a volatile-rich fluid phase and subsequent emplacement of minor plutons of muscovite-bearing leucomonzogranite, leucogranite, porphyry and pegmatite.

Albuquerque (1977) invoked partial melting of Meguma Group metasediments as the source of the parent magma for the granitoids in the southern Meguma Zone. Clarke and Halliday (1980) and Muecke and Clarke (1981) used trace element and isotopic data to indicate the Meguma Group, as exposed at present, cannot be the sole source of the South Mountain parent magma. They do concede, that whatever the source, it must have involved a large volume of metasedimentary rock. Considerable contamination of the magma by interaction with the Meguma Group rocks has probably occurred.

The age of intrusion of the granitic rocks of the Meguma Zone has been established on stratigraphic evidence and by isotopic age determinations. The richly fossiliferous Torbrook Formation of Early Devonian age is intruded by biotite granodiorite of the South Mountain Batholith (Smitheringale, 1973). Since the biotite granodiorite represents the oldest rock of the batholith, this relationship defines

time of first intrusion of the magma. All the granitic rocks are overlain nonconformably by the Early Carboniferous Horton and Windsor Group sedimentary rocks.

Radiometric age determinations from the various batholiths and plutons by a variety of techniques and authors places the bulk of intrusion in the 355-375 Ma interval (Fairbairn et al., 1960; Cormier and Smith, 1973; Reynolds et al., 1981). Clarke and Halliday (1980) use Rb/Sr mineral and whole-rock isochrons to define the ages of intrusion of the major granitic phases of the South Mountain Batholith as 371.8 ± 2.2 Ma for biotite granodiorite, 364.3 ± 1.3 Ma for monzogranite and 361.2 ± 1.4 Ma for late-stage porphyry. All of the above radiometric age determinations agree with the stratigraphic age bracket.

Chatterjee and Muecke (1982) document a paraintrusive suite of rocks within the South Mountain Batholith. A paraintrusive rock has an igneous texture and appearance but has a mineral assemblage which is not in magmatic equilibrium and is the result of interaction of a fluid phase with residual magma or previously crystallized granitic rock or both. This fluid phase was enriched (specialized) in such elements as Sn, U, Rb, Li, F, Be and Cs and resulted in formation of biotite leucogranite, sericitized granite, albitized granite, albitite and a variety of greisens. Volumetrically these "specialized" paraintrusive rocks represent a small portion of the granitic massifs, but they are of particular interest because of their close spatial and genetic relationship with significant Sn-U mineralizations (Chatterjee and Muecke, 1982; Richardson et al., 1982; O'Reilly et al., 1985).

Radiometric age determinations of samples from the paraintrusive suite commonly yield apparent ages in the 260-340 Ma interval (Reynolds et al., 1981; Chatterjee, 1983; O'Reilly et al., 1985; Elias, 1986; Reynolds et al., 1987). These younger dates are anomalous relative to the Middle Devonian dates (360-375 Ma) commonly obtained from rocks of the cogenetic suite. This time discrepency is believed to be the result of a Permo-Carboniferous event caused either by a separate magmatic event (Dallmeyer and Keppie, 1987) or by thermotectonism that resulted in overprinting of previously crystallized minerals (Reynolds et al., 1987). This aspect is important considering the economic significance of the paraintrusive rocks.

2.4 POST-GRANITIC SEDIMENTARY ROCKS

All the Meguma Zone Early to Middle Paleozoic metasedimentary r-ocks and the granitic rocks are overlain unconformably/nonconformably by Early Carboniferous sedimentary rocks of the Horton and Windsor Groups. The Horton Group as described in Bell (1929) and Bell and Blenkinsop (1960) consists of a lower Horton Bluff Formation of grey sandstone and shale and an upper Cheverie Formation of red-brown sandstone and shale. The Windsor Group conformably overlies the Horton sedimentary sequence. A number of authors describe this thick sequence of marine evaporites, limestones and lesser terrestrial red and green siltstones (Bell, 1929; Moore, 1967; Giles and Boehner, 1979; Boehner, 1984; Howie, 1984; Schenk, 1984).

The Carboniferous sedimentary rocks are truncated by major fault systems associated with the Cobequid-Chedabucto Fault Zone. Deform-

ation within these rocks varies in intensity but bears a close spatial relationship to the major fault traces.

The northwestern edge of the Meguma Zone is underlain by a sequence of Triassic sedimentary and rift-environment volcanic rocks (Wark and Clarke, 1980). These continental sedimentary rocks unconformably overlie all the Paleozoic strata and nonconformably overlie the granitic rocks in the northern regions of the Meguma Zone. The Mesozoic strata are relatively undeformed but they too are truncated by faults associated with the Cobequid-Chedabucto Fault Zone.

2.5 SUMMARY

The Meguma Zone of mainland Nova Scotia consists of a thick sequence of Lower to Middle Paleozoic metasedimentary rocks intruded by a number of peraluminous Devono-Carboniferous granitoid rocks. The granitoid rocks range in composition from tonalite to leucogranite many of which formed by fractional crystallization of quartz, plagioclase, biotite from a parent magma(s) derived by partial melting of metasedimentary rocks. A paraintrusive suite of rocks occurs within the granitoids. This suite is the result of interaction of melt and/or previously crystallized rock with a volatile-charged fluid phase exsolved during the later stages of magma evolution. The paraintrusive rocks are spatially and genetically associated with significant deposits of granophile elements.

CHAPTER 3

FIELD RELATIONS

3.1 INTRODUCTION

The study area for this thesis comprises the Larrys River and Sangster Lake Plutons and their enclosing metasedimentary country rocks (Fig. 3-1). This chapter describes the field relationships of the plutonic rocks to their metasedimentary country rocks while the next chapter describes the granitic rocks.

Keppie and Muecke (1979) placed the greenschist-amphibolite facies boundary in the area of the Sangster Lake and Larrys River Plutons. Schiller (1959; 1963), Nichols (1976) and Keppie (1985) documented the complex deformational and metamorphic histories of this area but none of these studies described the thermal metamorphic effects of emplacement of the Sangster Lake and Larrys River Plutons. In the current study, new observations shed further light on the history of this complex region.

The Larrys River Pluton is a roughly P-shaped body of 36 km^2. The Sangster Lake Pluton is roughly rectangular with an area of 25 km^2. Previous workers considered the two plutons to be connected by a narrow neck of granite (Fletcher and Faribault, 1887; Stevenson, 1964). Since geological mapping and air photo interpretation done for this project provide no evidence to support such a connection, thus in this thesis they are referred to as separate plutons. Fairbairn et al. (1960) referred to the granitic rocks in the vicinity of the fishing village

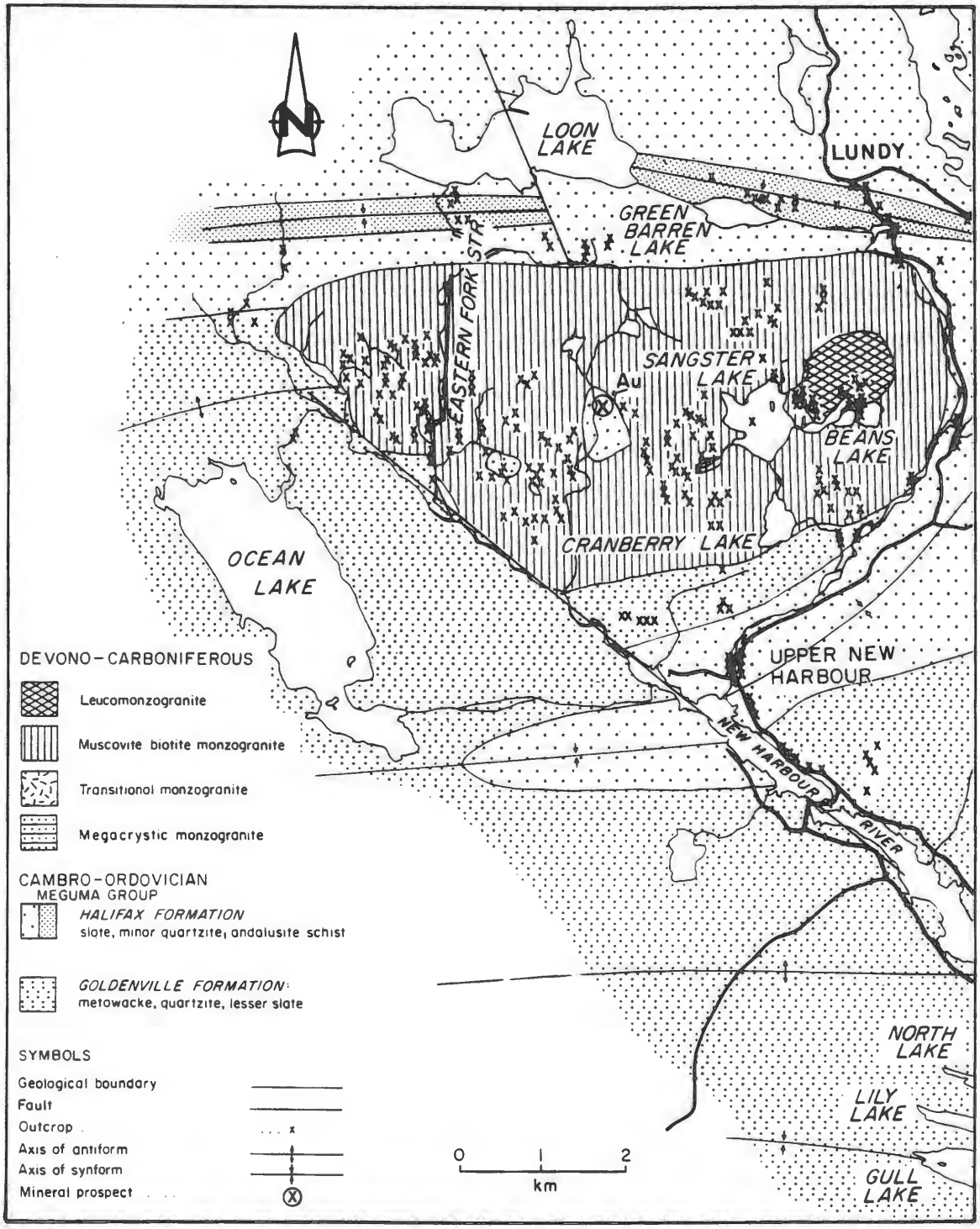

Figure 3-1 Geological setting of the Larrys River and Sangster Lake Plutons. Geology of the plutons is from this study while country rock geology is modified from existing geological maps listed in the text. F.L.C.Z. = Fougere Lake contact zone. Continued on following page.

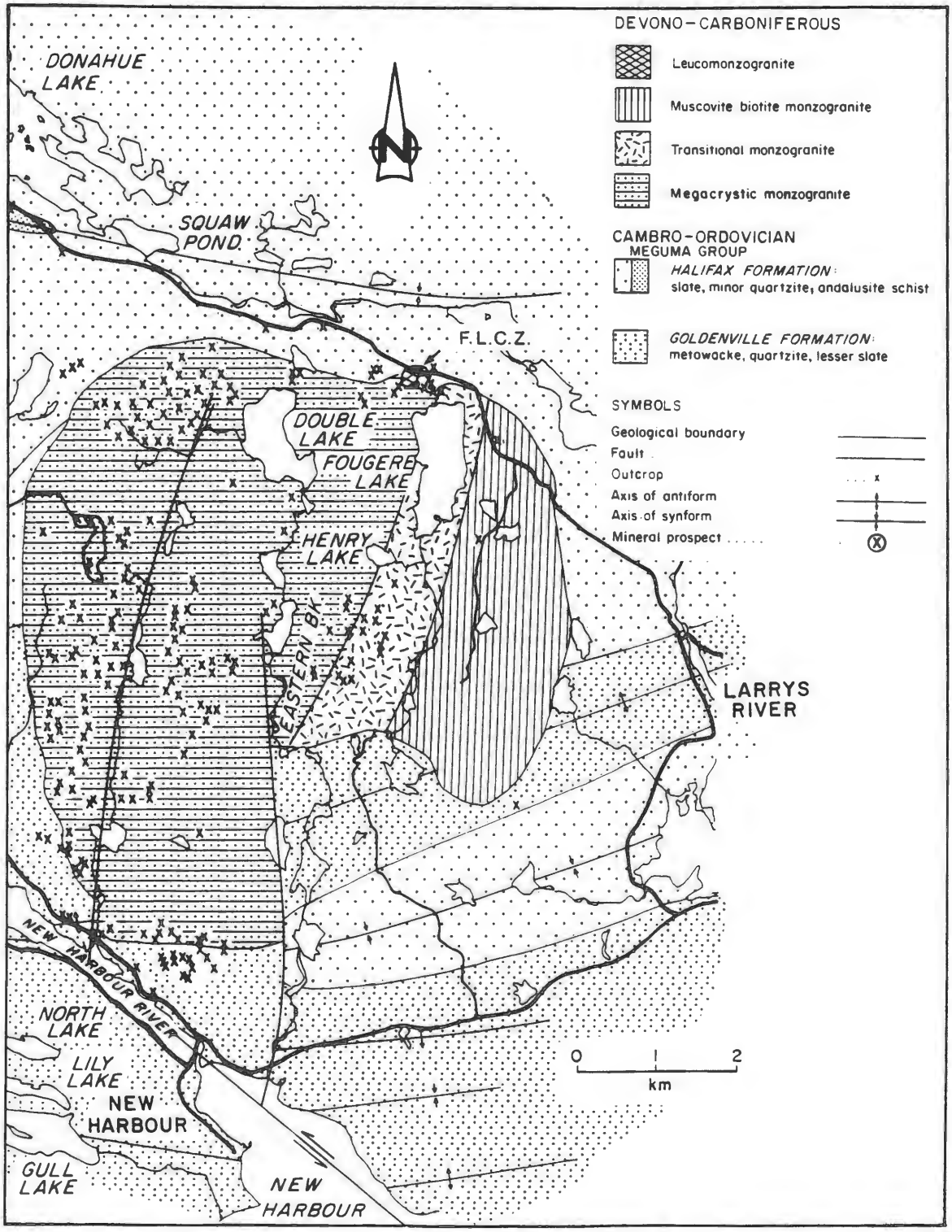

Figure 3-1 cont'd

of Larrys River as the Larrys River granitic terrain. From this the name Larrys River Pluton is derived. Ford and Ballantyne (1983) referred to the Larrys River Pluton as the Eastern Brook Pluton. As the name Larrys River was previously used to designate this granite, the name Eastern Brook Pluton is abandoned. The western pluton has Sangster Lake at its center so the name Sangster Lake Pluton is used to designate this body (Ford and Ballantyne, 1983).

3.2 CONTACT RELATIONS

The Sangster Lake and Larrys River Plutons are completely surrounded by metasedimentary rocks of the Meguma Group (Fig. 3-1), generally the Goldenville Formation in their southern halves and the Halifax Formation in the north. The overall outcrop exposure of these plutons is excellent and exposed or nearly exposed contact zones are common.

The Fougere Lake contact zone (FLCZ on Fig. 3-1) clearly shows the oldest and youngest rock types of the pluton intruding the Halifax Formation semi-pelitic and pelitic spotted slates. Andalusite-rich pelite and quartzite beds are resistent to weathering (Plate 3-1).

A hornfels sample from within one meter of the contact contains the mineral assemblage quartz-andalusite-cordierite-garnet-sillimanite (Plate 3-2). The sillimanite (var. fibrolite) occurs as fine needle-like mantles on both biotite and andalusite (Plate 3-3). Texturally this hornfels displays a well-developed foliation of the phyllosilicates and flattening of quartz grains. A post-tectonic origin for the

Plate 3-1 Thermally metamorphosed pelite from within one meter of the contact with the Larrys River Pluton at the Fougere Lake contact zone. The layered appearance is caused by resistant beds containing andalusite (And). Bracketed area shows an andalusite-rich band.

Plate 3-2 Photomicrograph of hornfels sample from within one meter of the contact. This pelite contains the assemblage quartz-andalusite-cordierite-garnet-sillimanite. Note the post-tectonic origin of the andalusite and cordierite as indicated by their overprinting of the foliation. A = andalusite; C = cordierite; G = garnet. Scale = 0.5mm

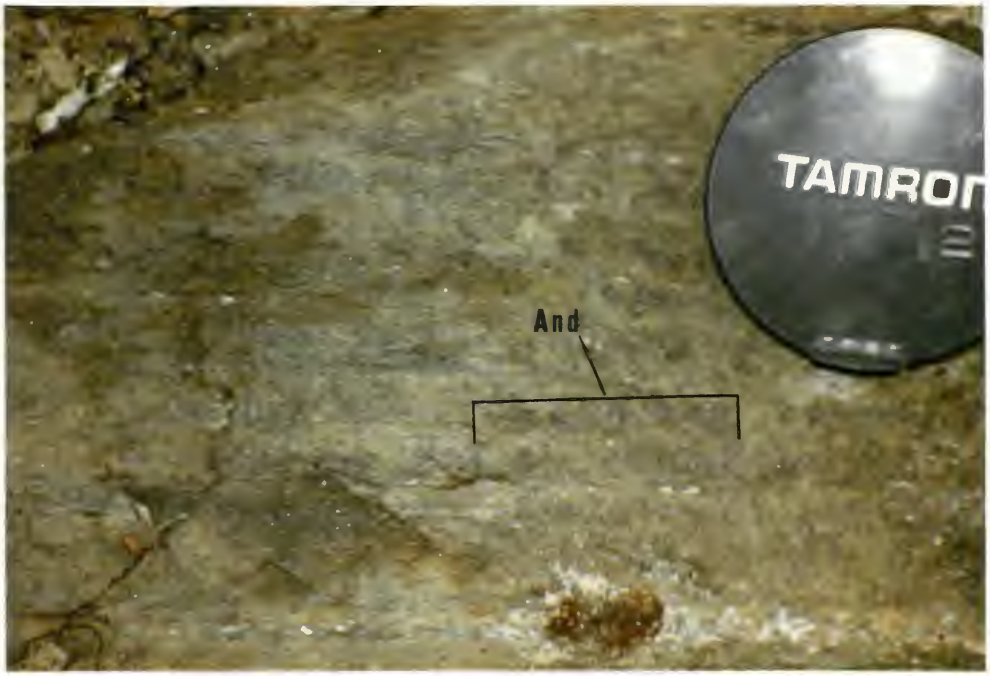

Plate 3-1

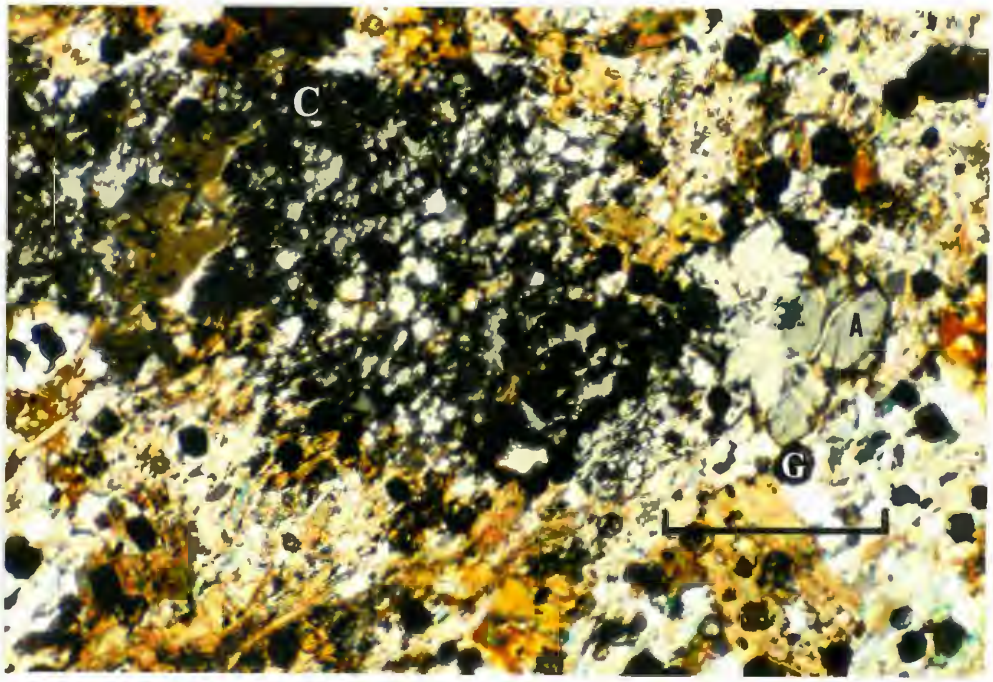

Plate 3-2

contact metamorphic andalusite and cordierite is indicated by their overprinting of this foliation (Plate 3-2).

The texture of these minerals is also significant. The andalusite occurs as small, clean, post-deformational crystals. Cordierite is found as small, rounded, inclusion-riddled patches that impart a typical spotted appearance to the rocks. Previous studies from the Meguma Zone found that andalusite and cordierite of regional metamorphic origin occur as large, blocky, inclusion-riddled, subhedral to euhedral porphyroblasts (Nichols, 1976; Schiller, 1959; 1963). To extend this observation, the overprinting of regional metamorphic assemblages by the Meguma Zone granitoids has also been described by McKenzie and Clarke (1975) and Clarke and Muecke (1985).

A contact zone of the Larrys River Pluton with Goldenville Formation country rocks is exposed immediately north of New Harbour (U.T.M. coordinates 4995500N, 621100E). The granitic rocks can be seen in sharp intrusive contact with the metasediments. The psammitic country rocks were more resistent to the contact metamorphic effects by the intrusion but some overprinting textures were observed. Baking and annealing of quartz grains results in a hard, dark rock with a cherty appearance. Semi-pelitic horizons have a typical spotted texture and often contain randomly oriented, elongate andalusite laths.

The Sangster Lake Pluton has been subjected to post-emplacement deformation (described in the Structural Geology section) which complicates recognition of the contact relationships, especially along the northern contact. A pluton-country rock contact in the undeformed, southwest region of the pluton is exposed along Eastern Fork Stream

(U.T.M. coordinates 5011450N, 623600E). Goldenville Formation semi-pelites and psammites are converted to hornfelses with the assemblage andalusite-sillimanite-cordierite. The fibrolite occurs as mantles on andalusite and biotite. Andalusite and cordierite occur as small undeformed poikiloblasts (Plate 3-4).

To the north and east the Sangster Lake Pluton intrudes the Halifax Formation. Along the road joining Upper New Harbour and Lundy, outcrops of Halifax Formation occur in the area of the stream draining Canter Lake. These outcrops contain large randomly oriented andalusite (chiastolite) laths. These poikiloblasts occur as large, clear crystals of post-deformational and contact metamorphic origin.

In the area of the small lake immediately south of Lundy, outcrops of highly metamorphosed Halifax Formation are found both along the road and in Patterson Brook (U.T.M. coordinates 5014100N, 617850E). In the brook an outcrop of schist occurs within one meter of the pluton, but the actual contact is obscured by water. The schist has an amphibolite facies assemblage of andalusite-cordierite-staurolite, but the relationship of these minerals to the fabrics in the rocks differs from the previously described contact zones. The crystals occur as large blocky, subhedral to euhedral poikiloblasts with inclusion trails discordant to the well-developed mica foliation.

Schiller (1963) describes an andalusite schist band(s) within the Halifax Formation in this region. One such band underlies the area between Loon Lake and Lundy to the north of the Sangster Lake Pluton (Fig.3-1). These rocks have been subjected to intense metamorphism and the assemblage consists of andalusite-cordierite-garnet ± staurolite.

Plate 3-3 Photomicrograph showing sillimanite (var. fibrolite)(F) mantles on biotite (B) and andalusite (A) from thermally metamorphosed pelite in the Fougere Lake contact zone. Small euhedral garnets (G) are also present. Scale = 0.5mm.

Plate 3-4 Photomicrograph from thermally metamorphosed semipelite from a contact zone of the Sangster Lake Pluton exposed along Eastern Fork Stream. Andalusite (A) occurs as undeformed, elongate poikiloblasts. Scale = 0.5mm.

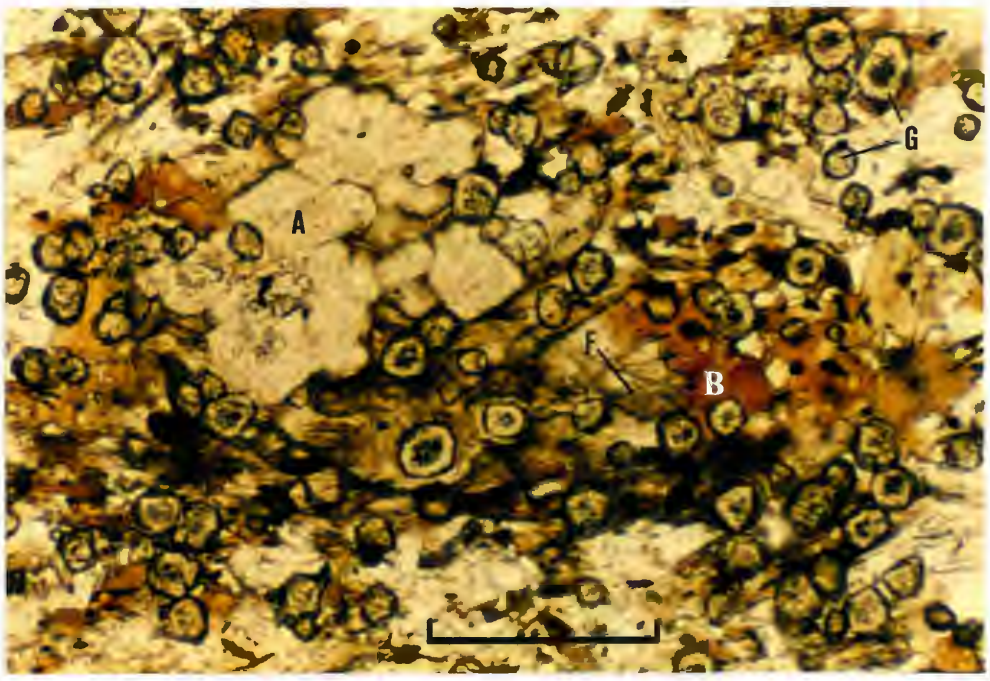

Plate 3-3

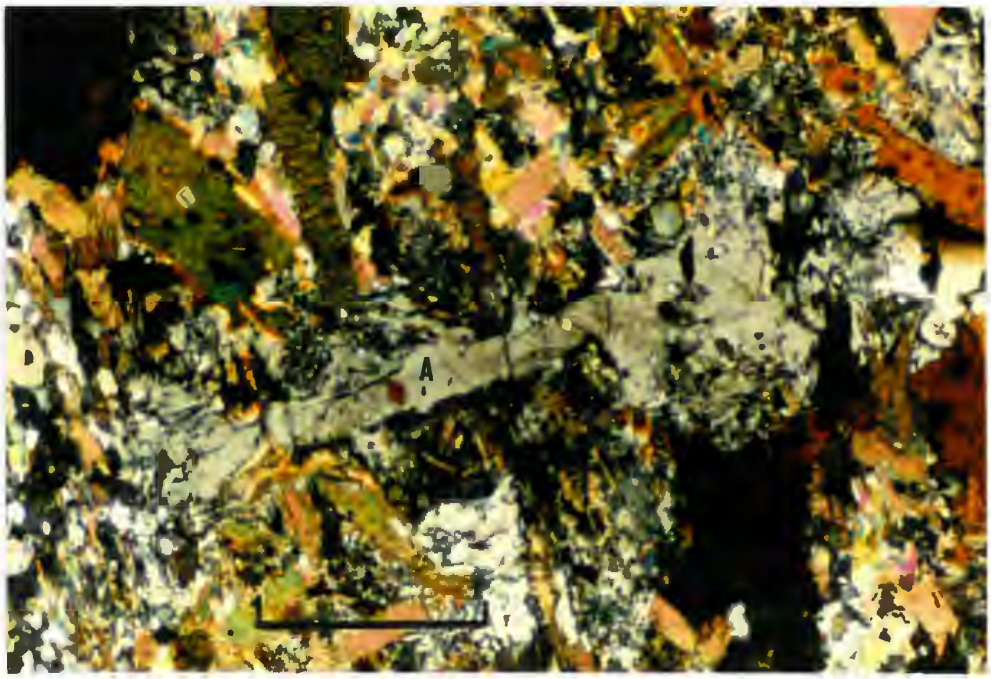

Plate 3-4

Schiller concluded that the metamorphism was related to the nearby plutons. The relationships described from the contact zones in this study show that the contact-derived metamorphic minerals overprint the regional foliation. Samples from the andalusite schist band have poikiloblasts of andalusite, cordierite and staurolite with internal fabrics that are discordant with the phyllosilicate foliation (Plate 3-6). Not only are the inclusion trails discordant, but their slight curvature indicates rotation during their growth. Identical relations were observed in similar rocks outcropping a short distance to the east (Nichols, 1976).

Keppie (1985) recognized a major dextral shear zone in the area of the andalusite schist band north of the Sangster Lake Pluton. This shear zone is discussed further in the following Structural Geology section and may have had a role in creation of the observed textures. Possibly, the thermally overprinted foliation in the Fougere Lake zone is not the same one that postdates the blocky poikiloblasts in the andalusite schist band near Lundy. P. K. Smith and J. D. Keppie (pers. comm.) suggest that the fabric related to this shear zone may exactly coincide with older Acadian fabrics. There are insufficient data to prove conclusively that the fabric overprinted in the Fougere Lake zone is the same as that which has rotated and deformed poikiloblasts in the Lundy area.

Some inferences may be drawn from the textures of the poikiloblasts in the Lundy area. The contact metamorphic andalusite observed in the various contact zones occurs as small, clear, anhedral to euhedral laths. The metamorphic minerals in samples from the Lundy

Plate 3-5 Photomicrograph of an andalusite poikiloblast (A) in pelite of the Halifax Formation from near the Sangster Lake Pluton south of Lundy (Fig. 3-1). Note its large, blocky, idioblastic texture and discordant relationship to the well-developed foliation as defined by the micas. Scale = 0.5mm.

Plate 3-6 Photomicrograph of andalusite poikiloblasts (A) from the andalusite schist band within the Halifax Formation east of Lundy (Fig. 3-1). The curved inclusion trails and deflection of the foliation around the crystals indicate that the poikiloblasts are syn-deformational. Scale = 0.5mm.

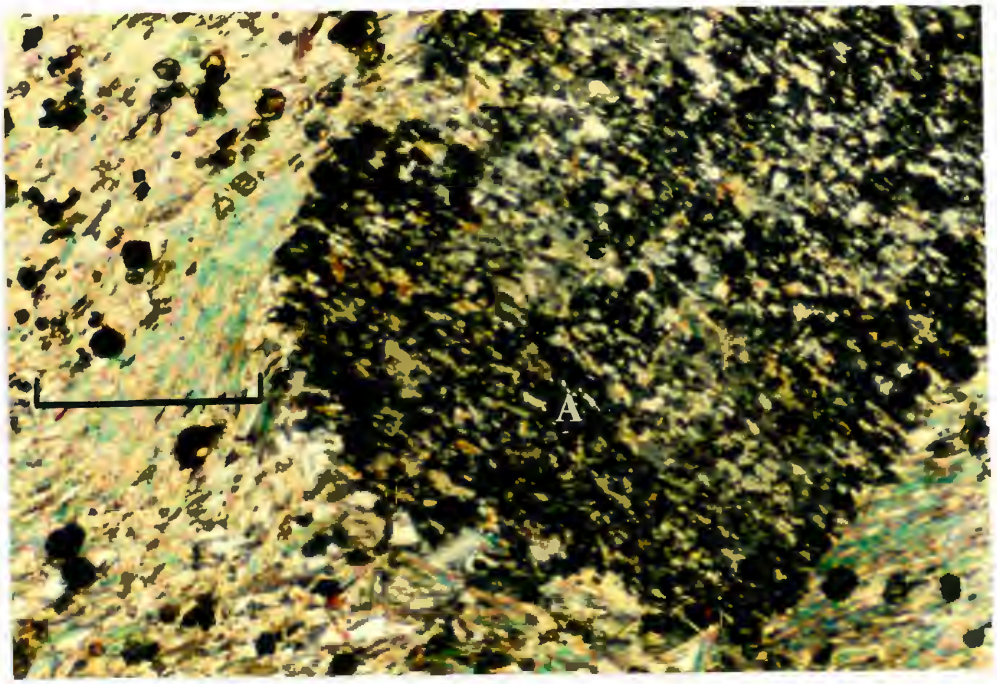

Plate 3-5

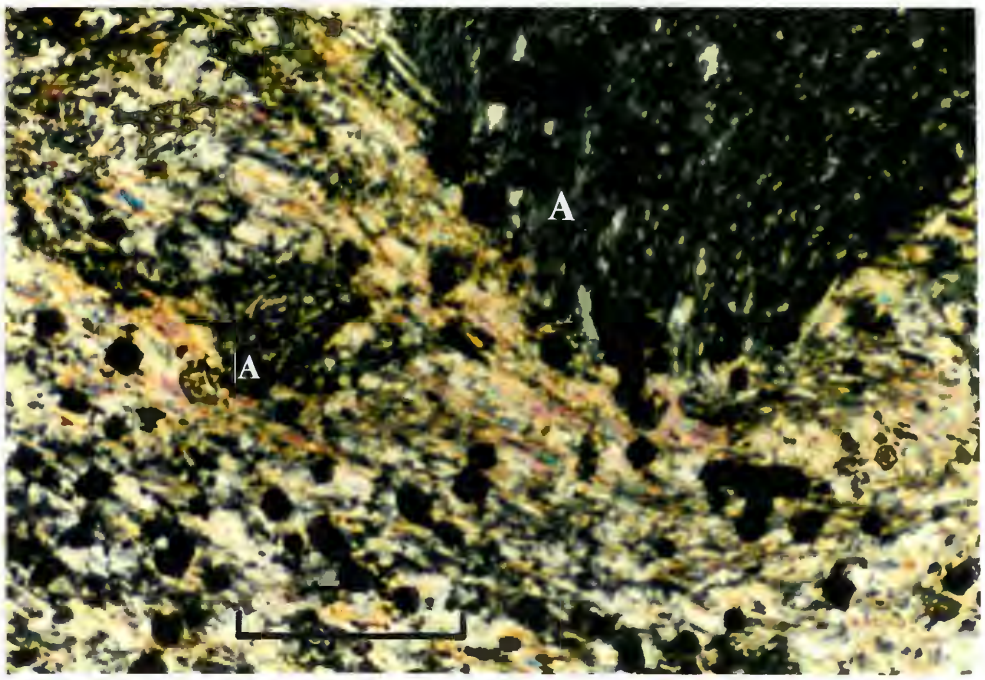

Plate 3-6

andalusite schists occur as large, blocky, inclusion-riddled, subhedral to euhedral poikiloblasts. Regional metamorphic mineral assemblages described from elsewhere in the Meguma Zone commonly have a similar mode of occurrence (G. K. Muecke, pers. comm.).

The great distance from the plutons at which the high-grade assemblages occur is another factor to consider. To the best knowledge of the author, Meguma Zone granitic rocks nowhere thermally alter their enclosing country rocks to the degree observed in the Lundy area for more than a few hundreds of meters from of the contact. For example, within 0.75 km north of the Fougere Lake contact zone, chlorite grade pelitic slates occur. These rocks should be receptive to metamorphism so their low grade quartz-chlorite-muscovite assemblage indicates the thermal effects of intrusion of the Larrys River Pluton did not extend this far from the contact.

The Sangster Lake Pluton has a sharp and straight northern contact which strongly suggests a faulted contact or, if intrusive, the contact is steeply dipping or vertical. It is unlikely then, that thermal metamorphism related to the pluton emplacement would be present in the metasediments over the distances that high grade assemblages are observed (>2 km). Nichols (1976) also concluded that regional, not contact metamorphism is the cause of high grade assemblages in some of the pelites in his study area.

3.3 STRUCTURAL GEOLOGY

The observations just described show the Sangster Lake and Larrys River Plutons were emplaced in a region of the Meguma Zone with a

complex pre- and post-intrusion deformational history. Prior to the plutonism, the Meguma Group in this area was subjected to at least two phases of deformation related to the Acadian Orogeny (Keppie et al. 1985). This resulted in tight east-west trending isoclinal folds. Both the plutons are discordant and cross-cut the pre-existing isoclinal fold structures and contact metamorphism associated with pluton emplacement overprints the main Acadian tectonic fabrics.

Deformation fabrics from the plutons and country rocks, combined with an air photo interpretation, appear in Figure 3-2. The Larrys River Pluton exhibits no deformational fabric, while the Sangster Lake Pluton is variably deformed. The northern region of the Sangster Lake Pluton, from Eastern Fork Stream to the Lundy-New Harbour road, displays a well-developed fabric. The highly deformed region of the pluton falls within the dextral Lundy shear zone of Keppie and Dallmeyer (1987). Granitic outcrops within this zone display a mineral alignment foliation (s planes) and shear planes (c planes) (Plate 3-7).

Such fabrics are typical of granitoid rocks within regional scale, mega-shear zones of orogenic fold belts (Ponce de Leon and Choukroune, 1980; Jegouzo, 1980; Vernon et al. 1982). These authors describe the progressive effects of ductile shearing in the heterogeneous deformation of granitic rocks. The most intense shearing usually occurs at the borders of the plutons. The shear zones may vary in width from a few kilometers down to a meter scale but the granitic rocks may carry the mineral alignment foliation (s planes) for a considerable distance from the actual shear zone. The s planes turn progressively into parallelism with the pluton-country rock contact. Within the shear

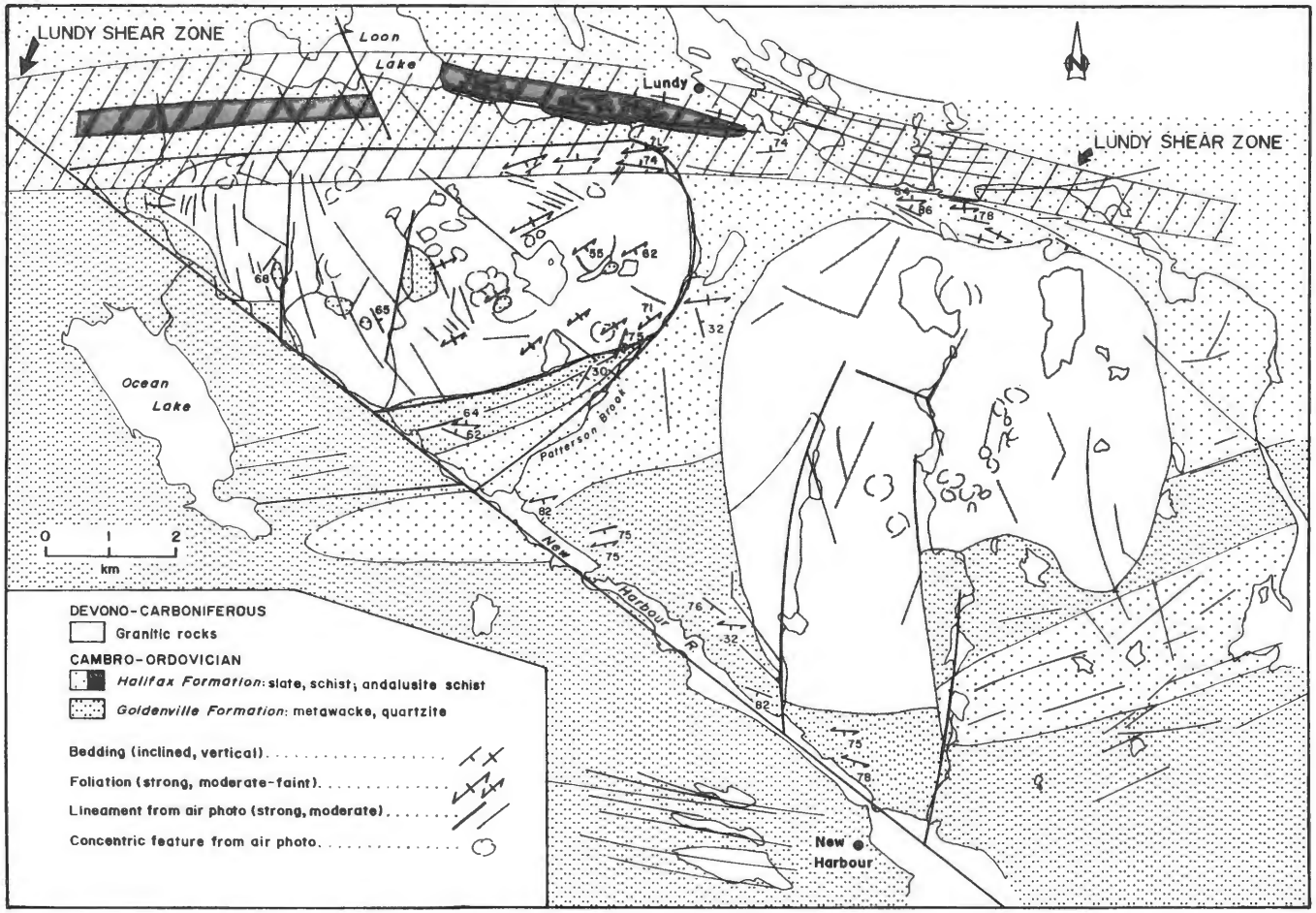

Figure 3-2 Air photo interpretation and structural data for the study area.

zone the area of most intense deformation is marked by appearance in the rocks of an additional fabric, the c planes (Plate 3-7). The c planes form oblique to the s planes (approx 30^{o}) to accommodate the imposed shear component of strain.

The Sangster Lake Pluton displays most of the deformational features described above describing the behavior granitic rocks in shear zones. A sample from the northeastern border of the Sangster Lake Pluton shows the occurrence of well-developed s and c planes within the pluton (Plate 3-7). Toward the south of the pluton the c planes decrease in number and intensity and eventually disappear. The compressional s plane fabric occurs throughout much of the rest of the pluton but varies greatly in intensity. An attempt to quantify this variation in intensity of the s plane fabric is included in Figure 3-2. A map of locations and relative orientations of structural features within the thesis area shows the coincidence of the orientation of s planes within the Sangster Lake Pluton with the east west trending Lundy shear zone (Fig. 3-2).

Much of the pluton west of the Eastern Fork Stream is undeformed except along its most northerly border. This region of the pluton has apparently escaped much of the shear-related deformation associated with the Lundy shear zone.

In outcrop the Larrys River Pluton shows no effects of the ductile shear although in thin section some deformational textures are recognizable (described in Chapter 4). This suggests the pluton was mildly affected by this deformational event.

Plate 3-7 Slab sample from the northern, highly deformed region of the Sangster Lake Pluton. Note the presence of a mineral alignment foliation (s plane; strike 080^{o}Az) and shear planes (c planes). These features indicate a dextral sense of shear. Scale = 5cm.

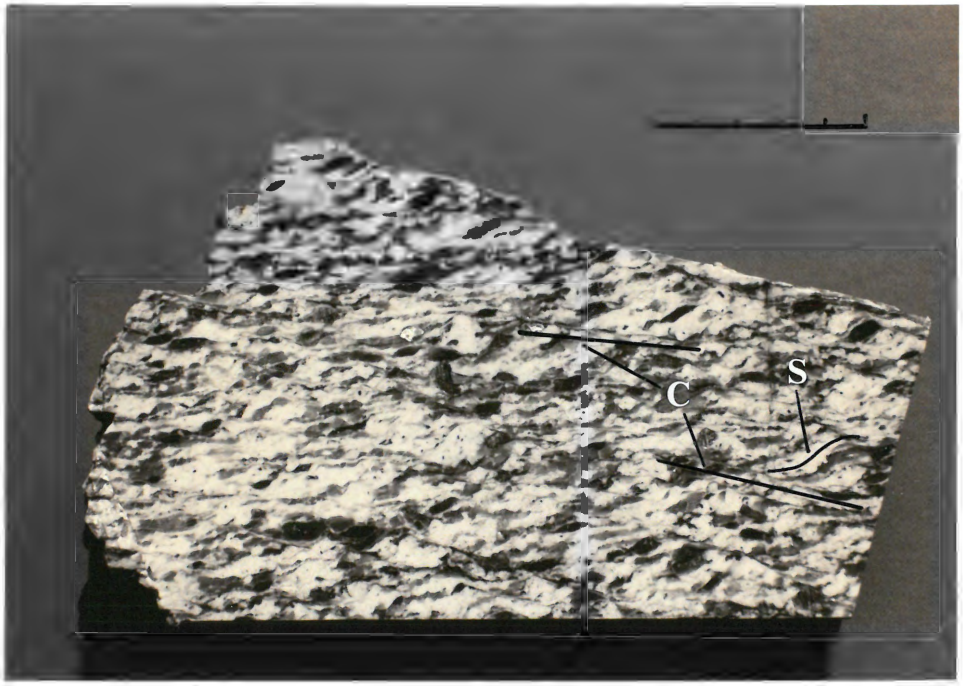

Plate 3-7

The regional trace of resistent Goldenville Formation metawacke units as well as lineaments within the plutons and country rocks are easily recognizable in the air photo interpretation because of the lack of surficial sediment cover over much of the study area. The Larrys River Pluton has two prominent north-south trending lineaments traversing the metasediment-pluton contact. The trace of these lineaments offsets the contact and subtends the trace of the regional fold structures of the Meguma Group strongly suggesting they represent faults.

The Sangster Lake Pluton is also traversed by a number of north-south trending lineaments. The most pronounced of these forms the path of the Eastern Fork Stream (Fig. 3-2). A slight offset of the pluton-country rock contact and the fact that this lineament separates a deformed region of the pluton from an undeformed region suggests the lineament is a fault. The pluton-metasediment contact along Patterson Brook north of Upper New Harbour forms a deep and persistent valley suggesting it may also be a fault. If so, a fault along Patterson Brook could be associated with, or be a subsidiary of, the Lundy shear zone. The mineral alignment foliation (s planes) within the immediately adjacent region of the Sangster Lake Pluton parallels the trend of the Patterson Brook valley (Fig. 3-2). This suggests that, during the period of the dextral east-west ductile shear the Sangster Lake Pluton behaved as a mega-augen, resistant to the shearing within the much more ductile pelites of the Halifax Formation. To accommodate the more resistant granitic pluton, shearing was localized along the pluton-schist contact.

Throughout the central and eastern portion of the Sangster Lake Pluton the northeast-trending s plane orientations may reflect compressional forces of the abutment or wedging of the pluton between the Patterson Brook fault and the Lundy shear zone. Toward the north of the pluton the s plane orientations trend roughly east-west, reflecting compressional forces associated with the Lundy shear zone.

Keppie and Dallmeyer (1987) describe a series of large northwest-southeast sinistral transcurrent faults within the Meguma Zone. These represent early Mesozoic movements along the Cobequid Chedabucto Fault Zone. One of these faults forms the trace of the New Harbour River (Fig. 3-2). Movement along these faults was very late in the structural development of the Meguma Zone and post-dated all plutonic and metamorphic activity.

3.4 MODE OF EMPLACEMENT

The shape of the Larrys River and Sangster Lake Plutons indicates their emplacement was not related to an obvious regional zone of weakness within the Meguma Zone. Country rock xenoliths occur within both plutons, but are small and not common. The Larrys River Pluton contains a number of small dykes and pods of pegmatite and highly-evolved leucogranite near its contacts with country rocks. This, and the fact that this pluton was intruded into metasediments of low regional metamorphic grade, suggests high level emplacement.

Although country rock xenoliths are uncommon within the Sangster Lake Pluton, a number of roof pendants or large xenoliths of Goldenville Formation occur. The air photo interpretation shows a number of

concentric circular structures throughout the pluton (Plate 3-8). In all instances, the metasedimentary roof pendants occur in low-lying areas along the perimeters of these circular structures. The relationship of these metasedimentary inliers and the concentric structures features provides clues as to the mode of emplacement of the pluton.

The circular structures may represent the sites of upwelling or convective cells within the larger underlying magma chamber (Fig. 3-3). Near the roof of the chamber some of these rose into the overlying country rocks and froze in place in the roof zone. Several of the metasedimentary blocks remained almost completely engulfed along the perimeter of the structures. Recent uplift and erosion dissected several of the upwellings exposing circular granitic structures with metasedimentary roof pendants occupying low-lying areas along their perimeters (Figs. 3-2; 3-3; Plate 3-8).

Abbott (1980) describes concentric circular structures of similar dimensions within the granitic rocks of the South Mountain Batholith near Halifax. At that location the structures also occur a short distance from the batholith-metasediment contact. Abbott concludes they are the result of shearing and convection within the magma chamber close to the metasediment contact.

If this interpretation is sound it verifies the Sangster Lake Pluton is exposed at its uppermost roof zone, especially in its southern and eastern regions where many of the circular features predominate. This interpretation is further strengthened by petrographic and geochemical evidence presented in subsequent chapters.

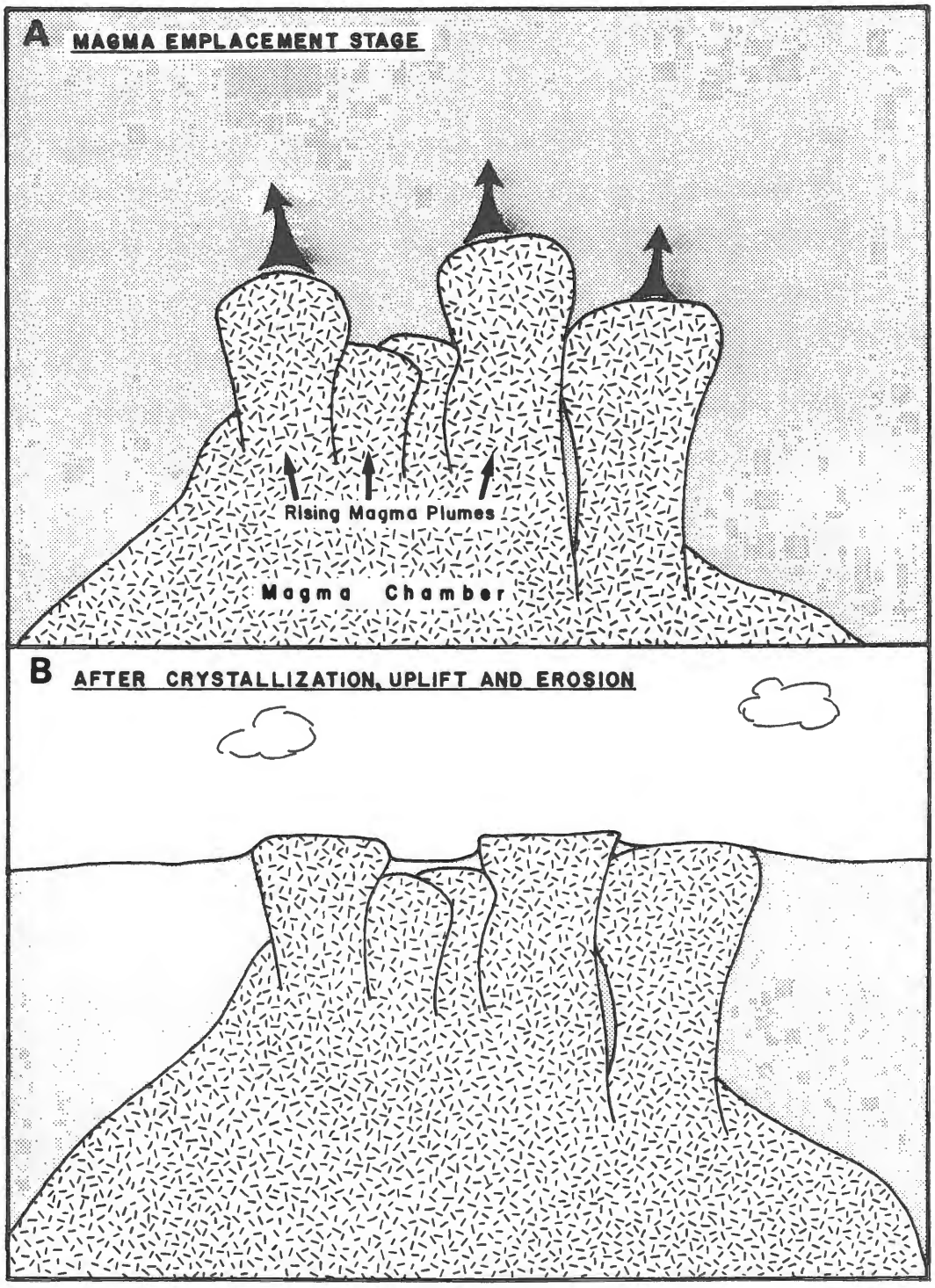

Figure 3-3 Schematic representation of the emplacement mechanism of the Sangster Lake Pluton and the origin of roof pendants underlying low lying areas.

Plate 3-8 Air photograph of an area immediately west of Sangster Lake (top right) showing a series of circular, concentric structures of monzogranite. Metasedimentary roof pendants commonly underlie topographic depressions along the perimeters of these structures (e.g. the wooded area surrounding small lake above the scale bar is underlain by metasediment). Scale = 100m.

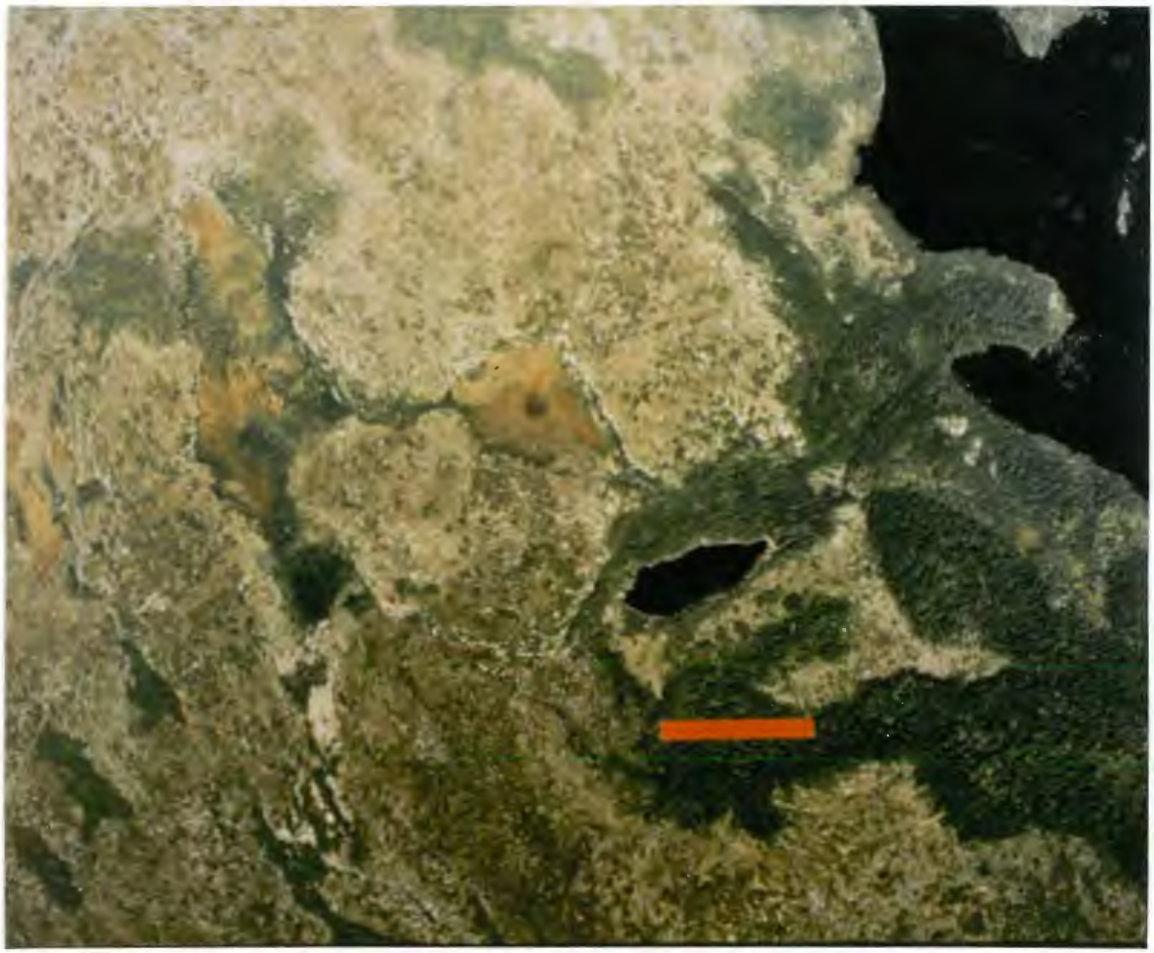

Plate 3-8

3.5 GEOPHYSICAL EXPRESSION

Since 1976 the Geological Survey of Canada has systematically collected high-sensitivity, airborne gamma-ray spectrometric data in Nova Scotia. The Eastern Meguma Zone, including the thesis area, was flown with 1 km line spacing (Geological Survey of Canada, Geophysical Maps 35611(3)G, 35611(4)G, 35611(5)G and 35611(6)G). The general principles of these surveys are described by Bristow (1979), Grasty (1979) and Killeen (1979).

The airborne gamma-ray spectrometric surveys show that the Sangster Lake Pluton has an anomalous and variable response for equivalent uranium (eU) and the equivalent uranium/equivalent thorium ratio (eU/eTh; Fig. 3-4). Ford and Ballantyne (1983) carried out in-situ gamma-ray spectrometric measurements which verify the airborne results.

The Larrys River Pluton has a relatively flat airborne spectrometric response, very similar to that over most of the granitic rocks throughout the Meguma Zone (Ford and O'Reilly, 1985). Airborne determinations of radioelement concentrations are generally less than actual bedrock concentrations because of a variety of factors. Thickness of overburden, wetness, and vegetative cover all have a shielding effect. Charbonneau et al. (1976) show that even though there are shielding effects, the relative proportions of uranium and thorium in the airborne data are consistent with bedrock concentrations.

The Sangster Lake Pluton has a significantly higher eU and eU/eTh response than the Larrys River Pluton (Fig. 3-4). Toward the east the

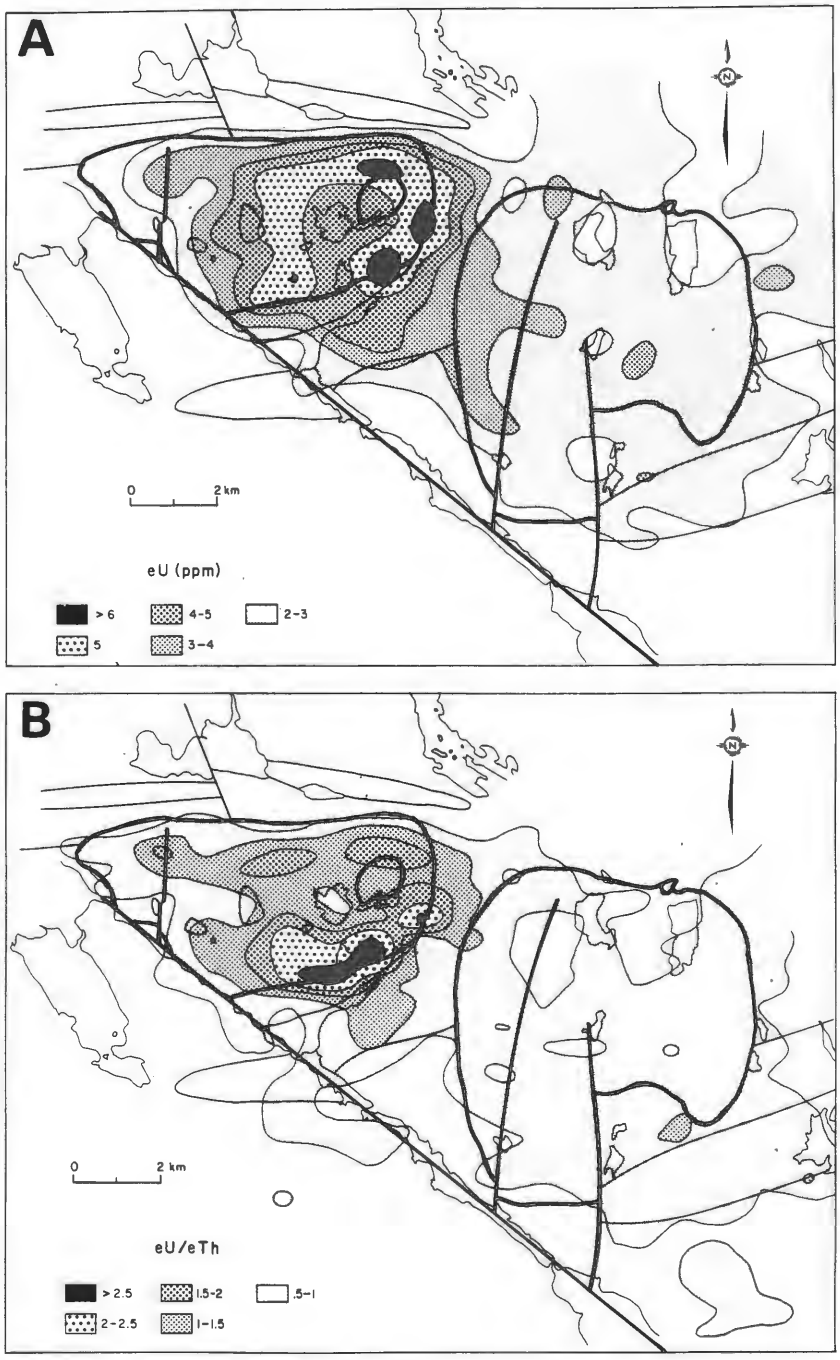

Figure 3-4 Airborne gamma-ray spectrometric response contour map for equivalent uranium (eU; map A) and the equivalent uranium/equivalent thorium ratio (eU/eTh; map B) over the study area. The major geological contacts from Figure 3-1 are also included.

airborne response over the Sangster Lake Pluton increases from background (2-3 eU ppm) up to anomalous levels (5-6 eU ppm). A similar relationship exists with the eU/eTh ratio. The ratio variation reflects either an increase of uranium or a decrease in thorium or both.

The ring-shaped pattern of the eU anomaly of the Sangster Lake Pluton is probably somewhat enhanced by the presence of Sangster and Cranberry Lakes (Fig. 3-4). The airborne data, although computer corrected for variables such as elevation, cannot be corrected for the presence of surface water. Gamma radiation is almost completely shielded by less than a meter of surface water. The presence of these lakes could be masking the response of underlying anomalous granite. Hence, the ring-shape may be misleading and in fact much of the southeastern end of the pluton may be anomalous.

3.6 AGE RELATIONS

The youngest rocks intruded by the Sangster Lake and Larrys River Plutons are those of the Halifax Formation. Lower Ordovician fossils occur in this Formation in the southwestern Meguma Zone (Keppie, 1977). Keppie and Dallmeyer (1987) summarize the results of K/Ar, $^{40}Ar/^{39}Ar$, Rb/Sr and U-Pb age determinations from granitic and metasedimentary rocks of the eastern Meguma Zone. The Larrys River and Sangster Lake Pluton ages from this summary appear in Table 3-1.

Monazite U-Pb age determinations of 372Ma and 375Ma are for samples of the Larrys River and Sangster Lake Plutons respectively. Both samples are biotite-muscovite monzogranite and come from the same

Table 3-1 Summary of radiometric age determinations for the Larrys River and Sangster Lake Plutons from Keppie and Dallmeyer (1987).

METHOD	LARRYS RIVER PLUTON (Ma)	SANGSTER LAKE PLUTON (Ma)	REFERENCE
Rb/Sr* muscovite	334		Fairbairn et al. (1960)
Rb/Sr* biotite	331		" "
K/Ar* muscovite	328		" "
K/Ar* biotite	369		" "
Rb/Sr whole rock isochron	396±21	364±7	Keppie et al. (1985)
U/Pb monazite	372±1	375±1	" "
$^{40}Ar/^{39}Ar$ muscovite	365.4±1.8	364.5±1.4	Keppie and Dallmeyer (1987)
$^{40}Ar/^{39}Ar$ biotite	365.9±1.9	363.8±1.7	" "

* Recalculated to decay constants and isotopic abundance ratios listed by Steiger and Jager (1977).

outcrops as sample F6-G004 of the Larrys River Pluton and F-G001 of the Sangster Lake Pluton collected for this study. The area of the Sangster Lake Pluton from which sample F-G001 was collected has the highest airborne radiometric response and, as is described in subsequent chapters, is an area that has undergone considerable mineralogical and chemical alteration. In both cases, Keppie and Dallmeyer (1987) interpret the monazite dates to represent the original, magmatic age of the plutons.

Keppie and Dallmeyer (1987) also give mica ages by the $^{40}Ar/^{39}Ar$ incremental release method (Table 3-1). The Larrys River sample yields plateau ages of 365.4 ± 1.9 Ma for muscovite and 363.8 ± 1.8 Ma for biotite while the Sangster Lake sample yields 364.5 ± 1.4 Ma and 365.9 ± 1.9 Ma respectively. They conclude that the plateaus are relatively undisturbed and interpret the mineral ages to represent the time of imposition of deformation associated with dextral shearing widespread throughout the eastern Meguma Zone. Since emplacement of the plutons occurred at approximately 372-375 Ma (monazite dates) and post-crystallization deformation occurred at 364 Ma (mica plateau ages) there is a 10 Ma interval between pluton emplacement and the shear deformation associated with the Lundy shear zone. This relationship is consistent with the findings presented in this and following chapters.

3.7 SUMMARY

The field relations described in this chapter show:

1. The Sangster Lake and Larrys River Plutons intrude Cambro-Ordovician Meguma Group metasedimentary rocks. Prior to intrusion

of the granites the metasediments were regionally metamorphosed to the greenschist and amphibolite facies. The plutons crosscut regional fold structures and superimpose thermal metamorphic mineral assemblages on those of regional metamorphic origin.

2. Deformation fabrics related to a dextral, east-west trending, shear zone overprint the Sangster Lake Pluton, especially in the northern region. The Larrys River Pluton has not been affected to the same degree by the shear deformation.

3. Concentric structures in the Sangster Lake Pluton are interpreted to represent upwellings or convective cells within the magma during emplacement. The presence of many large metasedimentary blocks or roof pendants in low-lying areas along the perimeters of the concentric structures suggest the pluton is exposed at its uppermost zone.

4. Airborne gamma-ray spectrometric response over the Larrys River Pluton is average. The response for eU and the eU/eTh ratio over the Sangster Lake Pluton is variable. The western portion of the pluton has average response while the eastern and northern regions are elevated by a factor of 2-3 times.

5. The published radiometric age determinations show that emplacement of the plutons occurred between 372-375 Ma. Mica-ages indicate the episode of shear deformation which overprints the

Sangster Lake Pluton occurred between 363-365 Ma. This brackets the emplacement and final cooling of the pluton to the 10 Ma interval between 363-373 Ma.

CHAPTER 4

FIELD RELATIONS AND PETROLOGY OF THE GRANITOID ROCKS

4.1 INTRODUCTION

The geology and distribution of granitic phases within the Larrys River and Sangster Lake Plutons are given in Figure 3-1. The classification scheme for plutonic rocks of Streckeisen (1976) was employed. Rock type designations are from modal counts on cut slabs stained for potassium feldspar with sodium cobaltinitrite. The results of the modal analyses are tabulated in Table 4-1 and presented in a quartz-alkali feldspar-plagioclase plot (QAP; Fig. 4-1). The modal analyses are further augmented by thin-section petrographic analyses. The petrography allowed delineation of the textural variations of the rock types as well as identification of the trace mineral assemblages and hydrothermal alteration effects.

4.2 LARRYS RIVER PLUTON

4.2.1 Megacrystic monzogranite

The western and central region of the Larrys River Pluton is underlain by a megacrystic biotite monzogranite (Fig. 3-1) in which muscovite is less than half as abundant as biotite. This rock type is variable in both texture and composition. Over small areas (< 10 m^2) it grades from an extremely megacrystic rock to one in which megacrysts are much less abundant. The variability is often accompanied by an

Table 4-1 Results of modal analysis counts on slabs from this study. Samples were stained for potassium feldspar with sodium cobaltinitrite.

PLUTON	SANGSTER LAKE PLUTON									
ROCK TYPE	LGT	HIGH-RESPONSE MONZOGRANITE				CENTRAL MONZOGRANITE				
SAMPLE #	F5-G004	F-G001	F-G003	F-G004	F-G005	F5-G001	F5-G010	SL-11	SL-12	SL-13
Quartz	31.7	27.1	31.7	35.1	36.7	31.5	25.3	33.6	28.7	37.5
K-spar	23.0	18.0	13.5	15.2	16.0	17.2	16.3	12.6	14.0	19.5
Plagioclase	35.2	36.8	38.0	38.8	34.3	36.2	42.3	35.3	40.5	33.7
Muscovite	8.1	15.0	14.0	8.1	8.1	9.5	10.4	10.9	12.4	7.1
Biotite	0.0	0.9	2.5	2.3	4.7	5.5	5.6	7.1	4.3	1.7
Chlorite	0.0	1.4	0.2	0.0	0.0	0.0	0.0	0.0	0.0	0.0
Other	1.7	0.2	0.1	0.2	0.2	0.1	0.1	0.5	0.1	0.5
Q/A/P	35/26/39	33/22/45	38/16/46	39/17/44	42/18/39	37/20/43	30/19/51	41/15/43	34/17/49	41/37/21

PLUTON	SANGSTER LAKE PLUTON			LARRYS RIVER PLUTON						
ROCK TYPE	CENTRAL MONZ		ARM	BIOT MUSC MONZ		TRANSITIONAL MONZOGRANITE			MEGA MONZ	
SAMPLE #	SL-14	SL-15	F-G018	F6-G004	LR-7	F3-G004	LR-5	LR-6	F3-G002	LR-G010
Quartz	30.8	30.7	25.2	28.0	43.2	28.5	32.2	28.6	40.1	37.2
K-spar	19.1	16.3	39.7	31.0	23.5	32.5	28.2	26.1	18.6	24.0
Plagioclase	34.5	39.4	28.7	29.7	27.0	28.7	33.2	36.1	29.1	25.7
Muscovite	13.0	9.4	3.7	7.0	2.2	2.3	1.8	3.8	2.8	5.2
Biotite	2.3	3.4	2.5	3.7	4.0	7.9	4.2	5.1	9.1	6.2
Chlorite	0.0	0.3	0.0	0.0	0.0	0.0	0.0	0.0	0.0	1.2
Other	0.3	0.5	0.2	0.2	0.1	0.1	0.4	0.3	0.3	0.2
Q/A/P	36/23/41	36/19/46	27/42/31	32/33/35	46/25/29	32/33/39	34/30/35	31/29/40	46/21/33	43/28/30

LGT = Leucomonzogranite ARM = Average-Response Monzogranite MEGA MONZ = Megacrystic Monzogranite

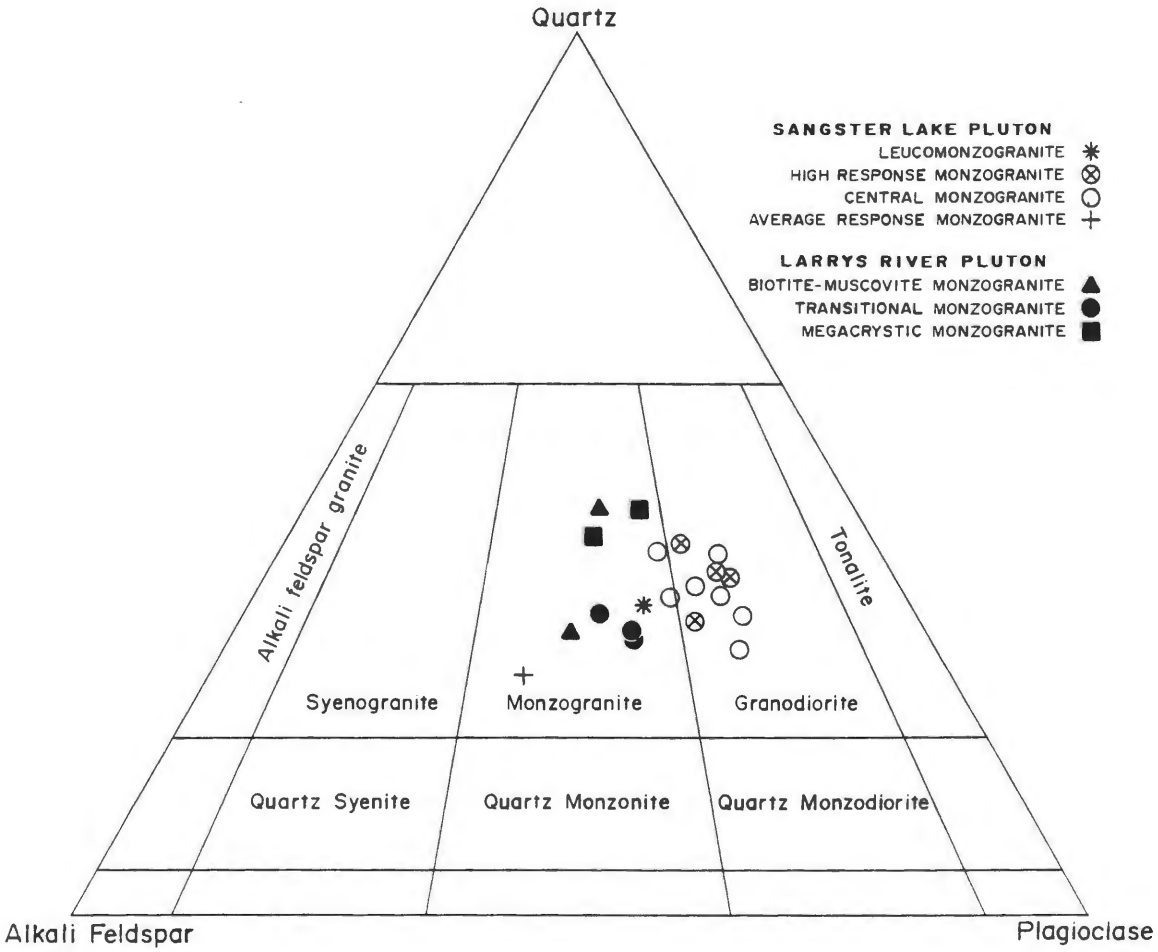

Figure 4-1 Quartz-alkali feldspar-plagioclase (QAP) ternary plot of modal analyses of selected samples of the Larrys River and Sangster Lake Plutons. Classification after Streckeisen (1976).

alignment of the megacrysts. The alignment is highly variable in orientation, often swirling within a single outcrop and is interpreted to be a primary, magmatic feature, the result of convective motion in the magma chamber (Abbott, 1980).

Texturally this rock resembles the biotite granodiorite of the South Mountain Batholith, but modally the rock is a monzogranite consisting of a megacrystic, hypidiomorphic granular mesh of quartz, plagioclase, potassium feldspar, biotite and muscovite (Fig. 4-1). Quartz occurs as anhedral coarse- and medium-sized crystals which display undulatory extinction. Potassium feldspar occurs mostly as megacrystic, strongly perthitic, subhedral to euhedral orthoclase which, in some cases, has albitic rims. The megacrysts often contain inclusions of one or all of quartz, oligoclase, biotite and muscovite.

Plagioclase occurs as euhedral-subhedral, medium-coarse grains of well-zoned (oscillatory) oligoclase. The central calcic cores are often clouded by secondary alteration to white mica, while the outer more sodic rims are clear. Biotite is variable in grain size and contains abundant zircons with pleochroic haloes. Muscovite occurs as secondary alteration of biotite and plagioclase as well as separate and discrete, blocky laths of possibly primary origin in the groundmass.

Accessory minerals are monazite (identified by SEM, Chapter 5), zircon, apatite, pyrite and rutile. Zircon and monazite occur solely as inclusions within biotite. Apatite occurs as fine- to medium-sized euhedral grains, both as discrete grains in the groundmass and as inclusions in biotite. Fe-oxides and rutile are associated with chloritization of biotite.

4.2.2 Transitional monzogranite

To the east the megacrystic monzogranite grades into a less megacrystic, gradational facies, the coarse-grained transitional monzogranite. This rock, although megacrystic, is much less so than the megacrystic monzogranite. The term transitional applies as this rock is a gradational facies between the megacrystic monzogranite and an equigranular biotite-muscovite monzogranite which outcrops to the east (Fig. 3-1). Modal analyses show that it is monzogranite (Fig. 4-1; Table 4-1).

The megacrystic and transitional monzogranites are texturally and compositionally distinct. The transitional monzogranite is typically coarse grained, with a hypidiomorphic granular groundmass of quartz, orthoclase, plagioclase, biotite and muscovite. The rock contains lath-shaped, perthitic orthoclase megacrysts (average 2.5-3.5 cm) but these, as stated earlier, are much less abundant than in the megacrystic monzogranite. The appearance of muscovite as a major mineral is significant, as in the megacrystic monzogranite muscovite occurs in minor amounts and mostly as a secondary mineral.

Quartz forms coarse- to medium-sized anhedral crystals with undulatory extinction. Perthitic orthoclase occurs as megacrysts and as a subhedral-anhedral constituent in the groundmass. The megacrysts are generally lath-shaped but relatively subhedral resulting from resorption along crystal boundaries. Plagioclase is oligoclase (An_{20-24}, microprobe determination, Chapter 5) and generally displays well-developed oscillatory zoning and clouded, sericitized cores.

Biotite exceeds muscovite in abundance and occurs in the groundmass as flakes riddled with zircons. Muscovite occurs both as discrete flakes within the groundmass and as small inclusions within plagioclase. The inclusions of muscovite are clearly secondary but whether the larger groundmass grains are primary or secondary could not be determined with certainty.

Accessory minerals consist of monazite (SEM identification, Chapter 5), zircon, apatite, magnetite, ilmenite, pyrite, rutile and chlorite. Apatite occurs as discrete subhedral crystals in the groundmass and as inclusions in biotite. Accessory amounts of andalusite and cordierite occur within other monzogranite plutons of the Meguma Zone (McKenzie and Clarke, 1975; MacDonald and Clarke, 1985). Neither these phases nor other aluminosilicates were recognized in the transitional monzogranite.

4.2.3 Biotite-muscovite monzogranite

The eastern and northern portion of the Larrys River Pluton is underlain by a massive, coarse-grained, biotite-muscovite monzogranite (Fig. 3-1). Unfortunately, this region of the pluton is poorly exposed and the following observations are based on a small number of outcrops. The biotite-muscovite monzogranite is a non-megacrystic end member of a progressive and gradational decrease in megacryst abundance within the pluton. Modal analyses show the rock is still monzogranite (Fig. 4-1; Table 4-1).

The biotite-muscovite monzogranite is coarse grained with a hypidiomorphic granular texture. The major minerals are quartz,

plagioclase, potassium feldspar, biotite and muscovite. Quartz, plagioclase and potassium feldspar occur roughly in equal proportions. Biotite predominates slightly over muscovite and together they comprise 6-10 volume %. Quartz occurs both as coarse-grained subhedral and/or anhedral crystals and as abundant fine-grained crystals as inclusions in the feldspars. Plagioclase is oligoclase (An_{24-28}, optical identification) and forms subhedral-euhedral laths. The plagioclase differs from that in the other monzogranites in having less oscillatory zonation and the presence of some normal zonation. The calcic cores are also less clouded by sericitic alteration.

The potassium feldspar is microcline and occurs as anhedral crystals and as interstitial fillings between other minerals. The microcline is only weakly perthitic, much less than in the previous monzogranites, with some examples being essentially devoid of albite exsolution lamellae. Biotite occurs as well-formed, medium-sized crystals with abundant zircon inclusions. Muscovite occurs both as medium- to coarse-grained, subhedral flakes and as fine-grained alteration of plagioclase.

Accessory minerals consist of monazite (SEM identification, Chapter 5), zircon, apatite, chlorite, rutile and opaque minerals. Monazite and zircon occur as inclusions in biotite while chlorite, rutile and opaques are associated with post-crystallization alteration of biotite. Apatite forms euhedral inclusions in biotite, and as interstitial fillings between other minerals (Plate 4-1).

4.2.4 Leucogranite and pegmatite

Minor intrusions and dykes of fine- to medium-grained leucogranite intrude all of the monzogranites of the Larrys River Pluton. These minor intrusions are often intimately associated with small pegmatitic segregations and occur most often close to metasedimentary contacts. Only one of these composite intrusions is large enough to show on Figure 3-1 (located in the Fougere Lake contact zone FLCZ).

This muscovite-bearing leucogranite is cream-colored and fine- to medium-grained. Biotite occurs in minor amounts in some samples as irregular wisps and patches. Where present the inhomogeneity of the micas gives the rocks a layered appearance. Zones of quartz veins with associated greisens are often present but are barren of significant concentrations of economic minerals.

The rock has an allotriomorphic granular texture of quartz, albitic plagioclase (An_{10}, optical determination), orthoclase and muscovite with albite twice as abundant as orthoclase. The orthoclase forms fine- to medium-grained, poikilitic non-perthitic anhedra. Muscovite occurs as medium-sized, subhedral flakes.

Apatite, biotite, zircon and garnet occur in accessory amounts. Biotite, where present, has zircon inclusions with pleochroic haloes.

The pegmatites are blocky, poorly-zoned intergrowths of quartz, perthitic orthoclase and large books of muscovite. No exotic minerals were observed except for one pegmatite boulder containing a large (2 x 5 cm), euhedral beryl crystal found in a glacial till cut west of Fougere Lake. The till is likely of very local provenance as it has a

minor component of metasedimentary clasts even though metasediments underlie the area a short distance to the north.

4.2.5 Deformation

In outcrop the Larrys River Pluton does not show any effects of the major, east-west trending shear zone which traverses the northern region of the study area (Fig. 3-2). However, in thin section the biotite-muscovite and northern region of the transitional monzogranite have definite deformational textures including quartz with moderate to strong undulatory extinction and sub-grain development, quartz and feldspar with sutured boundaries, and plagioclase with bent polysynthetic twin lamellae (Plate 4-2).

The presence of microcline in these rocks also suggests some deformation. Montoto (1973) concluded an inversion of orthoclase to microcline is a subtle indication of deformation of a previously crystallized granite. Although such an inversion can result from a variety of other factors, its coincidence with the other deformational textures is consistent with shearing related to the Lundy shear zone.

4.3 SANGSTER LAKE PLUTON

4.3.1 Two-mica monzogranite

The Sangster Lake Pluton consists almost entirely of a two-mica monzogranite (Fig. 3-1). Since a prime aim of this thesis is to examine the petrological and geochemical variation within a granite of anomalous and variable radiometric response, the pluton is subdivided

Plate 4-1 Photomicrograph of euhedral apatite (Ap) accompanying biotite (B) in the biotite-muscovite monzogranite of the Larrys River Pluton. Scale = 0.5 mm.

Plate 4-2 Photomicrograph from the transitional monzogranite of the Larrys River Pluton showing plagioclase (P) with bent polysynthetic twins. Scale = 0.5 mm.

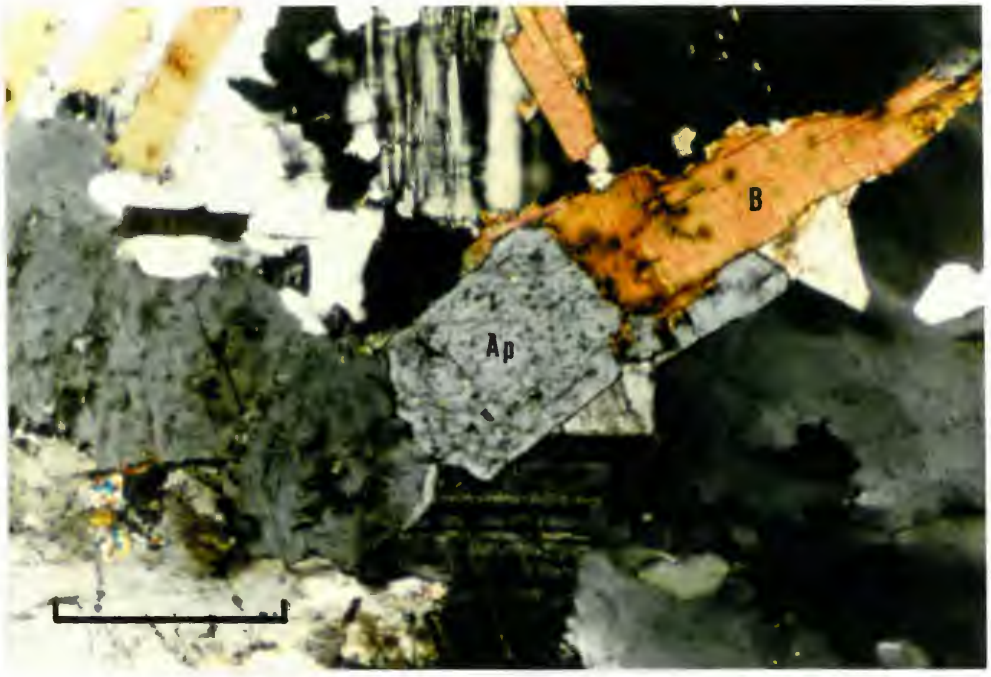

Plate 4-1

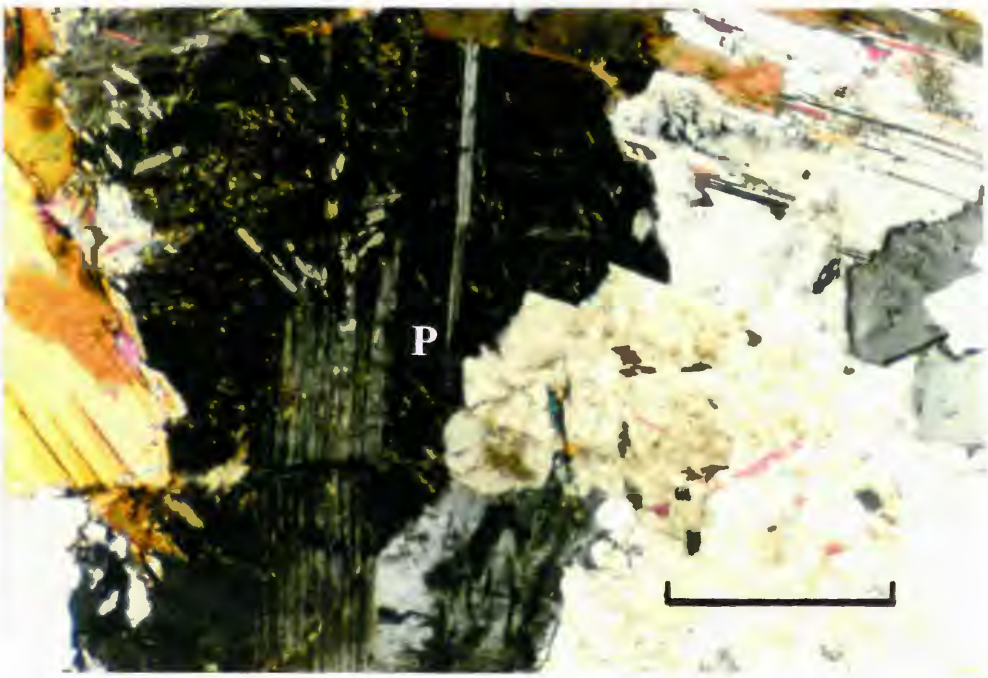

Plate 4-2

according to airborne radiometric response into three units: average-response monzogranite, central monzogranite and high-response monzogranite (Fig. 3-4). The average-response monzogranite has an average radiometric response, similar to that over the Larrys River Pluton (2-3 eU ppm). The central monzogranite has a radiometric response elevated by 2 to 3 times that over the average-response monzogranite, and the high-response monzogranite category is a suite of samples from across the area of highest radiometric response in the pluton (5-6.6 eU ppm; Fig. 3-4).

4.3.1.1 Average-response monzogranite

The average-response monzogranite underlies the portion of the pluton west of Eastern Fork Stream (Fig. 3-1). The rock is a coarse-grained, hypidiomorphic to allotriomorphic granular, non-megacrystic monzogranite. Major minerals are quartz, microcline, plagioclase, muscovite and biotite (Table 4-1). Microcline forms large, anhedral, perthitic (interpenetrating), poikilitic crystals which, in a few samples, is altered to muscovite. Plagioclase (An_{20-24}, microprobe analysis, Chapter 5) forms subhedral elongate laths which are, in general, normally zoned although some examples of patchy and oscillatory zoning are present. The calcic cores, and less so the sodic rims, are altered to sericite.

Muscovite is of at least two textural types: (A) large subhedral flakes distributed throughout the groundmass and (B) clearly secondary small flakes occurring as inclusions in plagioclase and mantles on microcline and biotite.

Biotite contains accessory monazite, zircon and apatite inclusions and is, in some instances, partly altered to muscovite, chlorite, rutile and Fe-oxide.

4.3.1.2 Central monzogranite

The central monzogranite underlies the central and northern regions of the pluton (Fig. 3-4) and has a major mineral assemblage of quartz, plagioclase, microcline, muscovite and biotite. Plagioclase is albite (microprobe identification, Chapter 5) and highly altered to fine-grained muscovite (Plate 4-3). This secondary muscovite, and coarse-grained muscovite occurring as discrete flakes in the groundmass and as alteration of biotite, results in these rocks having greater than 13% modal muscovite (the fine-grained secondary muscovite is not included in Table 4-1).

Biotite occurs as discrete flakes in the groundmass. In most sections it is altered to muscovite, quartz and Fe-oxide.

Accessory minerals are apatite, zircon, monazite, opaques and garnet. Apatite has at least two modes of occurrence: (1) fine- to medium-grained euhedral crystals in the groundmass; and (2) minute subhedral to euhedral inclusions within albite (Plate 4-4). The muscovite and apatite alteration shown in Plate 4-4 imparts a "dirty" appearance to the albite crystals.

Zircon, monazite and opaques are associated with biotite. An occurrence of zircon within muscovite is likely the result of muscovite pseudomorphing biotite. Garnet occurs as rare, small, euhedral, inclusion-free grains in the groundmass.

Plate 4-3 Photomicrograph from the central monzogranite showing albite (An_{5-10}) altered extensively to titanium-poor muscovite. Scale = 1.0 mm.

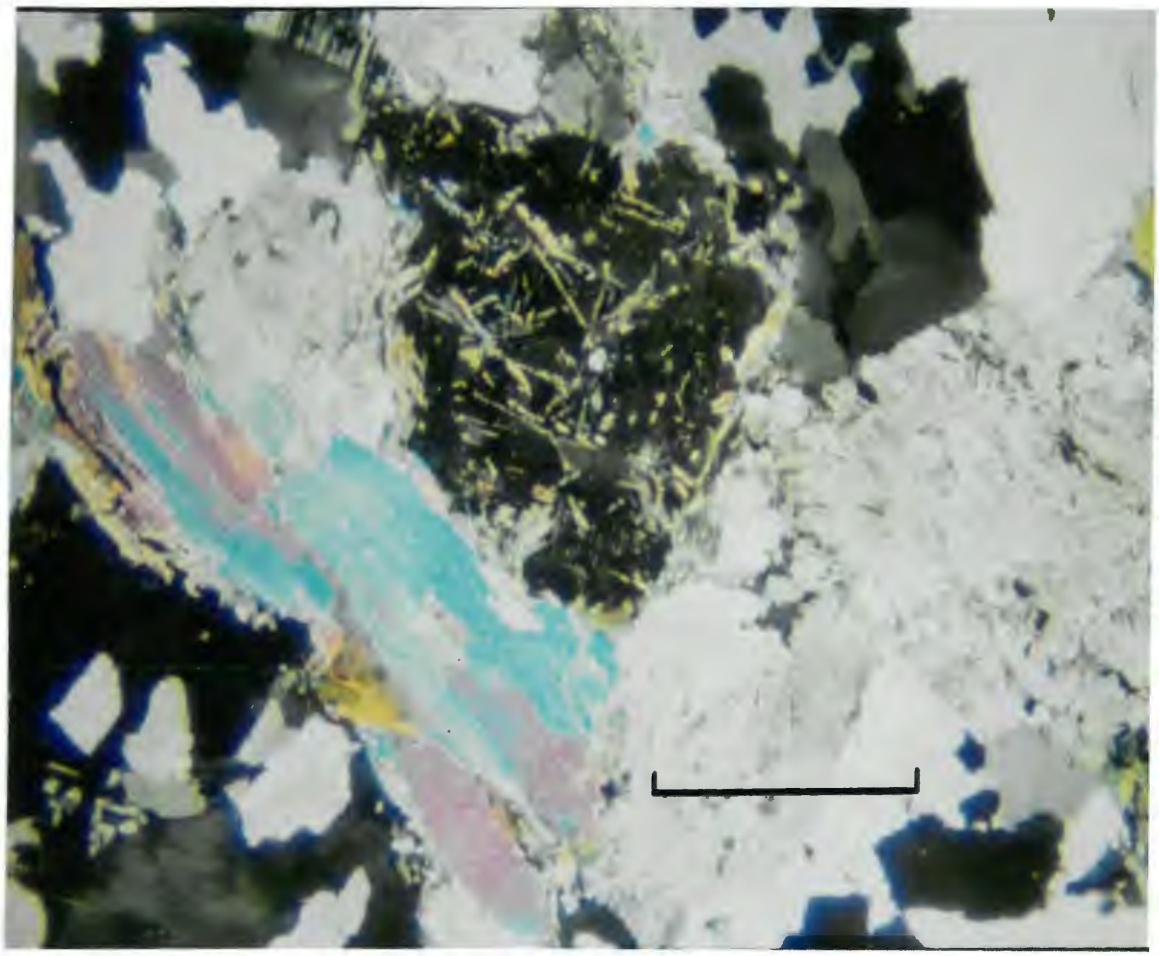

Plate 4-3

Plate 4-4 Photomicrograph from the central monzogranite showing albite altered to secondary muscovite (m) and apatite (a). Scale = 0.1 mm.

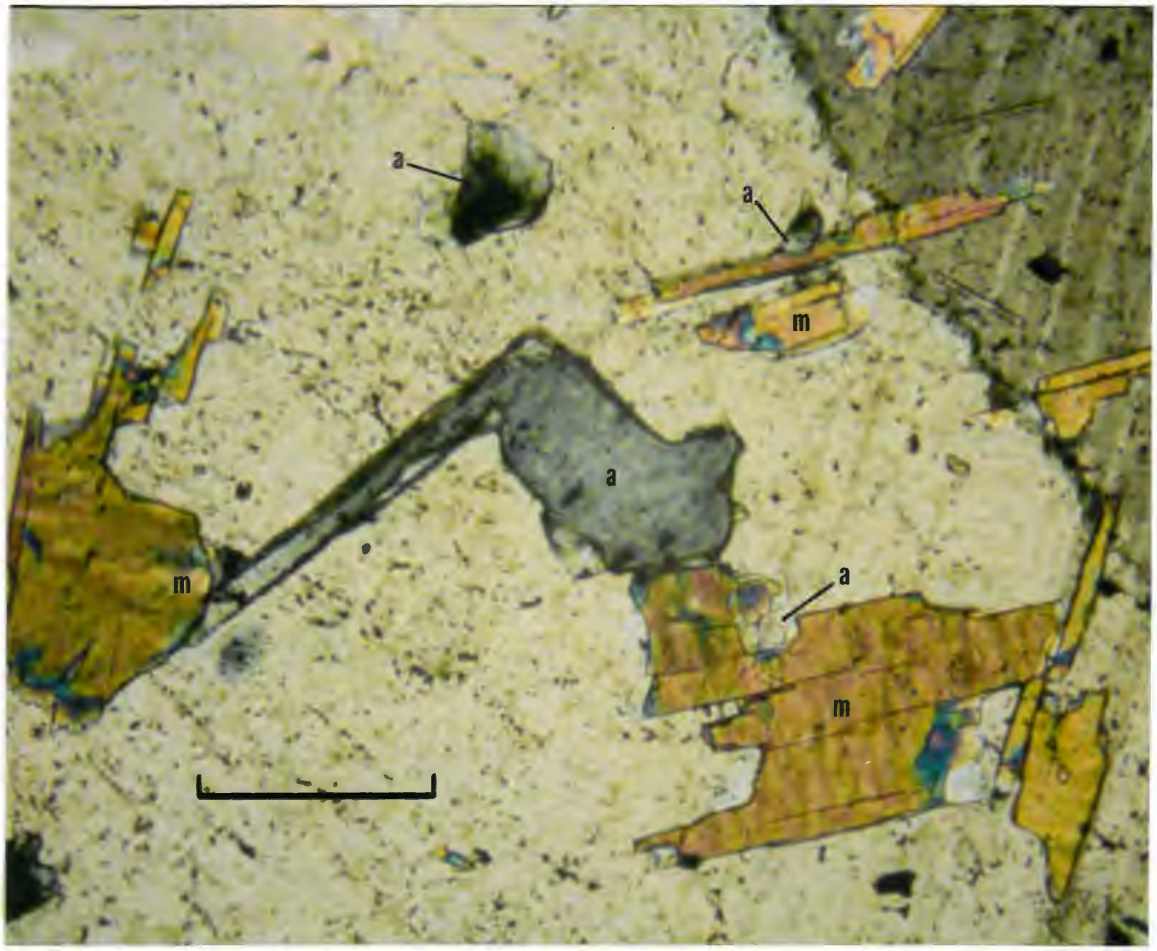

Plate 4-4

Modal abundances given in Figure 4-1 show that samples of the central monzogranite actually plot within the field of granodiorite. This not only conflicts with the muscovite-rich, highly-evolved appearance of these rocks but the abundance of secondary albite and extensive muscovite alteration indicate that the central monzogranite has clearly undergone sufficient fluid-rock alteration that it can no longer be considered a magmatic rock. The Streckeisen (1976) scheme was designed as a classification for "magmatic" rocks and should therefore not be strictly applied to highly-altered rocks. In addition, as is shown in the following chapter, these rocks have typically monzogranitic levels of most major elements (Fig. 6-3). For these reasons these rocks are called monzogranite for this study.

The relationship of microcline to the albite also suggests post-magmatic processes were important in formation of these rocks. Replacement textures shown in Plate 4-5 indicate that much of the microcline may be secondary after albite. The microcline has invaded along fractures within the albite and remnant patches of albite enclosed within the microcline have crystallographic continuity. The scalloped contact between the two minerals also indicates a reaction has occurred between them.

Replacement of secondary albite by microcline indicates that much, if not all of the K-feldspar is also secondary. If the central monzogranite, before secondary alteration, had modal proportions similar to the unaltered monzogranites the addition of secondary microcline would increase the proportion of K-feldspar. This is not the case as these rocks have less K-feldspar than the previously

Plate 4-5 Photomicrograph from the central monzogranite showing K-feldspar (Kf) replacing albite (Ab). Scale = 1.0 mm.

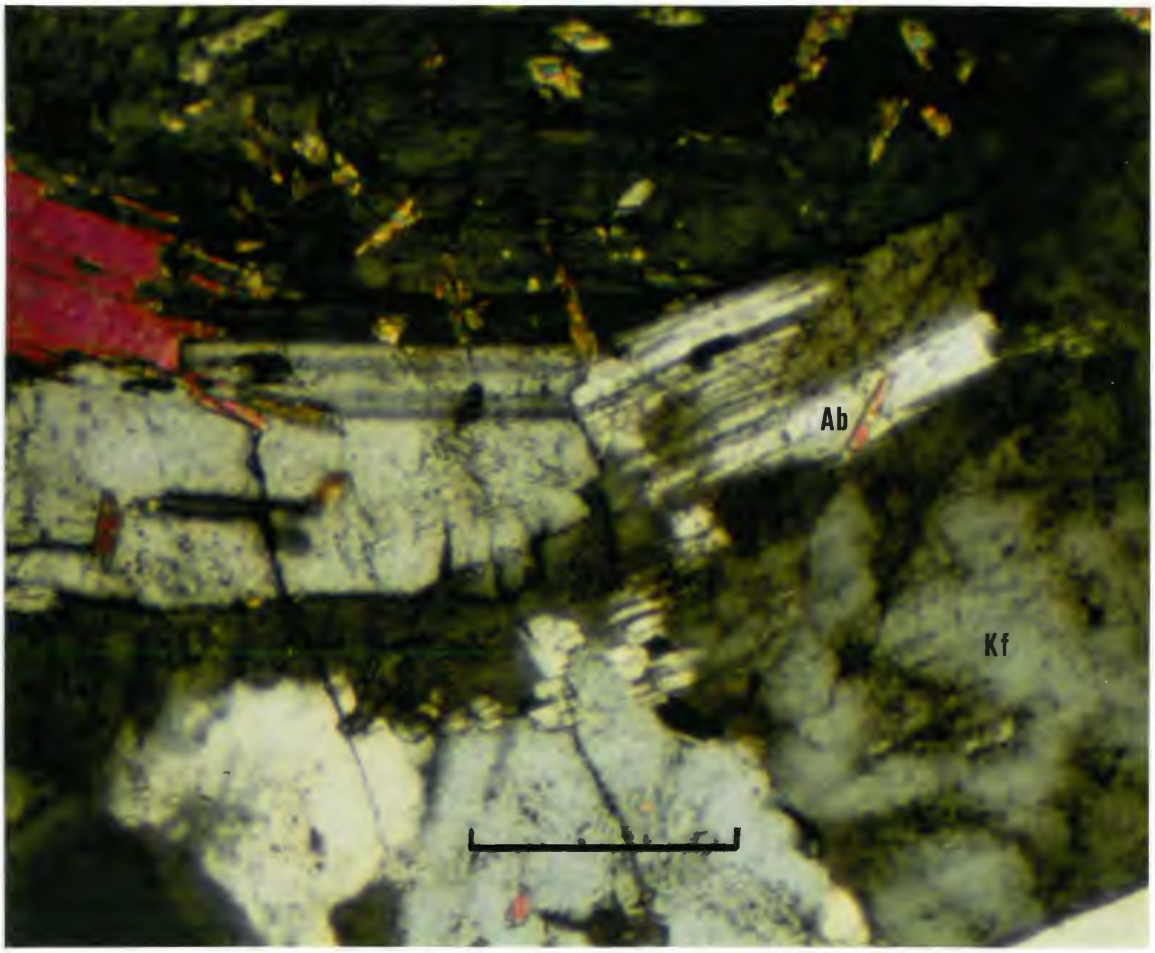

Plate 4-5

described monzogranites (Table 4-1). Possibly the central monzogranite had an original K-feldspar content that was much less than in the other monzogranites. Another interpretation is that the rocks originally had a comparable K-feldspar content but this was decreased prior to the formation of the secondary microcline. The Na-metasomatism (albitization of plagioclase) which affected the rocks prior to the microclinization may have obliterated some of the original K-feldspar. Unfortunately, there is no textural evidence to support either of these interpretations.

In any case, the modal percentages of K-feldspar do not reflect the original magmatic proportions and the low proportions of alkali feldspar on the QAP plot (Fig. 4-1) is actually a reflection of post-magmatic alteration.

4.3.1.3 High-response monzogranite

The high-response monzogranite occurs along the southern border of the pluton east of Cranberry Lake (Fig 3-1). The absence of glacial till assures that the anomalous radiometric response truly reflects the nature of the underlying granite.

The plagioclase is albite (An_{0-8}, microprobe identification, Chapter 5) and forms relatively unzoned, subhedral laths which are extensively altered to fine-grained muscovite and apatite (Plate 4-6). Microcline, as in the central monzogranite, forms anhedral, coarse-grained crystals which are unclouded and are secondary after albite. The muscovite also occurs as coarse-grained flakes within the groundmass and as alteration of biotite. Biotite occurs as chloritized flakes within the groundmass.

Accessory minerals include apatite, zircon, monazite, ilmenite and rutile. Apatite occurs as: (1) discrete subhedral-euhedral grains in the groundmass; (2) an alteration product forming inclusions within albite; and (3) associated with brown matted masses. The brown matted masses are of particular interest as K. L. Ford (pers. comm.), using autoradiograph and fission track methods, found that these masses are sites of increased radioactivity in these rocks. The masses are secondary and contain a texturally distinct apatite (Plate 4-7). Ford and Ballantyne (1983) identified a chlorine-bearing apatite and Fe-U-phosphate from a sample of the Sangster Lake Pluton. In the current study chloroapatite, Cl-bearing apatite and Fe-U-phosphate were identified in heavy mineral separates of samples of the high-response monzogranite (Chapter 5). These apatites are identical to the texturally distinct apatite associated with the brown masses (Plate 4-7). The association of Fe-U-phosphate with the brown masses suggests that the masses may be metamicts, the result of radioactive destruction of the crystal structure of an original unknown mineral.

Like the central monzogranite, the rocks of the high-response monzogranite are typically muscovite-bearing and monzogranitic in appearance although their modes plot within or near the granodiorite field on the QAP ternary plot (Fig. 4-1). They are called monzogranite with this study for the same reasons previously described for the central monzogranite. The textures observed within the central monzogranite which reflect fluid-rock alteration are even more distinctly developed in the high-response monzogranite.

Plate 4-6 Photomicrograph from the high-response monzogranite showing albite altered to fine-grained secondary muscovite (m) and apatite (a). Scale = 0.1 mm.

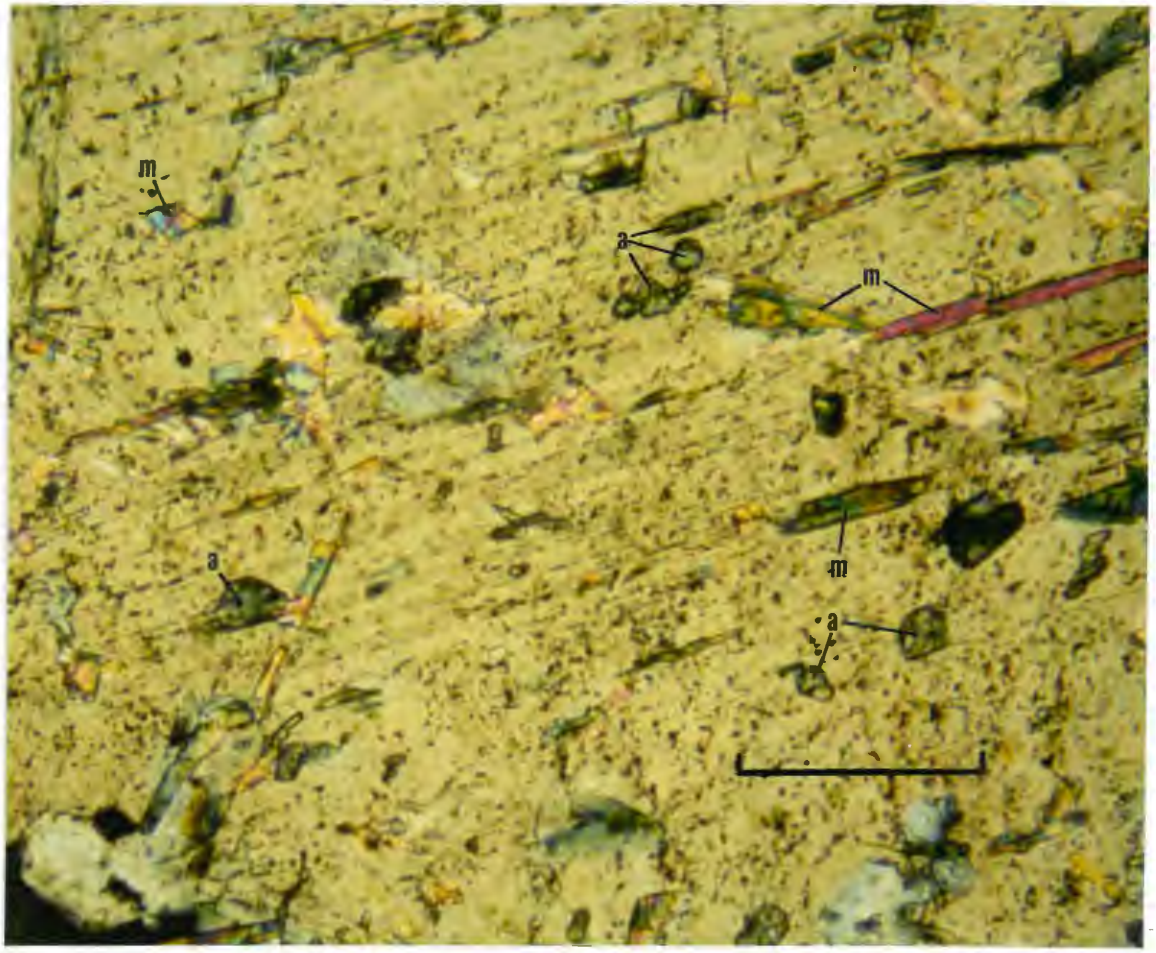

Plate 4-6

4.3.2 Beans Lake Leucomonzogranite and minor intrusions

Northeast of Sangster Lake, in the vicinity of Beans Lake, a small intrusion of muscovite-bearing leucomonzogranite forms a plug approximately 1 km^2 in area (Fig. 4-2). This plug is here named the Beans Lake Leucomonzogranite and is the only intrusion of this rock type large enough to be indicated on Figure 3-1. Smaller intrusions and dykes of leucomonzogranite and leucogranite intrude the pluton, especially close to country rock contacts.

The leucomonzogranite is cream- to buff-colored and varies from fine- to coarse-grained but most outcrops are medium grained. Texturally the rocks are allotriomorphic granular with a major mineral assemblage of quartz, plagioclase, orthoclase and muscovite. In only rare instances is biotite present. A sample of this rock type falls in the monzogranite field near the granodiorite boundary on QAP ternary plot (Fig. 4-1).

The plagioclase is albite (An_6, optical determination) and occurs as subhedral, unzoned laths with resorbed boundaries. There is secondary alteration to fine-grained white mica, but this texture is not as developed as in the central and high-response monzogranites. Orthoclase forms coarse- to medium-grained, anhedral crystals which display little or no twinning. Textures showing replacement of albite by quartz and orthoclase are particularly well-developed in these rocks (Plate 4-8). Both orthoclase and quartz have invaded the albite forming resorbed boundaries and remnant patches of albite in crystallographic continuity with the adjacent albite grains. Muscovite occurs both as medium- to coarse-grained books within the groundmass

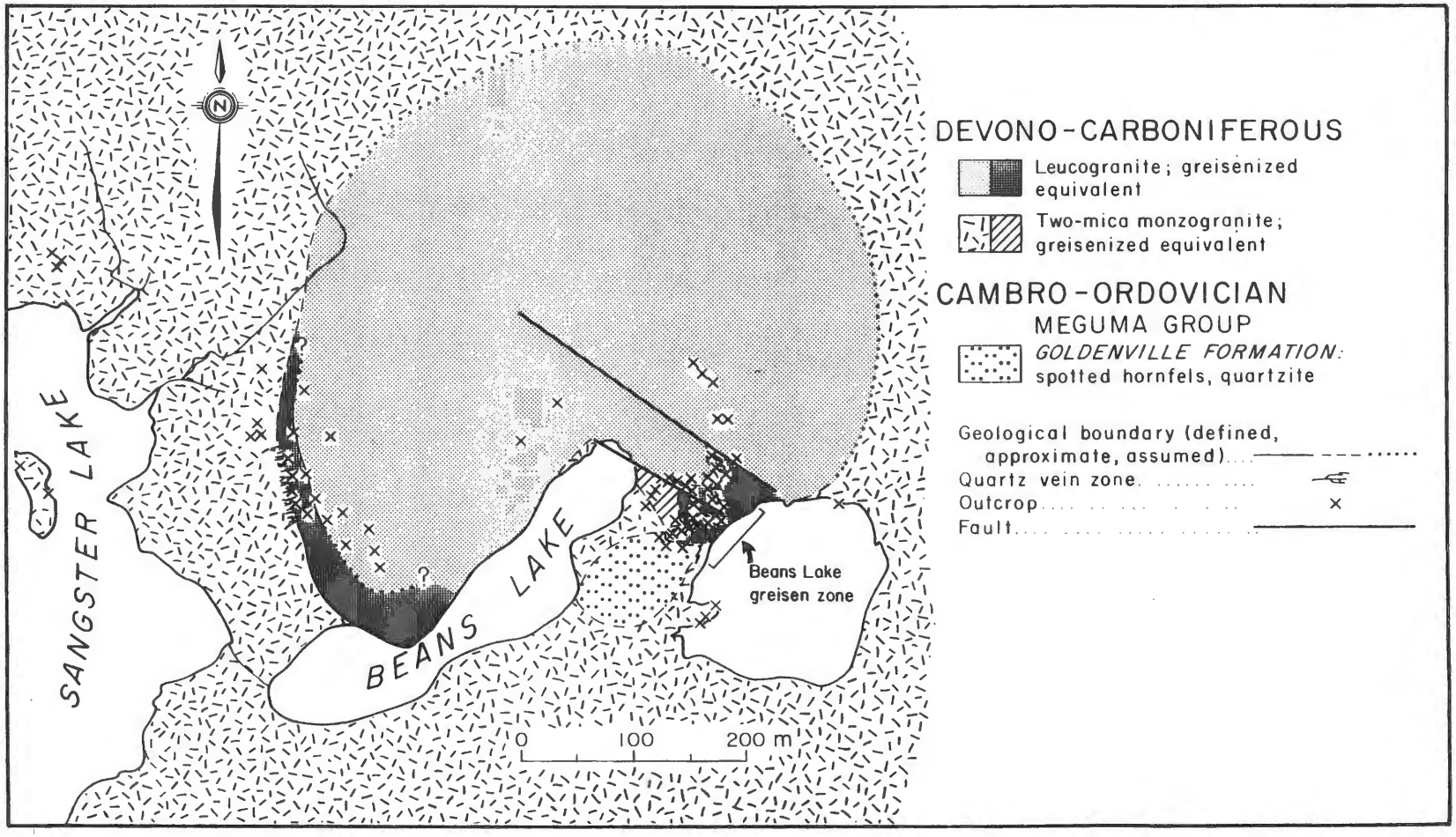

Figure 4-2 Geology of the Beans Lake Leucomonzogranite.

Plate 4-7 Photomicrograph from the high-response monzogranite showing a brown matted mass (metamict?) and associated texturally distinct chlorine-bearing apatite (Cl-Ap). Scale = 0.5 mm.

Plate 4-8 Photomicrograph from the Beans Lake Leucomonzogranite showing replacement of albite (A) by quartz (Q) and orthoclase (K). Scale = 0.5 mm.

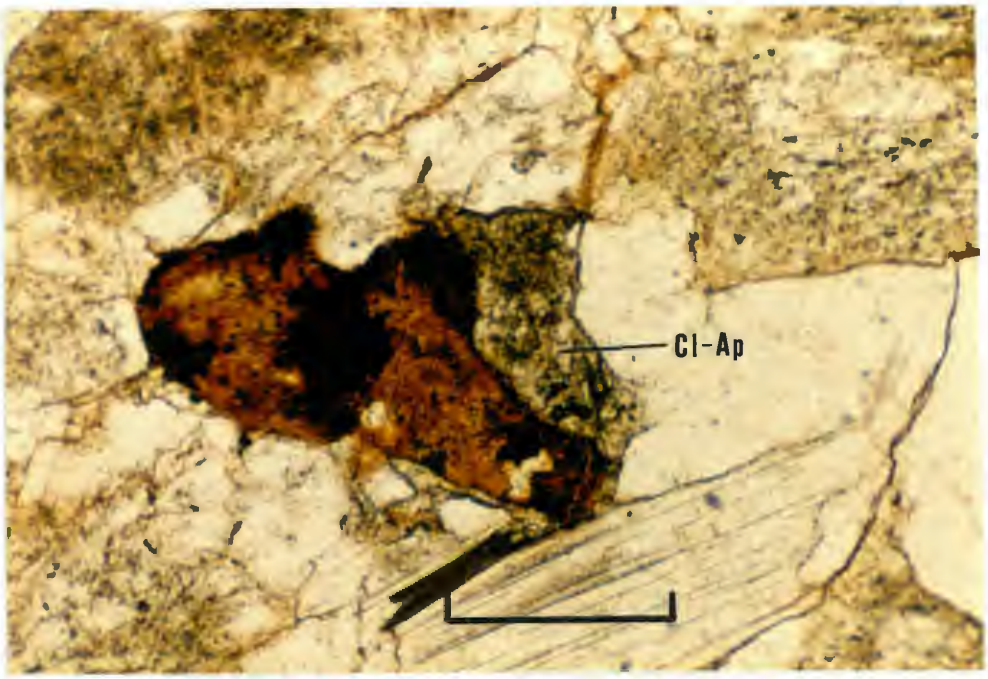

Plate 4-7

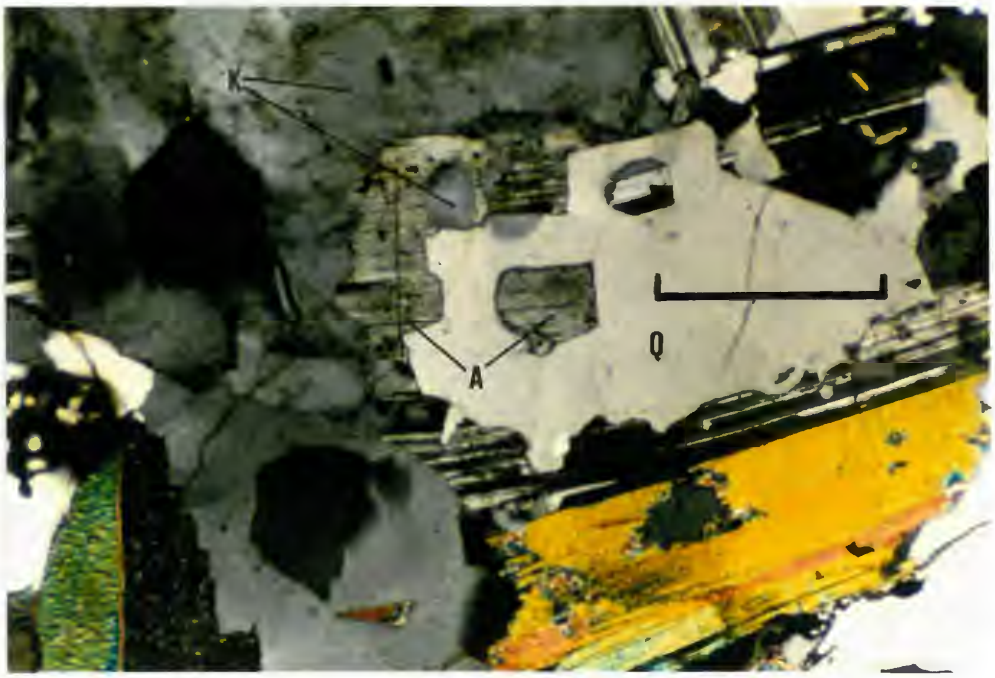

Plate 4-8

and as small flakes within albite. These textures suggest that much of this intrusion has undergone considerable fluid-rock interaction.

Accessory minerals include apatite, garnet, lepidolite and the brown masses (metamicts) with associated apatite previously described from the high-response monzogranite.

4.3.3 Beans Lake greisen zone

A contact zone of the Beans Lake Leucomonzogranite with the monzogranite is exposed near the northeast end of Beans Lake (the Beans Lake greisen zone; Fig. 4-2). Both the host monzogranite and the leucomonzogranite in this zone are extensively metasomatized. Within 30 m the outcrop grades from massive, coarse-grained monzogranite into medium- to coarse-grained, muscovite-rich leucomonzogranite. This transition is gradational, and striking considering the composition of the end members.

The metasomatized monzogranite host is texturally similar to the central monzogranite except for the presence of abundant (approximately 5-7%) euhedral to subhedral, inclusion-free, garnet crystals (Plate 4-9). The garnets are not associated with any particular mineral and occur as discrete grains and as inclusions in quartz and the feldspars. Near the leucomonzogranite the abundance of biotite decreases and muscovite increases. The overall effect of these changes results in the rock becoming leucomonzogranitic. The leucomonzogranite, although garnet-bearing, does not have the abundance of garnet observed in the adjacent metasomatized monzogranite. This suggests that the garnets are metasomatic and the result of interaction of a fluid phase with the

Plate 4-9 Photomicrograph from the metasomatized monzogranite from within the Beans Lake greisen zone showing abundant, subhedral, inclusion-free garnet crystals. Scale = 0.3 mm.

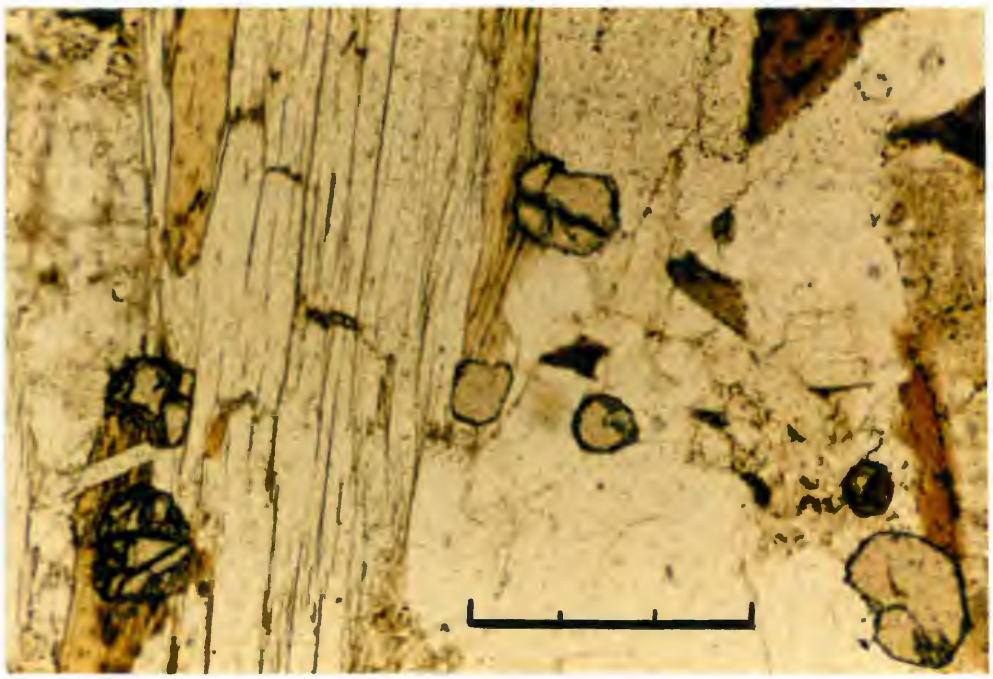

Plate 4-9

previously crystallized monzogranite. Such an alteration implies high temperatures similar to those described by Kontak and Corey (1988) for metasomatic garnet formation in the South Mountain Batholith. The high temperature alteration has apparently obliterated many of the original intrusive contact features and resulted in a gradational relation.

Greisen-bordered quartz veins (1-3 cm wide) overprint the entire contact zone, but for the most part, are confined to the leucomonzogranite. The swarms trend consistently between 110° and 130° Az. The veins are barren except for tourmaline clusters, but their greisenized borders contain tourmaline, garnet, greenish apatite and lepidolite. No concentrations of minerals of economic significance were observed.

A similar quartz vein swarm intrudes the contact of the Beans Lake Leucomonzogranite with monzogranite along a prominent ridge overlooking Sangster Lake (Fig. 4-2). At this location the actual contact is not exposed, but the existing outcrops indicate the swarm is located within the contact zone. The veins are up to 1 m wide but are essentially barren.

4.3.4 Deformation

In outcrop the average-response monzogranite is apparently undeformed but in thin section undulatory extinction of quartz and the presence of microcline suggest a small degree of deformation.

Deformation in the central monzogranite varies from faint to intense (Fig. 3-2). Subgrains, bent polysynthetic twin lamellae in albite, bent cleavage traces in muscovite, sutured grain boundaries, and c and s fabrics in all cases post-date the fluid-rock alteration textures described previously. The presence of secondary albite with

deformed twin lamellae is particularly useful for establishing the relationship of deformation and hydrothermal alteration. The fact the grains are albite and have lamellae that are bent indicates the process of albitization of the original plagioclase occurred prior to the deformation. These relationships indicate that pluton emplacement and subsequent hydrothermal alteration are both pre-deformational.

The rocks of the high-response monzogranite have only a very weak deformational fabric in the form of stretching and rodding of quartz and feldspar. The presence of slightly-deformed polysynthetic twins in the secondary albite and mica with bent cleavage traces suggest the hydrothermal alteration was pre- or syn-deformational.

The Beans Lake Leucomonzogranite and similar smaller intrusions are not deformed to the same degree as their enclosing monzogranite host. In many cases, outcrops of monzogranite with a moderately developed and obvious preferentially oriented fabric are intruded by leucomonzogranite which shows no fabric. However, in thin section deformational textures such as undulatory extinction of quartz, albite with slightly bent polysynthetic twins (Plate 4-8), and muscovite with bent cleavage traces are present. The difference in deformational intensity between the two is consistent with late-tectonic intrusion of the leucomonzogranite. The monzogranite must have been undergoing post-crystallization deformation prior to intrusion of the leuco-monzogranite, otherwise an explanation for the more strongly developed foliation in the monzogranite is difficult to explain. If this reasoning is correct, the leucomonzogranite was intruded during the later or waning stages of this episode of deformation.

Shear-related deformation affected the alteration mineral phases in the Beans Lake greisen zone. In the well-developed greisen borders of the quartz vein swarms, the micas have a preferred orientation. The fabric orientation coincides with that observed in the monzogranite. The leucomonzogranite away from the greisen-bordered vein systems does not have the same intensity of fabric development. In fact, many of the leucomonzogranite outcrops appear to be undeformed and it is only in thin section that mild deformational textures are recognizable.

This relationship may be interpreted in two ways. First, the more pronounced foliation within the greisens may reflect of the increased amount of mica within the greisens. The micaceous greisens were more susceptible to deformation. Alternatively, emplacement of the leucomonzogranite occurred during the waning stages of the shear deformation which, by that time, had already deformed the enclosing monzogranite. Conceivably, by the time the leucomonzogranite had crystallized, the deformation had decreased to a level such that only the more ductile greisens took on a strong preferred orientation. This assumes that the hydrothermal fluids which formed the vein swarms and greisens are related to the latest stages of evolution of the leucomonzogranite. The observed field relations and radiometric age data (Table 3-1) support both interpretations.

4.4 SUMMARY

1. The Larrys River Pluton consists predominantly of a megacrystic biotite monzogranite. Toward the east the monzogranite grades into a less megacrystic, transitional monzogranite which in turn

grades into a massive biotite-muscovite monzogranite. This sequence represents a trend towards more evolved rocks. Small intrusions and dykes of leucogranite and pegmatite intrude the monzogranites near the contacts with the Meguma Group country rocks.

2. In outcrop the Larrys River Pluton appears to be undeformed. In thin section subtle deformational textures indicate the north-eastern region of the pluton is mildly deformed.

3. The Sangster Lake Pluton consists almost entirely of coarse-grained, two-mica monzogranite. Variations in the airborne gamma-ray spectrometric data over the pluton correspond to textural and mineralogical changes within the pluton related to fluid-rock interaction. The western region of the pluton has average radiometric response and is characterized by a typical magmatic mineral assemblage and appearance. The eastern region of the pluton has anomalous radiometric response. This corresponds to increasing intensity of features indicative of hydrothermal alteration such as: (1) the presence of secondary albite and microcline (2) secondary alteration of albite to fine-grained muscovite and apatite and (3) formation of secondary Cl-bearing apatite and Fe-U-phosphate.

4. The Sangster Lake Pluton hosts a small intrusion of leuco-monzogranite, the Beans Lake Leucomonzogranite. The contact zone

of this minor intrusion has undergone considerable metasomatism as the result of interaction of the rocks with a fluid phase which probably emanated from the leucomonzogranite. The quartz vein swarms and greisens are associated with this alteration.

5. A deformational fabric overprints all granitoid rocks of the Sangster Lake Pluton. The fabric is most intense along the northern border, but some degree of deformation persists throughout most of the central and eastern region of the pluton. The Beans Lake Leucomonzogranite appears to be devoid of this fabric, but in thin section mild deformational features are recognizable. Micaceous greisen zones associated with the leucomonzogranite distinctly reflect the deformational fabric. The fact that the leucomonzogranite is only mildly deformed while associated greisens have a pronounced fabric suggests either: (a) the intrusion was emplaced during the waning stages of the deformational episode; or (b) the more micaceous greisens behaved in a ductile manner and took on a more pronounced foliation.

CHAPTER 5

MINERAL CHEMISTRY

5.1 INTRODUCTION

The field evidence and petrographic and textural criteria in the previous chapter show that some of the rocks of the thesis area have undergone post-crystallization hydrothermal alteration. The increased intensity of the alteration in regions of anomalous airborne gamma-ray spectrometric response is also highlighted. Such widespread alteration processes must have had an impact on the primary mineralogy of the rocks. This chapter examines the chemistry of the major, minor and trace minerals.

5.1.1 Methods

Polished thin sections were prepared from samples of the various rock types and classes described in Chapter 4. Plagioclase and muscovite were analysed at Dalhousie University using the energy dispersive system of a Cambridge Mark V electron microprobe. Potassium feldspar and apatite were analysed using the wavelength dispersive system of a JEOL 733 electron microprobe also at Dalhousie.

Representative samples were crushed and heavy minerals were separated from the fine sand-sized fraction using s-tetra-bromoethane (S.G. 2.95). The heavy mineral separates were examined using a Cambridge S4-10 SEM (scanning electron microscope) at the University of New Brunswick, Fredericton. The SEM is equipped with a Tracor Northern

NS-880 EDS (energy dispersive system) and backscatter detector, operated at 20 kV.

5.2 PLAGIOCLASE

The composition of the plagioclase within each of the rock groupings is given in Table 5-1. The analyses are averages of between 3 and 5 spots on each crystal. A plot of Or-Ab-An proportions of the groupings is given in Figure 5-1. The data field for plagioclases from monzogranites of the South Mountain and Musquodoboit Batholiths from Logothetis (1984) and MacDonald (1981) are included for comparison.

The transitional and average-response monzogranites have plagioclase compositions comparable with those from the South Mountain and Musquodoboit Batholiths. The optical normal zoning is confirmed and typically magmatic, subhedral, clear oligoclase laths (Ab_{85-90}) have albitic rims (Ab_{89-95})(Plate 5-1).

The plagioclases from the central monzogranite differ in that they have a higher Ab content (Ab_{92-99}) and display little or no zonation. The high-response monzogranite has plagioclases which are essentially unzoned and even more albitic in composition (Ab_{98-100}). The data show a definite soda enrichment or albitization trend in plagioclases which correlates with increased airborne gamma-ray response and increased intensity of alteration.

The plagioclases from the central and high-response monzogranites are typically unzoned and markedly albitic in composition. Albite-bearing granitoids can crystallize by magmatic processes if certain conditions are met (Manning, 1981; Pollard, 1983; London, 1987). To

Table 5-1 Geochemical analyses of plagioclases from the Sangster Lake and Larrys River Plutons.

ROCK TYPE	HIGH RESPONSE MONZOGRANITE															
SAMPLE #	F-G001	F-G001	F-G001	F-G001	F-G001	F-G001	F-G001	F-G001	F-G001	F-G001	F-G003	F-G003	F-G003	F-G003	F-G003	F-G003
SiO_2	69.02	69.05	68.62	68.27	68.98	69.00	68.87	68.33	68.50	68.83	68.58	66.87	68.60	68.31	68.67	68.53
TiO_2	0.00	0.00	0.00	0.00	0.00	0.04	0.00	0.10	0.04	0.08	0.00	0.00	0.00	0.00	0.00	0.00
Al_2O_3	19.66	19.54	19.36	19.23	19.60	19.49	19.45	19.24	19.37	19.44	19.43	20.59	19.63	19.80	19.47	19.30
FeO	0.03	0.00	0.00	0.00	0.00	0.03	0.06	0.00	0.14	0.15	0.02	0.00	0.00	0.00	0.00	0.00
CaO	0.03	0.04	0.06	0.07	0.00	0.00	0.00	0.00	0.00	0.00	0.03	0.78	0.05	0.10	0.07	0.00
Na_2O	11.68	11.61	11.74	11.56	11.50	11.57	11.91	11.70	11.51	11.64	11.50	10.94	11.33	11.26	11.44	11.35
K_2O	0.17	0.20	0.18	0.38	0.08	0.19	0.00	0.17	0.23	0.18	0.20	0.13	0.10	0.10	0.11	0.11
TOTAL	100.59	100.44	99.96	99.51	100.16	100.39	100.29	99.54	99.79	100.32	99.76	99.31	99.71	99.57	99.76	99.29
Or	0.92	1.14	0.98	2.11	0.46	1.04	0.00	0.95	1.27	1.01	1.13	0.74	0.57	0.57	0.64	0.65
Ab	98.96	98.66	98.76	97.56	99.54	98.96	100.00	99.05	98.73	98.99	98.66	95.50	99.20	98.94	99.03	99.36
An	0.12	0.20	0.28	0.33	0.00	0.00	0.00	0.00	0.00	0.00	0.20	3.76	0.23	0.49	0.33	0.00

ROCK TYPE	CENTRAL MONZOGRANITE														AVG RESP MONZ	
SAMPLE #	SL-13	SL-13	SL-13	SL-11	SL-11	SL-11	SL-11	SL-11	SL-13		SL-11		SL-11		SL-7	
									CORE	RIM	CORE	RIM	CORE	RIM	CORE	RIM
SiO_2	66.16	67.89	66.86	67.49	67.41	67.47	68.52	67.84	66.63	68.20	66.76	66.62	67.13	68.45	64.51	66.57
TiO_2	0.00	0.00	0.02	0.00	0.00	0.00	0.10	0.00	0.00	0.00	0.00	0.00	0.00	0.00	0.02	0.00
Al_2O_3	20.67	19.28	20.22	19.98	19.84	20.43	19.79	19.75	20.32	19.36	20.86	20.87	20.99	19.53	21.31	20.26
FeO	0.04	0.04	0.05	0.04	0.00	0.10	0.00	0.02	0.01	0.04	0.06	0.03	0.00	0.04	0.02	0.00
CaO	1.24	0.06	0.71	0.82	0.53	0.98	0.38	0.34	0.90	0.05	1.26	1.11	1.39	0.30	2.34	0.82
Na_2O	10.69	11.49	11.15	10.96	11.15	11.03	11.20	11.23	11.03	11.72	10.79	10.97	10.82	11.48	9.96	11.23
K_2O	0.22	0.02	0.22	0.18	0.10	0.19	0.20	0.10	0.20	0.19	0.22	0.25	0.29	0.10	0.23	0.09
TOTAL	99.02	98.96	99.23	99.47	99.03	100.20	100.12	99.28	99.09	99.56	99.95	99.85	100.62	99.90	98.39	98.97
Or	1.23	1.10	1.22	1.00	0.55	1.07	1.14	0.55	1.15	1.05	1.22	1.40	1.59	0.53	1.34	0.50
Ab	92.84	98.64	95.42	95.09	96.89	94.30	97.04	97.81	94.57	98.71	92.82	93.37	91.88	98.05	87.35	95.64
An	5.93	0.26	3.36	3.91	2.56	4.63	1.82	1.64	4.28	0.23	5.97	5.23	6.53	1.42	11.34	3.86

ROCK TYPE	AVERAGE RESPONSE MONZOGRANITE						TRANSITIONAL MONZOGRANITE							
SAMPLE #	SL-7		F-G018		F-G018		LR-5		LR-5		LR-5		LR-5	
	CORE	RIM	CORE	RIM	CORE	RIM	CORE	RIM	CORE	RIM	CORE	RIM	CORE	RIM
SiO_2	66.40	67.00	65.67	68.54	65.34	66.63	64.85	65.76	64.89	65.56	64.87	66.15	65.81	67.53
TiO_2	0.00	0.00	0.00	0.00	0.00	0.00	0.00	0.00	0.00	0.00	0.00	0.00	0.00	0.00
Al_2O_3	20.71	19.94	21.61	20.06	21.98	20.69	21.60	21.59	21.83	21.28	21.60	20.54	20.81	19.58
FeO	0.04	0.00	0.02	0.00	0.00	0.00	0.00	0.00	0.00	0.00	0.00	0.00	0.00	0.00
CaO	1.26	0.52	2.32	0.30	2.83	1.27	2.59	2.25	2.79	2.12	2.66	1.81	1.58	0.49
Na_2O	10.81	11.20	9.92	11.47	9.81	10.42	10.21	10.55	10.29	10.60	10.38	10.77	10.95	11.37
K_2O	0.16	0.17	0.17	0.16	0.21	0.09	0.21	0.19	0.20	0.16	0.20	0.13	0.17	0.22
TOTAL	99.38	98.83	99.71	100.53	100.17	99.10	99.46	100.36	100.00	99.72	99.71	99.40	99.32	99.19
Or	0.91	0.96	0.98	0.88	1.20	0.52	1.18	1.03	1.10	0.86	1.09	0.71	0.95	1.20
Ab	93.12	96.58	87.67	97.70	85.20	93.20	86.69	88.56	85.95	89.27	86.62	90.87	91.73	96.53
An	5.98	2.45	11.34	1.42	0.14	0.06	12.12	10.42	12.95	9.88	12.29	8.42	7.32	2.27

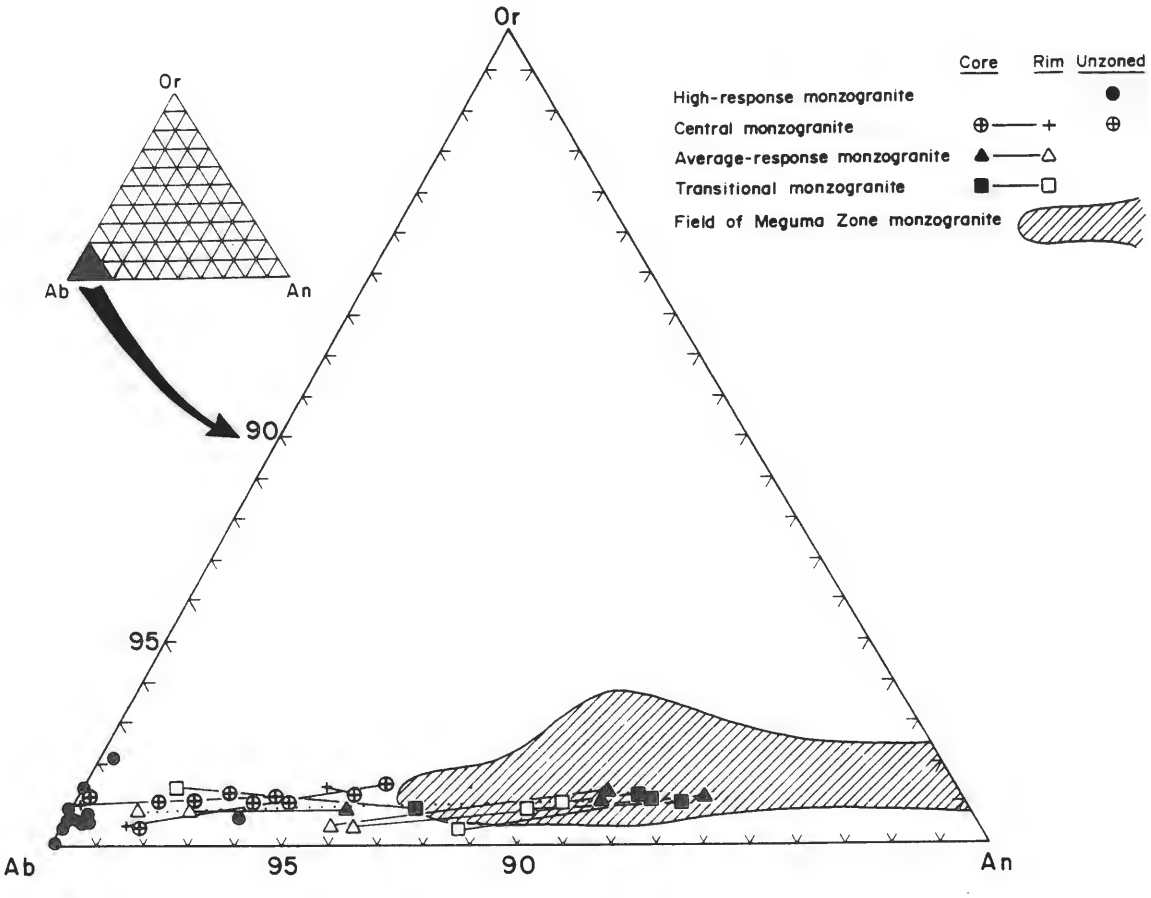

Figure 5-1 Ternary plot of Or-Ab-An proportions of plagioclases from samples of the Sangster Lake and Larrys River Plutons. Data from the South Mountain and Musquodoboit Batholiths are from MacDonald (1981) and Logothetis (1984).

Plate 5-1 Zoned, unaltered plagioclase (An_{15-20}) from the average-response monzogranite of the Sangster Lake Pluton. Scale = 1mm.

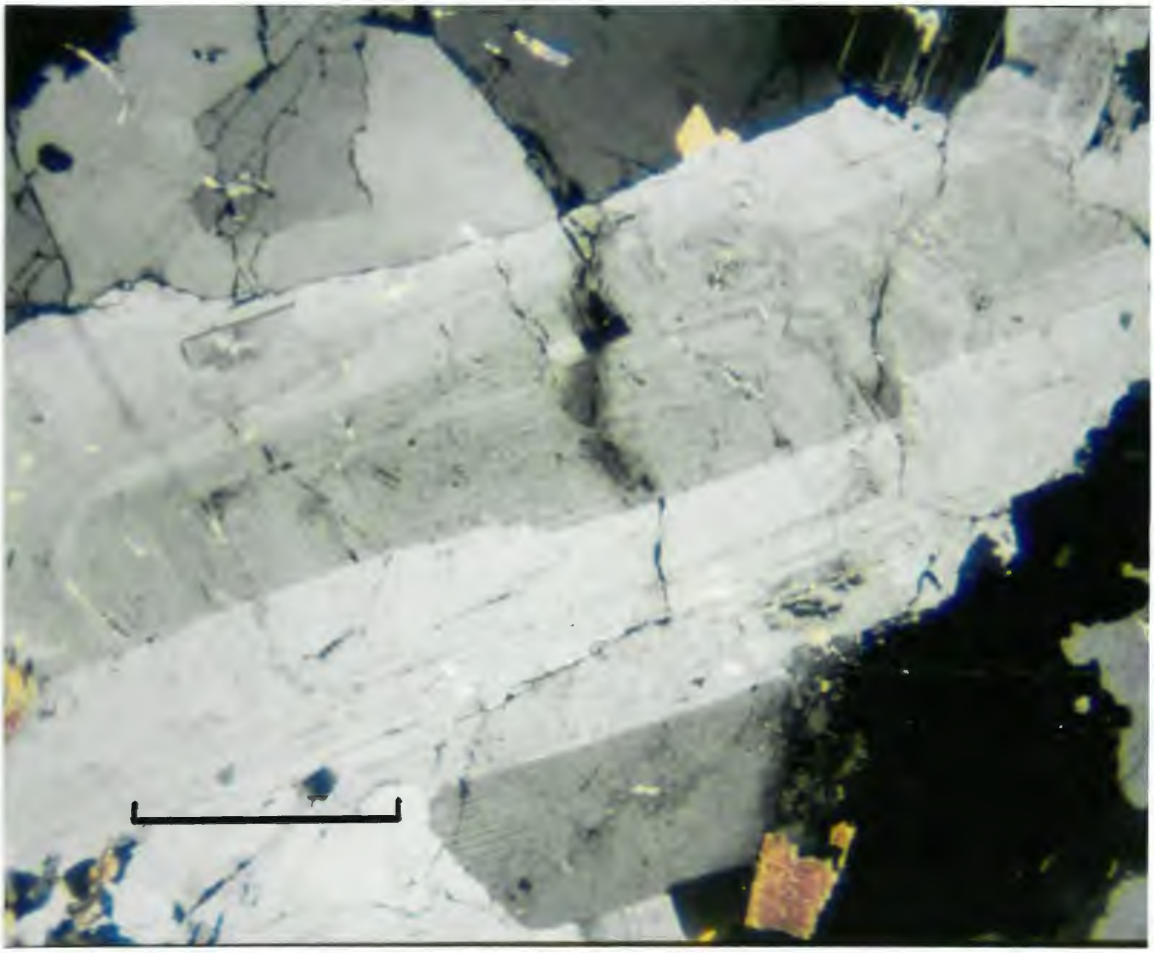

Plate 5-1

crystallize albite from a magma, greatest importance lies with the role of the volatile components (F, B, H_2O) and anions such as P during the late stages of differentiation of a water-saturated magma. The overall effect of enrichment of these elements is to lower the temperature of the granite minimum, thus allowing continued magmatic crystallization to temperatures in the order of 550-600 ^{o}C and to shift the granite minimum toward the Ab apex in the Qz-Ab-Or system, thus permitting crystallization of progressively more albitic plagioclase (Manning, 1981). The Manning (1981) study deals solely with the water-saturated Qz-Ab-Or system. The influence of an An component is not addressed. This limits application of these experimentally derived results in evaluating the influence of volatiles on naturally occurring granite systems.

Hence, albite-bearing granitoids and albitites can be produced by magmatic processes only under certain extreme situations of volatile enrichment. Such melts are not common and give rise to granitoid rocks with peculiar textures and mineralogy. None of these features is evident in the hydrothermally altered rocks in the Sangster Lake Pluton which are typically monzogranitic in appearance. These criteria indicate that the albite in the altered monzogranites and the leuco-monzogranite is of secondary origin.

5.3 POTASSIUM FELDSPAR

The potassium feldspar (K-feldspar) occurs as: (A) large sub-hedral-euhedral megacrysts, (B) small anhedral grains in the groundmass and (C) secondary replacement of albite. They are generally perthitic,

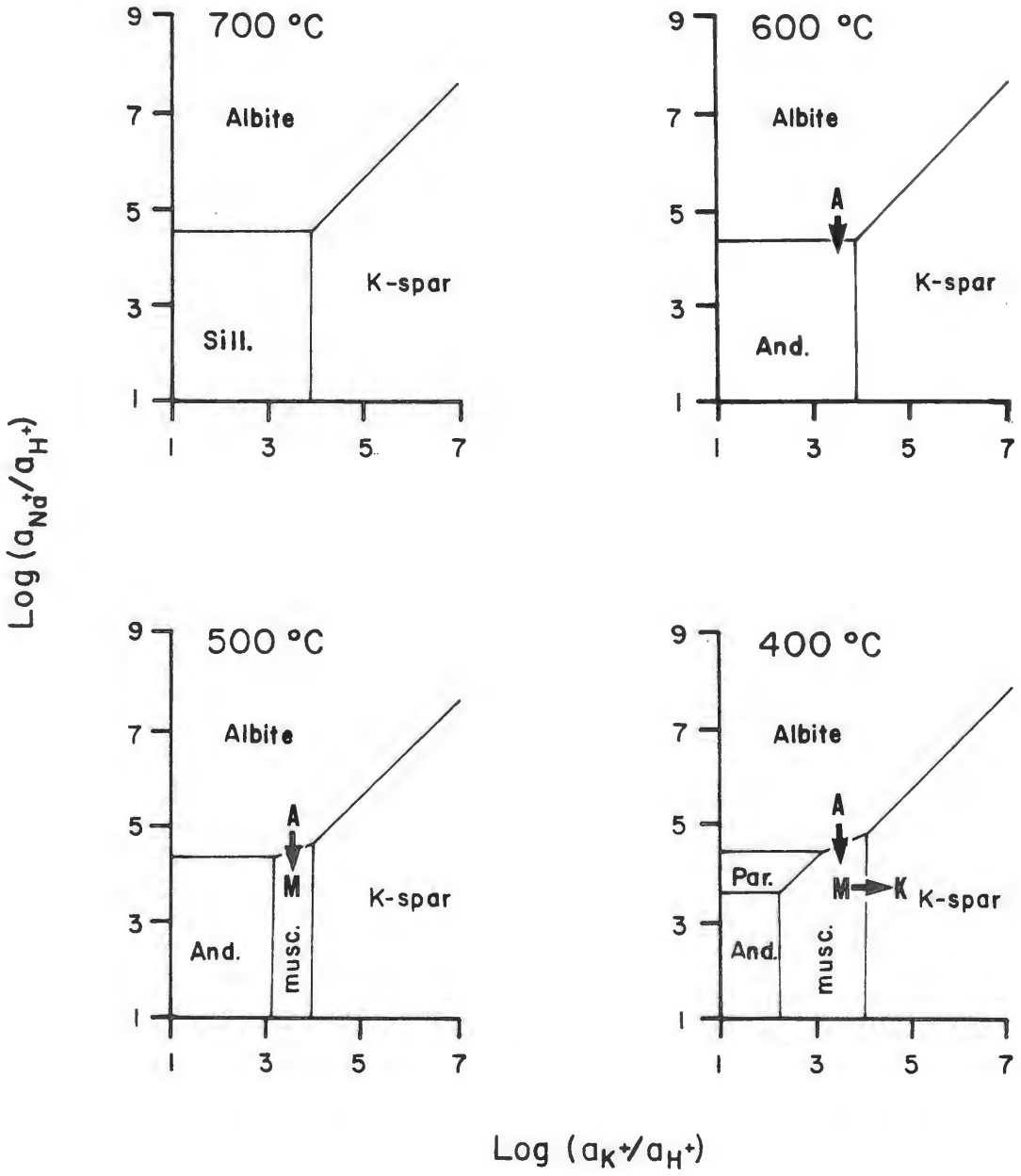

Figure 5-2 Logarithmic activity diagrams for the system Na_2O-K_2O-Al_2O_3-SiO_2-H_2O-HCl in the presence of quartz at 2kb and temperatures 400° to 700°C (from Helgeson, 1985). Trend A-M-K is discussed in text. And = andalusite; musc = muscovite; Sill = sillimanite; Par = paragonite

twinned and poorly zoned. The K-feldspars in all the monzogranites except the central and high-response monzogranite and the leuco-monzogranite appear to be typically magmatic in that they are in apparent equilibrium with the major rock-forming minerals.

K-feldspar in the central and high-response monzogranites has replaced albite (Plate 4-5). This replacement texture is particularly well developed in the Beans Lake Leucomonzogranite (Plate 4-8). Since the formation of the albite is probably post-magmatic (see previous discussion on plagioclase compositions) the replacement of the albite by K-feldspar dictates the K-feldspar is also the result of post-magmatic alteration.

The observed textures require that the hydrothermal fluid change its behavior to dominantly potassic. Experimental studies in the system Na_2O-K_2O-Al_2O_3-SiO_2-H_2O-HCl show that in the 700-400°C range at 2 kb, a change in temperature does not appreciably change the stability fields of albite and K-feldspar (Fig 5-2; Helgeson, 1985). In order to crystallize K-feldspar and obtain the texture shown in Plates 4-3 and 4-8, there would have to be either an increase in the activity of K in the fluid such that K-feldspar instead of albite becomes the stable phase or, if the original fluid had a sufficient content of both Na and K, a decrease in the activity of Na (Fig. 5-2). Below 500°C the stability field of muscovite expands greatly, mostly at the expense of the andalusite and K-feldspar fields, while the albite field remains virtually unchanged.

The textures observed within the hydrothermally altered rocks can be used to estimate the relative activities of Na and K in the fluid.

The secondary albite in both the altered monzogranites and leucomonzogranites is replaced by muscovite (Plate 4-4). The albite with fine-grained muscovite is in turn replaced by K-feldspar. To explain the observed sequence of mineralogical transformations the fluid must have followed a path similar to that schematically depicted by the trend A-M-K in Figure 5-2, where position A refers to albitization, M to muscovitization, and K to K-feldspathization.

According to the stability diagrams, to develop this textural sequence the fluid must first attain equilibrium within the albite field (position A, Fig. 5-2). With evolution of the system the activity of Na must decrease such that at T<500-600°C (position M, Fig.5-2) muscovite becomes the stable phase, explaining the observed replacement of albite by muscovite. With further cooling the field of muscovite expands so that the muscovite-K-feldspar boundary shifts slightly toward higher $\log(a_{K+}/a_{H+})$. Therefore, to replace the albite-muscovite assemblage by K-feldspar, the fluid must reach a higher K^+/H^+ ratio. A simple drop in temperature would not allow this to happen so an increase of the activity of K in the fluid must occur (position K, Fig. 5-2).

The increase in the activity of K in the fluid is problematic. A possible source of K for the fluid is inferred from the position of the hydrothermally altered rocks on the QAP plot (Fig. 4-1). These rocks plot within the granodiorite field, a position inconsistent with their monzogranitic appearance and mineralogy. As described in Chapter 4, some of the original K-feldspar may have been replaced during albitization of the rocks. This breakdown of K-feldspar would release K to

the fluid unless a secondary mineral phase was forming to accommodate it.

5.3.1 Chemistry

The analyses of K-feldspars (average of 3 to 5 spots on each crystal) are given in Table 5-2. The K-feldspars are unzoned and range from Or_{87} Ab_{13} to Or_{95} Ab_5 (Fig. 5-3). The development of a perthitic texture in the K-feldspars indicates that these are not the original compositions (i.e. at time of formation). Textures suggestive of metasomatic replacement of the K-feldspar by the albite, such as albite mantles and invasion perthite, are absent.

While there is no difference in the major Or-Ab-An contents among the various rock types, there are distinct minor-element chemical differences. A plot of K_2O vs P_2O_5 shows separation between the unaltered and altered rocks (Fig. 5-4). The separation is significant considering the potassium feldspar in the hydrothermally altered rocks is secondary. The increase of both K_2O and P_2O_5 likely reflects increasing activity of potassium and phosphorus in the hydrothermal fluids which pervaded these rocks.

5.3.2 Phosphorus Content of Potassium Feldspar

Phosphorus can occur in minor amounts in the tetrahedral sites of the feldspar crystal lattice (Ribbe, 1983). Both K-feldspar and plagioclase can accommodate up to 0.33 wt.% P (Smith, 1983). The K-feldspar analyses show that the unaltered monzogranites (biotite-muscovite, transitional and megacrystic monzogranites in Table 5-2) have from 0 to 0.22 wt.% P_2O_5 (0-0.10 wt.% P). By contrast, the

Table 5-2 Geochemical analyses of potassium feldspars from the Sangster Lake and Larrys River Plutons.

SAMPLE #	F-G001	F-G001	F-G001	F-G001	F-G001	F-G005	SL-13	SL-13	SL-13	F6-G004	F6-G004	LR-6	LR-6	LR-6
ROCK TYPE	HIGH-RESPONSE MONZOGRANITE						CENTRAL MONZOGRANITE			BIOT-MUSC MONZ		TRANSITIONAL MONZ		
SiO2	64.39	63.01	63.23	64.09	64.46	64.65	63.93	63.91	64.43	64.77	64.37	64.10	64.40	64.11
TiO2	0.00	0.00	0.00	0.00	0.00	0.00	0.00	0.00	0.00	0.00	0.00	0.00	0.00	0.00
Al2O3	18.58	19.04	18.64	18.40	18.46	18.84	18.47	18.73	18.68	18.21	18.16	18.63	18.68	18.52
FeO	0.02	0.00	0.03	0.01	0.02	0.00	0.02	0.02	0.03	0.02	0.04	0.01	0.03	0.02
MnO	0.02	0.02	0.04	0.04	0.02	0.05	0.08	0.05	0.07	0.02	0.05	0.07	0.03	0.02
MgO	0.00	0.00	0.01	0.00	0.00	0.00	0.00	0.00	0.01	0.00	0.00	0.01	0.00	0.01
CaO	0.01	0.02	0.00	0.00	0.02	0.01	0.03	0.01	0.02	0.00	0.03	0.04	0.02	0.03
Na2O	0.81	1.14	0.87	0.66	0.99	0.48	0.96	0.78	1.06	0.62	0.79	0.98	0.78	1.03
K2O	16.33	16.32	16.21	16.50	16.18	15.14	15.70	15.15	15.31	15.65	15.49	15.42	14.99	14.81
BaO	0.01	0.00	0.02	0.02	0.00	0.04	0.02	0.02	0.02	0.09	0.05	0.26	0.29	0.31
P2O5	0.33	0.66	0.51	0.31	0.36	0.41	0.40	0.39	0.60	0.00	0.00	0.14	0.13	0.19
TOTAL	100.49	100.21	99.55	100.03	100.49	99.64	99.61	99.07	100.23	99.37	98.97	99.67	99.36	99.03
Or	92.96	90.31	92.45	94.28	91.67	95.35	91.40	92.99	90.37	94.35	92.64	91.10	92.57	90.34
Ab	6.99	9.61	7.54	5.72	8.26	4.57	8.47	6.97	9.51	5.65	7.21	8.70	7.31	9.51
An	0.05	0.08	0.01	0.00	0.07	0.08	0.13	0.04	0.12	0.00	0.15	0.20	0.12	0.15

SAMPLE #	LR-G010	LR-G010	F-G020	F-G020	F-G020	F-G020	F-G020	F-G020	F-G024	F-G024
ROCK TYPE	MEGA MONZ		LEUCOMONZOGRANITE							
SiO2	64.29	64.86	63.52	63.97	64.64	64.06	64.44	65.13	64.21	64.33
TiO2	0.00	0.00	0.00	0.00	0.00	0.00	0.00	0.00	0.00	0.00
Al2O3	18.81	18.47	18.90	18.62	18.66	18.62	18.74	18.40	18.78	18.65
FeO	0.02	0.08	0.04	0.05	0.09	0.16	0.09	0.04	0.11	0.06
MnO	0.11	0.05	0.10	0.10	0.06	0.08	0.13	0.08	0.10	0.12
MgO	0.00	0.01	0.00	0.03	0.02	0.01	0.01	0.01	0.01	0.00
CaO	0.05	0.03	0.01	0.04	0.03	0.02	0.02	0.00	0.04	0.02
Na2O	1.47	0.46	0.77	0.76	0.62	0.48	1.15	1.04	0.69	1.09
K2O	14.72	15.00	16.17	15.77	15.81	15.39	14.91	15.15	15.54	15.67
BaO	0.32	0.46	0.02	0.00	0.02	0.00	0.03	0.03	0.01	0.03
P2O5	0.22	0.14	0.81	0.70	0.53	0.52	0.33	0.41	0.65	0.60
TOTAL	100.01	99.56	100.32	100.04	100.48	99.34	99.85	100.29	100.14	100.57
Or	86.61	95.39	93.24	92.99	94.23	95.37	89.42	90.55	93.49	90.35
Ab	13.15	4.45	6.71	6.81	5.62	4.52	10.48	9.45	6.31	9.55
An	0.25	0.16	0.05	0.20	0.15	0.10	0.10	0.00	0.20	0.10

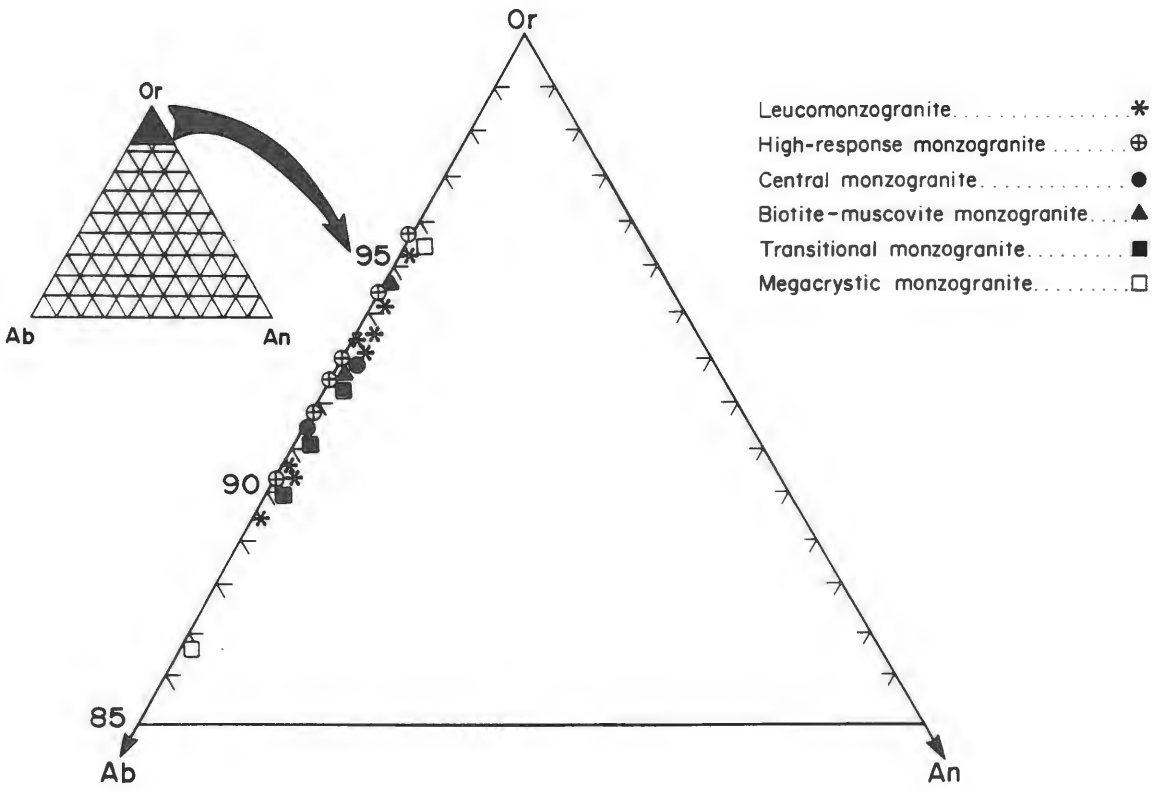

Figure 5-3 Ternary plot of Or-Ab-An proportions of potassium feldspar from samples of the Sangster Lake and Larrys River Plutons.

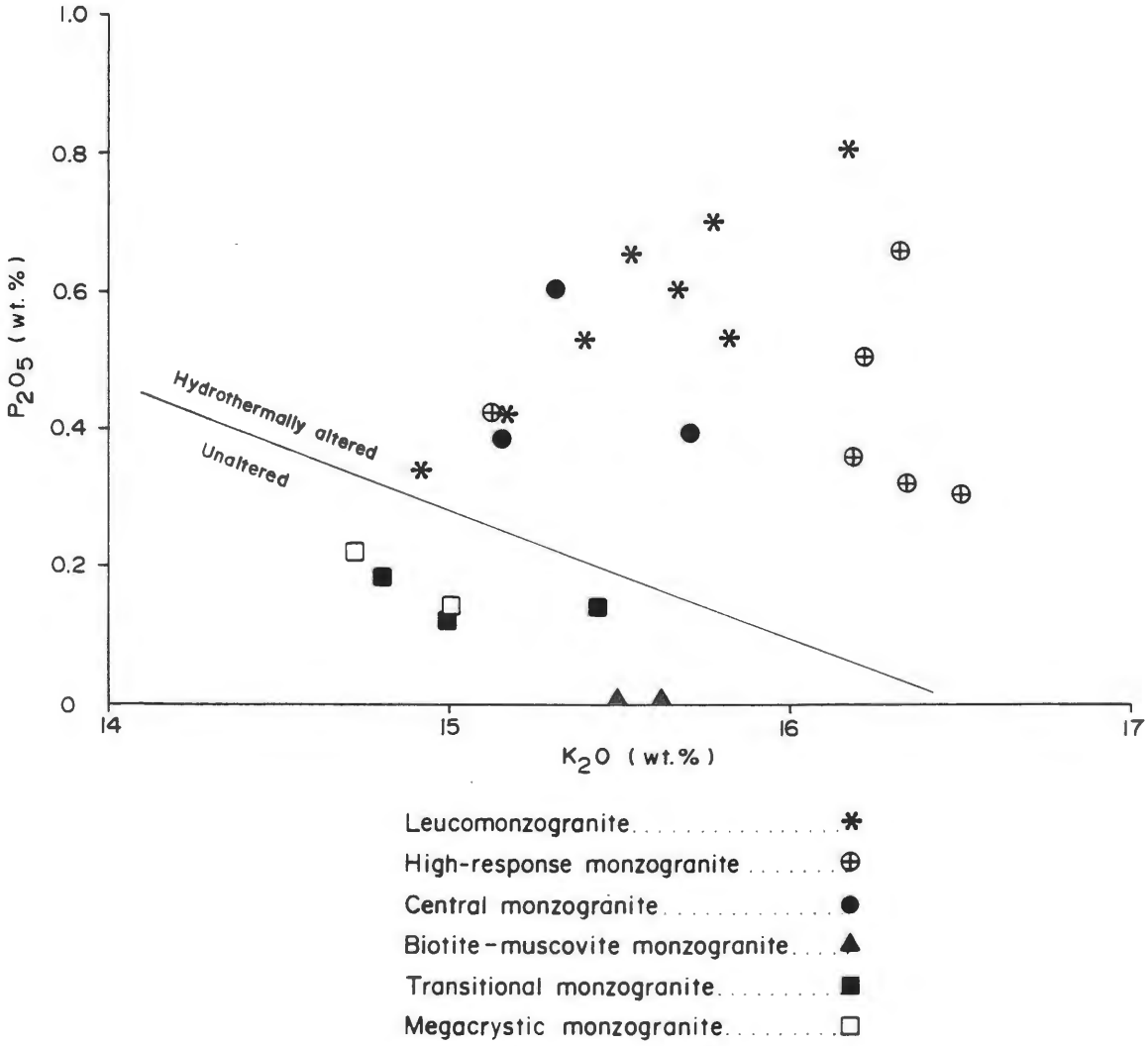

Figure 5-4 Plot of P_2O_5 vs K_2O for potassium feldspars from the various rock types and radiometric categories of the Sangster Lake and Larrys River Plutons.

altered monzogranites (high-response and central monzogranites) and, in particular, the leucomonzogranite have markedly elevated levels ranging from 0.31 to 0.81 wt.% P_2O_5 (0.14-0.36 wt.% P). Conceivably, in light of the occurrence of minute apatite in the altered plagioclases, submicroscopic apatite inclusions could be the source of elevated P in the K-feldspars. If these inclusions are present, there should an increase of CaO with P_2O_5. The data show that, if anything, there are lower levels of CaO in the K-feldspar of the altered rocks than in the unaltered.

Logothetis (1984) found that primary K-feldspars from the South Mountain Batholith have a P_2O_5 content ranging up to 0.36 wt.% (0.16 wt.% P). He concludes that the destruction of these primary feldspars during albitization released significant amounts of phosphorus to the fluid. The secondary albites produced by the alteration contain, on average, much less phosphorus (approx. 0.04 wt.% P_2O_5, 0.02 wt.% P). The excess phosphorus, together with other factors, allowed the formation of secondary phosphate minerals (apatite, autunite and torbernite) in many hydrothermal mineral deposits within the batholith.

The K-feldspars from the unaltered rocks have phosphorus levels comparable to those reported by Logothetis (1984) for the primary K-feldspars of the South Mountain Batholith. The phosphorus levels of K-feldspars from the hydrothermally altered rocks are markedly higher than those in the fresh rocks. By comparison, the secondary feldspars in the South Mountain Batholith (Logothetis, 1984) have levels of P lower than both the unaltered and altered rocks in this study. This

discrepancy may have arisen through differences in physical conditions and composition of the fluids within the two systems.

5.4 MUSCOVITE

Muscovite is a common, but not necessarily diagnostic, constituent of peraluminous granitoid rocks. Muscovite in peraluminous granitic rocks can be the result of magmatic crystallization at high pressures or can be formed at lower pressures and subsolidus temperatures through reaction of a fluid and/or vapor phase with pre-existing aluminous minerals (Clarke et al., 1976; Clarke, 1981). This potential diversity in origin requires that petrologic and genetic inferences based on muscovite be made with caution.

Miller et al. (1981) stipulated that the presence of primary muscovite in a granitic rock indicates crystallization from a strongly peraluminous magma at a depth of >11 km. However, there have been reported occurrences of apparently primary muscovite in granites emplaced at depths of 5 to 10 km. This can explained in three ways: 1) the primary muscovites were crystallized when the magma was at a level >11 km and were intruded with the melt to a higher level after they crystallized; 2) the muscovites are secondary in origin despite their "primary" appearance; or 3) interpretations based on experimental data are not representative of real granitic systems. Any of these explanations is possible therefore the use of muscovite alone as a petrologic indicator can be suspect if close attention is not given to textural observations.

5.4.1 Textural Criteria for Primary and Secondary Muscovite

Miller et al. (1981) showed that there are compositional differences in muscovites of primary (P) and secondary (S) origin. Logothetis (1984) found compositional differences between secondary muscovites of differing facies of alteration. The former study concluded that P-muscovites are richer in Ti, Na and Al and poorer in Mg and Si than S-muscovites. In both studies the conclusions are based on mineral grains which are, on textural criteria, irrefutably of either primary or secondary origin. Miller et al. (1981) referred to the textural criteria of Saavedra (1978) for designation of a primary mica. These criteria are:

1. coarse grain size, comparable to the obvious primary phases.
2. cleanly terminated subhedral-euhedral grains.
3. not enclosed by or enclosing another mineral phase from which the muscovite may have been formed.
4. be in a rock of clean, unaltered, hypidiomorphic granular texture.

Secondary micas occur as small, ragged grains confined to the margins of, or as inclusions within, other minerals. Benoit (1971) observed that micas of primary origin can occur within rocks which have been altered and therefore micas of several generations can be found within a single sample. This is an important consideration in this study because, although the textural criteria for P- and S-muscovites

Plate 5-2 Typical primary (P) muscovite analysed in this study. Note the coarse grain size, cleanly terminated plates and hypidiomorphic granular texture. Scale = 1.0mm.

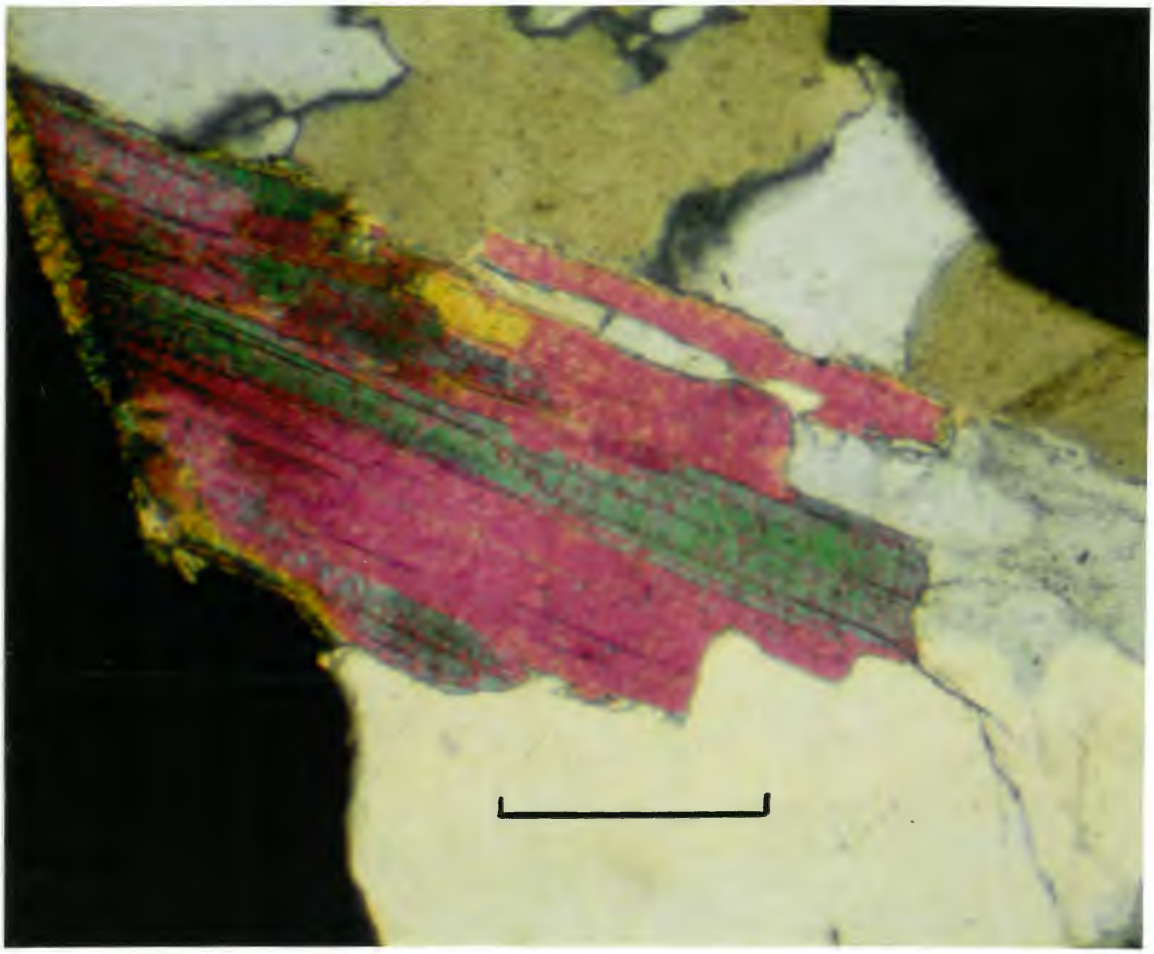

Plate 5-2

described above were employed, there is a very gradual transition between the unaltered and altered rocks.

In this study P-muscovites were selected for analysis according to the first three criteria of Miller et al. (1981; Plate 5-2). The first and third criteria were rigidly adhered to, but the second could not be strictly followed as grains with cleanly terminated boundaries were rare. The fourth criterion could not be met because some of the rocks are hydrothermally altered. These limitations imply that an undetermined amount of the muscovites classified as primary with this study may actually be secondary. At best then, the P-muscovite category consists of more than one population of muscovite.

The S-muscovites were selected for analysis from those occurring solely as inclusions within plagioclase grains (Plate 5-3). Their textural relationship dictates that they are definitely secondary.

5.4.2 Chemistry

Analyses of P- and S-muscovites are given in Table 5-3. The P-muscovite analyses are an average of 3 to 5 spots from each crystal. As the S-muscovites are typically small, their analyses are the average of 3 separate counts on the same spot. The muscovites of both origins are phengitic in composition on the basis of having $Si:Al^{IV}$ ratios greater than 3:1 and having moderately high amounts of octahedral Fe and Mg (Deer et al. 1962). Both the primary and secondary muscovites vary significantly from end-member muscovite compositions (Fig. 5-5). This plot also shows that the two textural categories cannot be distinguished based on their end member components.

Plate 5-3 Typical secondary (S) muscovite analysed in this study, formed by alteration of albite in the rocks of anomalous radiometric response of the Sangster Lake Pluton. Scale = 0.1mm.

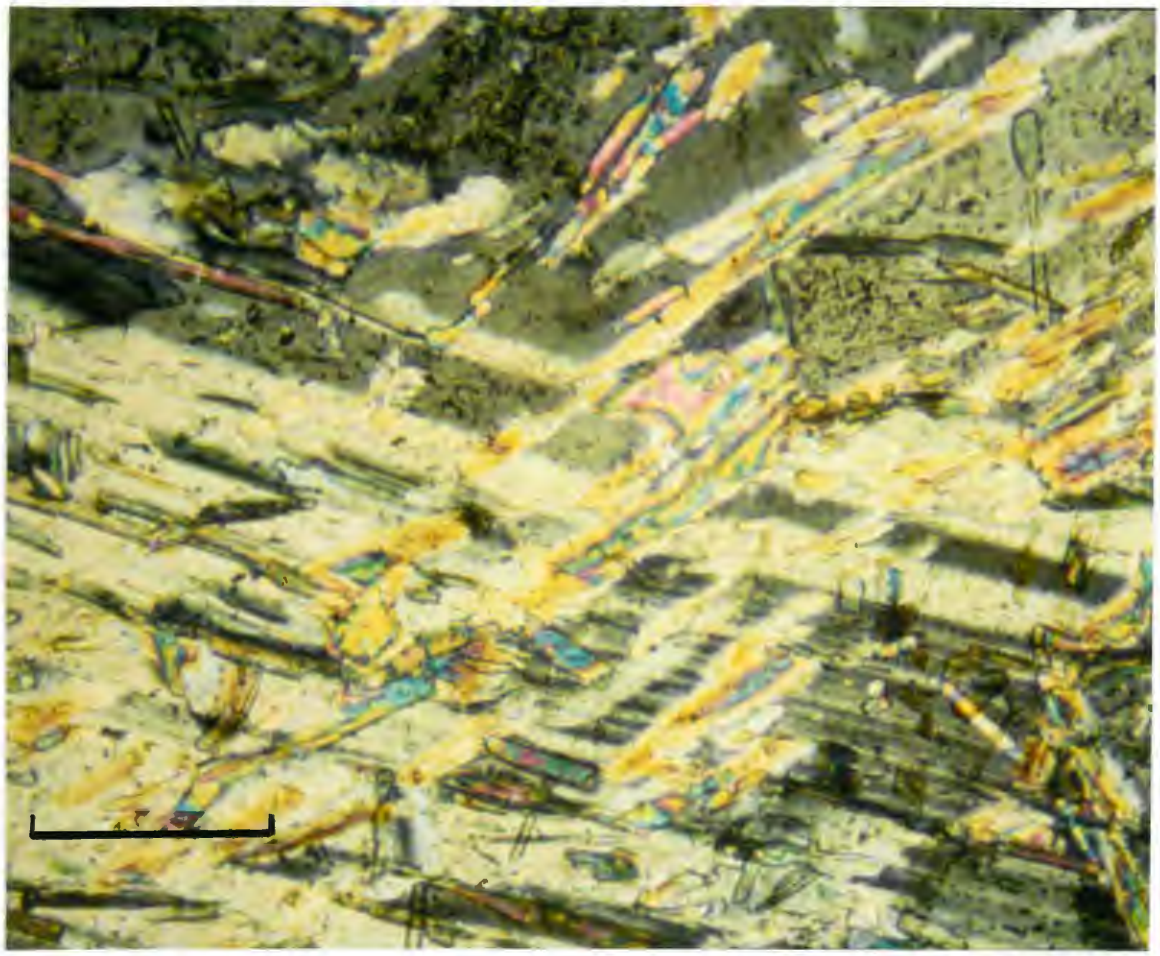

Plate 5-3

Table 5-3 Geochemical analyses of primary (P) and secondary (S) muscovites from the Sangster Lake and Larrys River Plutons.

MICA TYPE	PRIMARY (P) MUSCOVITES																				
SAMPLE #	F-G018	F-G018	F-G018	F-G018	F-G018	F-G018	F-G018	SL-15	SL-15	SL-15	LR-5	LR-5	LR-5	LR-5	LR-5	LR-5	LR-5	F-G003	F-G003	F-G003	F-G001	F-G001
ROCK TYPE	AVERAGE-RESPONSE MONZOGRANITE							CENTRAL	MONZOGRANITE		TRANSITIONAL MONZOGRANITE							HIGH-RESPONSE MONZOGRANITE				
SiO_2	46.30	46.41	45.73	46.16	46.70	46.00	45.57	46.70	46.01	45.98	45.75	45.50	45.52	45.39	45.35	45.45	45.47	45.17	45.65	45.76	46.08	45.90
TiO_2	0.83	0.51	1.02	0.70	0.72	2.16	1.04	0.67	0.28	0.41	0.00	0.62	0.71	0.37	0.87	0.83	0.86	0.50	0.35	0.29	0.34	0.58
Al_2O_3	36.29	35.70	35.78	36.08	35.12	34.52	35.56	34.77	35.48	34.78	35.55	35.91	35.19	35.87	35.45	35.65	35.57	35.04	34.97	35.36	35.68	35.37
FeO_{tot}	1.31	1.49	1.25	1.40	1.62	1.52	1.17	1.81	1.72	1.84	1.43	1.37	1.59	1.20	1.12	1.02	1.24	1.94	1.89	1.66	1.70	1.50
MnO	0.00	0.00	0.00	0.00	0.00	0.00	0.00	0.00	0.00	0.00	0.00	0.00	0.00	0.00	0.00	0.00	0.00	0.00	0.00	0.00	0.00	0.00
MgO	0.42	0.59	0.46	0.48	0.64	0.56	0.38	0.82	0.63	0.49	0.70	0.50	0.65	0.40	0.52	0.43	0.52	0.53	0.49	0.53	0.41	0.30
Na_2O	0.28	0.18	0.28	0.38	0.17	0.15	0.30	0.00	0.06	0.33	0.00	0.00	0.00	0.14	0.52	0.46	0.22	0.12	0.14	0.17	0.35	0.33
K_2O	10.89	10.80	10.57	10.67	10.85	10.70	10.43	11.06	10.86	10.53	11.04	11.29	10.91	10.76	10.30	10.33	10.44	10.67	10.71	10.71	10.61	10.51
H_2O	4.54	4.52	4.49	4.53	4.52	4.50	4.47	4.51	4.48	4.45	4.59	4.61	4.59	4.59	4.59	4.60	4.60	4.59	4.58	4.59	4.49	4.47
TOTAL	100.86	100.20	99.58	100.40	100.34	100.11	98.92	100.34	99.59	98.81	99.06	100.02	99.16	98.72	98.72	98.77	98.72	98.56	98.78	99.07	99.66	98.96
	FORMULA 24 (O, OH)																					
Si	6.108	6.154	6.092	6.109	6.189	6.120	6.110	6.202	6.149	6.191	6.163	6.107	6.134	6.117	6.116	6.114	6.118	6.171	6.173	6.152	6.148	6.161
Al^{IV}	1.892	1.846	1.904	1.892	1.811	1.880	1.890	1.798	1.851	1.809	1.837	1.893	1.866	1.883	1.884	1.886	1.882	1.829	1.827	1.848	1.852	1.840
Al^{VI}	3.749	3.733	3.716	3.735	3.683	3.531	3.728	3.642	3.736	3.709	3.765	3.743	3.864	3.791	3.711	3.727	3.721	3.701	3.708	3.745	3.757	3.744
Ti	0.070	0.051	0.103	0.070	0.072	0.216	0.105	0.066	0.028	0.042	0.000	0.061	0.070	0.036	0.085	0.001	0.084	0.050	0.035	0.029	0.034	0.059
Fe	1.440	0.165	0.139	0.155	0.179	0.169	0.132	0.201	0.192	0.021	0.167	0.160	0.186	0.140	0.131	0.119	0.145	0.205	0.221	0.190	0.190	0.169
Mn	0.000	0.002	0.000	0.002	0.003	0.000	0.000	0.000	0.000	0.000	0.000	0.000	0.000	0.000	0.000	0.000	0.000	0.000	0.002	0.000	0.000	0.000
Mg	0.080	0.116	0.092	0.095	0.126	0.111	0.076	0.161	0.125	0.098	0.126	0.081	0.117	0.072	0.095	0.084	0.095	0.097	0.091	0.089	0.082	0.059
Na	0.072	0.045	0.073	0.098	0.043	0.039	0.079	0.000	0.016	0.085	0.000	0.055	0.000	0.035	0.132	0.049	0.056	0.061	0.036	0.031	0.091	0.085
K	1.832	1.827	1.797	1.800	1.834	1.816	1.784	1.870	1.851	1.808	1.947	1.876	1.924	1.900	1.818	1.820	1.839	1.883	1.896	1.900	1.805	1.799
H	4	4	4	4	4	4	4	4	4	4	4	4	4	4	4	4	4	4	4	4	4	4
O	24	24	24	24	24	24	24	24	24	24	24	24	24	24	24	24	24	24	24	24	24	24

Table 5-3 cont'd

MICA TYPE	SECONDARY (S) MUSCOVITES																				
SAMPLE #	F-G018	F-G018	SL-15	SL-15	SL-15	SL-15	F-G003	F-G003	F-G003	F-G003	F-G001	F-G001	F-G001	F-G001	F-G001	F-G001	F-G001	F-G005	F-G005	F-G005	F-G005	F-G005
ROCK TYPE	AVG-RESP	MONZ	CENTRAL MONZOGRANITE				HIGH-RESPONSE MONZOGRANITE															
SiO_2	46.04	46.25	46.10	46.50	45.79	47.40	47.02	46.75	46.16	46.28	46.20	46.17	46.26	46.05	45.44	46.24	46.18	46.44	46.07	46.03	46.93	45.69
TiO_2	0.00	0.30	0.07	0.00	0.00	0.11	0.07	0.02	0.00	0.06	0.27	0.40	0.02	0.00	0.00	0.00	0.22	0.29	0.18	0.06	0.34	0.00
Al_2O_3	35.93	36.16	35.59	35.95	36.39	33.94	34.48	34.51	33.98	34.77	34.69	35.00	35.60	36.12	36.42	37.32	34.59	34.46	34.10	36.24	34.45	36.06
FeO_{tot}	1.12	1.27	1.65	1.56	1.39	1.89	1.86	1.95	2.39	1.86	2.33	2.61	1.83	1.58	1.55	1.34	3.20	1.99	2.26	1.19	2.53	1.70
MnO	0.00	0.00	0.00	0.00	0.00	0.00	0.00	0.00	0.00	0.00	0.00	0.00	0.00	0.00	0.00	0.00	0.00	0.00	0.00	0.00	0.00	0.00
MgO	0.43	0.22	0.46	0.39	0.30	0.51	0.64	0.70	0.80	0.51	0.65	0.56	0.30	0.12	0.00	0.00	0.60	0.63	0.83	0.16	0.53	0.27
Na_2O	0.08	0.21	0.18	0.17	0.27	0.91	0.00	0.49	0.00	0.20	0.00	0.21	0.25	0.00	0.21	0.11	0.05	0.24	0.00	0.44	1.02	0.32
K_2O	10.80	10.82	10.78	10.95	10.94	9.35	10.64	10.60	10.58	10.79	10.90	10.63	10.70	10.80	10.62	10.92	10.54	10.62	10.74	10.67	10.67	10.15
H_2O	4.47	4.51	4.48	4.51	4.49	4.47	4.62	4.60	4.56	4.59	4.48	4.49	4.48	4.48	4.45	4.54	4.48	4.46	4.43	4.48	4.50	4.46
TOTAL	98.87	99.73	99.31	100.03	99.57	98.58	99.35	99.62	98.47	99.06	99.72	100.07	99.44	99.15	98.69	100.47	99.86	99.13	98.61	99.27	100.02	98.65
	FORMULA 24 (O, OH)																					
Si	6.170	6.150	6.172	6.178	6.114	6.352	6.302	6.284	6.265	6.236	6.209	6.162	6.186	6.164	6.112	6.104	6.186	6.235	6.230	6.148	6.253	6.138
Al^{IV}	1.830	1.848	1.829	1.822	1.886	1.648	1.698	1.716	1.735	1.764	1.791	1.838	1.814	1.836	1.888	1.896	1.814	1.765	1.770	1.852	1.745	1.862
Al^{VI}	3.844	3.820	3.785	3.806	3.839	3.712	3.710	3.661	3.664	3.719	3.678	3.667	3.795	3.861	3.885	3.909	3.647	3.689	3.664	3.852	3.665	3.847
Ti	0.000	0.300	0.007	0.000	0.000	0.011	0.007	0.002	0.000	0.006	0.027	0.040	0.002	0.000	0.000	0.000	0.022	0.029	0.018	0.006	0.034	0.000
Fe	0.126	0.141	0.185	0.174	0.155	0.212	0.217	0.234	0.281	0.217	0.261	0.291	0.205	0.177	0.174	0.148	0.359	0.223	0.256	0.133	0.282	0.191
Mn	0.000	0.000	0.000	0.000	0.000	0.000	0.004	0.001	0.000	0.000	0.000	0.000	0.000	0.000	0.000	0.000	0.000	0.000	0.000	0.000	0.000	0.000
Mg	0.086	0.044	0.092	0.077	0.060	0.102	0.115	0.129	0.147	0.094	0.130	0.111	0.059	0.024	0.000	0.000	0.120	0.125	0.167	0.031	0.105	0.054
Na	0.021	0.054	0.047	0.043	0.070	0.236	0.000	0.123	0.000	0.164	0.000	0.054	0.064	0.000	0.055	0.028	0.015	0.061	0.000	0.114	0.018	0.083
K	1.846	1.836	1.841	1.860	1.863	1.598	1.866	1.862	1.880	1.904	1.860	1.810	1.824	1.844	1.822	1.839	1.800	1.819	1.852	1.818	1.814	1.739
H	4	4	4	4	4	4	4	4	4	4	4	4	4	4	4	4	4	4	4	4	4	4
O	24	24	24	24	24	24	24	24	24	24	24	24	24	24	24	24	24	24	24	24	24	24

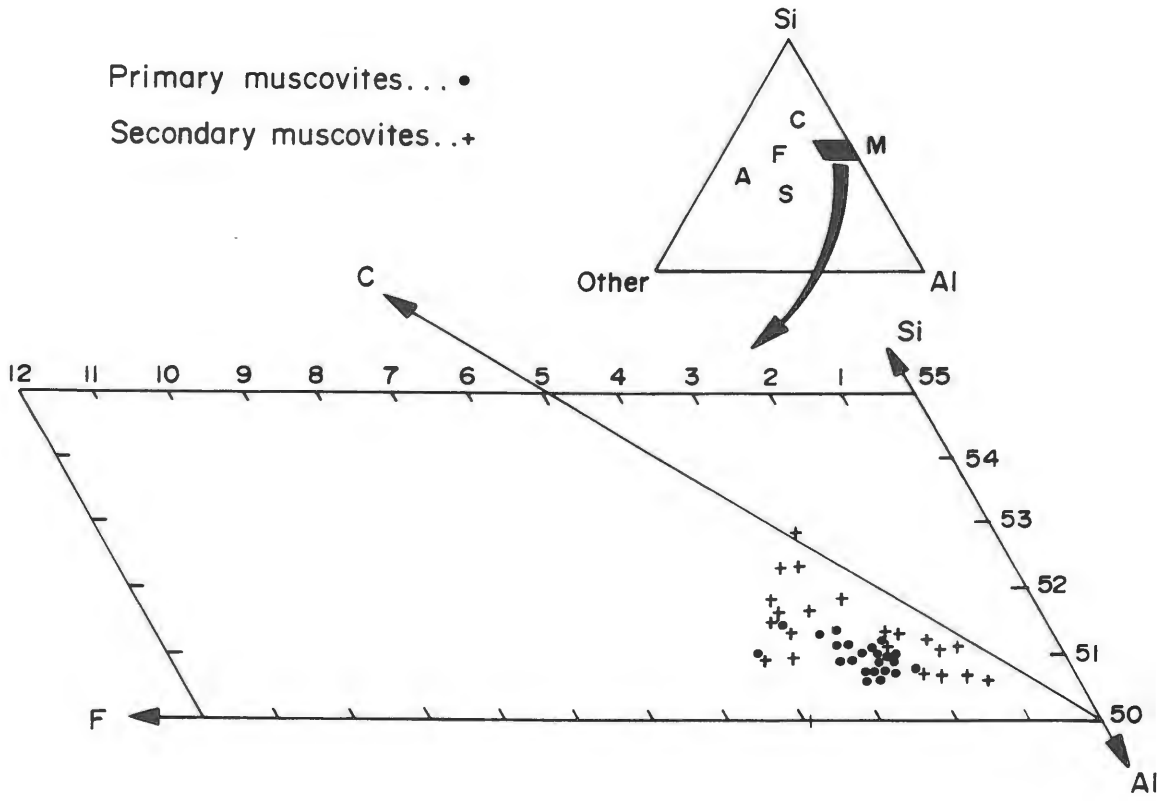

Figure 5-5 Plot of Si, Al and other (octahedral cations Fe, Mg, Ti, Mn, Cr) atomic proportions of primary and secondary muscovites from the Sangster Lake and Larrys River Plutons. M = pure muscovite; C = celadonite; F = ferrimuscovite; A = annite; S = siderophyllite.

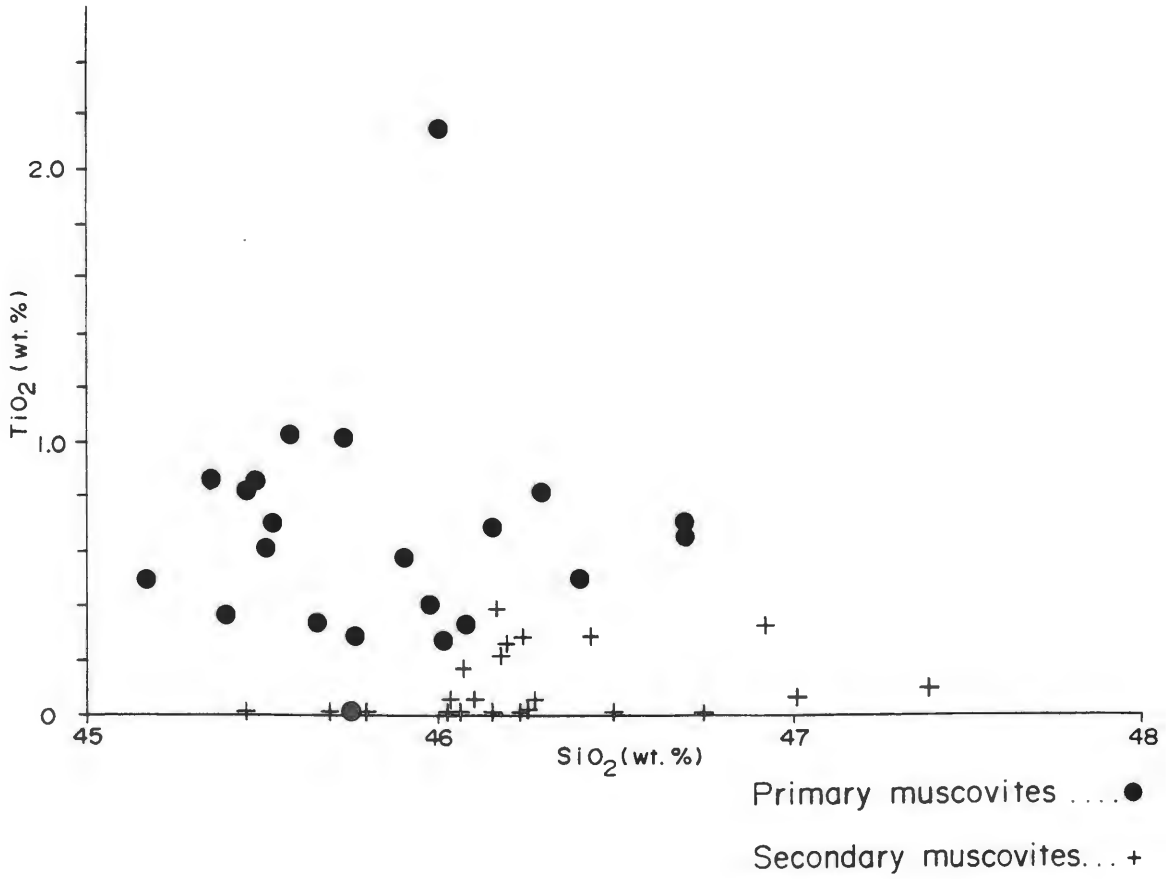

Figure 5-6 Plot of TiO_2 vs SiO_2 of primary and secondary muscovites from the Sangster Lake and Larrys River Plutons.

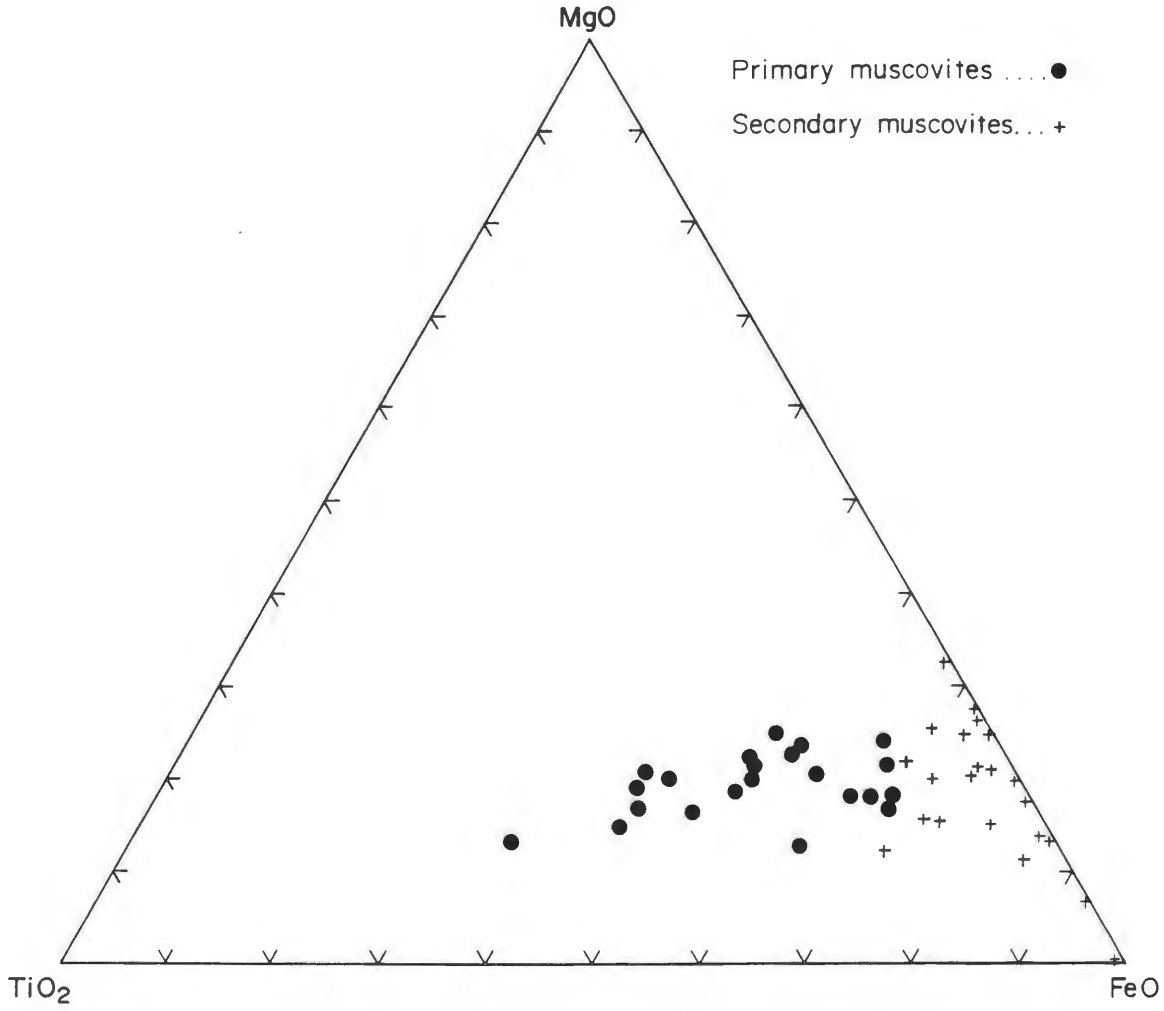

Figure 5-7 Plot of MgO-TiO_2-FeO for primary and secondary muscovites from the Sangster Lake and Larrys River Plutons.

The largest compositional difference among the data involves Ti, with muscovites of secondary origin having markedly less TiO_2 (mean 0.13 wt.%, s.d. 0.13) than those of the primary category (mean 0.67 wt.%, s.d. 0.42). Miller et al. (1981), Logothetis (1984) and Ham and Kontak (1987) also found that Ti variation is the most useful discriminator between different muscovite generations. In addition, S-muscovites are richer in Si and Mg (Miller et al., 1981). This negative relationship between Ti and Si is reflected in the data from this study (Fig. 5-6). A plot of MgO-TiO_2-FeO also shows the elevated Ti content of the P-muscovite category, while showing that the Mg/Fe ratio remains relatively constant (Fig. 5-7).

Miller et al. (1981) found that P-white micas are enriched in Na relative to the S category. The reverse holds with this study where most S-micas are enriched in Na relative to the P-micas (Fig. 5-8). The S-micas analysed in this study occur as inclusions within secondary albite. The Na enrichment in the S-micas could result from: (1) their formation from a fluid phase with a significant Na component or; (2) their Na enrichment is a reflection of their formation from an Na-rich phase like albite. Logothetis (1984) reported a similar Na enrichment in white mica formed within albitized and greisenized rocks at the Long Lake Prospect in the South Mountain Batholith.

5.4.3 Discriminant Analysis

The muscovite data set of P- and S-micas was subjected to discriminant analysis using the Systat Statistical Package, Version 3.0. The details of the discriminant analyses and its application here are given in Appendix III.

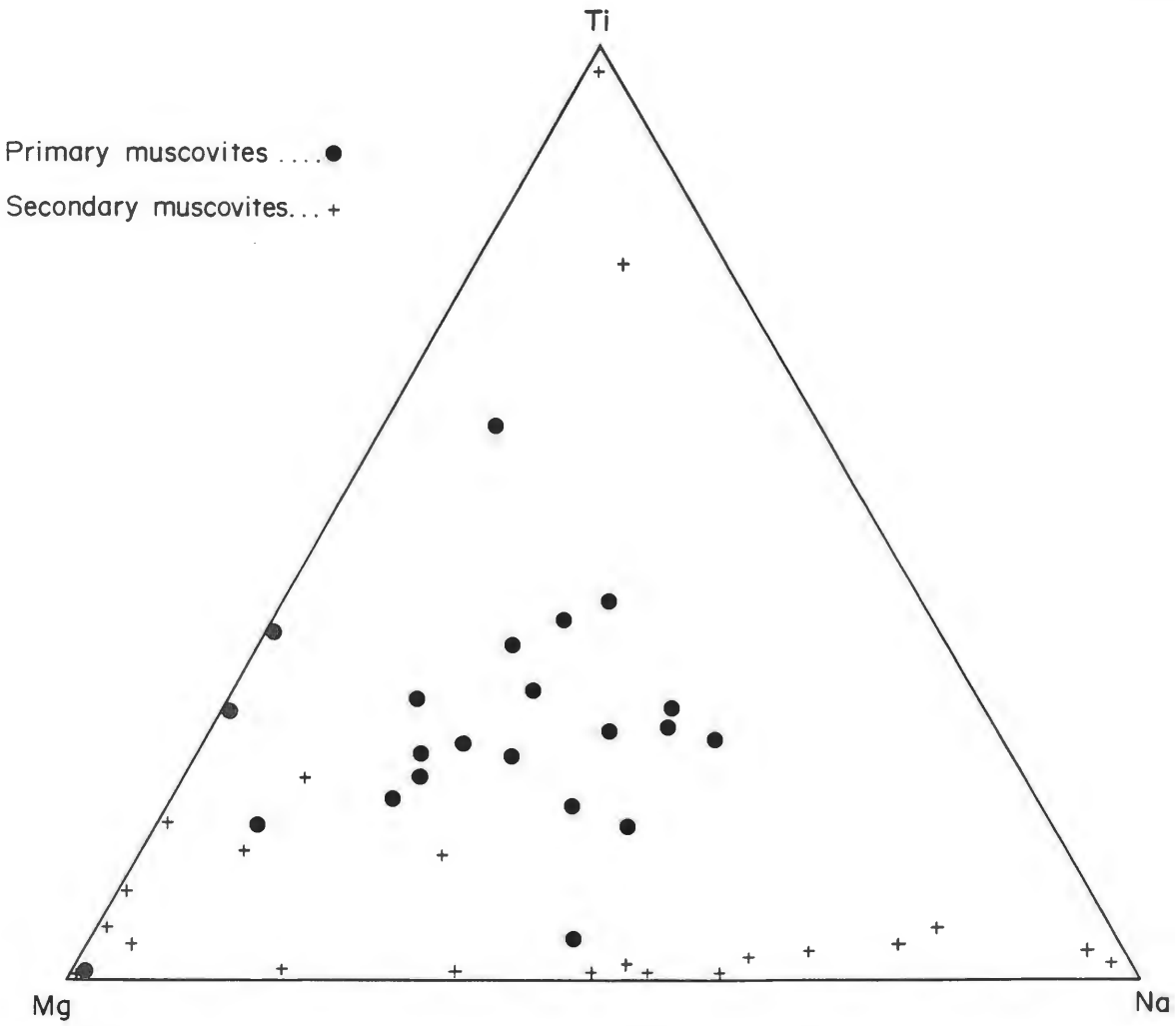

Figure 5-8 Plot of Ti-Mg-Na for primary and secondary muscovites from the Sangster Lake and Larrys River Plutons.

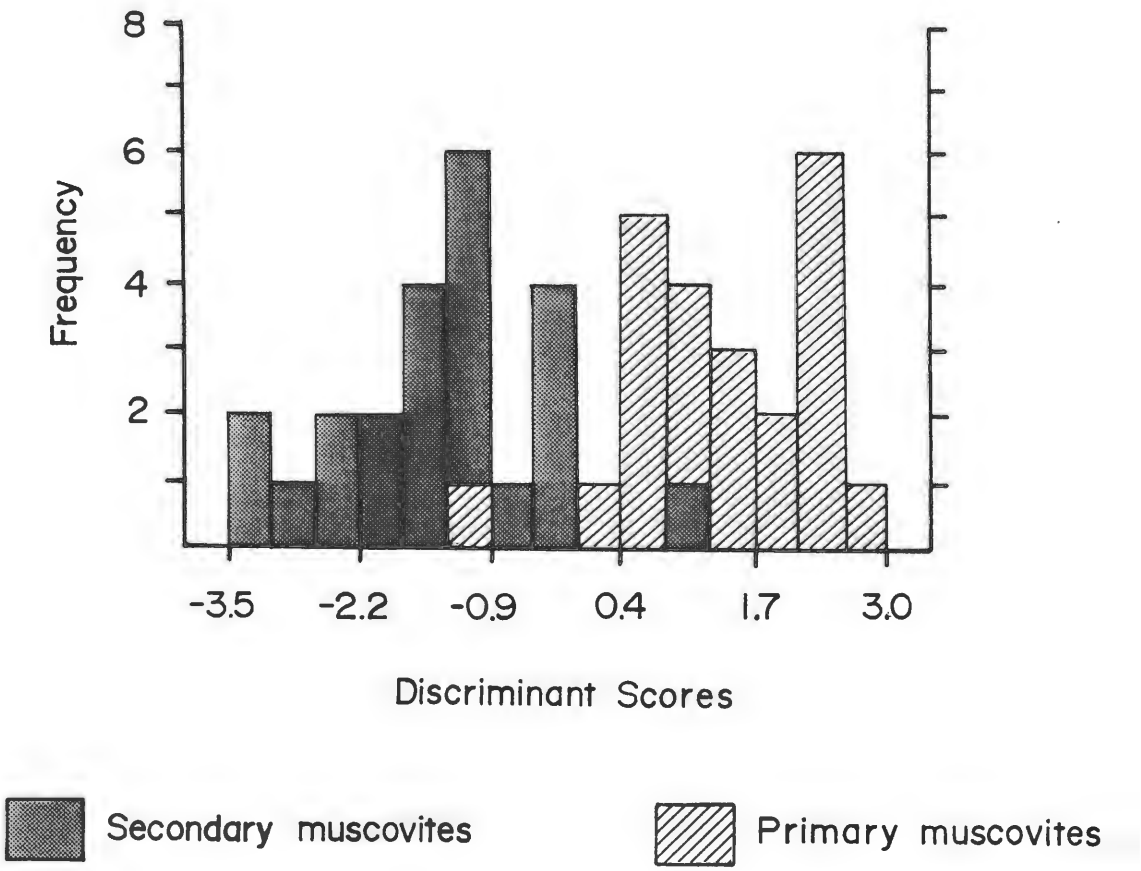

Figure 5-9 Stacked histogram of discriminant function scores of primary and secondary muscovites from the Sangster Lake and Larrys River Plutons.

The results of the discriminant analysis gave standardized discriminant function coefficients in order of importance (regardless of sign) of 0.911 (TiO_2), 0.740 (Al_2O_3), 0.576 (MgO) and -0.343 (FeO). These are consistent with the plots of these elements presented previously except for the absence of Na_2O as a discriminator. Figure 5-8 shows that some S-micas have higher Na_2O levels relative to the P-micas. Although there are examples of Na-enrichment, there is considerable scatter (i.e. within group variation) and this likely lessens the use of Na as a discriminator.

The discriminant scores are plotted as a histogram in Figure 5-9. The discriminant scores are derived using Fisher discriminant function, group classification coefficients according to the following formulae. For S-micas D_S = -8.06 (TiO_2) -2128.805 (Al_2O_3) -163.839 (FeO) -28.448 (MgO) -653.956. For P-micas D_P = -6.053 (TiO_2) - 2051.853 (Al_2O_3) - 167.965 (FeO) -26.631 (MgO) - 627.368. There is good separation of the two categories with only one sample of each group misclassified. This shows that, based on the criteria outlined previously, the S-muscovites can be distinguished from the P-muscovites by their levels of TiO_2, Al_2O_3, MgO and FeO. A muscovite of unknown origin can also be classified if the levels of the important variables are known simply by deriving discriminant scores by using the above formulae. The formula which yields the highest value indicates the mica category in which the unknown falls. Take note that the data for the unknown mica must first be treated according to the procedure outlined in Appendix III, i.e. normalized to SiO_2 and then log transformed.

5.5 PHOSPHATES

5.5.1 Introduction

Phosphorus in granitic rocks is usually manifest as apatite which occurs in trace to minor quantities. Apatite occurs as a cumulate phase, generally associated with biotite, in other Meguma Zone granitoids (McKenzie, 1974; MacDonald, 1982). Granitoid rocks containing most biotite (e.g. granodiorite and biotite monzogranite) have the greatest abundance of the mineral.

Apatite and other phosphate minerals formed by metasomatic and hydrothermal processes are described in several recent studies (Neiva, 1982; O'Reilly et al., 1982; Logothetis, 1984; Chatterjee et al., 1985). Phosphates associated with late-stage alteration are anomalous in their concentration of the volatiles F, Cl and OH (Deer et al. 1966: Neiva, 1982; Logothetis, 1984).

Primary apatites analysed in this study occur as euhedral to subhedral grains intimately associated with biotite and as discrete grains within the groundmass of all monzogranitic phases of both plutons (Plate 4-1). Secondary apatites occur as minute euhedral to subhedral inclusions in secondary albite (Plate 4-6). Chlorine-bearing apatites were analysed from grain mounts of heavy mineral separates as all grains of this mineral were lost from polished thin sections during preparation.

5.5.2 Chemistry

The analyses of apatites are tabulated according to rock type in Table 5-4. The primary apatites (INT) and the secondary chlorine-bearing apatites (Cl) are the average of 3 to 5 spots on particular grains. Analyses of secondary apatites as inclusions in albite (ALT) are averages of 3 successive counts on particular crystals. The coefficients of a Spearman Rank Correlation (Appendix III) using the Systat Statistical Package, Version 3.0 are tabulated as a correlation matrix in Figure 5-10. The matrix shows positive and negative inter-element relationships of 99% significance, especially among MnO, CaO and FeO. Both MnO and FeO have a strong negative correlation with CaO suggesting substitution of Fe and Mn for Ca in the apatite crystal lattice. Most of the apatites can be classified as F-rich or fluoro-apatite based on their F levels (Table 5-4). The Cl-bearing apatites have low levels of F and hence F shows a negative correlation with Cl in Figure 5-10.

When the data are examined solely on mode of occurrence there is no consistent geochemical difference between primary and secondary apatites. A plot of MnO vs CaO (Fig. 5-11) for the textural varieties of apatite shows that, although there is an excellent linear trend, there is no difference between the modes of occurrence except for those from the leucomonzogranite and the Cl-apatites. This suggests that, although there are distinct textural varieties of apatites, there was either partial re-equilibration during subsequent secondary alteration or there never was a chemical difference.

Table 5-4 Geochemical analyses of apatites from the Sangster Lake and Larrys River Plutons.

SAMPLE #	F-G024	F-G024	F-G024	F-G024	F-G024	F-G001	F-G001	F-G001	F-G001	F-G001	F-G001	F-G005	F-G005	F-G005	F-G005	F-G005	F-G005	F-G005	F-G005	F-G005
MODE*	INT	INT	INT	INT	INT	Cl	Cl	Cl	Cl	Cl	INT	INT	INT	ALT	ALT	ALT	ALT	ALT	ALT	ALT
ROCK TYPE	LEUCOMONZOGRANITE					HIGH-RESPONSE MONZOGRANITE														
P_2O_5	41.64	41.66	41.97	41.91	41.98	41.69	41.38	42.36	41.71	42.15	43.06	42.24	41.93	42.18	42.35	42.55	42.11	41.83	41.80	41.05
CaO	47.54	46.89	47.69	46.88	46.55	46.62	46.78	50.97	49.39	52.95	51.79	50.97	50.94	50.58	51.05	54.12	51.46	53.97	51.46	52.11
MnO	6.51	6.66	5.97	6.79	6.52	4.42	5.34	3.17	3.39	1.59	3.40	3.17	3.39	3.55	3.29	0.62	2.73	0.80	2.68	2.82
FeO	0.78	1.01	0.64	0.78	0.91	3.11	2.71	0.83	2.40	1.08	0.47	0.37	0.25	0.43	0.52	0.00	0.17	0.00	0.43	0.38
Cl	0.06	0.05	0.04	0.06	0.07	3.00	3.36	2.09	2.66	1.89	0.07	0.05	0.05	0.02	0.05	0.04	0.05	0.05	0.05	0.03
F	3.34	3.63	3.38	3.30	3.40	0.18	0.15	0.64	0.10	0.66	1.76	3.15	3.23	3.17	2.61	3.09	3.31	3.73	3.81	3.87
TOTAL	99.87	99.90	99.67	99.72	99.42	99.01	99.72	100.05	99.64	100.31	100.54	99.94	99.80	99.92	99.87	100.40	99.83	100.37	100.22	100.26
	# IONS 26 (O,OH,F,CL)																			
P	6.09	6.09	6.12	6.13	6.14	6.23	6.17	6.20	6.18	6.15	6.21	6.12	6.09	6.11	6.14	6.10	6.10	6.02	6.04	5.96
Ca	8.80	8.67	8.80	8.67	8.62	8.81	8.83	9.44	9.27	9.78	9.45	9.34	9.36	9.28	9.37	9.82	9.43	9.83	9.41	9.58
Mn	0.95	0.97	0.87	0.99	0.95	0.66	0.80	0.46	0.50	0.23	0.49	0.46	0.49	0.51	0.48	0.09	0.40	0.12	0.39	0.41
Fe	0.11	0.15	0.09	0.11	0.13	0.46	0.40	0.12	0.35	0.16	0.07	0.05	0.04	0.06	0.07	0.00	0.02	0.00	0.06	0.05
Cl	0.02	0.01	0.01	0.02	0.02	0.90	1.00	0.61	0.79	0.55	0.02	0.01	0.01	0.01	0.01	0.01	0.01	0.01	0.01	0.01
F	1.82	1.98	1.84	1.80	1.86	0.10	0.08	0.35	0.06	0.36	0.95	1.70	1.75	1.72	1.41	1.66	1.79	2.00	2.06	2.10

SAMPLE #	SL-15	SL-15	SL-15	SL-15	SL-13	SL-13	SL-13	SL-13	SL-11	SL-11	SL-11	SL-7	LR-6	LR-G009	LR-G009	LR-G009	LR-G009
MODE*	ALT	ALT	ALT	INT	INT	INT	INT	INT	INT	INT	INT	INT	INT	INT	INT	INT	INT
ROCK TYPE					CENTRAL	MONZOGRANITE						AVG-RES	TRANS	MEGACRYSTIC		MONZOGRANITE	
P_2O_5	42.71	43.01	42.56	43.03	41.13	42.28	41.92	41.77	42.90	41.52	41.93	42.72	42.56	43.50	43.25	41.11	43.20
CaO	51.59	51.19	52.86	51.54	53.32	52.84	50.35	50.90	52.93	52.06	53.48	53.56	53.03	52.09	53.22	55.68	52.96
MnO	3.55	3.53	3.01	3.32	1.63	2.00	3.68	2.92	1.94	1.86	1.36	0.99	1.24	2.10	1.10	0.23	1.49
FeO	0.56	0.53	0.46	0.50	0.19	0.10	0.43	0.33	0.23	0.16	0.12	0.17	0.44	0.27	0.21	0.09	0.28
Cl	0.05	0.03	0.04	0.05	0.05	0.05	0.05	0.06	0.05	0.03	0.04	0.01	0.07	0.07	0.06	0.04	0.05
F	1.90	1.99	1.82	1.83	3.39	3.23	3.09	3.53	2.34	3.88	3.45	2.75	2.75	2.12	2.26	2.74	2.19
TOTAL	100.30	100.26	100.74	100.25	99.71	100.50	99.50	99.50	100.34	99.49	100.37	100.21	100.09	100.13	100.08	99.90	100.17
	# IONS 26 (O,OH,F,CL)																
P	6.18	6.21	6.14	6.21	5.99	6.08	6.11	6.08	6.17	6.03	6.04	6.14	6.13	6.25	6.21	5.98	6.21
Ca	9.44	9.35	9.65	9.42	9.83	9.62	9.28	9.37	9.63	9.57	9.75	9.74	9.67	9.47	9.67	10.25	9.63
Mn	0.51	0.51	0.43	0.48	0.24	0.29	0.54	0.42	0.28	0.27	0.20	0.14	0.18	0.30	0.16	0.03	0.21
Fe	0.08	0.08	0.07	0.07	0.03	0.01	0.06	0.05	0.03	0.02	0.02	0.02	0.06	0.04	0.03	0.01	0.04
Cl	0.01	0.01	0.01	0.01	0.01	0.01	0.01	0.02	0.01	0.01	0.01	0.00	0.02	0.02	0.02	0.01	0.01
F	1.03	1.07	0.98	0.99	1.84	1.74	1.68	1.92	1.26	2.11	1.86	1.48	1.48	1.14	1.21	1.49	1.18

* MODE OF OCCURRENCE: ALT = Apatite as minute, secondary grains within albite
INT = Apatite as interstitial grains in groundmass
Cl = Chlorine-bearing apatite

P_2O_5	CaO	MnO	FeO	Cl	F	
1.000	0.302	-0.195	-0.101	-0.005	**-0.476**	P_2O_5
	1.000	**-0.928**	**-0.744**	-0.389	0.028	CaO
		1.000	**0.769**	0.271	-0.079	MnO
			1.000	**0.550**	-0.428	FeO
				1.000	**-0.441**	Cl
					1.000	F

Figure 5-10 Matrix of Spearman Rank Correlation Coefficients of geochemical analyses (n=37) of apatites from the Sangster Lake and Larrys River Plutons. The 99 % level of significance (one-tailed test) for n=37 is p = ± 0.432 (Appendix III).

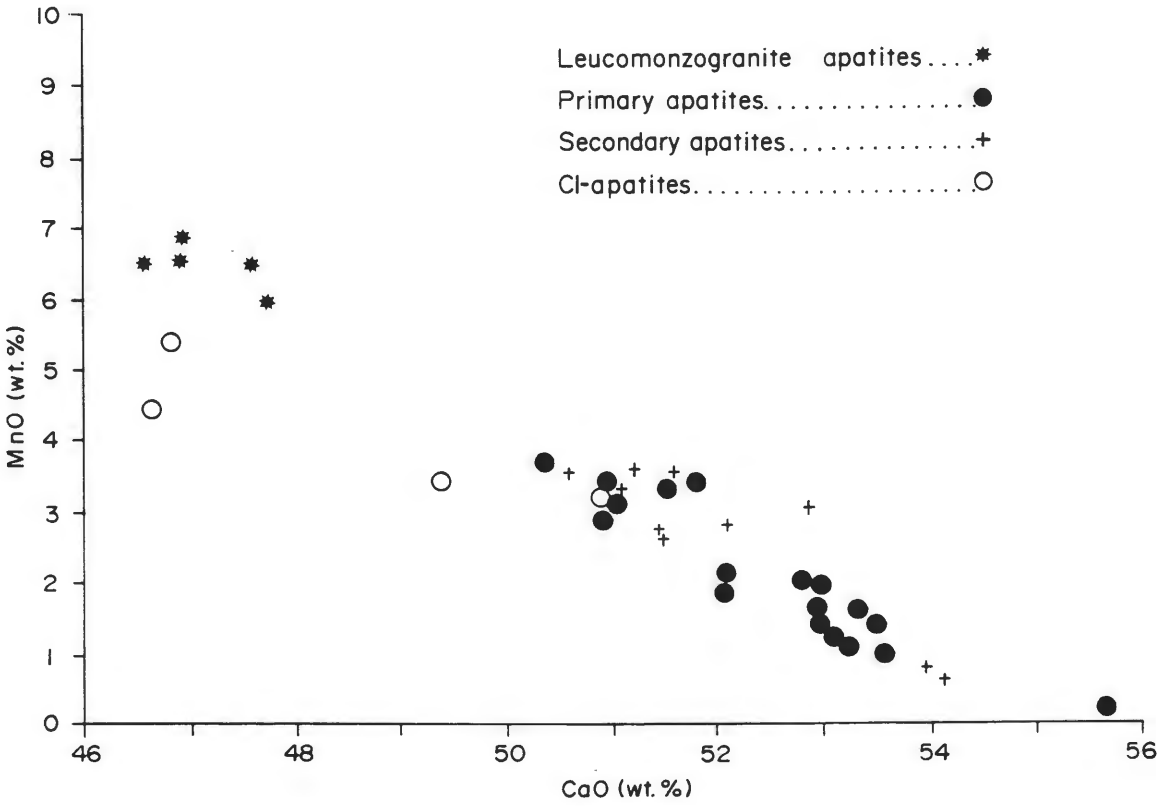

Figure 5-11 Plot of MnO vs CaO for apatites of primary and secondary modes of occurrence from the Sangster Lake and Larrys River Plutons. Apatites from the leucomonzogranites and Cl-bearing apatites from the high-response monzogranite are also designated as they have a distinct mode of occurrence.

When the data are examined according to rock type and radiometric response category, there are trends which separate the apatites in the altered rocks from those in the unaltered rocks (Fig. 5-12). The levels of MnO, FeO and CaO best show the separation and are interpreted to reflect substitution of Mn and Fe for Ca in the apatite lattice.

Calcium may be partially replaced by Mn in the apatite structure and Mn-rich apatites are often associated with granitic pegmatites (Deer et al., 1966). This implies that Mn enrichment in apatites may therefore be an indicator of late-stage, volatile-rich conditions during formation. Logothetis (1984) found that secondary apatites in greisens at the Long Lake Prospect in the South Mountain Batholith are also enriched in Mn and Fe. He concluded that the apatites are related to greisenization that accompanied Fe- and Mn-metasomatism.

The rocks of the high-response monzogranite contain small, brown, matted masses (metamicts, Chapter 4) which contain a weakly birefringent, dirty apatite (Plate 4-7). This mode of occurrence is distinctly different from the others and compositionally they to range from chlorine-bearing apatite to true chloroapatite (Cl in Table 5-4) and Fe-U-phosphate (described later, Table 5-5).

5.6 ACCESSORY MINERALS

Heavy mineral separates from samples from both plutons were examined using a scanning electron microscope (SEM) equipped with an energy dispersive system (Table 5-5). An attempt is made to quantify the relative abundance of each mineral in the separates as well as

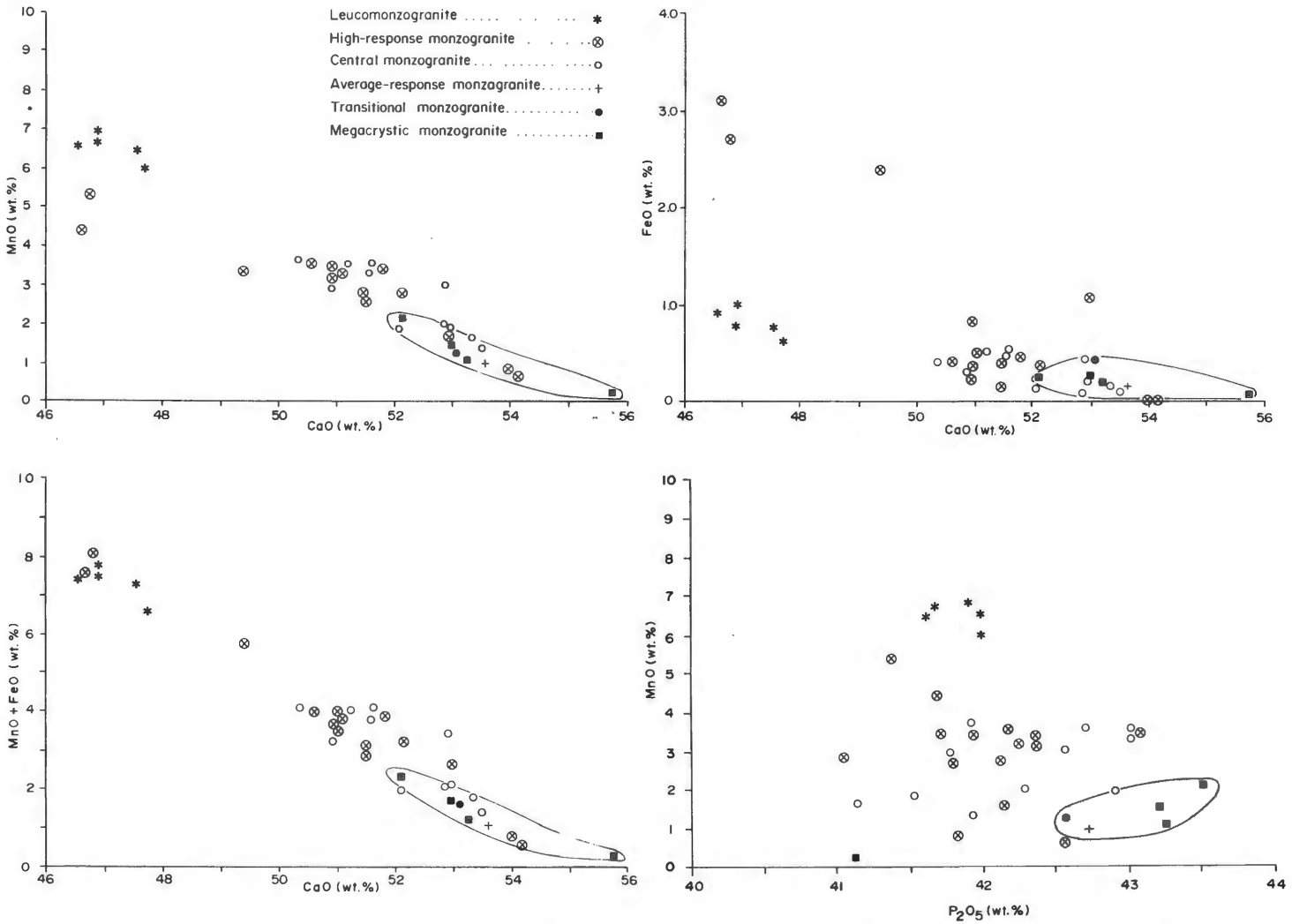

Figure 5-12 Plots of major element analyses of apatites from the Sangster Lake and Larrys River Plutons. Circled areas represent field of unaltered rocks.

indicate significant textural and compositional criteria. A description of some of the observed mineral species in Table 5-5 follows.

5.6.1 Mineralogy

5.6.1.1 Monazite

Monazite occurs in all samples except the greisen from the Beans Lake greisen zone. It invariably occurs as minute inclusions in biotite except in one instance where it occurs as an inclusion in muscovite (Table 5-5). The muscovite grain may be secondary after biotite but as the samples are grain mounts the textural characteristics of the muscovite (i.e secondary or primary) cannot be determined.

Monazite and zircon have a similar mode of occurrence (i.e. inclusions in biotite), but in all instances monazite is more abundant than zircon. In thin section the minerals are difficult, if not impossible, to distinguish from one another. A distinguishing feature may be that the zircon has an elongate, subhedral-euhedral habit, while monazite forms smaller, subhedral-anhedral grains.

The association of monazite with biotite indicates that, although monazite was observed in all rock types, its abundance in each sample may be directly proportional to the amount of biotite.

5.6.1.2 Zircon

Zircon was observed in almost all samples and has two modes of occurrence. Most commonly, it occurs as minute inclusions in biotite although an example of a zircon inclusion in chloroapatite (F5-G007; Table 5-5) was observed. Less commonly separate, euhedral grains of zircon occur. The separate grains may have originally been inclusions

Table 5-5 Accessory mineral species identified in heavy mineral separates from the rocks of the study area.

	GREISEN	LEUCOMONZ		MONZOGRANITES											
				High-Response				Central			Avg-Response		BM Mgt*	Trans**	Mega***
MINERAL	F-G020	F5-G007	F6-G005	F-G001	F-G003	F-G004	F-G005	SL-11	SL-13	SL-15	SL-7	F-G018	F6-G004	LR-5	LR-G011
Monazite		e[3]	r	r	u-r	p	p	r	r-u	u	c	c	c	p-c	c
Zircon[1]		e[4]		u[6]	r	u	r			u	u	u	c	p-c	c
Zircon[2]					r[6]			p-u							u
Apatite	c	p	c						p		p	p-u		u	c
Mn-apatite			c	c	a	a	c	p	p	a					r
Chloroapatite		a		c			c-p			a					
Fe-Mn-garnet	a	p	c	c-p	c		c		u	p	r	p	u		
Rutile					u-r	p	r	r			r	r			
Wolframite	r	r			r-e				e						
Cassiterite	r														
Topaz		c													
Fe-U-phosphate				u			r		r						
Magnetite										r	u			c	
Ilmenite					r						r		r	r-u	
Fe-Mn-oxide			r								u				
Pyrite		p												p	c
Chalcopyrite		e-r									r				
Sphalerite															e
Stibnite				r											
Native silver			e[5]				e								

1. zircon as inclusions in biotite.
2. zircon as separate, euhedral grains.
3. occurs as minute grain in muscovite.
4. occurs as minute grain in chloroapatite.
5. occurs as minute grain in biotite.
6. contains elevated Hf.

a = abundant
c = common
u = uncommon
p = present
r = rare
e = extremely rare

* biotite-muscovite monzogranite
** transitional monzogranite
*** megacrystic monzogranite

within biotite and were liberated during crushing, however, their larger grain size suggests that they were discrete grains within the groundmass.

Two samples from the high-response monzogranite have zircon grains with a distinct Hf peak (Table 5-5). Whether the Hf-enrichment in the zircon is of magmatic or hydrothermal origin is not known.

As with the monazite, the close association of zircon with biotite indicates that rocks of low biotite content also have a low zircon content.

5.6.1.3 Apatite

The composition of apatites in the plutons was described previously but the SEM examination provides further insight as to the distribution and relative abundances of the various apatites. Normal apatites, for the purpose of discussion, are those without Mn or Cl enrichment. Normal apatite is relatively abundant in many of the rock types (Table 5-5). There is no correlation of normal apatite with degree of differentiation, as it is found in the more primitive biotite-bearing rocks as well as the leucomonzogranite and greisen samples. However, normal apatite is almost completely absent from the hydrothermally altered high-response and central monzogranite categories. By contrast, these are the rocks which contain Cl- and Mn-rich apatite. This further suggests a relationship between hydrothermal alteration and apatite composition.

5.6.1.4 Mn-apatite

Manganese-bearing apatite is abundant in the central and high-response monzogranites and the leucomonzogranite. One grain is present in a megacrystic monzogranite sample of the Larrys River Pluton. The Mn-apatite is more abundant in samples where normal apatite is absent or rare. The limitation of Mn-apatite to samples from areas of elevated radiometric response suggests a relationship between these two phenomena.

5.6.1.5 Chloroapatite

For this study the term chloroapatite includes true chloroapatite and Cl-rich apatite. As SEM analysis is only semi-quantitative, distinguishing the two species is impossible other than to say their spectra include a definite Cl peak. Chloroapatite was recognized in one sample of the central monzogranite, two of the high-response monzogranite and is most abundant in a sample of leucomonzogranite from the Beans Lake greisen zone.

Chlorine-bearing apatite occurs associated with brown masses in the high-response monzogranite (previously described). This generation of apatite is associated with hydrothermal alteration.

5.6.1.6 Fe-U-phosphate

A few examples of Fe-U-phosphate occur in samples from the regions of anomalous radiometric response. They have a similar mode of occurrence to the chloroapatite. Ford and Ballantyne (1983) described

Fe-U-phosphate in a sample from the Sangster Lake Pluton and found it contains a significant portion of the radioactivity in the rocks.

5.6.1.7 Fe-Mn garnet

Garnet (Fe-Mn variety) occurs in all rock types except the most primitive rock types of the Larrys River Pluton. Although present in many of the rocks, it is most abundant in the hydrothermally altered rocks of the Sangster Lake Pluton. It comprises 70-80% of the heavy mineral separate in a sample from the Beans Lake greisen zone.

5.6.1.8 Topaz

Topaz is a common constituent of a sample of leucomonzogranite from the Beans Lake greisen zone where it occurs as coarse, anhedral grains. It was not recognized in any other sample.

5.6.1.9 Wolframite and cassiterite

Both wolframite and cassiterite occur rarely in samples from the hydrothermally altered regions of the Sangster Lake Pluton and the Beans Lake greisen zone. Their presence is consistent with the hydrothermally altered nature of these rocks, but their scarcity is disappointing considering the advanced stage of alteration some of these rocks exhibit. Their restriction to the altered rocks from areas of anomalous radiometric response is significant.

5.6.1.10 Sulphides

Chalcopyrite, sphalerite and stibnite occur rarely in several samples (Table 5-5). Pyrite is common in the biotite-rich megacrystic monzogranite. This coincides with the petrography as pyrite occurs associated with biotite. Excluding the biotite-pyrite association, the remaining sulphides are not associated with any particular rock type or radiometric response category.

5.6.1.11 Native silver

A minute grain of native silver occurs in each of two samples. In one, it forms a minute inclusion in a biotite grain in the leucogranite from the Larrys River Pluton (F-6-G005; Table 5-5). In the second it occurs as a discrete, but small, grain in a high-response monzogranite sample. Whether or not the silver is associated with the magmatic or hydrothermal processes or silver paint from the electron microscope could not be determined. They remain mineralogical curiosities.

5.6.2 Comparison of Assemblages in Altered and Unaltered Rocks

The heavy mineral assemblages in unaltered versus altered rocks are distinctly different. The monzogranites of the Larrys River Pluton and the average-response monzogranite of the Sangster Lake Pluton (unaltered rocks) have heavy mineral assemblages dominated by monazite, zircon, normal apatite, ilmenite, magnetite and pyrite. This assemblage is typical of granitic rocks derived by magmatic processes. In fact, some of these phases (monazite, zircon, apatite) are used in

explaining the geochemical trends in Meguma Zone granitoids (Muecke and Clarke, 1981; Clarke and Muecke, 1985; MacDonald and Clarke, 1985).

The central and high-response monzogranites, leucomonzogranite and greisen (altered rocks) have a heavy mineral assemblage dominated by Mn-apatite, chloroapatite, garnet, Fe-U-phosphate, topaz, cassiterite and wolframite. Monazite and zircon are much less abundant than in the unaltered, biotite-rich monzogranites.

The assemblage of accessory phases in the altered rocks indicates the alteration fluid was enriched in P, Cl, Mn, F, U, Sn and W). The possibility exists that the accessory minerals are magmatic, but if so their composition confirms that the environment in which they formed was highly evolved.

5.7 SUMMARY

The geochemistry of the minerals within the rocks of the Sangster Lake and Larrys River Plutons is summarized below:

1. The rocks of both plutons from areas of average airborne radiometric response have plagioclases comparable in composition to those in the monzogranites of the South Mountain and Musquodoboit Batholiths (Ab_{80-90}).

2. The rocks from areas of the Sangster Lake Pluton that have anomalous radiometric response have plagioclases of more albitic composition (Ab_{90-100}). The plagioclase chemistry shows that albitization was a dominant alteration process.

3. Potassium feldspars from all phases and radiometric categories cannot be distinguished on their Or-Ab-An systematics. However, K-feldspars in unaltered and altered rocks can be distinguished by their levels of K_2O and P_2O_5.

4. Secondary muscovites and those of possible primary origin have subtle chemical differences. Secondary muscovites are enriched in Na and Si and depleted in Ti relative to primary muscovites.

5. Apatites in the plutons are of primary (magmatic) and secondary origin. The apatites have no consistent compositional difference between the modes. Regardless of mode of occurrence, apatites in the unaltered rocks are compositionally distinct from those in the altered rocks. Apatites in the altered rocks are enriched in Mn, Fe, Cl and U and are depleted in Ca relative to those in the unaltered rocks. This suggests that there has been at least partial compositional re-equilibration of the primary apatite during hydrothermal alteration that produced the secondary apatites.

7. The heavy mineral assemblage in the altered rocks is distinctly different from that in the unaltered rocks. The altered rocks have an assemblage dominated by Mn-apatite, chloroapatite, garnet, Fe-U-phosphate, topaz, cassiterite and wolframite. This assemblage is consistent with crystallization from either a

volatile-rich magma or a hydrothermal fluid. The unaltered rocks have an assemblage dominated by monazite, zircon, apatite, ilmenite, magnetite and pyrite. This assemblage is consistent with a magmatic origin.

CHAPTER 6

GEOCHEMISTRY

6.1 INTRODUCTION

This chapter presents major, minor and trace element analyses of 20 samples from the Sangster Lake Pluton and 13 from the Larrys River Pluton. The analyses include the major elements, CIPW normative calculations, Thornton-Tuttle differentiation indices (TTDI) and a minor and trace element suite consisting of Ba, Cu, F, Mo, Pb, Rb, Sn, Sr, Zn, U, W, B, Be, Li, Th, Zr, Ag and Au (Table 6-1). The analyses include all rock types and radiometric categories defined in the previous chapters. The sample locations relative to geology and airborne radiometric response are given in Figure 6-1.

Only two samples collected from the average-response monzogranite were fresh enough for analysis. To define better this rock type two unpublished analyses were provided by K. L. Ford of the Geological Survey of Canada.

Seventeen representative samples were analysed for the rare earth elements (La, Ce, Nd, Sm, Eu, Tb, Yb and Lu) and a suite of additional trace elements (Ta, Cs, Hf and Sc) (Table 6-2).

6.2 NON-PARAMETRIC CORRELATION

The entire data set (n=33) was treated statistically to produce Spearman Rank Correlation Coefficients using the Statistical Package for Social Sciences program at Dalhousie. The results are plotted as a

Table 6-1 Major, minor and trace element data and CIPW norms for samples of the Sangster Lake and Larrys River Plutons. Sample locations are given on Figure 6-1.

	LARRYS RIVER PLUTON												
SAMPLE #	F6-G002	LR-G009	LR-G010	LR-G011	LR-G012	F3-G004	LR-5	LR-6	F6-G004	F6-G008	F6-G009	LR-7	F6-G005
ROCK TYPE		MEGACRYSTIC MONZOGRANITE				TRANSITIONAL MONZOGRANITE			BIOTITE-MUSCOVITE MONZOGRANITE				LGNT
SiO_2	75.87	72.78	71.86	70.53	70.40	73.69	72.91	72.71	73.67	72.84	72.29	74.10	74.27
TiO_2	0.33	0.40	0.40	0.34	0.34	0.24	0.21	0.23	0.17	0.24	0.17	0.22	0.09
Al_2O_3	13.49	14.85	15.17	15.89	15.63	14.70	15.30	14.98	14.52	14.70	14.88	14.40	14.71
Fe_2O_3	0.04	0.56	0.12	0.05	0.36	0.04	0.00	0.01	0.00	0.00	0.00	0.04	0.00
FeO	1.82	1.70	2.03	1.68	1.56	1.52	1.42	1.49	1.47	1.59	1.33	1.37	0.69
MnO	0.05	0.05	0.05	0.04	0.04	0.05	0.07	0.05	0.05	0.04	0.04	0.04	0.06
MgO	0.64	0.75	0.73	0.60	0.65	0.53	0.55	0.58	0.51	0.47	0.39	0.46	0.14
CaO	0.69	1.08	1.03	0.95	1.01	0.69	0.78	0.85	0.65	0.74	0.58	0.68	0.39
K_2O	3.26	3.85	4.43	5.44	5.09	4.68	5.04	4.82	4.44	4.38	5.21	4.45	3.67
Na_2O	3.21	3.47	3.49	3.52	3.58	3.44	3.56	3.56	3.45	3.61	3.45	3.57	4.37
H_2O^+	0.66	1.02	0.81	0.73	0.57	0.80	0.85	0.82	0.70	0.66	0.58	0.42	0.38
H_2O^-	0.12	0.07	0.15	0.12	0.13	0.14	0.12	0.14	0.11	0.08	0.14	0.07	0.18
P_2O_5	0.25	0.26	0.25	0.26	0.27	0.25	0.26	0.25	0.27	0.30	0.30	0.29	0.38
CO_2	0.16	0.05	0.13	0.16	0.10	0.19	0.16	0.15	0.16	0.19	0.07	0.26	0.13
TOTAL	100.47	100.82	100.5	100.19	99.60	100.82	101.11	100.50	100.06	99.76	100.29	100.30	99.08
FE_2O_3 TOT	2.06	2.45	2.38	1.92	2.09	1.73	1.58	1.66	1.63	1.77	1.48	1.56	0.77
TTDI	92.52	89.50	91.13	92.21	91.15	93.42	93.11	92.91	93.66	93.56	94.57	93.94	95.39
CIPW NORMS (wt. %)													
Qz	45.03	36.36	33.94	28.73	29.06	35.63	32.31	33.06	36.85	35.57	33.27	36.42	35.56
Or	19.76	23.22	26.93	32.99	30.99	28.21	30.21	29.07	26.87	26.62	31.21	26.79	22.13
Ab	27.74	29.92	30.26	30.50	31.09	29.57	30.59	30.78	29.94	31.37	30.08	30.73	37.70
An	1.83	3.75	3.57	3.11	3.36	1.82	2.27	2.64	1.51	1.71	0.89	1.52	0.00
En	1.64	1.91	1.87	1.55	1.64	1.35	1.39	1.45	1.30	1.21	1.00	1.17	0.33
Fs	2.96	2.61	3.25	2.67	2.47	2.54	2.43	2.50	2.57	2.68	2.30	2.27	1.27
Ilm	0.64	0.77	0.78	0.65	0.66	0.47	0.39	0.45	0.31	0.47	0.31	0.41	0.16
Ap	0.59	0.59	0.60	0.60	0.62	0.59	0.59	0.59	0.62	0.72	0.72	0.66	0.90
Cor	4.14	3.73	3.47	3.20	3.13	3.39	3.23	3.03	3.59	3.53	3.43	3.24	3.61
TRACES (ppm)													
Ba	219	327	401	591	540	347	433	429	178	174	354	169	12
Cu	1	13	8	31	6	3	10	3	1	1	4	2	1
F	470	570	540	440	500	420	370	370	890	470	350	820	660
Mo	2	1	1	1	1	2	1	1	1	1	1	1	1
Pb	24	27	24	30	27	26	35	29	24	25	29	23	18
Rb	213	210	223	229	229	213	210	200	231	237	225	232	333
Sn	8	5	5	1	3	3	5	4	6	10	2	11	19
Sr	79	106	108	123	124	101	117	121	63	61	82	59	13
Zn	55	73	69	58	65	50	77	74	56	53	56	49	28
U	6.6	8.5	8.3	8.1	6.8	5.5	3.4	6.8	4.4	5.1	4	4.5	14
W	7	1	1	4	1	2	3	2	2	3	3	2	3
B	25	25	20	25	25	25	30	25	25	25	20	25	20
Be	6	2.5	3	4.5	2.5	5.5	5.5	4.5	5	6	5.5	3.5	10.5
Li	161	130	125	113	122	152	129	141	159	174	116	173	104
Th	12	14	16	12	12	8	8	9	7	7	8	7	2
Zr	100	122	115	97	108	79	80	85	71	71	81	70	29
Ag	0.1	0.1	0.1	0.1	0.1	0.1	0.1	0.1	0.2	0.1	0.1	0.1	0.1
Au(ppb)	8	21	1	10	1	5	6	1	1	1	1	3	1

Table 6-1 continued

	SANGSTER LAKE PLUTON										
SAMPLE #	F5-G001	F5-G010	SL-11	SL-12	SL-13	SL-14	SL-15	F-G018	SL-7	81-45	81-46
ROCK TYPE			CENTRAL MONZOGRANITE					AVERAGE-RESPONSE MONZOGRANITE			
SiO_2	72.99	73.06	72.19	72.21	72.68	71.82	73.00	73.41	75.07	73.80	75.50
TiO_2	0.17	0.15	0.29	0.23	0.21	0.24	0.17	0.10	0.17	0.14	0.14
Al_2O_3	14.99	15.36	15.43	15.34	15.27	15.83	15.11	14.95	13.87	14.40	13.50
Fe_2O_3	0.11	0.14	0.41	0.31	0.19	0.69	0.00	0.09	0.05	-	-
FeO	1.33	1.26	1.50	1.39	1.39	1.35	1.22	0.92	0.91	-	-
MnO	0.04	0.06	0.05	0.07	0.06	0.07	0.05	0.03	0.03	0.02	0.02
MgO	0.35	0.29	0.49	0.40	0.39	0.48	0.28	0.28	0.29	0.27	0.26
CaO	0.43	0.48	0.47	0.46	0.46	0.42	0.48	0.56	0.62	0.69	0.63
K_2O	3.94	3.95	4.13	3.98	4.03	4.33	3.81	5.23	4.55	4.70	4.37
Na_2O	3.89	4.03	3.59	3.89	3.82	3.80	4.08	3.51	3.31	3.76	3.54
H_2O^+	0.92	0.93	0.79	0.97	0.73	0.80	0.63	0.48	0.6	-	-
H_2O^-	0.14	0.14	0.19	0.20	0.10	0.13	0.16	0.25	0.1	-	-
P_2O_5	0.50	0.50	0.34	0.43	0.39	0.32	0.49	0.27	0.28	0.28	0.24
CO_2	0.09	0.17	0.13	0.08	0.13	0.01	0.07	0.11	0.15	-	-
TOTAL	99.55	100.38	99.81	99.58	99.75	100.16	99.39	99.94	99.90	100.00	100.10
FE_2O_3 TOT	1.59	1.54	2.08	1.85	1.73	2.19	1.34	1.11	1.06	0.91	0.91
TTDI	94.11	93.79	92.38	93.12	93.49	92.05	94.30	94.68	94.53	97.19	97.32
CIPW NORM (wt. %)											
Qz	36.68	35.18	36.06	35.06	35.89	33.09	35.76	33.04	38.55	33.72	37.97
Or	23.95	23.83	25.07	24.21	24.48	26.18	23.12	31.42	27.43	27.44	25.46
Ab	33.48	34.79	31.25	33.85	33.11	32.78	35.41	30.22	28.54	32.16	30.23
An	0.00	0.00	0.18	0.00	0.00	0.00	0.00	1.05	1.33	1.12	1.08
En	0.87	0.71	1.26	1.02	1.00	1.22	0.69	0.68	0.71	0.90	0.87
Fs	2.30	2.20	2.45	2.35	2.40	2.24	2.10	1.61	1.49	0.07	0.07
Ilm	0.31	0.29	0.55	0.45	0.39	0.47	0.31	0.19	0.31	0.87	0.00
Ap	0.84	1.18	0.79	1.00	0.93	0.76	1.17	0.61	0.63	0.67	0.57
Cor	4.55	4.54	5.14	4.75	4.75	5.00	4.38	3.19	3.07	2.75	2.58
TRACES (ppm)											
Ba	26	72	52	26	34	28	20	371	261	360	310
Cu	1	2	1	2	1	3	2	1	1	9	5
F	610	660	570	570	570	700	700	310	220	355	400
Mo	1	1	1	1	1	1	1	2	1	-	-
Pb	17	8	20	19	18	18	17	30	26	21	20
Rb	293	385	267	339	294	357	367	208	191	180	160
Sn	12	19	9	14	11	15	20	2	1	10	4
Sr	17	57	22	19	17	17	51	99	79	100	70
Zn	59	75	80	81	72	94	63	44	39	29	44
U	10	15.4	12.2	17.8	10.9	20.1	15.5	4.6	3.9	3.5	2.5
W	4	4	4	4	5	5	5	4	4	2	2
B	25	15	20	25	40	20	65	15	25	-	-
Be	7.5	23.0	4.5	5.0	4.5	4.5	7.5	5.5	3.0	4.0	3.5
Li	217	271	135	234	210	263	246	92	95	75	60
Th	4	3	7	5	4	6	6	4	5	3	4
Zr	57	100	78	61	62	94	45	57	61	30	40
Ag	0.1	0.05	0.2	0.1	0.1	0.2	0.1	0.1	0.1	-	-
Au(ppb)	1	10	2	4	3	1	1	1	1	-	-

Table 6-1 continued

	SANGSTER LAKE PLUTON								
SAMPLE #	F-G022	F5-G004	F5-G007	F-G024	F-G020	F-G001	F-G003	F-G004	F-G005
ROCK TYPE		LEUCOMONZOGRANITE			GREISEN	HIGH-RESPONSE MONZOGRANITE			
SiO_2	73.19	73.25	73.55	74.38	62.34	72.62	72.30	72.41	72.86
TiO_2	0.02	0.03	0.07	0.03	0.10	0.11	0.11	0.16	0.12
Al_2O_3	14.81	15.05	15.27	14.60	22.16	15.05	15.31	15.09	14.92
Fe_2O_3	0.00	0.00	0.09	0.00	0.86	0.10	0.11	0.44	0.11
FeO	0.52	0.45	0.37	0.58	1.19	1.02	1.03	1.05	1.02
MnO	0.06	0.03	0.04	0.05	0.07	0.05	0.05	0.05	0.05
MgO	0.10	0.05	0.06	0.06	0.39	0.24	0.25	0.34	0.25
CaO	0.50	0.47	0.63	0.77	0.34	0.61	0.44	0.47	0.50
K_2O	3.61	3.58	3.38	3.15	6.91	3.76	3.84	3.97	3.69
Na_2O	4.67	4.58	4.89	4.65	3.18	4.14	4.06	3.91	4.03
H_2O^+	0.56	0.60	0.52	0.56	2.06	1.23	1.15	0.95	1.02
H_2O^-	0.18	0.17	0.12	0.17	0.28	0.12	0.20	0.11	0.09
P_2O_5	0.33	0.62	0.75	0.87	0.53	0.62	0.48	0.47	0.51
CO_2	0.19	0.19	0.10	0.10	0.32	0.19	0.15	0.19	0.19
TOTAL	98.56	98.70	99.72	99.79	100.45	99.74	99.28	99.50	99.27
FE_2O_3 TOT	0.58	0.50	0.50	0.64	2.18	1.23	1.25	1.61	1.24
TTDI	95.57	94.86	93.49	94.45	86.64	93.82	93.79	93.01	93.89
CIPW NORM	(wt. %)								
Qz	33.11	33.73	32.41	33.30	16.87	35.09	34.98	32.55	33.77
Or	21.91	21.56	18.94	18.20	42.05	22.84	23.41	24.16	22.48
Ab	40.56	39.56	42.44	42.32	27.72	35.89	35.40	36.12	37.38
An	0.00	0.00	0.00	0.00	0.00	0.00	0.00	0.00	0.00
En	0.26	0.13	0.15	0.15	1.00	0.61	0.64	0.85	0.64
Fs	1.04	0.83	0.64	1.10	2.18	1.85	1.88	1.79	1.82
Ilm	0.04	0.06	0.16	0.06	0.20	0.20	0.20	0.31	0.24
Ap	0.79	1.47	2.04	2.04	1.27	1.48	1.15	1.12	1.22
Cor	3.22	3.73	4.25	3.58	9.73	4.30	4.61	4.50	4.43
TRACES (ppm)									
Ba	11	14	38	8	12	26	17	24	21
Cu	6	8	2	2	7	1	1	2	2
F	370	236	310	760	970	760	700	500	635
Mo	2	1	0.7	2	1	2	2	1	1
Pb	15	13	11	14	22	14	16	19	17
Rb	315	423	506	441	917	432	391	347	375
Sn	30	25	15	27	72	19	21	22	20
Sr	12	95	53	88	42	72	32	33	29
Zn	12	16	25	15	66	43	52	69	57
U	9.7	23	16.4	15.5	56.7	16	13.9	13.4	13.8
W	2	1	4	1	3	4	10	5	3
B	20	25	9	20	25	20	30	30	20
Be	5.5	29.5	50.0	12.5	11.5	12.5	9.0	14.0	13.0
Li	69	64	60	47	237	248	246	252	228
Th	1	1	2	1	2	3	3	5	4
Zr	19	20	18	15	38	42	40	57	48
Ag	0.1	0.1	0.05	0.1	0.2	0.1	0.1	0.1	0.1
Au(ppb)	2	1	25	1	6	2	1	18	2

Table 6-2 Rare earth element data and levels of Cs, Hf, Sc and Ta for representative samples of the Sangster Lake and Larrys River Plutons.

	GREISEN	LEUCOMONZOGRANITE		MONZOGRANITES												
				HIGH-RESPONSE			CENTRAL		AVG-RESP	TRANSITIONAL		BIOT-MUSC		MEGACRYSTIC		
SAMPLE #	F-G020	F-G022	F5-G004	F6-G005	F-G001	F-G003	F-G005	SL-13	SL-15	SL-7	LR-5	LR-6	LR-7	F6-G004	LR-G009	LR-G010	LR-G011
La	13.28	0.83	0.85	3.70	6.76	6.35	7.76	11.93	7.52	9.80	15.80	17.70	12.90	13.30	29.80	28.60	20.20
Ce	9.17	2.86	3.10	7.74	14.00	14.98	15.96	22.46	15.66	19.50	31.00	33.60	26.40	26.90	56.70	55.40	39.90
Nd	5.93	1.31	1.58	3.64	7.67	7.07	7.42	11.58	7.42	9.80	11.10	16.50	14.90	13.10	29.00	28.00	15.70
Sm	1.43	0.27	0.29	0.92	2.06	1.97	2.20	3.16	2.05	3.00	3.90	4.42	3.50	3.63	6.71	6.60	4.68
Eu	0.07	0.04	0.04	0.06	0.09	0.11	0.09	0.12	0.09	0.492	0.701	0.725	0.342	0.342	0.684	0.743	0.799
Tb	0.31	0.05	0.06	0.13	0.26	0.25	0.27	0.40	0.26	0.362	0.573	0.495	0.531	0.483	0.594	0.557	0.413
Yb	0.50	0.20	0.16	0.47	0.29	0.36	0.30	0.44	0.28	-	1.00	0.60	0.685	0.86	1.25	1.02	1.00
Lu	0.061	0.032	0.022	0.057	0.042	0.055	0.049	0.06	0.039	0.05	0.085	-	0.13	0.088	0.182	0.162	0.131
SUM 8 REE	30.75	5.59	6.10	16.72	31.17	31.15	34.05	50.15	33.32	43.00	64.16	74.04	59.39	58.70	124.92	121.08	82.82
La_N/Lu_N	22.2	2.6	3.4	6.6	16.5	11.9	16.3	19.9	19.9	20.6	19.3	-	10.3	15.6	16.8	18.1	15.8
Eu/Eu^*	0.14	0.43	0.39	0.20	0.14	0.18	0.13	0.12	0.14	0.53	0.56	0.54	0.30	0.30	0.35	0.39	0.58
Cs	41.5	20.9	20.3	28.1	37.0	36.0	35.3	26.5	49.8	9.3	12.4	11.8	17.4	16.7	13.1	13.0	10.8
Hf	2.47	1.35	1.15	1.46	1.81	1.57	1.78	2.08	1.72	1.90	2.30	2.60	2.30	2.40	4.00	3.90	2.80
Sc	2.33	0.70	0.51	1.52	2.29	2.35	2.34	3.35	2.39	2.08	3.39	3.73	3.80	3.87	5.51	5.49	4.34
Ta	10.30	5.49	7.68	5.25	6.69	5.97	5.17	3.40	4.23	2.90	3.50	2.90	3.90	4.00	1.30	2.90	2.80

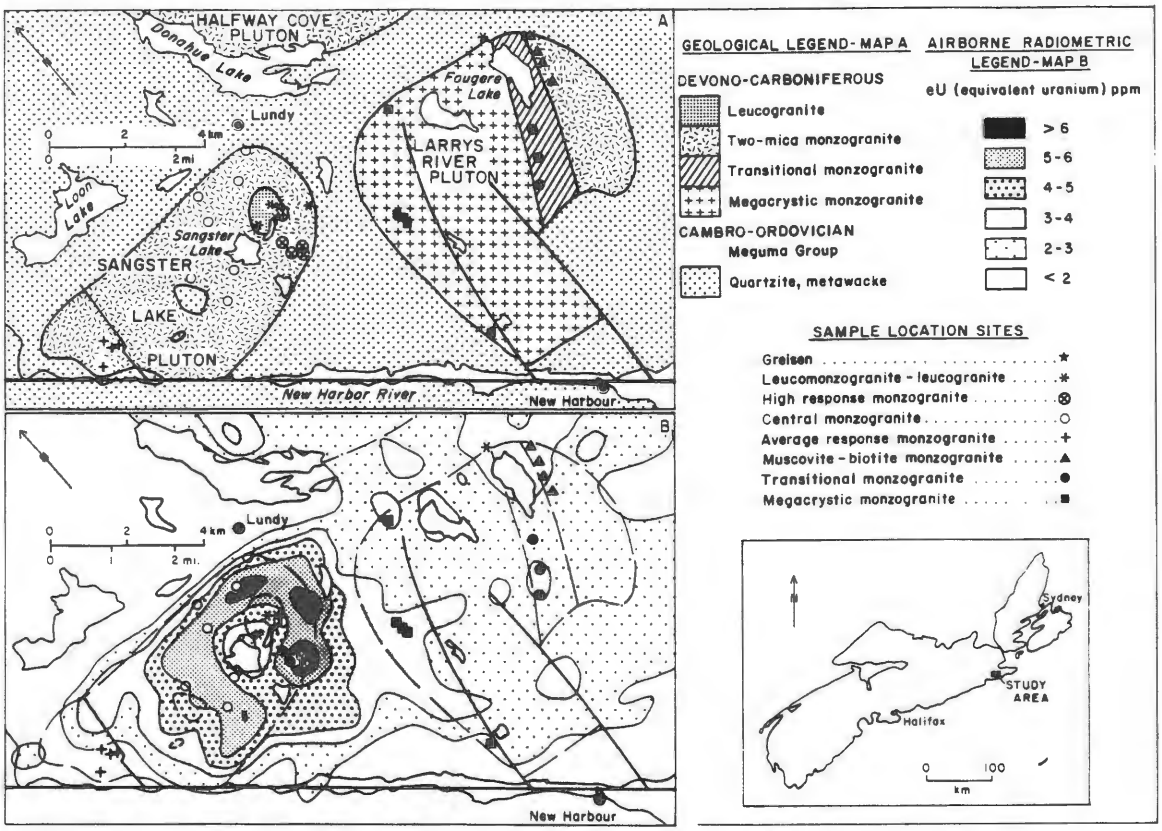

Figure 6-1 A. Generalized geologic map with sample locations, Sangster Lake and Larrys River Plutons. B. Map showing the sample location sites relative to airborne spectrometric results for equivalent uranium (eU).

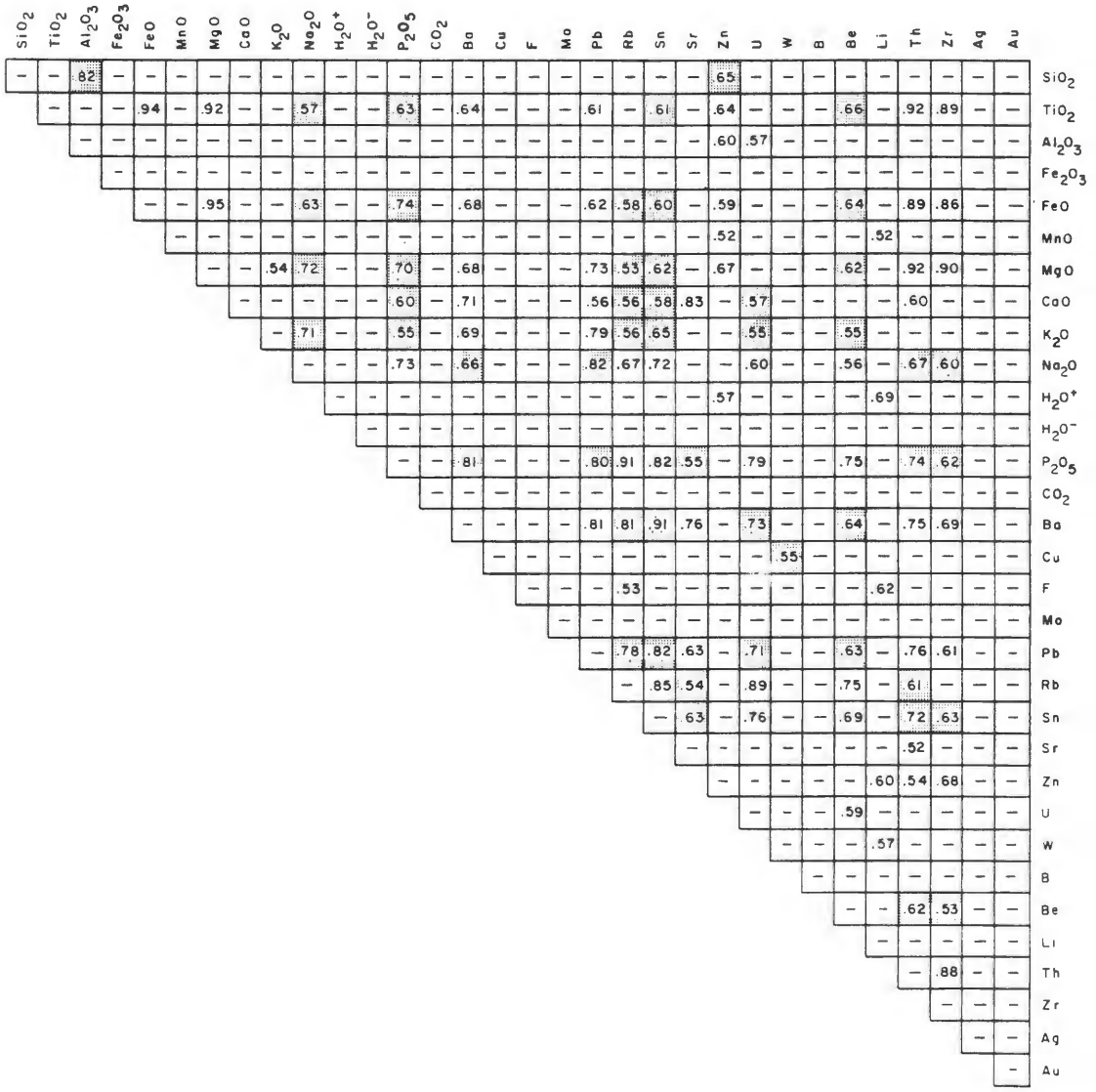

Figure 6-2 Spearman Rank Correlation Matrix of coefficients of the total major and trace element data from the Sangster Lake and Larrys River Plutons (n=33). Coefficients of >99.9% significance are indicated as positive (clear) and negative (screen) correlations.

correlation matrix in Figure 6-2. This non-parametric statistical method was used to determine inter-element relationships within the data set (Appendix III). The coefficients define a positive association of 99.9% significance for a granophile element suite consisting of U, Sn, Rb, Be, P_2O_5, Na_2O, Li and F. In contrast, the elements of this granophile suite have a negative correlation with such elements as K_2O, Th, Pb, Ba and Sr. The observed positive and negative inter-element relationships have significance when considered in conjunction with the geological and petrographic data.

6.3 MAJOR ELEMENTS

Harker variation plots of the major oxides, normative corundum and TTDI are compared with the data fields for granodiorite, monzogranite and minor intrusions of leucomonzogranite, porphyry and aplite for the South Mountain and Musquodoboit Batholiths (Fig. 6-3). These plots show the rock types from the thesis area have major element geochemical compositions comparable to similar rocks within other Meguma Zone intrusions and fall outside the granodiorite field.

Harker plots are poor indicators of differentiation for rocks with SiO_2 levels confined to a range from 70-75%. They are included here though, as they allow the major element levels in the rocks from this study to be compared with those in other Meguma Zone granitoid suites. This has value for mineral exploration and bedrock mapping purposes as it shows that, although some of the monzogranites have been extensively altered, this is not necessarily recognizable in major element geochemical levels.

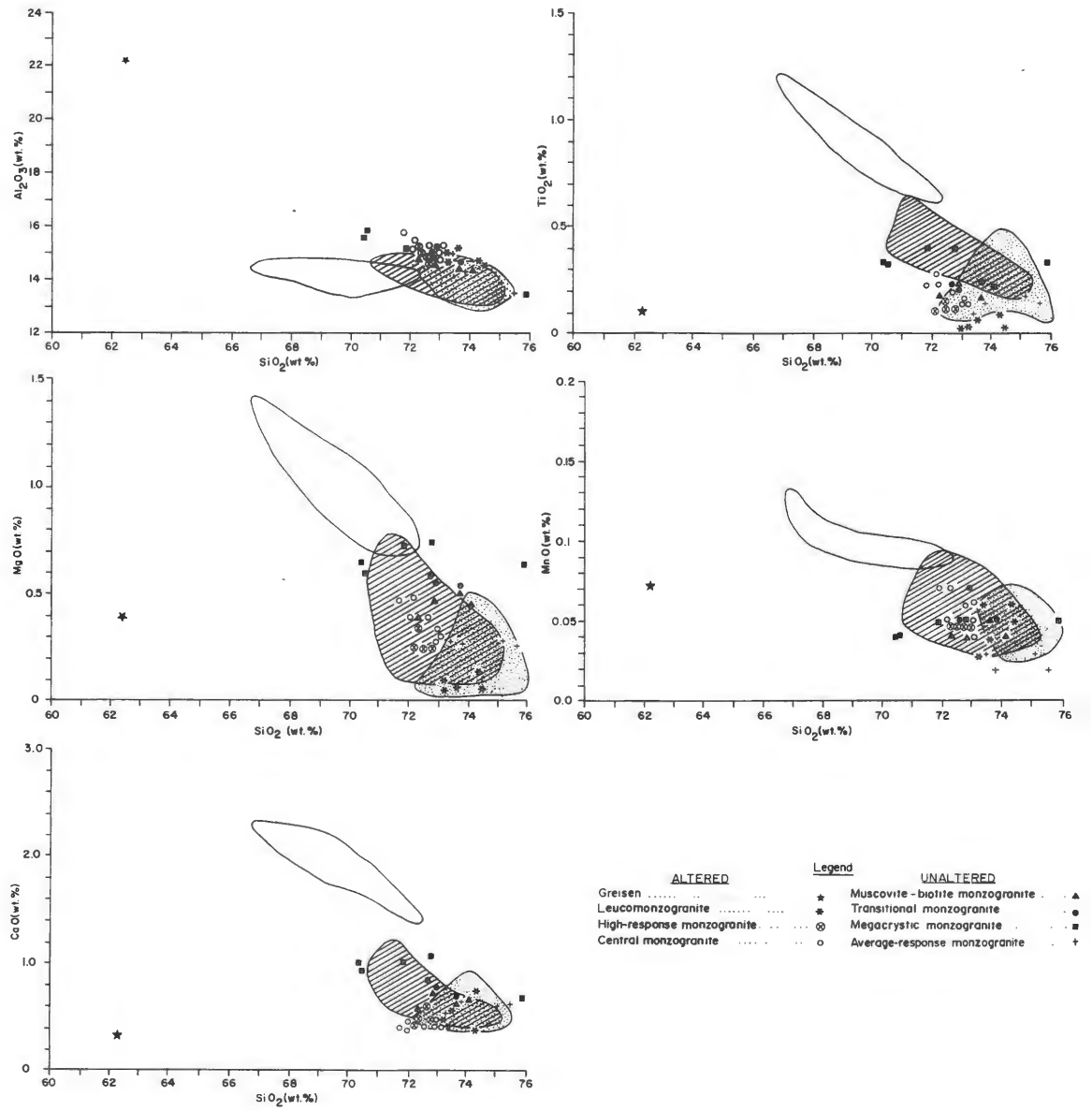

Figure 6-2 Spearman Rank Correlation Matrix of coefficients of the total major and trace element data from the Sangster Lake and Larrys River Plutons (n=33). Coefficients of >99.9% significance are indicated as positive (clear) and negative (screen) correlations.

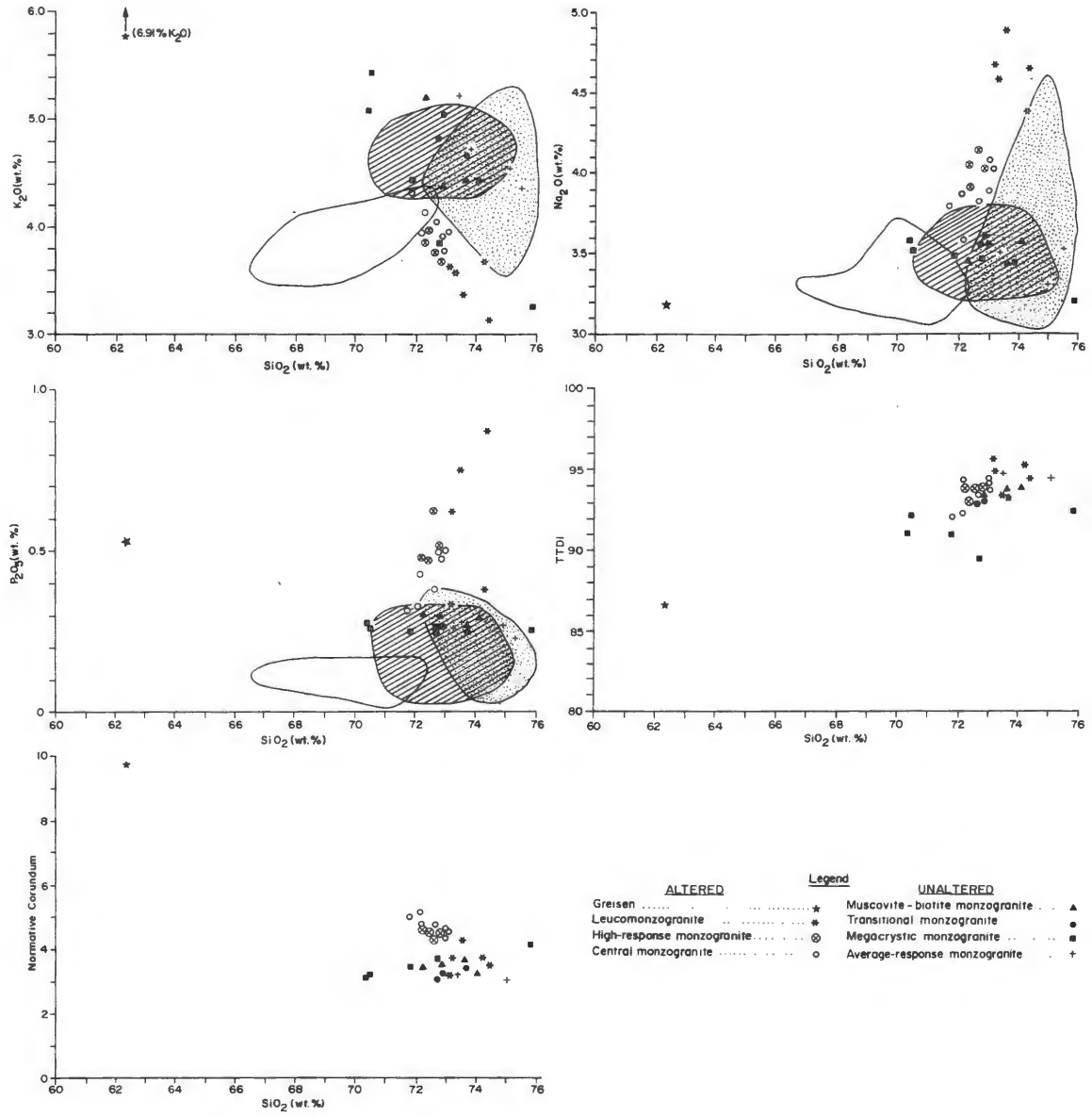

Figure 6-3 cont'd

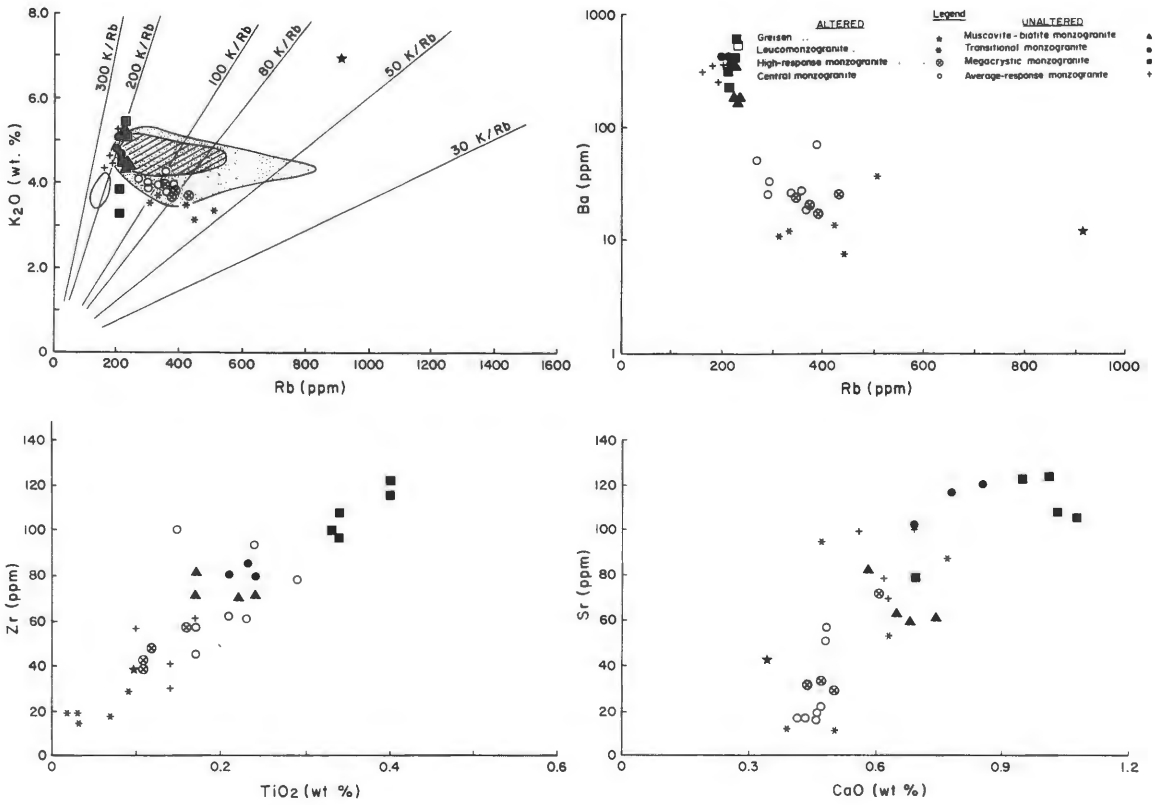

Figure 6-4 Plots of K_2O, CaO, TiO_2, Zr, Ba, Rb and Sr in combinations as indicators of differentiation. Fields of Meguma Zone granitoids are designated in Figure 6-3.

Better elemental indicators of differentiation are plots using the major elements TiO_2 and CaO and the trace elements Zr, Rb, Sr and Ba. These are provided in Figure 6-4 and are discussed in the text.

6.3.1 Larrys River Pluton

The three varieties of monzogranite of the Larrys River Pluton have major element, TTDI and normative corundum contents that fall within, or straddle the monzogranite field of the South Mountain and Musquodoboit Batholiths.

Exceptions are the five samples of megacrystic biotite monzogranite. This rock type underlies most of the pluton (Fig. 6-1), but because of its characteristic deep weathering, only 5 samples were fresh enough for whole-rock analysis. The rock has a considerable range of SiO_2 and K_2O, but the remainder of the major oxides exhibit little variation. Potassium feldspar megacrysts comprise 20-50% of the rock. Conceivably, the 3 kg sample size used for coarse-grained granitoid rocks was too small and even with a considerably larger sample, the large variation in modal K-feldspar may have a significant effect on the overall chemistry, especially, SiO_2, K_2O and Ba. An increasing amount of modal K-feldspar decreases the amount of free quartz and increases the amount of K_2O and Ba. The scatter shown by samples of this monzogranite in Figure 6-3 is likely a reflection of the extreme variability of modal K-feldspar. Smooth trends exhibited by elements such as Zr and Ti, which do not enter the K-feldspar structure, further support this conclusion (Fig. 6-4). Perhaps the overall chemical composition of the megacrystic monzogranite may be better approximated by an average of the 5 samples.

The transitional and the biotite-muscovite monzogranites are less megacrystic and more homogeneous and hence do not have the large variability in SiO_2 and K_2O. The major element levels of these rocks invariably fall within the monzogranite field of the South Mountain and Musquodoboit Batholiths.

A leucogranite from the pluton (F6-G005 in Table 6-1) has major element concentrations comparable to those of the minor intrusions of leucomonzogranite and porphyry of the South Mountain Batholith.

The monzogranites are all peraluminous (i.e. $Al_2O_3/CaO+Na_2O+K_2O>1$) and the levels of normative corundum (avg. 3.43 wt.%) are considerably higher than those of monzogranites from both the South Mountain (avg. 2.16 wt.%; McKenzie and Clarke, 1975) and Musquodoboit Batholiths (avg. 2.75 wt.%; MacDonald and Clarke, 1985). MacDonald and Clarke (1985) found the Musquodoboit Batholith is more peraluminous than the western portion of the South Mountain Batholith (McKenzie and Clarke, 1975), but comparable to the eastern portion (Smith, 1974). They also note that two small intrusions adjacent to the Musquodoboit Batholith have higher normative corundum levels, suggesting the granitoid rocks of the eastern Meguma Zone may be characteristically more peraluminous. The data from this study support their contention although the reason for the elevated peraluminous levels is not known.

McKenzie and Clarke (1975), Muecke and Clarke (1981) and MacDonald and Clarke (1985) found that fractional crystallization of biotite, plagioclase and accessory zircon and apatite is the differentiation process by which the South Mountain and Musquodoboit Batholiths formed. The chemical data from the Larrys River Pluton are consistent with this

model. Smooth, decreasing trends exhibited by elements in Figure 6-4 are consistent with magmatic differentiation by crystallization of plagioclase (Sr vs CaO), K-feldspar (Ba vs Rb; K_2O vs Rb), zircon and biotite (Zr vs TiO_2).

6.3.2 Sangster Lake Pluton

The geochemical results from samples from the Sangster Lake Pluton are also given in Figures 6-3 and 6-4. There are some interesting deviations from the Larrys River Pluton and the established trends for Meguma Zone granitoids.

The average-response monzogranite has major element concentrations comparable to the levels from the monzogranites of the Larrys River Pluton and the South Mountain and Musquodoboit Batholiths. The central and high-response monzogranites, on the other hand, vary significantly in that their levels of TiO_2, CaO and K_2O are lower and Al_2O_3, Na_2O and P_2O_5 are higher than the established trends (Fig. 6-3). The variation is most striking with K_2O, Na_2O and P_2O_5 where their levels are more comparable to the field of highly evolved minor intrusions than to that of the monzogranites from the South Mountain and Musquodoboit Batholiths.

The leucomonzogranite samples also deviate from the established trends of similar rocks in the Meguma Zone granitoids. Most variation is with K_2O, which is lower, and Na_2O and P_2O_5, which are higher.

The monzogranites of the Sangster Lake Pluton are even more corundum normative (avg. 4.17 wt.%) than the Larrys River Pluton. The normative corundum vs SiO_2 plot shows a trend of constant to slightly increasing normative corundum with increasing SiO_2 (Fig. 6-3). The

central and high-response monzogranite categories deviate from this trend by having lower SiO_2 and higher normative corundum. This is possibly a reflection of fluid-rock interaction involving alkalis in these rocks. The elemental indicators of magmatic differentiation (Fig. 6-4), particularly the K_2O vs Rb plot, show the altered rocks have elemental levels typical of rocks in which a highly evolved fluid phase has had an important evolutionary role.

6.3.3 Albitization Trend

The behavior of K_2O, Na_2O, CaO and P_2O_5 is of particular interest. Ford and Ballantyne (1983) recognized an "albitization trend" in their geochemical data from the Sangster Lake Pluton. They defined this as a positive correlation of U content associated with an increase of the Na_2O/K_2O ratio.

The plots of Na_2O versus SiO_2 (Fig. 6-3) and K_2O-Na_2O-CaO (Fig. 6-5) verifies that there is a trend toward Na enrichment in the Sangster Lake Pluton. The trend is manifest within samples from the central and high-response monzogranites and the leucomonzogranite. Firstly, note that in both these plots, the average-response monzogranite and the monzogranites of the Larrys River Pluton fall within the field of Meguma Zone monzogranites. Secondly, note the deviation toward Na_2O enrichment shown by the hydrothermally altered samples. A mineralogical expression of the albitization trend is the widespread presence of secondary albite in these rocks (Chapter 5; Fig. 5-1).

A plot of P_2O_5 vs Na_2O/K_2O reveals a strong positive correlation of elevated P associated with the progressive Na-enrichment (Fig. 6-6). Mineralogically this is reflected in formation of discrete apatite

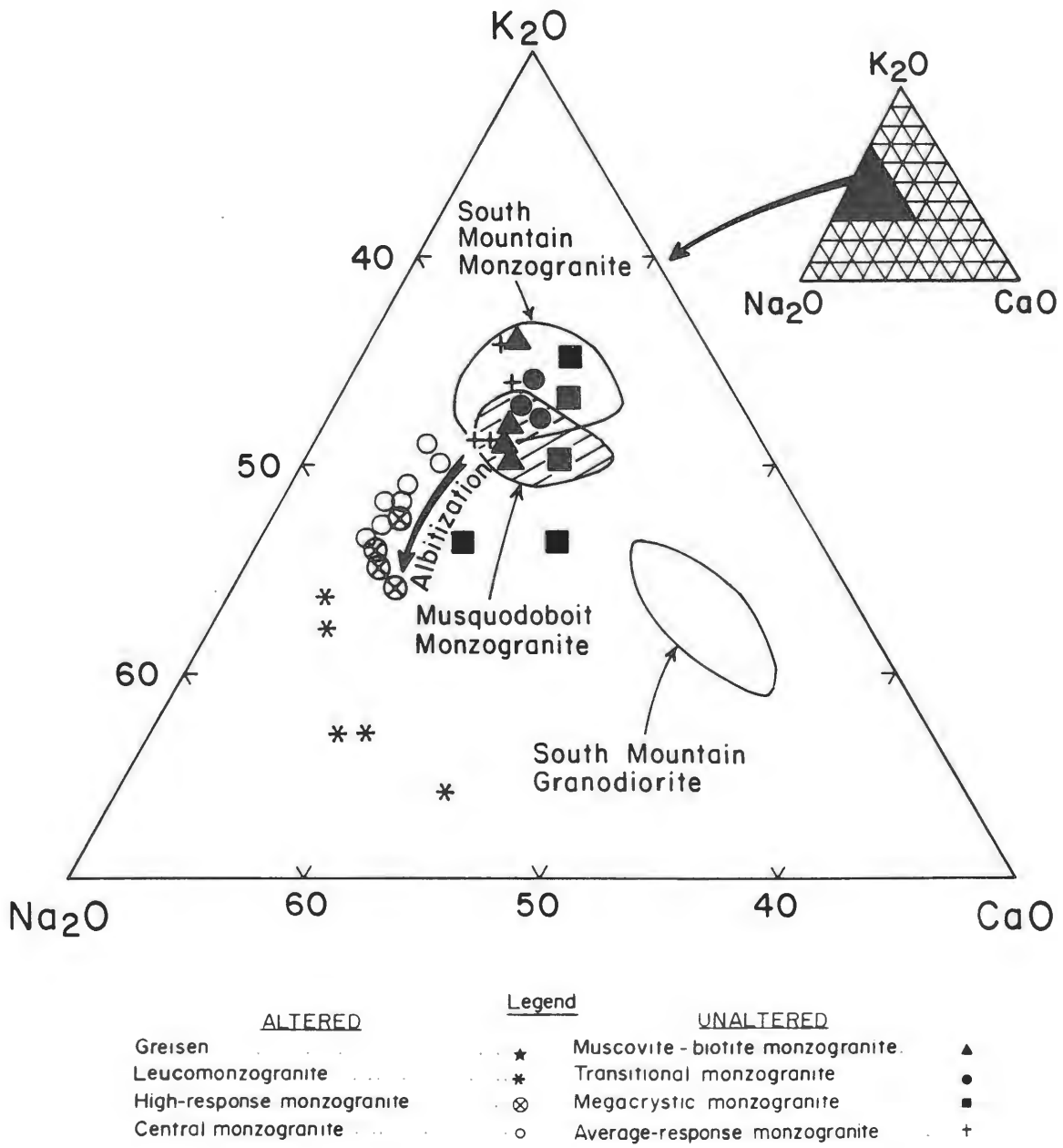

Figure 6-5 A plot of K_2O-Na_2O-CaO for geochemical data from the Sangster Lake and Larrys River Plutons.

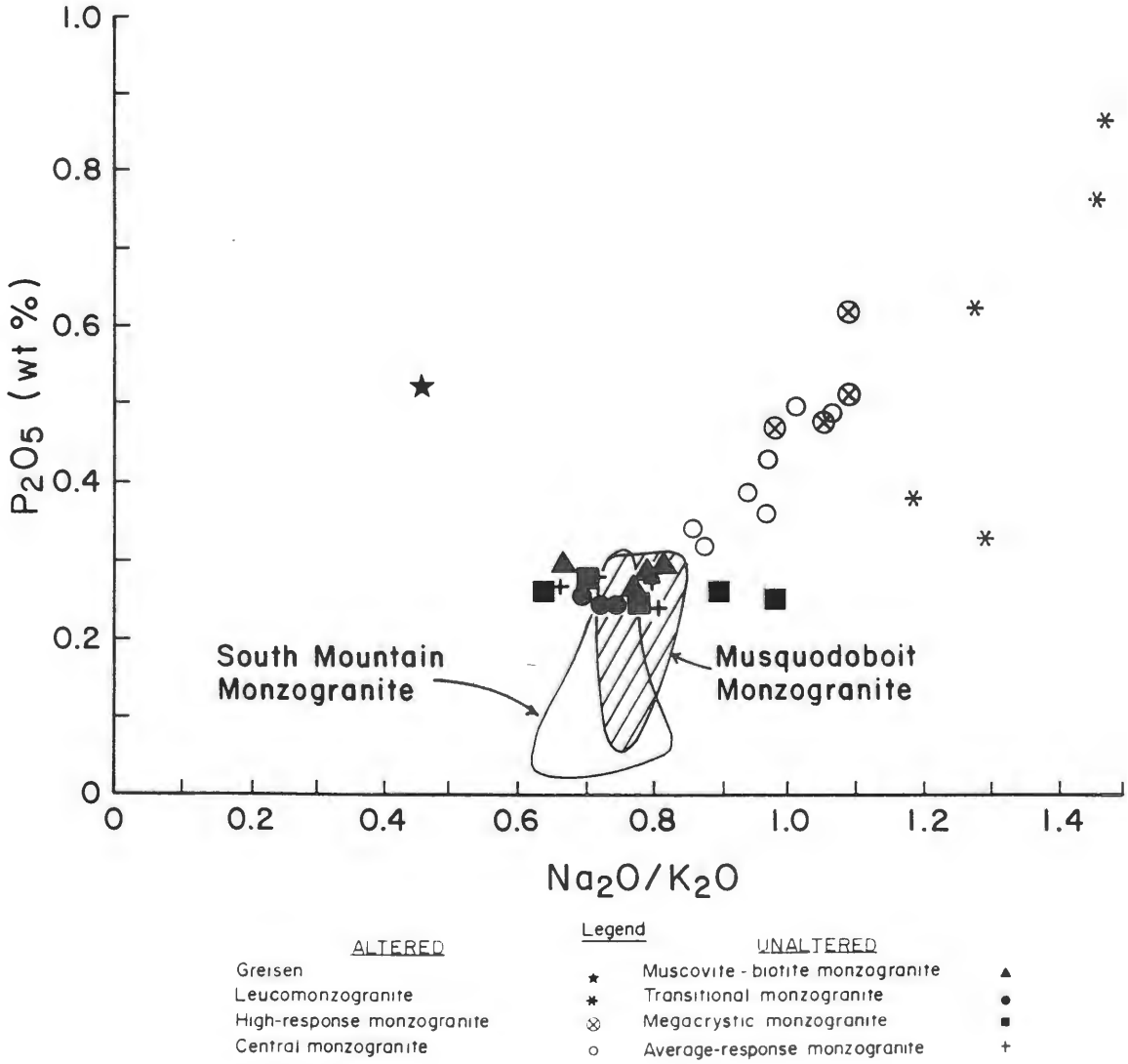

Figure 6-6 A plot of P_2O_5 vs the Na_2O/K_2O ratio for the Sangster Lake and Larrys River Pluton data.

grains within the secondary albites. This suggests that P was mobile during the late-stage fluid-rock interactions. The Ca released by albitization of the original plagioclase was immediately combined with P in the fluid phase to produce the secondary apatite.

Logothetis (1984) described the mobility of P and subsequent phosphate precipitation during albitization at some mineral deposits in the South Mountain Batholith. He cited a breakdown of primary K-feldspar and release of its minor amount of phosphorus as a source for the element to the hydrothermal fluid.

This model, although attractive, cannot be directly applied in this study as there is an increase in P_2O_5 content in K-feldspar in the hydrothermally altered rocks compared with that in unaltered rocks (Chapter 5). Another significant difference is the scale over which the two hydrothermal systems were operative. With this study, the volume of rock that has been albitized is in the order of cubic kilometers while the examples described by Logothetis (1984) are metasomatized selvages to fractures in the order of cubic meters or less. Even though there are these differences, both studies show a mobility of P with hydrothermal alteration.

The arguments presented above indicate that the Na_2O/K_2O ratio and the level P_2O_5 can be used effectively as alteration indices whereby the behavior of trace elements during progressive alteration can be assessed.

6.3.4 Source of Sodium and Phosphorus in the Hydrothermal Fluid

The geochemical and petrographic data just described show both Na and P were dominant in the hydrothermal fluid. It remains to be

demonstrated that these elements can be enriched to such levels by magmatic differentiation or whether either or both were introduced from a non-magmatic source.

6.3.4.1 Sodium

Sodium enrichment with magmatic differentiation is well established, but experimental studies show that in order to crystallize albite from a granitic melt the system must contain a highly elevated concentration of volatiles (Manning, 1981; Pichavant, 1981; Cerny et al., 1985; London, 1987). Much of the Sangster Lake Pluton was altered by a Na-rich fluid phase. Such Na enrichment is a feature common to late-stage granitoid differentiates, but the assumption that the Na is entirely of magmatic origin needs discussion.

A possible source for introduced Na are the metasediment sequences the plutons intrude. Previous studies of the metasediments found that greenschist facies regional metamorphic wackes contain a significant amount of albite of metamorphic origin (An_{0-4}; Chu, 1978; Liew, 1979; Cullen, 1983). A granitic pluton intruding such rocks will encounter a metamorphic water which is in equilibrium with the surrounding low-grade mineral assemblage (i.e. rocks in which albite is a major constituent). Therefore the water will likely have a significant Na component.

A melt intruding such metasediments will likely interact, to some degree, with the rocks through which it passes. A melt digesting metawacke will assimilate large quantities of major elements such as SiO_2, Al_2O_3, Na_2O, K_2O, FeO and H_2O. These major elements could alter

the overall composition of the melt, but all are easily accommodated in the normal rock-forming minerals.

If, at the time of emplacement, the melt coexists with an exsolved fluid phase, then mixing of the magmatic fluid with the metamorphic pore fluid is likely to occur. The mixing will produce a fluid with a concentration of elements intermediate between that of the two component fluids and dependent on the respective volumes of each fluid. The content of Na will therefore be intermediate between that of the magmatic and metamorphic fluids.

If albitization such as has affected the Sangster Lake Pluton is predominantly the result of Na introduced by influx of metamorphic water, then examples of such alterations should be commonplace throughout the Meguma Zone wherever plutons are emplaced in greenschist facies metawacke sequences. This is not the case, for example the Larrys River Pluton has intruded identical rocks but albitization of any significance is absent even within contact zones. In fact, significant albitization is only associated with the latest stage granitoid and paraintrusive rocks both of which are likely sources of considerable magmatic water.

The whole-rock ^{18}O data with this study (described later) only indicate the hydrothermal alteration was either solely the result of an internally generated magmatic fluid or the result of a magmatic fluid which has mixed with a fluid of similar $\delta^{18}O$ composition. Kontak (1987), however, documented sulphur isotope data from the East Kemptville Sn deposit that show the mineralizing fluids were dominantly of

magmatic origin. Since albitized rocks are common at East Kemptville, enrichment of Na in a dominantly magmatic fluid is possible.

Lastly, the geochemical data (described earlier) show a positive correlation of Na with the granophile elements both with the comagmatic and paraintrusive rocks (Figs. 6-2; 6-7). This implies the fluid phase had a significant magmatic component, as many of the granophile elements would not be enriched in metamorphic waters.

6.3.4.2 Phosphorus

Phosphorus in low-calcium granite melts decreases with magmatic differentiation (Gribble, 1969). The petrography and geochemical data of the present study show that, in the comagmatic rocks, normal levels of P are found, but in the paraintrusive rocks elevated levels occur (Figs. 6-6; 6-7). As with Na, the metasedimentary country rocks, especially slate sequences, are a possible source of P.

Recent studies have shown that, although in purely magmatic systems P decreases with differentiation, once the system becomes increasingly dominated by an exsolved fluid phase P increases concomitantly with the volatiles (Cerny et al., 1985; London, 1987). Examples of P mobility in fluid-dominated systems in the Meguma Zone are described by Chatterjee et al. (1982) and Logothetis (1984).

In this study P has a positive correlation with the granophile elements as well as indicator elements of extreme magmatic differentiation. This suggests the P in this system is magmatically derived with little or no input from the metasediments. Similar correlations were found by Kontak (1987) in the paraintrusive rocks hosting the East Kemptville Sn deposit. He also presents sulphur isotope data to show

the system was dominantly magmatic through all alteration facies including the Sn-rich topaz greisens.

6.4 TRACE ELEMENTS

The trace element analyses for samples of the Larrys River and Sangster Lake Plutons are given in Table 6-1. The following description of the geochemical relations deals essentially with the positively and negatively correlated element suites defined by the non-parametric statistical treatment in Figure 6-2. The positively correlated suite consists of the trace elements U, Sn, Rb, Be, Li and F and the major elements P_2O_5 and Na_2O. An elemental suite consisting of K_2O, Th, Pb, Ba and Sr is negatively correlated with the elements of the positive suite.

6.4.1 Uranium

The trace element levels of U decrease slightly (Fig. 6-7) from the megacrystic monzogranite (mean 7.7 ppm) to the average-response monzogranite (mean 4.5 ppm). Decreasing U is opposite to the established behavior of this element with increasing differentiation. Possibly, the decrease is simply a result of the small number of samples defining each group. An alternative interpretation is that U in the unaltered rocks occurs in accessory minerals such as zircon and monazite and thus, with Th, decreases concomitantly with them. The U vs Th plot supports this interpretation (Fig. 6-7).

The central and high-response monzogranites and the leucomonzogranites (altered rocks) show a well-defined, positive correlation with both Na_2O/K_2O and P_2O_5. The presence of secondary apatite, Cl-apatite

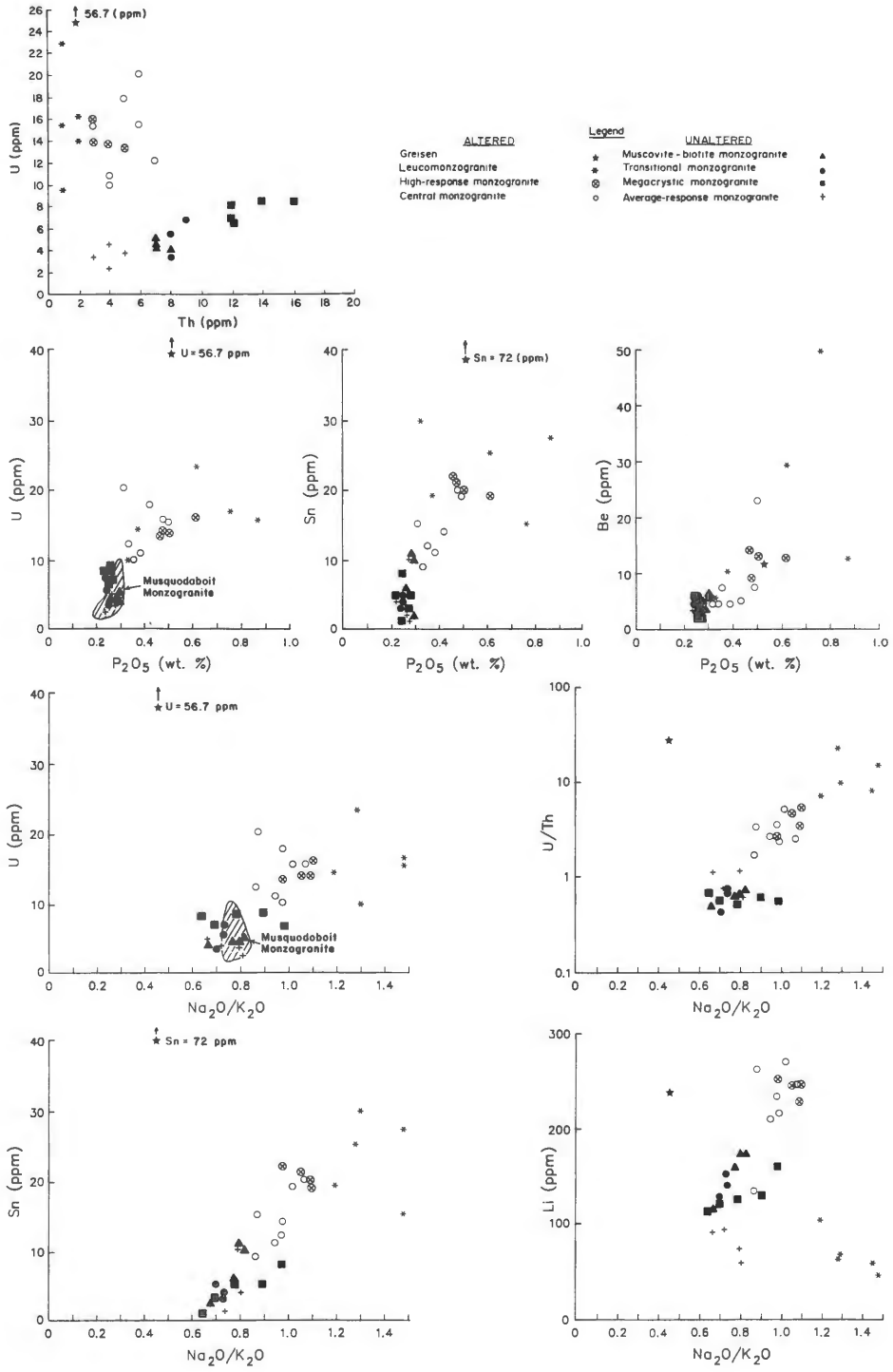

Figure 6-7 Plots of selected trace and major elements from the Sangster Lake and Larrys River Plutons.

and Fe-U-phosphate within the altered rocks is described in Chapter 5. The occurrence of these minerals explains the increase of U with increase of P_2O_5 and the Na_2O/K_2O ratio.

6.4.2 Tin

Tin follows an identical trend to U (Fig. 6-7). A Sn-bearing mineral phase was not recognized in the petrography, but cassiterite occurs in the heavy mineral separates (Table 5-5). Tin can be accommodated in significant amounts in other minerals. Richardson et al. (1982) found that, at the East Kemptville Sn deposit in southwest Nova Scotia, upwards of 100 ppm Sn occurs in greisenized leucomonzogranite samples which are not cassiterite-bearing. They believe that Sn in the muscovite crystal structure accounts for the elevated levels.

The processes that altered the Sangster Lake Pluton were accompanied by formation of titanium-poor, secondary muscovite which is the likely site for the elevated Sn levels.

6.4.3 Rubidium

The level of Rb and especially the K/Rb ratio is an established indicator of degree of magmatic differentiation or fluid-rock interaction (Heier and Billings, 1972). Rubidium does not form its own minerals, but its similarity in physical and chemical properties to K results in its incorporation into K-bearing phases. Rubidium has a slightly higher ionic radius (1.49 Å) than K (1.33 Å) resulting in K being preferentially incorporated during crystallization of the main K-bearing phases. Rubidium therefore becomes progressively enriched in the residual liquid phase during magmatic differentiation. This

results in late-stage differentiates becoming enriched in Rb with a corresponding decrease in the K/Rb ratio.

Heier and Billings (1970) found that most igneous rocks have a K/Rb ratio between 160-300 and that only rarely do the common rock types fall outside this range. Reynolds (1972) noted that the most differentiated granites and pegmatites can have a K/Rb ratio much less than 160. Cerny et al. (1985) reported examples of leucogranites with a K/Rb as low as 41 and pegmatites less than 10. They suggest that rocks crystallizing in a fluid-rich environment are preferentially enriched in Rb and thus have a low K/Rb ratio.

A plot of K_2O vs Rb, including the various equivalent K/Rb lines, is given in Figure 6-4. The granodiorites of the South Mountain Batholith have a K/Rb in the order of 200, and the Meguma Zone monzogranites extend down to a K/Rb of 70, but only 2 samples are below 150 (McKenzie and Clarke, 1975). Most of the monzogranite samples fall between ratio values of 150-200. Perhaps the two samples that fall below this range have undergone alteration.

The monzogranite samples of the Larrys River Pluton and the average-response monzogranite of the Sangster Lake Pluton have a K/Rb in the order of 150-200. The central and high-response monzogranites and the leucomonzogranite samples deviate from this and have ratios as low as 70 for the monzogranites and 55 for the leucomonzogranites. This trend toward low K/Rb ratios strongly suggests that these rocks have undergone considerable fluid-rock or fluid-melt interaction.

6.4.4 Lithium

Lithium is a member of the alkali metal family with Rb and Cs and concentrates in late-stage differentiates and the accompanying hydrothermal fluid phase (Heier and Billings, 1970). Lithium increases with magmatic differentiation in Meguma Zone granitoids (McKenzie, 1974; and Charest, 1976). In this study Li is highest in the hydrothermally altered monzogranites and shows a positive correlation with the Na_2O/K_2O ratio (Fig. 6-7). This suggests that Li was mobile during the alteration. Farley (1979) found similar high Li levels in South Mountain Batholith rocks associated with granophile element mineralizations.

The low levels of Li in the leucomonzogranites relative to both the unaltered and altered monzogranites is contradictory (Fig. 6-7). The high levels of the alteration indices (Na_2O/K_2O and P_2O_5) in the leucomonzogranites suggests that these rocks are altered. Therefore, their low Li levels are inconsistent with the fluid-enriched environment in which they formed. Possibly, the reason for the low Li is that the leucomonzogranites are less micaceous than the hydrothermally altered monzogranites (Table 4-1). Muscovite is known to be a common site for Li in granitic rocks (Heier and Billings, 1970). As no other Li-bearing phase such as lepidolite, amblygonite or spodumene is present in the rocks, a likely residence for the elevated levels of Li is the secondary muscovite which was forming during the alteration.

6.4.5 Fluorine

Fluorine content is elevated among the altered samples, although less pronounced than some other Meguma Zone granitoid rocks associated

with deposits of Sn (Charest, 1976; Farley, 1979; O'Reilly et al., 1982; Richardson et al., 1982; Logothetis, 1984). The absence of fluorite as an accessory mineral in any of the rocks of the thesis area, including late-stage pegmatites and greisens, was noted previously. The only common F-bearing phase is fluoroapatite (Chapter 5) although topaz is common in one sample of leucomonzogranite (Table 5-5). Therefore, secondary muscovites and fluoro-apatites are the probable sources for the elevated F levels. A similar absence of fluorite was noted within rocks of the Musquodoboit Batholith by MacDonald and Clarke, (1985). The significance of this feature is further discussed in Chapter 8.

6.4.6 Beryllium

Beryllium levels increase among rocks of anomalous radiometric response of the Sangster Lake Pluton. One sample of leucomonzogranite from the Beans Lake Leucomonzogranite is highly anomalous (50 ppm; F5-G007) but no Be-bearing minerals were identified. A positive correlation of Be vs P_2O_5 (Fig. 6-7) suggests that elevated Be levels may accompany the secondary apatites in these rocks.

6.4.7 Barium and Strontium

Barium and strontium are members of the alkaline earth metal series and thus behave chemically in a similar manner. Strontium (1.18 Å) is intermediate in size between K (1.33 Å) and Ca (1.02 Å) and can isomorphously replace Ca and K-bearing (El Bouseily and El Sokkary, 1975). In granitic rocks, both Sr and Ca decrease with differentiation with the decrease in Sr accounted for by acceptance of in Ca-bearing phases, especially plagioclase.

Barium (1.34 Å) is almost identical in size to K and is therefore hosted by K-bearing phases such as K-feldspar in granitic rocks (El Bouseily and El Sokkary, 1975).

In this study both Ba and Sr have a negative correlation with members of the granophile element suite (Fig. 6-2; Table 6-1). In the monzogranites of the Larrys River Pluton they show a depletion which corresponds to the suggested differentiation sequence (Fig. 6-4). In the average response monzogranite of the Sangster Lake Pluton the plagioclase and K-feldspar are probably the main sites for Sr and Ba. Although feldspar fractionation would account to some degree for their reduced levels, their strong depletion in the altered rocks (Fig. 6-4) is likely the result of destruction of the primary feldspars. If none of the secondary phases being formed was able to retain the Ba and Sr, these elements would have been removed by the alteration fluids.

As Sr behaves like Ca, the precipitation of a calcic phase such as apatite during the albitization of plagioclase would be expected to provide an appropriate depositional site for both the Ca and Sr released. The data do not support this as both elements show a negative correlation with P_2O_5 (Fig. 6-2).

6.4.8 Lead

The main residence site for Pb within a granitic rock is in K-feldspar. The observed strong negative correlation of Pb with the granophile element suite is consistent with destruction of K-feldspar during hydrothermal alteration. As with Ba and Sr, if the liberated Pb is not accommodated in a suitable secondary phase, then it will show a

depletion with increasing degree of hydrothermal alteration. The secondary K-feldspar in the altered rocks (Plates 4-5 and 4-8) apparently provides a suitable site, but the Pb levels remain low in these rocks. This can be explained by one of the following:

1. the liberated Pb was present in the fluid but the physical and chemical conditions under which the secondary K-feldspar formed were not suitable for incorporation of the Pb;
2. during destruction of the original K-feldspar there was not a suitable secondary mineral forming to incorporate the liberated Pb, therefore it left the system with the fluid. The formation of secondary K-feldspar followed albitization suggesting it may not have been available to incorporate Pb released during destruction of the original K-feldspar.

6.4.9 Thorium

The Th content of granitoid rocks decreases with increasing differentiation and this trend is apparent in Meguma Zone granitic rocks (Farley, 1979; MacDonald and Clarke, 1985). However, Chatterjee and Muecke (1982) found that within the South Mountain Batholith some bodies show Th increases along with U.

In this study decrease of Th corresponds with the differentiation sequence established in Chapter 4 (Fig. 6-7). Within the altered monzogranites and the leucomonzogranites Th remains roughly constant, but U markedly increases by three to four. The corresponding increase in the U/Th ratio (Fig. 6-7) coincides with a pronounced eU/eTh anomaly in the airborne radiometric data (Ford and Ballantyne, 1983; Fig. 3-4).

The Th decrease is likely the result of crystallization of zircon, rutile and monazite during formation of the biotite-rich rocks. The processes which resulted in an increase of U in the altered rocks have, apparently, not affected the Th content.

6.5 RARE EARTH ELEMENTS

6.5.1 Introduction

The concentrations of the REE suite consisting of La, Ce, Nd, Sm, Eu, Tb, Yb and Lu, the sum 8 REE, Eu/Eu^* and the concentrations of Cs, Hf, Sc and Ta are given in Table 6-2. The analytical techniques are given in Appendix II.

The results of the REE analyses are normalized using the chondritic average of Haskin et al. (1968).

6.5.2 Analytical Results

The chondrite-normalized REE compositions according to sample grouping are presented in Figure 6-8. The patterns show that the megacrystic biotite monzogranite samples have the highest total REE content (average Sum 8 REE = 109.61 ppm), small negative europium anomalies (average $Eu/Eu^* = 0.44$) and light-REE (LREE) enrichment (average $La_N/Lu_N = 16.9$), similar to those of the granodiorites of the South Mountain Batholith (Muecke and Clarke, 1981). This correlation is consistent with this study where the megacrystic monzogranite, except for its high content of K-feldspar megacrysts, is granodioritic in composition.

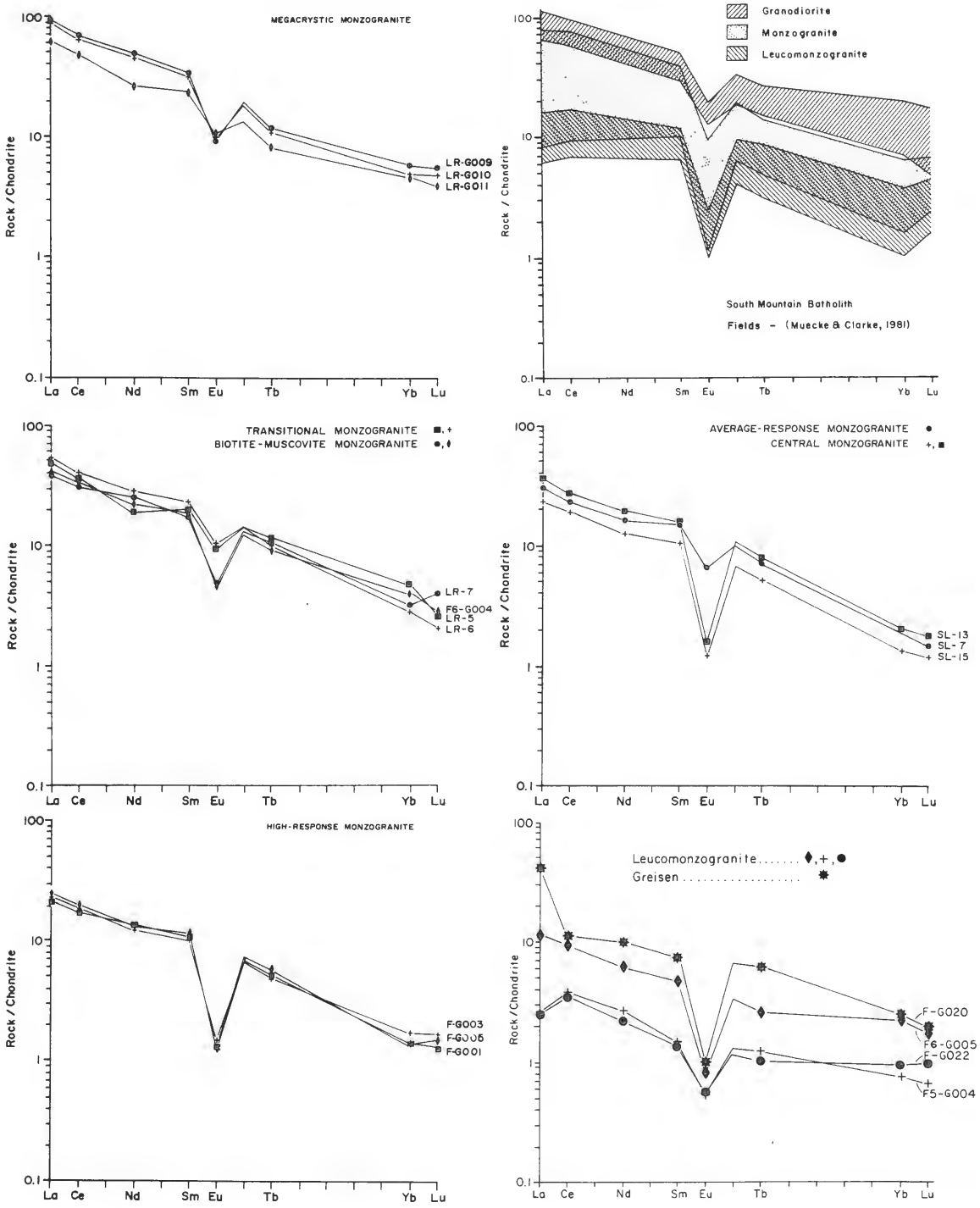

Figure 6-8 Chondrite-normalized REE patterns for samples from the Sangster Lake and Larrys River Plutons and the South Mountain Batholith. The data are tabulated in Table 6-2.

The transitional and biotite-muscovite monzogranites are more highly evolved than the megacrystic monzogranite. The REE patterns support this observation by having lower total REE (average Sum 8 REE = 64.07 ppm), similar negative Eu anomaly (average Eu/Eu^* = 0.42) and similar LREE content (average La_N/Lu_N = 15.1). The values are comparable to the monzogranite data of Muecke and Clarke (1981).

The average-response monzogranite of the Sangster Lake Pluton has a REE pattern comparable to the monzogranites of the Larrys River Pluton and the South Mountain Batholith (Fig. 6-8). Total REE (average Sum 7 REE = 43.00 ppm), small negative Eu anomaly (average Eu/Eu^* = 0.53) and level of LREE (average La_N/Lu_N = 20.6) are all similar to those just described.

The hydrothermally altered monzogranites of the Sangster Lake Pluton have patterns distinct from the unaltered monzogranites and from those of the South Mountain Batholith. The central monzogranite has lower total REE (average Sum 8 REE = 41.73 ppm), a large negative Eu anomaly (average Eu/Eu^* = 0.13) and similar LREE (average La_N/Lu_N = 19.9). The high-response monzogranite also has comparatively low total REE (average Sum 8 REE = 32.12 ppm), large negative Eu anomalies (average Eu/Eu^* = 0.15) and similar LREE (average La_N/Lu_N = 14.9).

The leucomonzogranite has patterns that are variable but continue the LREE depletion trend. They have very low total REE (average Sum 8 REE = 9.47 ppm), a moderate negative Eu anomaly (average Eu/Eu^* = 0.34) and further decreased LREE levels (average La_N/Lu_N = 4.2). The results from the present study are comparable to those from the leucogranites of the South Mountain Batholith except that the sum of

REE and the magnitude of the negative Eu anomaly are slightly less (Fig. 6-8).

The single sample of greisen from the Beans Lake greisen zone has REE contents intermediate between the leucomonzogranites and the monzogranites (Fig. 6-8). The sample contrasts with the trend of LREE depletion and shows LREE enrichment (La_N/Lu_N = 22.2) the result of an anomalous increase in La content.

6.5.3 Rare Earth Elements in Felsic Magmas

Rare earth element abundances in felsic igneous rocks commonly show progressive depletion with increasing differentiation. This trend is marked by reduction of LREE and increase of a negative Eu anomaly and is a feature common to felsic igneous suites of varying compositional affinity (calc-alkaline, peralkaline, peraluminous) from both plutonic and volcanic rocks (Miller and Mittlefehldt, 1982). There are two main explanations for the observed trends.

One school believes that the above trends are the result of progressive depletion of REE in the melt by fractional crystallization of REE-rich accessory minerals (Miller and Mittlefehldt, 1982; Gromet and Silver, 1983; Mittlefehldt and Miller, 1983; Sawka et al., 1984; Higgins et al., 1985; Jefferies, 1985; Charoy, 1986). Between 50 % (Alderton et al., 1980) and 95% (Gromet and Silver, 1983) of the REE in granitic rocks reside in the accessory minerals, and in some cases (eg. monazite) these minerals are so REE-rich that only minute amounts are required to account for the observed levels in the whole rock. A common conclusion is that fractional crystallization of accessory minerals such as monazite, allanite, zircon, apatite, sphene, rutile

and plagioclase (to deplete Eu levels) will progressively deplete a melt in REE.

A second school holds that an important and contributing factor to the observed trends is the result of REE being mobilized during fluid/melt and fluid/rock interactions with a volatile-enriched fluid phase exsolved during the late stages of fractional crystallization (Alderton et al., 1980; Muecke and Clarke, 1981; Taylor and Fryer, 1983; Logothetis, 1984; Chatterjee and Strong, 1984; Baker, 1985; Higgins et al., 1985; Kontak et al., 1988).

The mobility of REE in hydrothermal fluids has been confirmed by a number of studies (Beus, 1958; Kosterin, 1959; Martin et al., 1978; McLennan and Taylor, 1979). The mobility is achieved by dissolved anionic species in the fluids (Cl^-, F^- and CO_3^{2-}) forming stable REE-bearing complexes (Muecke and Moller, 1988). These same anions are also important in the transportation and precipitation of such economically important elements as Cu, Mo, W, Sn, U, Nb and Ta and, therefore, there is a correspondence between mobility of REE and the ore metals (Taylor and Fryer, 1983; Chatterjee and Strong, 1984).

A review of the existing experimental data shows that Cl-rich fluids preferentially mobilize LREE (Flynn and Burnham, 1978; Kamineni, 1986) and F- and CO_3-rich fluids show a preference for heavy REE (HREE) (Balashov and Krigman, 1975; Wendlandt and Harrison, 1979).

Fractional crystallization of a peraluminous magma may result in water saturation and exsolution of an aqueous fluid (Burnham and Ohmoto, 1980). The fluid phase becomes enriched with complexing agents and incompatible elements as differentiation progresses. The chemical

activity of the anion-charged fluid phase becomes a dominant factor and governs the subsequent physical and chemical processes during the remaining evolution of the system (Burnham and Ohmoto, 1980; Manning, 1981; Pichavant, 1981; Pollard, 1983; Cerny et al., 1985; London, 1987; Pichavant et al., 1987). The REE signature of the resulting rocks is, in part, a function of this chemically active fluid phase.

6.5.4 Interpretation

In this section the REE data are discussed in light of the existing experimental, petrographic and chemical information in the literature.

The plots of chondrite-normalized REE data show that the plutons have levels typical of felsic granitoid rocks (Fig. 6-8). These trends are consistent with felsic rocks derived by fractional crystallization involving plagioclase (Eu depletion) and REE-rich accessory minerals such as monazite, zircon and apatite in particular.

Several workers have invoked this model to explain REE patterns in granitoid suites from both within the Meguma Zone (Muecke and Clarke, 1981) and elsewhere (Mittlefehldt and Miller, 1983; Jefferies, 1983; Higgins et al., 1985; Charoy, 1986). However, Muecke and Clarke (1981) stated that crystal fractionation of major and accessory minerals accounts for observed trends up to monzogranite, but that for the more evolved and depleted rock types fluid interaction has to be invoked. They invoked interaction of the melt or previously crystallized rock with a volatile-rich fluid (F-dominated) exsolved during the latest stages of differentiation.

The two models used to explain REE depletion during differentiation diverge at this point. Miller and Mittlefehldt (1982) contend that late-stage felsic melts have very low saturation levels of accessory minerals and hence REE-rich phases can crystallize in the very latest rocks of a granitoid suite. In contrast, irrefutable examples of REE mobility by hydrothermal fluids are reported, but these involve locations where the alteration was intense and widespread (Chatterjee and Strong, 1984; Baker, 1985). Less obvious examples exist, and are to be expected, considering that: (1) the transition from a water-undersaturated system dominated by magmatic processes to a saturated system dominated by fluid/melt interaction is gradational (Burnham and Ohmoto, 1980; Pollard, 1983) and (2) with further differentiation the fluid phase becomes progressively enriched in anions and incompatible elements. Hence the activity of anionic ligands in the fluid increases in importance (Muecke and Clarke, 1981; Taylor and Fryer, 1983; Kontak et al., 1988).

Most granitic systems likely involve some combination of these processes. This holds especially for peraluminous granites where the initial H_2O content was high enough that exsolution of an aqueous phase during differentiation was probably inevitable.

The altered rocks in the study area all have REE patterns comparable to those which are cited in the literature as typical of fluid-melt or fluid-rock interaction (Fig. 6-8). The patterns for the central and high-response monzogranites are particularly interesting in that they are significantly lower than those in the unaltered rocks and

are more similar to the leucocratic monzogranite of Muecke and Clarke (1981).

Pichavant et al. (1987) in a study of the Macusani glasses of southeast Peru concluded they are examples of quenched peraluminous melt, roughly leucogranite in composition. The geochemistry indicates the melt was strongly peraluminous and alkali- and volatile-rich. The REE abundances in the glasses are comparable to those of the leuco-monzogranite of both this study and those of the South Mountain Batholith. Although the glasses represent quenched melt, their incompatible element enrichment coupled with the fact they are riddled with fluid inclusions indicates the melt co-existed with a highly evolved fluid phase.

In fluid-dominated systems examples of REE-depleted rocks are commonly accompanied by rocks (generally greisens) in which the leached REE are deposited (Alderton et al., 1980; Taylor and Fryer, 1983; Chatterjee and Strong, 1984). The sites of deposition commonly display highly variable patterns which depend on the dominant anion species.

In this study only one sample of greisen was analysed (F-G020; Fig. 6-8). Most REE species in this sample are slightly elevated compared to levels in the country rock leucomonzogranite, except for La which shows a marked increase and Eu which is more depleted. The enrichment of most REE is believed to be the result of deposition from the greisenizing fluid while the Eu depletion likely represents alteration of plagioclase to muscovite and quartz.

Albitization was a dominant alteration process within the rocks of the Sangster Lake Pluton. Several workers believe that albitization

can result in the depletion of REE and production of large negative Eu anomalies (Baker, 1985; Higgins et al., 1985). Others believe that potassic alteration is equally as efficient in stripping and mobilizing REE (Martin et al., 1978; Alderton et al., 1980). Thus the two cannot be effectively differentiated by REE geochemistry.

6.5.5 Role of Accessory Minerals

The importance of the role of accessory mineral phases in governing observed REE trends in a rock was previously stated. Higgins et al. (1985) found that accessory minerals are resistant to metasomatism and are unaffected by alteration processes until an advanced stage. A slightly contrasting view is presented by Kamineni (1986) who found an example of REE mobilization by low temperature interaction with groundwater.

Plots of REE data against TiO_2, P_2O_5, TTDI, Hf, Sc, Th and Zr for thesis area rocks are given in Figure 6-9. These parameters are good indicators of magmatic differentiation and hence allow estimation of REE behavior during this process. The extremely smooth trends exhibited by the indicator elements vs REE data strongly suggest that magmatic differentiation was an important process in the depletion of REE levels in these rocks. The marked decreases (e.g. Sum REE vs Zr) apparent in Figure 6-9 can be best achieved by crystallization of mineral phases such as monazite (for LREE) and zircon (for HREE).

A SEM scan of heavy mineral separates (Table 5-5) confirms the presence of both these minerals in almost all samples examined but that they are strongly associated with the occurrence of biotite. Therefore, rocks with little or no biotite have a correspondingly very low

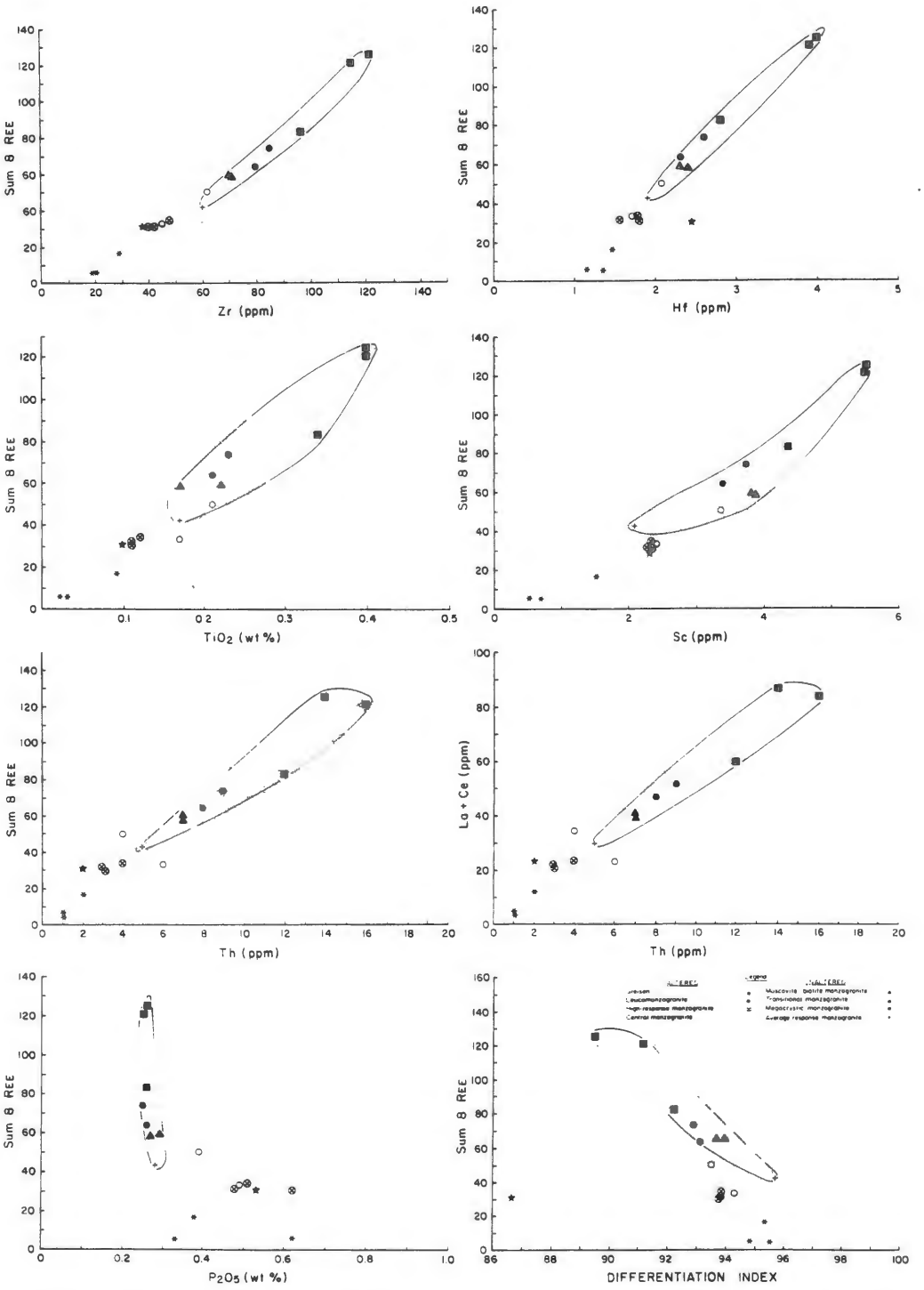

Figure 6-9 Plots of Sum REE vs TiO_2, P_2O_5, CaO, TTDI, Th, Zr, Hf, La, Ce and Sc from the Sangster Lake and Larrys River Plutons. The data are tabulated in Tables 6-1 and 6-2. Circled area represents field of unaltered rocks.

amount of these minerals. Gromet and Silver (1983) found that only minute amounts of monazite are required to give rise to the observed REE levels in granitic rocks. A La+Ce vs Th plot indicates the behavior of this important LREE-rich accessory phase (Fig. 6-9).

In light of the petrographic data the sum REE vs P_2O_5 plot is surprising (Fig. 6-9). The hydrothermally altered monzogranites, leucomonzogranites and greisen contain significant secondary apatite. Since apatite is an excellent host for REE, especially middle-REE, any increase in P_2O_5 could be accompanied by an increase of REE. The plot shows this is not the case. This can be explained by one of the following: 1) during the albitization of plagioclase and precipitation of secondary apatite the abundance of REE in the hydrothermal fluid was very low and the original REE-rich phases were unaffected by the alteration, 2) in the volatile-rich environment during the formation of secondary apatite the REE had a much stronger affinity for the fluid phase than for the apatite.

The first explanation can only be partially refuted because of the limited number of samples, particularly greisens, analyzed with this study. The REE levels in the one greisen sample are enriched relative to the leucomonzogranite from which it formed (Fig. 6-8). The enrichment, although modest except for La, suggests REE were mobilized by the hydrothermal fluid and subsequently deposited during greisenization. This conflicts somewhat with the smooth, continuous trends shown in Figure 6-9. These suggest that the REE-rich accessory minerals maintained their inherent magmatic signature and were virtually unaffected by the hydrothermal alteration.

With the second explanation, the data show that in the leucomonzogranite and the hydrothermally altered monzogranites, there are extremely low levels of REE. This suggests during alteration, the REE may have had a strong affinity for the fluid phase until the greisenization stage. In silicate melts, P has a strong affinity for cations of high charge such as Ca and REE (Ryerson and Hess, 1980; London, 1987). In aqueous systems REE have strongest affinity for anion species like F^-, Cl^- and CO_3^{2-} relative to species such as SO_4^{2-}, OH^-, HCO_3^- and PO_4^{4-} (Balashov and Kligman, 1975; Flynn and Burnham, 1978; Wendlandt and Harrison, 1979). The presence of anionic species such as Cl^- in the fluid phase may have kept the REE preferentially in solution during formation of secondary apatite.

The depleted REE levels and their smooth continuous trends versus differentiation indicator elements show no break between altered vs unaltered rocks (Fig. 6-9) suggesting the original magmatic trend was unaffected by the hydrothermal alteration. However, the REE patterns exhibited by the altered rocks are typical of rocks in which a fluid phase played an important evolutionary role (Muecke and Clarke, 1981; Fig. 6-8). This means, that if a fluid phase was important in deriving the observed REE levels it was the result of fluid-melt interaction. Evidence to suggest that post-crystallization hydrothermal alteration further depleted the REE levels is lacking.

Kontak et al. (1988) present petrographic, geochemical and isotopic data from the South Mountain Batholith which show that, in the late-stage environment, fluid-melt interaction was important in the evolution of the observed highly depleted REE patterns (esp. LREE).

They define a leucogranite I suite in which the fluid played a minor role and a leucogranite II suite in which the fluid phase played a dominant evolutionary role. The REE levels of the leucogranite II suite are comparable to the leucocratic monzogranite samples of Muecke and Clarke (1981) and the leucomonzogranite samples from this study.

6.6 OXYGEN ISOTOPES

6.6.1 Method

Whole-rock oxygen isotope analyses were carried out on eleven samples from the plutons. The samples were analyzed at Kruger Enterprises Inc., Geochron Laboratories Division, Cambridge, Massachusetts and are reported as $\delta^{18}O$ in per mil ($^{o}/_{oo}$) relative to Standard Mean Ocean Water (SMOW). The analyses are accurate to $\pm$ 0.36 $^{o}/_{oo}$ (2σ).

6.6.2 Results

The whole-rock oxygen isotope results are tabulated according to rock type and radiometric category in Table 6-3. The values vary from 9.7-12.4 $^{o}/_{oo}$ and show no systematic correlation among the rock types and radiometric categories. The results compare well with whole-rock $\delta^{18}O$ data reported by Longstaffe et al. (1980; 10.1-12.0 $^{o}/_{oo}$), Chatterjee et al. (1985; 10.18-12.38 $^{o}/_{oo}$) and Kontak et al. (1988; 9.5-11.3 $^{o}/_{oo}$) for the various granitic phases of the South Mountain Batholith and satellite plutons. They also fall within the range of peraluminous granitoid rocks on a world-wide scale (Sheppard, 1986; 10-14 $^{o}/_{oo}$). The previous workers in other Meguma Zone granitoids also found there is no correlation of granite type with $\delta^{18}O$ value.

Table 6-3 Oxygen isotope compositions for whole rocks from the Sangster Lake and Larrys River Plutons.

SAMPLE NUMBER	ROCK TYPE	DEGREE OF ALTERATION	DEGREE OF DEFORMATION	$\delta^{18}O$
F-G020	Greisen	Extreme	Light	+10.0
F-G022	Leucomonzogranite	Strong	Light	+12.4
F5-G004	Leucomonzogranite	Intense	Light	+10.2
F5-G007	Leucomonzogranite	Intense	Light	+9.7
F6-G005	Leucogranite	Moderate	Undeformed	+11.1
F-G001	High-Response Monzogranite	Intense	Moderate	+11.2
F-G005	High-Response Monzogranite	Intense	Moderate	+11.6
SL-15	Central Monzogranite	Intense	Very Strong	+11.3
SL-7	Average-Response Monzogranite	Weak	Undeformed	+12.0
F6-G004	Biotite-Muscovite Monzogranite	Weak	Light	+11.4
LR-G010	Megacrystic Monzogranite	Absent	Undeformed	+10.7

Longstaffe et al. (1980), using a combination of whole-rock and mineral $\delta^{18}O$ data, further concluded that the $\delta^{18}O$ values reflect those of the magma and that there was only slight isotopic fractionation from the original melt.

Chatterjee et al. (1985) and Kontak et al. (1988) found an enrichment of $\delta^{18}O$ resulting from interaction of the granitoid rocks with a fluid phase.

6.6.3 Parameters for Isotopic Fractionation

The partitioning of oxygen isotopes between a rock and an aqueous fluid during hydrothermal alteration is dependent on the following variables:

1. the isotopic composition of the fluid and the original unaltered rock,
2. the temperature of the exchange,
3. the water/rock ratio,
4. type of system (i.e. open or closed).

Taylor (1977) describes the relationships of these variables and shows that a change in any one can significantly alter the resulting ^{18}O abundance in a hydrothermally altered rock.

The isotopic composition of the altering fluid phase is of particular importance if it is markedly different from the initial rock with which it interacts. For example, a peraluminous granitic rock with a typically magmatic $\delta^{18}O$ value ($\approx$ 7-12 $^{o}/_{oo}$) interacting with meteoric water (<-5 $^{o}/_{oo}$) will result in an altered rock of different $\delta^{18}O$ than if the alteration fluid had a ^{18}O composition closer to that of the initial rock.

The temperature of the interaction becomes increasingly important below approximately 700-600°C. At the higher temperatures, more typical of the magmatic environment (i.e. >750°C), the degree of fractionation of oxygen isotopes is much less significant (Taylor, 1977). In the temperature range of pneumatolytic-hydrothermal alterations (≈600-300°C) fractionation can increase significantly with decreasing temperature.

The water/rock ratio (W/R) is the ratio of the amount of water oxygen versus the amount of rock oxygen in the total system. The final ^{18}O composition of a rock undergoing alteration will be dependent on the volume of water with which it has interacted (low versus high W/R).

Whether a system is closed or open can be important to the resulting ^{18}O composition of the altered rock. In nature, pure end member systems (i.e. totally open or totally closed) are unlikely and there is usually some combination of the two. A purely closed system involves continuous re-circulation and cyclic re-equilibration of a set volume of H_2O. In a purely open system each increment of H_2O passes through the system once and is then lost to the environment.

6.6.4 Oxygen Isotope Modelling

The interplay of the variables described above makes interpretation of oxygen isotope abundances in rocks very complex. If certain assumptions are made, and sufficient data are available, the fluid-rock interactions can be modelled. A series of plots of $\delta^{18}O$ of hydrothermally altered rock versus W/R ratio calculated using Equation 6-1

according to the oxygen isotope exchange model of Taylor (1977) is given in Figure 6-10.

$$W/R = \frac{\delta^{i}_{H_2O} - \delta^{i}_{Rock}}{\delta^{i}_{H_2O} - (\delta^{f}_{Rock} - delta)} \qquad \text{(Equation 6-1)}$$

Where: $\delta^{i}_{H_2O}$ = initial δ value of the hydrothermal fluid

δ^{i}_{Rock} = initial δ value of the rock before alteration

δ^{f}_{Rock} = final δ value of rock after alteration

W/R = ratio of atom % oxygen in water and rock

$delta^{*} = A\ (\frac{10^6}{T^2})\ - B$

* A and B are mineral-H_2O partitioning coefficients used in determining delta. This assumes the mineral-H_2O approximates rock-H_2O at equilibrium and at given temperature in degrees Kelvin. For albite A = 2.91, and B = 3.41.

Each plot illustrates the relationship of temperature, W/R ratio and the resultant ^{18}O in the altered rock for the specified composition of $\delta^{18}O$ of the initial fluid involved in the hydrothermal alteration. To construct the models the following assumptions were necessary:

(1) An approximation of the $\delta^{18}O$ value of the initial, unaltered rock. Data on the regional distribution of $\delta^{18}O$ in granitic rocks of the Meguma Zone are limited (Longstaffe et al., 1980; Chatterjee et al., 1985; Kontak et al., 1988). The ^{18}O abundances in the more primitive rock types, granodiorite and biotite monzogranite, allows an approximation of the original $\delta^{18}O$ of the parental magma. These rocks crystallized from high temperature melt fractions in which an aqueous fluid component was probably minor; thus they best reflect the ^{18}O

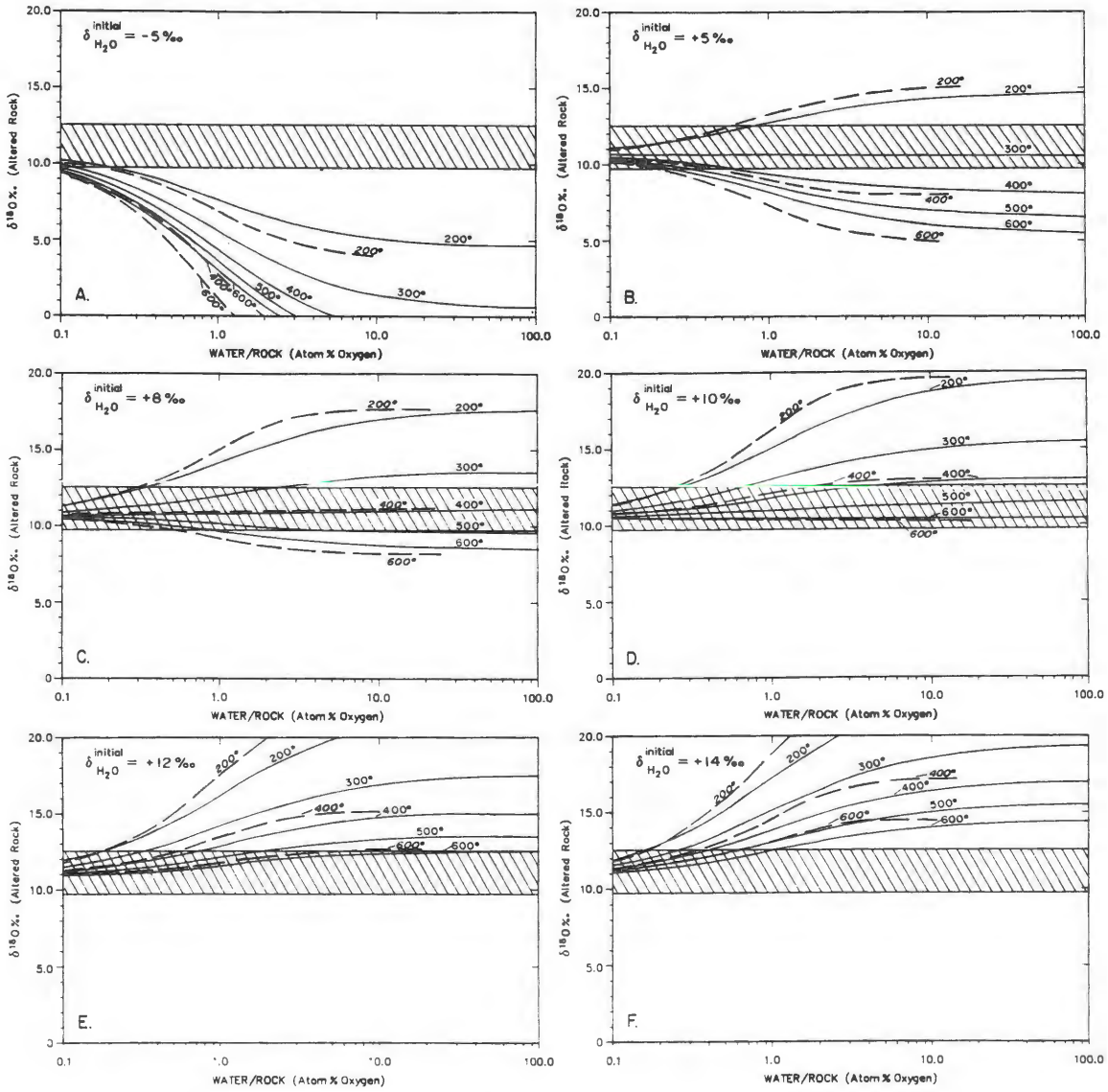

Figure 6-10 Plots of $\delta^{18}O$ in altered rocks vs water/rock ratio (W/R) for various initial compositions of hydrothermal fluids and closed system (solid) and open system (dashed) temperature curves. The range of $\delta^{18}O$ values for samples from this study are designated (diagonal lines) and are tabulated in Table 6-3. Derivation of the models and assumptions are discussed in the text.

value of the parental magma before any fractionation resulting from interaction with an exsolved fluid.

Existing data show the $\delta^{18}O$ levels in granodiorite and biotite monzogranite vary throughout the South Mountain Batholith and to simply take the average may be erroneous. It seems that, on a regional scale, the isotopic variation may reflect the nature of the basement rocks from which the magmas were formed.

With this study the most primitive rock type analysed is the biotite monzogranite of the Larrys River Pluton (Table 6-3). This sample has a $\delta^{18}O$ of +10.7 $^{o}/_{oo}$ which varies only slightly from the average of granodiorite samples (+10.67 $^{o}/_{oo}$) from the New Ross area reported by Longstaffe et al. (1980). Based on these criteria a value of +10.7 $^{o}/_{oo}$ reasonably approximates the initial $\delta^{18}O$ of the magma from which the study area plutons formed.

(2) Estimates of the temperature of the fluid-rock interactions are necessary. Temperature estimates are possible from the textural relationships and phase equilibria of alteration mineral assemblages described in Chapter 4. These indicate that albitization of plagioclase was followed by muscovitization and K-feldspathization in the hydrothermally altered monzogranites and leucomonzogranites. Phase equilibria in the system Na_2O-K_2O-Al_2O_3-SiO_2-H_2O-HCl at 2kb (Fig. 5-2; Helgeson, 1985) shows this alteration sequence is consistent with a temperature range of 500-400^{o}C. A further assumption is that the lower temperature alterations continuously re-equilibrated the oxygen in all the alteration minerals formed at higher temperature. There is also a possibility that re-equilibration of oxygen between the fluid and rock

continued as the system cooled below 400°C. This is thought to be minimal as there is no mineralogical expression of low temperature interaction (e.g. development of sericite or kaolin). Based on these data and assumptions, the temperature of pervasive hydrothermal alteration in the thesis area rocks was in the 500-400°C range.

(3) The isotopic composition of the initial hydrothermal fluid is an important factor governing the $\delta^{18}O$ abundance of an altered rock. For the purpose of this discussion the models in Figure 6-10 are calculated for a variety of initial H_2O compositions.

(4) The $\delta^{18}O$ abundance of a hydrothermally altered rock is partially dependent on whether the system was open or closed. The models illustrated in Figure 6-10 show the temperature curves for 600, 500, 400, 300 and 200°C for a closed system, and the 600, 400 and 200°C curves for an open system. The temperature curves for a purely open system vary from those of a purely closed system according the equation of Taylor (1977):

$$(W/R)_{open} = Log_e\ [(W/R)_{closed} + 1] \qquad \text{(Equation 6-2)}$$

The models represent minimum values for the W/R ratio, especially for the open system, as appreciable amounts of H_2O may move through the system without exchanging with the rocks.

(5) Derivation of the model requires a knowledge of the δ value of the resultant rock at equilibrium and any given temperature. To be strictly accurate, calculation of separate water/mineral ratios for each of the major mineral species in a rock is necessary and these

ratios should be weighted against modal abundances of the minerals in the rock. In the absence of these data the $\delta^{18}O$ value of plagioclase is often accepted as a reasonable approximation of the δ_{Rock} at equilibrium (Taylor, 1977). This assumption allows an estimation of delta in Equation 6-1 for any temperature. For this study the partitioning coefficients for albite-H_2O (Equation 6-1) were chosen as albite is the plagioclase species in the hydrothermally altered rocks.

(6) The models presented in Figure 6-10 were derived to determine the W/R ratio in a hydrothermal system. Taylor (1977) states that a W/R ratio determined by this method is a minimum value. Ohmoto (1986) stresses this point and argues that, in natural systems, the real value may differ considerably from that calculated using the Taylor model. Nevertheless, with the present study this parameter could not be constrained. The intent of the discussion is to use the isotope modelling to draw preliminary inferences as to the isotopic composition of the fluid phase necessary to result in the observed spread of $\delta^{18}O$ in the altered rocks. No attempt is made to quantify the W/R ratio except in general terms.

6.6.5 Interpretation

The oxygen isotope results of this study show no systematic difference in relation to rock type, radiometric category, degree of hydrothermal alteration or degree of deformation (Table 6-3). The sample suite includes rocks ranging in composition from the least differentiated megacrystic biotite monzogranite to the most differentiated leucomonzogranite. Their degree of hydrothermal alteration ranges from unaltered to highly albitized rocks and greisen. The

degree of deformation is also considered and undeformed examples as well as strongly deformed samples with c/s fabrics are represented.

Based on the assumptions outlined above, open and closed system oxygen isotope models for hydrothermal fluids of a variety of initial $\delta^{18}O$ values are given in Figure 6-10. The range of $\delta^{18}O$ values for all samples for the study area (+9.7 to +12.4 $^{o}/_{oo}$) is also indicated (diagonal lines).

The model of fluid-rock interactions involving a fluid of predominantly meteoric water (Fig. 6-10A) illustrates that for all temperatures and most W/R ratios the observed $\delta^{18}O$ values are not possible. A value for meteoric water of -5 $^{o}/_{oo}$ was selected for the purpose of this modelling as it represents a level in which the latitude effect is minimal. In any event, at high latitudes the δ value of meteoric water decreases (i.e <-5 $^{o}/_{oo}$) and if such values are used in the modelling the result is even more pronounced depression of the temperature curves toward low $\delta^{18}O$ altered rock values.

A model involving a mixture of a meteoric water (-5 $^{o}/_{oo}$ or less) with an internally derived water from a granitic magma ($\approx$+7 to +12 $^{o}/_{oo}$; Sheppard, 1986) is illustrated in Figure 6-10B (+5 $^{o}/_{oo}$). Under these conditions and in the temperature range suggested for alteration with this study (500-400^{o}C) the observed range of $\delta^{18}O$ is only produced at low W/R ratios. In addition, values of $\delta^{18}O$ in the altered rock greater than that estimated for the initial rock (+10.7 $^{o}/_{oo}$) can only arise from low temperature alteration.

Conversely, the models invoking interaction of the initial rocks with isotopically heavy waters (>+12 $^{o}/_{oo}$; Fig. 6-10 E and F) illus-

trate that within the inferred 500-400°C temperature range the observed range of $\delta^{18}O$ can only occur with low W/R ratios. In addition, interaction with such isotopically heavy water would result in a trend of increasing $\delta^{18}O$ in all the altered rocks. Such a trend is not observed in the data (Table 6-3).

The models using a fluid of +8 $^{o}/_{oo}$ and +10 $^{o}/_{oo}$ (Fig. 6-10 C and D) best fit the observed range of $\delta^{18}O$ in the samples. With such a fluid, interactions occurring at a variety of temperatures (including the deduced range), at both low through high W/R ratios and in either closed or open systems are consistent with the observed narrow spread of $\delta^{18}O$. From this a general conclusion is that the hydrothermal fluid which altered the Sangster Lake Pluton had a $\delta^{18}O$ of approximately 8-10 $^{o}/_{oo}$.

Longstaffe et al. (1980) found the Meguma Group metasediments have a similar range of $\delta^{18}O$ (+10.1 to +12.9 $^{o}/_{oo}$) to the granitoid rocks. The similarity between the two and a lack of data on the $\delta^{18}O$ composition of coexisting minerals in the metasediments makes inferences of the composition of metamorphic fluid in equilibrium with the metasediments during granite emplacement difficult. A crude estimate can be made that at temperatures in the 250-400°C range the fluid would have a $\delta^{18}O$ value 3-4 $^{o}/_{oo}$ lower than the coexisting rocks (i.e. $\approx$+6 to +10 $^{o}/_{oo}$)

From the models presented in Figure 6-10, it cannot be distinguished what proportion of the hydrothermal fluid was internally generated from the granitic magma and what proportion was derived from mixing with metamorphic water derived from the metasediments. The only

conclusion allowable is that the magmatic-hydrothermal system remained closed to input from outside fluids or if a fluid was introduced it had a similar $\delta^{18}O$ value.

Although there is no apparent correlation of $\delta^{18}O$ values with degree of differentiation (Longstaffe et al., 1980; Chatterjee et al., 1985; Kontak et al., 1988) there are examples in which hydrothermal fluids have significantly altered original ^{18}O signatures. Chatterjee et al. (1985) show progressive enrichment in whole-rock $\delta^{18}O$ values with degree of alteration at the Millet Brook U deposit in the South Mountain Batholith. Unaltered granodiorite clusters between +10.18 and +10.86 $^{o}/_{oo}$ while altered and mineralized samples range from +11.12 to +12.38 $^{o}/_{oo}$ and +12.3 to +15.3 $^{o}/_{oo}$ respectively. They invoke mixing of internally generated, CO_2-rich magmatic fluids with an $\delta^{18}O$ enriched fluid of probable metamorphic origin to attain the elevated whole-rock $\delta^{18}O$.

Kontak et al. (1988) recognize deviations from the typically magmatic range of $\delta^{18}O$ values in the South Mountain Batholith. The isotopic composition of coexisting minerals in some greisens shows deviation from the normal magmatic equilibrium ratios. They invoke input of an ^{18}O-enriched fluid of possible metamorphic origin to mix with the magmatic reservoir to arrive at the resulting signatures.

Both the above studies invoke mixing of magmatic-derived fluid with isotopically heavy water. However, altered rocks with $\delta^{18}O$ values elevated from those of the original, unaltered rocks are possible without invoking an isotopically heavy water. Increasing δO^{18} can result by interaction of a fluid with a $\delta^{18}O$ value less than that of

the original rock through low temperature alteration. For example, interaction of unaltered rock with $\delta^{18}O$ of +10.7 $^{o}/_{oo}$ (equivalent to the granodiorite) with a fluid of $\delta^{18}O$ of +8 to +10 $^{o}/_{oo}$ (Fig. 6-10 C and D) will result in altered rocks of elevated $\delta^{18}O$ if the interaction occurs at temperatures below 400-300°C.

6.7 SUMMARY

The examination of major, minor, trace element, and isotopic geochemistry of the Larrys River and Sangster Lake Plutons established the following trends:

1. The monzogranites of the Larrys River Pluton and the average-response monzogranite of the Sangster Lake Pluton have major, minor and trace element levels comparable to similar granitoid rocks of the South Mountain and Musquodoboit Batholiths. These trends are consistent with fractional crystallization of plagioclase, biotite and the accessory minerals zircon, apatite and monazite from a granodioritic parent magma.

2. Regions of the Sangster Lake Pluton of anomalous airborne radiometric response have major, minor and trace element signatures indicating that these rocks have undergone widespread albitization by a hydrothermal fluid exsolved from the magma during the later stages of differentiation. The hydrothermal alteration elevated the levels of Na_2O, P_2O_5, U, Sn, Rb, Li, F and Be in the rocks.

3. Conversely, the altered regions are depleted in K_2O, CaO, Ba, Sr and Pb. Depletion of these elements is consistent with albitization of plagioclase and decrease of modal K-feldspar.

4. Two main trends are recognizable in the REE geochemical data: 1) Abundances in the monzogranites of the Larrys River Pluton and the average-response monzogranite of the Sangster Lake Pluton are comparable to similar monzogranitic rocks throughout the Meguma Zone. The patterns are consistent with fractional crystallization being an important process by which these peraluminous granitoid rocks formed. 2) The leucomonzogranites and hydrothermally altered monzogranites have extremely low REE levels. These levels are consistent with interaction of the melt and/or previously crystallized rock with a aqueous fluid phase enriched in complexing agents.

5. Decreasing REE contents with decreasing Zr, Th, TiO_2 and P_2O_5 suggest most of the REE reside in accessory mineral phases rich in these elements. Likely REE-rich accessory phases are zircon, monazite, primary apatite and rutile, all of which are present in heavy mineral separates from these samples. The smooth, continuous trends of REE versus the above elements show no break between altered and unaltered rocks. This suggests the REE-bearing phases were unaffected by the alteration and that the low REE levels in the altered rocks resulted from fluid-melt interaction.

6. The whole-rock oxygen isotope data allow only poorly constrained conclusions. Oxygen isotope modelling suggests that the hydrothermal fluid had a $\delta^{18}O$ in the order of +8 $^{o}/_{oo}$ to +10 $^{o}/_{oo}$. This is consistent with a magmatic fluid generated from a peraluminous granitic magma, but whether or not this fluid mixed with a metamorphic fluid of similar isotopic composition could not be determined. Therefore, the hydrothermal alteration pervasive in the Sangster Lake Pluton could be either the result of an internally generated magmatic fluid or the result of a magmatic fluid which has mixed with a metamorphic fluid of similar $\delta^{18}O$ composition. A significant component of meteoric water in the hydrothermal fluid was unlikely. Further isotopic data are required from coexisting mineral phases of the Sangster Lake Pluton and the Meguma metasediments to allow more definitive conclusions.

CHAPTER 7

PETROGENESIS

7.1 INTRODUCTION

This chapter explains the origin and emplacement histories of the Larrys River and Sangster Lake Plutons by bringing together the findings described in the previous chapters. For clarity of presentation, the emplacement history of each pluton is presented separately. This is not intended to suggest the two plutons have separate, unrelated origins, because it is believed the two plutons are genetically linked to a single parent magma.

7.2 LARRYS RIVER PLUTON

The intrusive history of the study area commenced with development of a parent magma of an overall granodioritic composition (Fig. 7-1A). The Meguma Group country rocks, at the time of development of the magma, had already undergone deformation, folding and amphibolite facies regional metamorphism related to the Acadian Orogeny.

The Larrys River Pluton is believed to be an offshoot of a parental magma which rose to its present position at a time when the parent magma had differentiated into granodiorite to biotite monzogranite (Fig. 7-1B). The main driving force for the separation and rise of a portion of the melt was likely a progressive decrease in density of the melt resulting from fractional crystallization and hence, depletion of more dense mafic constituent minerals. Once

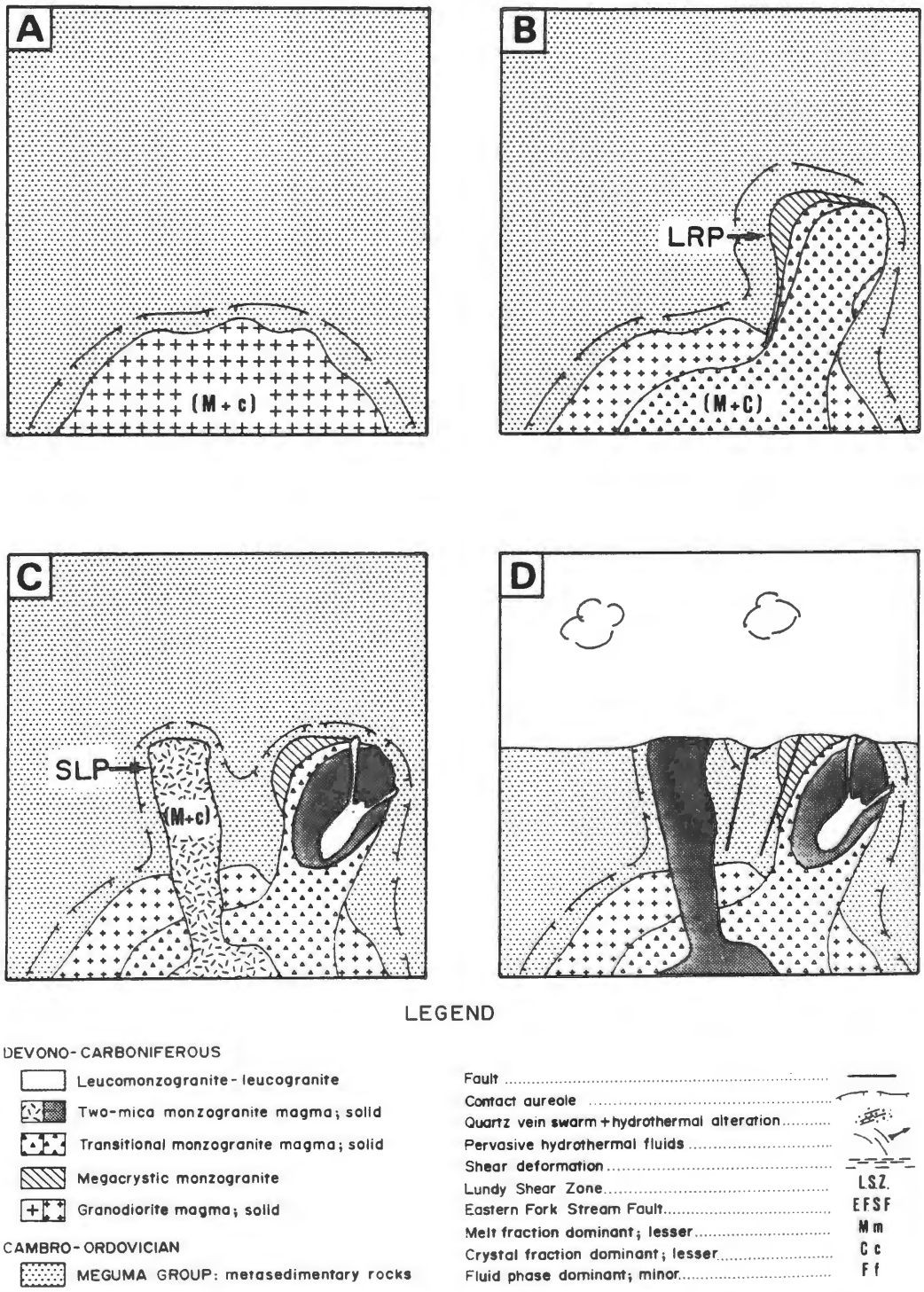

Figure 7-1 Schematic representation of the petrogenetic history of the Larrys River Pluton. See text for explanation. Vertical scale is greatly exaggerated. LRP = Larrys River Pluton; SLP = Sangster Lake Pluton. Note, legend also applies to Figure 7-2.

emplaced, the offshoot continued to differentiate inward by fractional crystallization from the contact with the country rocks. Thermal metamorphism related to the intrusion overprinted regional folds as well as the regional metamorphic assemblages.

Continued differentiation of the magma resulted in evolution of the melt into the transitional monzogranite and biotite-muscovite monzogranite, and a decrease in the proportion of K-feldspar megacrysts (Fig. 7-1B). This suggests many of the megacrysts present within the biotite monzogranite originally crystallized in the parent magma chamber and were emplaced along with the melt fraction. Eventually, the magma evolved to an overall two-mica monzogranite composition at which time a fraction of melt separated and rose to form the Sangster Lake Pluton (Fig. 7-1C). The development of the Sangster Lake Pluton is described further in the following section.

The melt fraction remaining at the core of the Larrys River Pluton reached a leucomonzogranite-leucogranite composition. At some point the remaining melt became oversaturated in water resulting in separation of an aqueous fluid phase (Burnham and Ohmoto, 1980). This process, known as second boiling, is accompanied by increased fluid pressure which can result in fracturing of the previously crystallized rock. Fracturing permits the rise of highly evolved melts and development of a hydrothermal system.

The fluid phase escaping from the minor intrusions can cause autometasomatism of the leucogranites as well as hydrothermal alteration of the enclosing rocks. These alterations are present within and adjacent to the leucogranite intrusions in the Larrys River Pluton

(e.g. Fougere Lake contact zone; Chapter 3). The minor development of these alterations within this pluton is an indication that either the fluid was not rich in anionic species and complexes such as Cl, F, B, P and CO_2 or only a small amount of fluid was exsolved.

The final stage of evolution of the Larrys River Pluton was accompanied by east-west trending, dextral shear deformation (Lundy shear zone; Chapter 3). This event only slightly deformed the pluton. After solidification of the pluton the area was affected by a series of brittle NW-SE trending major faults and lesser subsidiary faults (Fig. 7-1D). Following these events the area was uplifted and eroded to its present exposure level.

7.3 SANGSTER LAKE PLUTON

A two-mica monzogranitic magma separated from the parent magma and rose to form the Sangster Lake Pluton (Fig. 7-2A). Once emplaced, the melt continued to differentiate and crystallize inward from the cooler outer regions of the pluton (Fig. 7-2B). At some stage, the melt became saturated in water and second boiling occurred. The resulting fluid was strongly enriched in volatiles and granophile elements. With further differentiation and evolution of the melt, the proportion of fluid relative to remaining melt increased and both became further enriched with granophile elements.

Eventually, the fluid phase became a dominant component within the highly evolved remaining melt. At some point the remaining magma chamber was tapped, allowing offshoots of this highly evolved melt and fluid to escape and rise through the previously crystallized rock.

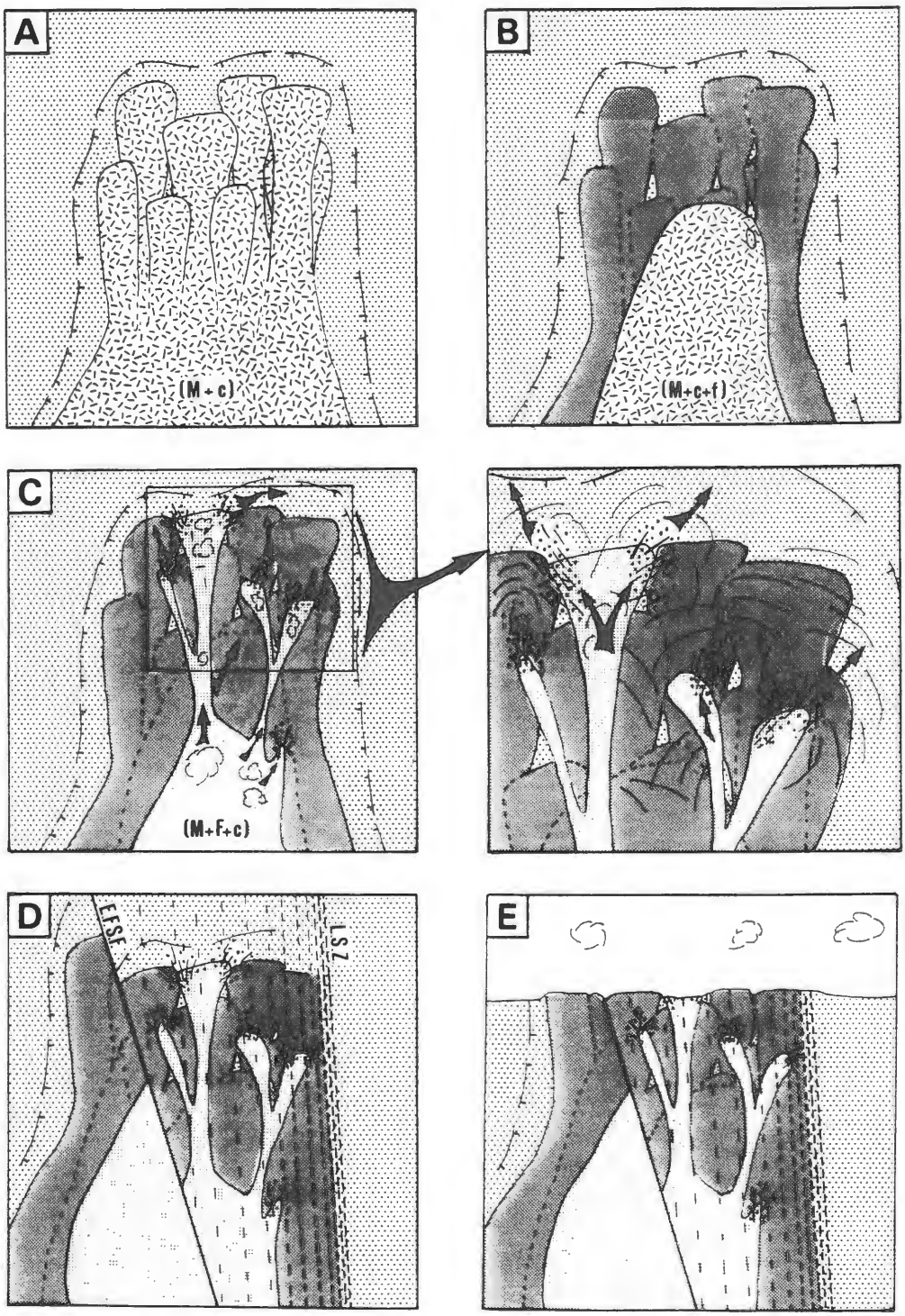

Figure 7-2 Schematic representation of the petrogenetic history of the Sangster Lake Pluton. See text for explanation. Vertical scale is greatly exaggerated. Legend as in Figure 7-1.

Overpressure related to buildup of the fluid phase and perhaps a vapour phase within the magma chamber may have been important in creating the fractures necessary to allow the melt to rise (Fig. 7-2C).

Interaction of the fluid with previously crystallized rocks resulted in mineralogical transformations in two main styles (Fig. 7-2C). Hydraulic fracturing accompanying second boiling allowed for release of the fluid causing structurally controlled swarms of quartz veins and associated greisens (e.g. the Beans Lake greisen zone). These zones are characterized by well-developed alteration and associated intense metasomatism over a relatively short distance (few hundred meters).

A second, more pervasive style, involved a widespread alteration of the mineral phases comprising the previously crystallized rocks throughout much of the eastern portion of the pluton. This resulted in formation of a considerable volume of altered rock which has no obvious structural control other than its location at the roof of the pluton (Fig. 7-2C). Perhaps the overlying contact aureole of annealed metasedimentary rocks served as a barrier to the escaping fluids, trapping them in the roof zone.

The only mechanism which would permit such widespread, pervasive alteration with no obvious structural control is fluid transfer along grain boundaries and joints. A number of theoretical studies have shown that circulating hydrothermal systems on the order of 10-20 km diameter may form in roof zones of newly consolidated granite (Norton and Knight, 1977; Parmentier and Schedl, 1981). Within such a system,

the pathway for the fluid transfer is by a combination of large scale fractures and grain boundary diffusion (Norton and Knapp, 1977).

Manning and Exley (1984) invoked this combination of processes for intrusion of a non-megacrystic lithium-mica leucogranite at St. Austell, Cornwall. This leucogranite intrudes a previously crystallized biotite granite and the fluids associated with the intrusion caused an aureole of mineralogical transformations extending a considerable distance into the biotite granite. These studies show that pervasive alterations on the scale of those in the current study are quite feasible.

The pluton is overprinted by deformation related to the Lundy shear zone (LSZ in Fig. 7-2D). The monzogranites, including the alteration mineral assemblage, exhibit a penetrative foliation related to this deformational event while much of the leucomonzogranite is relatively undeformed. This places the peak of the deformational event during emplacement of the leucomonzogranite and early formation of the paraintrusive rocks.

The last significant event which affected the Sangster Lake Pluton was a series of regional NW-SE trending faults and lesser subsidiary faults. One such fault, Eastern Fork Stream fault (EFSF in Fig. 7-2D), juxtaposed a block of undeformed and relatively unaltered biotite-muscovite monzogranite against variably deformed two-mica monzogranite (Fig. 7-2E). The sense and magnitude of displacement along this fault are not known but the western, undeformed block may represent a deeper part of the system relative to the eastern deformed and hydrothermally

altered block. The pluton has since been uplifted and eroded to its present position (Fig. 7-2E).

CHAPTER 8

ECONOMIC GEOLOGY

8.1 INTRODUCTION

Felsic granitoid rocks, in particular those of peraluminous composition, host economic deposits of granophile elements (Tischendorf, 1977; Stemprok, 1979; Taylor, 1979; Strong, 1981). An abundant geological literature about this association within the granitic terrains of the world deals with every aspect of their origin, evolution and emplacement, as well as diagnostic petrographic and geochemical characteristics. Since the early 1970's, the peraluminous granitoid rocks of the Meguma Zone, in particular the South Mountain Batholith, have been the focus of such studies. This resulted in discovery and development of the 56 million tonne, greisen-hosted East Kemptville Sn deposit, and a sizable vein-type U deposit (Millet Brook) within the South Mountain Batholith (Chatterjee et al., 1982; Richardson et al., 1982).

The exploration activity and, to a lesser extent, the research studies resulted in discovery of numerous other Sn-U showings, as well as a re-evaluation of many previously known granite-hosted prospects and occurrences (Charest, 1976; Farley, 1979; Chatterjee and Muecke, 1982; Ford and Ballantyne, 1983; O'Reilly et al., 1982; Chatterjee, 1983; Ford and O'Reilly, 1985).

The Sangster Lake and Larrys River Plutons have no known deposits of Sn or related elements, although the geological and geochemical

evidence suggests the Sangster Lake Pluton, in particular, is fertile ground.

This chapter describes:

1. the known mineral occurrences within this area;
2. the geological and geochemical features of the granitoid rocks which attest to their economic potential.

8.2 MINERAL OCCURRENCES

8.2.1 Sangster Lake Au Prospect

The Sangster Lake Au prospect occurs within a metasedimentary roof pendant approximately 1.5 km west of Sangster Lake (Fig 3-1). Gold-bearing glacial drift was discovered in this area in the early 1930's which led to follow-up prospecting during the next decade. Exploration at the site was restricted to overburden trenching and pitting (Goudge, 1934). One trench reached bedrock, and uncovered a 3 m wide belt of auriferous quartz veins in whin (quartzite). The veins are interbedded with a strike of 150°Az and a dip of 30° east. There was no attempt to define the bedrock extent of the zone, and by the late 1930's the prospect was abandoned and no significant exploration has been carried out at the site since.

The workings at the prospect have long since collapsed and are now overgrown. Since there are no metasedimentary outcrops in the immediate area of the prospect all conclusions are based on examination of dump samples, the descriptions of Goudge (1934), and conversations with

an Upper New Harbour resident who worked as a laborer at the site in the 1930's.

Goudge (1934) reported that the source of the gold-rich drift was likely the auriferous quartz vein belt uncovered during the drift trenching. He concluded the veins are bedding-parallel and identical in form and structure to veins mined at the many Au camps throughout the Meguma Zone. An 8 m wide granitic dyke cuts the belt at a high angle suggesting a pre-granitic origin of the vein system. The limited extent of the auriferous zone and the gold-rich drift, and the fact that the metasedimentary roof pendant is surrounded and cut off by the nearby granite are probable reasons as to why exploration ceased at the site,

Dump samples collected for this study confirm that the veins are bedding-parallel, but the relationship of the contact metamorphism to the veins could not be determined. Pink andalusite occurs in the veins but this is not diagnostic in determining their origin. Small dykes and veins of monzogranite cut the veins suggesting that the two have no obvious genetic relationship.

Approximately 1.3 km southwest of the prospect is another metasedimentary roof pendant which has outcrops with a 2-5 cm thick bedding-parallel quartz vein. This vein has a similar orientation to those at the prospect (153^{o}Az and dipping 63^{o} east; Fig. 3-8). There is no previous record of this vein and gold was not observed.

8.2.2 Green Barren Pegmatite

A small, 1-2 m wide pegmatite dyke intrudes Halifax Formation andalusite schists north of the Sangster Lake Pluton, between Green

Barren Lake and Lundy (Fig. 3-1). The dyke was obviously test-pitted at some time in the past although there is no record of any past exploration in this immediate area.

The pegmatite is somewhat irregular, pod-shaped, and poorly zoned. It consists of a large central zone of quartz, with K-feldspar and muscovite confined to the outer margins. A few grains of apatite were found, but for the most part, there is no significant mineralization.

The occurrence is hosted by amphibolite facies andalusite schists within the Lundy shear zone (Chapter 3). The pegmatite intrudes the 095° Az shear trend at 065° Az and is less deformed than the enclosing schists. This suggests one of two situations:

1. the intrusion occurred during the later stages of development of the shear episode, an observation that is consistent with the syn- or post-deformational relation between the Beans Lake Leucomonzogranite and the fabric produced by this shear deformation;

2. the difference in mechanical properties between the pegmatite and the enclosing pelites is such that the pelites may have shielded the more competent pegmatite from the brunt of the deformational effects.

If situation 1 is valid than the pegmatite occupies a similar position in time to the Beans Lake intrusion therefore suggesting the pegmatite is a late-stage offshoot of the Sangster Lake Pluton.

8.3 ECONOMIC POTENTIAL

Although there are no mineral deposits of economic significance known within the Sangster Lake or Larrys River Plutons, there are many features attesting to a high economic potential for this area. The literature contains an abundance of information outlining field, petrographic and geochemical criteria with which mineralized or specialized plutons can be separated from so called "barren" plutons (Beus and Zalashkova, 1964; Tischendorf, 1977; Stemprok, 1979; Taylor, 1979; Van de Pijpekamp, 1982; Smith and Turek, 1976). In theory, these criteria are applicable to any granitic terrain to evaluate its economic potential.

MacDonald and Clarke (1985) summarize the main features of "specialized granites" originally defined by Tischendorf (1977) and compare these with the Musquodoboit Batholith. The features are:

1. post-tectonic emplacement;
2. palingenic or anatectic origin of the parental magma (S-type granite);
3. an intrusive mode of emplacement;
4. polyphase high-level intrusions;
5. importance of the apical portion of individual plutons or the host batholith;
6. strong and progressive increase of incompatible and granophile elements with differentiation;
7. association of accessory minerals reflecting the incompatible and granophile element enrichment (eg. cassiterite, topaz, fluorite, tourmaline, beryl, columbite-tantalite);

8. an unusual sequence of crystallization of the rock-forming minerals;
9. late-stage, often widespread, autometasomatic alteration (eg. microclinization and albitization);
10. post-magmatic alteration, often with associated economic mineralization (greisens, quartz veins).

The various rock types of the Sangster Lake and Larrys River Plutons are compared with the criteria of Tischendorf (1977) in Table 8-1. The Larrys River Pluton does not satisfy many of the criteria other than its occurrence as a peraluminous pluton within the Meguma Zone (criteria 1-4). The remaining criteria indicating the presence of late-stage intrusions and alterations associated with hydrothermal fluids are absent or weakly developed (criteria 5-10).

The Sangster Lake Pluton, to varying degrees, satisfies all of the above criteria except for the occurrence of economic mineralization. Economically significant mineralization has not been recognized, although examples of post-magmatic alteration are well developed (e.g. Beans Lake greisen zone; Chapter 4). Criteria (1), (2), (3) and (4) are evident from the regional setting of the pluton within the Meguma Zone peraluminous terrain and the field data reported with this study.

The air photo interpretation and field mapping show that the Sangster Lake Pluton is exposed at its uppermost apical zone thus satisfying criterion (5). The geochemical data presented in Chapter 6 satisfy criterion (6) and show a progressive increase of granophile and incompatible elements with both differentiation and subsequent fluid-

Table 8-1 Comparison of the Sangster Lake and Larrys River Plutons with criteria of economic potential as defined by Tischendorf (1977).

ECONOMIC POTENTIAL INDICATORS after Tischendorf, 1977	SANGSTER LAKE PLUTON					LARRYS RIVER PLUTON			
	ARMg	CMg	HRMg	LMg	Gr	MMg	TMg	BMg	Lgt
1. post-tectonic emplacement of the granite	y	y	y	y	y	y	y	y	y
2. S-type parental granite	y	y	y	y	y	y	y	y	y
3. intrusive mode of emplacement	y	y	y	y	y	y	y	y	y
4. polyphase high level intrusions	y	y	y	y	y	y	y	y	y
5. apical region in the granitoid	n	y	y	y	y	n	n	n	y
6. increase of granophiles with differentiation	a	s	s	s	s	a	a	a	m
7. accessories reflecting granophile enrichment	w	s	s	s	s	a	a	w	s
8. unusual sequence of crystallization of minerals	n	y	y	y	y	n	n	n	y
9. late stage, widespread autometasomatism	a	s	s	s	s	a	a	a	m-s
10. postmagmatic alteration (greisenization, quartz veining)	a	w	w	s	s	a	a	a	w-m

Explanation: y = yes, n = no, a = absent; w = weak, m = moderate, s = strong

ARMg = Average Response Monzogranite
CMg = Central Monzogranite
HRMg = High-Response Monzogranite
LMg = Leucomonzogranite
Gr = Greisen

MMg = Megacrystic Monzogranite
TMg = Transitional Monzogranite
BMg = Biotite-Muscovite Monzogranite
Lgt = Leucogranite

rock alterations. Petrography shows that within the hydrothermally-altered rocks there is a peculiar replacement of secondary albite by K-feldspar and quartz. This unusual sequence (criterion 8) is best explained by autometasomatic processes acting on previously crystallized rock.

The most convincing feature suggesting a high economic potential is the widespread, pervasive hydrothermal alteration (predominantly albitization) of the entire central and eastern portion of the pluton (criterion 9). Alteration is important for the leaching, transport and precipitation of rare-element deposits. In addition, previous workers established that there is a correlation of elevated radiometric signature with plutons that have undergone hydrothermal alteration and associated mineralization (Chatterjee and Muecke, 1982; Yeates et al., 1982; and Ford and O'Reilly, 1985).

Several previous studies of Meguma Zone granites report a close association of F-enrichment with granophile element mineralization (Charest, 1976; Farley, 1979; Muecke and Clarke, 1981; O'Reilly et al., 1982; Richardson et al., 1982; Logothetis, 1984). The accessory mineral assemblages in rocks from this study (Table 5-5) show that granophile element-rich accessory minerals are present in significant proportions in the late-stage and hydrothermally-altered rocks. In addition, the presence of secondary apatite, chloroapatite and Fe-U-phosphate confirms the presence of P and Cl in the hydrothermal fluid. Conversely, the complete absence of fluorite from any of the samples examined and the fact that topaz was recognized in only one sample of leucomonzogranite suggests the fluid phase was either not enriched in F

or that it was dominated by other anions, namely P and Cl. Little information exists as to the relative activities of P vs F in hydrothermal systems. The data from this study suggest that the activity of P in the fluid dominated over F with respect to Ca released during albitization of primary plagioclase. This is evident from the formation of apatite and chloroapatite instead of significant amounts of F- and Ca-bearing phases such as fluorite and topaz. Conceivably, in a hydrothermal system with high P, Cl and F, a dominance in the activity of P and Cl relative to interaction with the cations and incompatible elements may be prohibitive to formation of economic concentrations of rare-element accessory minerals.

This, of course, assumes that F was also present in the fluid. A valid alternative explanation is that there was simply a low concentration of F. Either alternative is consistent with the available data.

One must also consider that mineral deposits exist but simply have not been recognized, were eroded away or are not exposed. These explanations may be valid but the abundance of outcrop and the excellent exposure of the pluton at its uppermost level suggest otherwise.

8.4 SUMMARY

The Larrys River Pluton has only weakly developed features suggesting it has potential to host economic mineralization. On the other hand, the Sangster Lake Pluton satisfies most criteria indicative of a potentially mineralized pluton. The fact that deposits of

economic significance have not been recognized may be the result of one or more of:

1. a lack of F-specialization in the hydrothermal fluid;
2. the presence of other anions (e.g. Cl and P) dominated over F in the fluid resulting in dispersal of rare-element accessory minerals throughout the rocks;
3. lack of significant concentrations of rare elements in the fluid phase.
4. deposits of granophile elements exist but have not been recognized, are not exposed or have been eroded.

CHAPTER 9

CONCLUSIONS AND RECOMMENDATIONS FOR FUTURE WORK

9.1 CONCLUSIONS

This thesis concerns the geology, mineralogy and geochemistry of a granitic terrain with a variable airborne gamma-ray spectrometric response. These data allow the following conclusions to be made.

1. The Larrys River and Sangster Lake Plutons consist almost entirely of various textural facies of monzogranite. These plutons intruded metasedimentary rocks of the Cambro-Ordovician Meguma Group during Devono-Carboniferous times. Small, cogenetic intrusions of leucomonzogranite, leucogranite and pegmatite intruded the monzogranites of both plutons.

2. The plutons have contact aureoles which overprint regional metamorphic assemblages which grade up to amphibolite facies.

3. Much of the Sangster Lake Pluton is overprinted by a deformational fabric related to a dextral shear zone forming the northern contact of the pluton. In some instances the intrusion of the late-stage leucomonzogranites, occurred during the peak to later stages of this shear episode. The Larrys River Pluton has only been mildly affected by this deformation.

4. The Sangster Lake Pluton intruded as a series of convective upwellings of plume-like form. The pluton is exposed at its uppermost roof zone and contains several metasedimentary roof pendants of varying size along the perimeters of the plume structures.

5. A lack of metasedimentary xenoliths within both plutons suggests that either stoping was not an important method of intrusion, or such material, if it existed, was completely digested.

6. Petrography shows that the monzogranites of the Larrys River Pluton compare in texture and mineralogy with similar rock types described from other Meguma Zone granitoids, namely the Musquodoboit and South Mountain Batholiths. The Sangster Lake Pluton, although monzogranitic in composition, underwent considerable hydrothermal alteration. The alteration was predominantly sodic in nature and resulted in albitization of plagioclase, appearance of secondary muscovite and apatite and destruction of K-feldspar. A late, potassic pulse is associated with K-feldspathization of the secondary albite.

7. The major, minor and trace element geochemistry of the plutons is, for the most part, comparable to the other peraluminous granitic rocks of the Meguma Zone. There are, however, certain chemical trends within the Sangster Lake Pluton which correlate well with the progression of hydrothermal alteration. These rocks show a pronounced albitization trend which has a positive correlation with P_2O_5 and a granophile

element suite comprising U, Sn, Rb, Li, Be and F. Conversely, these positive elemental trends are negatively correlated with K_2O, CaO, Pb, Sr and Ba which can be related to the breakdown and/or alteration of the primary feldspars.

8. Rare earth element levels in the unaltered monzogranites are comparable to similar monzogranitic rocks of the Meguma Zone. The patterns are consistent with fractional crystallization of REE-rich accessory minerals and plagioclase. The hydrothermally altered rocks have extremely low REE levels suggesting interaction of a volatile-rich aqueous fluid with melt and/or previously crystallized rock. However, smooth, continuous, decreasing trends of REE versus decreasing Zr, Th, TiO_2 and P_2O_5 show no break between altered and unaltered rocks. This suggests the REE reside in accessory minerals that were unaffected by the alteration, indicating the low REE levels in the altered rocks are inherited from melt-fluid, not fluid-rock, interaction.

9. The hydrothermally altered area of the Sangster Lake Pluton has elevated response of eU and the eU/eTh ratio in airborne gamma-ray spectrometric data. The geochemical data confirm that U is elevated in these altered areas as a result of the hydrothermal alteration. It follows that airborne spectrometric surveys are a useful exploration tool in defining plutons or areas of large plutons which have undergone similar hydrothermal alteration. These plutons have potential to host economic deposits of granophile elements.

10. Although no deposits of economic significance are known, the Sangster Lake Pluton has strongly developed features of a pluton with potential to host deposits of Sn and related elements. The absence of such deposits may simply reflect a lack of exposure or detailed exploration. Geochemical evidence provides two other alternatives: (1) the hydrothermal fluid may not have had a sufficient specialization of volatiles (esp. F) for concentration, transport and precipitation of the granophile elements into economic deposits; (2) the presence of other anions in the fluid (e.g. Cl and P) resulted in dispersion of granophile elements.

9.2 RECOMMENDATIONS FOR FUTURE WORK

A number of further research projects may amplify certain topics only initially addressed by this thesis:

1. This study examined, in two dimensions, a well-exposed pluton of anomalous radiometric response. The evidence presented here shows that the alterations resulting in this elevated response occurred in the uppermost roof zone of this particular pluton. Examination of these processes in the third dimension (i.e. depth) is lacking. A study initiated to examine this aspect will require deep diamond-drilling by an exploration company or government agency. A recommended location for this drill hole is atop the outcrop knoll marking the highest eU response in the pluton (sample F-G001, Appendix I).

2. Geochemistry in this, and in other recent investigations, defined an increased activity and mobility of P in the aqueous fluid-rich environment associated with the later stages of evolution of peraluminous granites. Little is known about this interesting phenomenon and further investigations are required to determine why and how this takes place, and what its economic significance may be.

3. The granitoid rocks of the eastern Meguma Zone have markedly higher levels of normative corundum compared with the rest of the Meguma Zone. The cause(s) for this feature remains unknown and could be the focus of a future study.

4. Rare earth elements show extremely low levels associated with fluid-melt interaction. Similar results are reported in studies from other hydrothermally altered Meguma Zone granitoid rocks. More information is required on REE systematics among the various rock-forming minerals (especially the heavy mineral suite) in these or similar rocks. The emergence of electron microprobe techniques capable of analyzing REE levels in minute accessory minerals make such a project possible.

5. The Beans Lake Leucomonzogranite has extensively metasomatized and greisenized contact zones with its enclosing monzogranite. One such zone, the Beans Lake greisen zone, is well exposed and thus would lend itself well to a detailed study of the effects of high temperature metasomatism.

6. The entire Meguma Zone has been covered by airborne gamma-ray spectrometric surveys. This study dealt with a terrain of elevated uranium and the uranium/thorium ratio. Different forms of radiometric response systematics are found over other areas of the Meguma Zone including some granitic terrains. For example, areas of anomalous eTh, eTh/eU, K, eU/K and eTh/K response have not been investigated in detail. Similar studies to this thesis should be carried out in these areas to document fully the significance of these relationships and to evaluate further the usefulness of airborne gamma-ray spectrometric surveys as an exploration and mapping tool.

7. The Sangster Lake Pluton provides an excellent opportunity for isotopic geochemical studies of the transition from the magmatic-postmagmatic stages of granitoid evolution. For instance, this study dealt with whole-rock oxygen isotope abundances but data on the ^{18}O abundances of the constituent rock-forming minerals throughout the stages are lacking. In addition, the behavior of other isotopic species (e.g. Sr, Nd, Pb and H) in the magmatic-hydrothermal transition could be examined.

8. The oxygen isotope study in this thesis highlights the lack of data on the ^{18}O systematics in the Meguma Group metasedimentary rocks. There are very limited data on the abundances in the major rock-forming minerals both relative to geographic distribution in the Meguma Zone

and throughout the various metamorphic zones. Such data should allow inferences as to the isotopic composition of the metamorphic waters.

APPENDIX I

PETROGRAPHIC DESCRIPTION OF CHEMICALLY ANALYSED SAMPLES

I.1 DEFINITION OF TERMS

I.1.1 Rock Type

Most rock type names used in this thesis were assigned according to the classification scheme for plutonic rocks of Streckeisen (1977). For comparative purposes, samples of monzogranite from areas of the Sangster Lake Pluton exhibiting anomalous radiometric response were categorized according to their relative level of response.

I.1.2 Location

The location of each sample site is given relative to existing roads and/or geographical recognizable landforms. The location of samples is also given in Figure 6-1.

I.1.3 Outcrop Description

The outcrop from which each sample was collected is described giving the size, extent and morphology of the outcrop as well as the degree of weathering (fresh, slight, moderate and intense). Outcrops with moderate or intense surface weathering were first drilled and blasted (Appendix II) in order to eliminate or minimize the weathered material. The terms used to describe the degree of weathering are not to be confused with degree of hydrothermal alteration.

I.1.4 Grain Size

The grain size designations used in the following descriptions are as follows:

coarse grain size: >0.5 cm

medium grain size: 0.1-0.5 cm

fine grain size: <0.1 cm

I.2 PETROGRAPHIC DESCRIPTIONS

I.2.3 Larrys River Pluton

Sample No.: F6-G002

Rock Type: Megacrystic monzogranite

Location: The sample was collected from the north edge of an area of abundant outcrop west of Double Lake. Immediately north of the outcrop is a large peat bog.

Outcrop Description:

The outcrop is a smooth glacial pavement. Drilling and blasting was required to obtain fresh material because of deep weathering.

Description: The rock is a megacrysitc, coarse-grained biotite monzogranite. In outcrop the rock contains randomly oriented K-feldspar megacrysts in a coarse-grained groundmass of quartz, plagioclase and biotite. In thin

section the rock is hypidiomorphic granular with anhedral quartz and subhedral oligoclase. Biotite is euhedral with abundant inclusions of zircon and monazite. Muscovite occurs in minor amounts and usually after biotite. Accessory minerals consist of monazite, zircon and apatite. Apatite occurs as euhedral grains associated with biotite. The rock displays no deformation textures.

Sample No.: LR-G009

Rock Type: Megacrystic monzogranite

Location: Collected from a road circling an abandoned blueberry barrens along the western margin of the pluton. The barrens is accessible by a poor-quality woods road off the Lundy to Upper New Harbour road.

Outcrop Description:

The outcrop consists of a $8m^2$, very smooth glacial pavement forming the bed of the woods road. The outcrop was uncovered during construction of the road and hence was shielded from deep weathering except for the upper few centimeters. Although fresh, the smooth form of the outcrop required blasting in order to obtain a sample.

Description: The rock has megacrysts of K-feldspar, randomly oriented in a hypidiomorphic granular groundmass of quartz, plagioclase and biotite. Minor amounts of muscovite are present both as separate grains and replac-

ing biotite. Accessory minerals consist of monazite, zircon, apatite, rutile and opaques. The monazite and zircon occur as inclusions in biotite. Apatite, and pyrite occur spatially associated with biotite. Opaques and rutile occur associated with chloritized biotite. The rock displays no deformation textures.

Sample No.: LR-G010

Rock Type: Megacrystic monzogranite

Location: Collected from a road circling an abandoned blueberry barrens along the western margin of the pluton. The barrens is accessible by a poor-quality woods road off the Lundy to Upper New Harbour road.

Outcrop Description:

The outcrop consists of a $25m^2$, very smooth glacial pavement forming the bed of the road. The outcrop was uncovered during construction of the woods road and hence has been shielded from deep weathering. Although fresh, the smooth form of the outcrop required blasting in order to obtain a sample.

Description: Randomly oriented megacrysts of K-feldspar in a coarse grained hypidiomorphic granular groundmass of quartz, plagioclase, K-feldspar and biotite. Plagioclase is oligoclase in composition and occurs both within the

groundmass and occasionally as megacrysts. Biotite of two generations occurs, one with abundant inclusions of zircon and monazite and one relatively free of inclusions. The inclusion-free variety occurs after the inclusion-rich variety. Apatite occurs as euhedral grains associated with biotite. The rock displays no megascopic or microscopic deformation textures.

Sample No.: LR-G011

Rock Type: Megacrystic monzogranite

Location: Collected from an abandoned blueberry barrens along the western margin of the pluton. The barrens is accessible by a poor quality woods road off the Lundy to Upper New Harbour road. The outcrop is located near the center of the barrens as defined by the circular woods road surrounding it.

Outcrop Description:

The sample was collected from a $30m^2$ weathered outcrop in an area of abundant boulders of this rock type. The deep weathering of the outcrop required two blasts before sufficiently fresh material was uncovered.

Description: Randomly oriented megacrysts of K-feldspar in a coarse-grained hypidiomorphic granular groundmass of quartz, plagioclase, K-feldspar and biotite. Plagioclase is subhedral and oligoclase in composition and occurs

mostly within the groundmass although megacrysts are present. Biotite of two generations occurs, one with abundant inclusions of zircon and monazite and one relatively free of inclusions. Apatite occurs as euhedral grains within and adjacent to biotite. The rock displays no megascopic or microscopic deformation textures.

Sample No.: LR-G012

Rock Type: Megacrystic monzogranite

Location: Collected from a high outcrop knoll immediately southwest of an unnamed lake near the southwest corner of the pluton. The outcrop is accessible from the New Harbour to Upper New Harbour road by a privately owned, woods road.

Outcrop Description:

The outcrop knoll is ten meters high and roughly circular in shape. It occurs at the contact with Meguma Group metasedimentary rocks. Weathering required one blast along a vertical joint plane to obtain a sample.

Description: The rock contains abundant K-feldspar megacrysts in a coarse-grained hypidiomorphic granular groundmass of quartz, oligoclase and biotite. Biotite is euhedral with abundant inclusions of zircon and monazite. Muscovite and chlorite occur in minor amounts replacing biotite.

Accessory minerals consist of monazite, zircon and apatite all of which are associated with biotite. Rutile and opaques (Fe-oxide) occur associated with chloritization of biotite. The rock displays no deformation textures.

Sample No.: F3-G004

Rock Type: Transitional monzogranite

Location: Collected from an outcrop knoll in a boulder-strewn barrens near the center of the pluton. The knoll is located approximately 0.5km north of the north end of a fire road accessing the area from the highway connecting Larrys River with New Harbour.

Outcrop Description:

The outcrop consists of a series of ledges forming a knoll rising from a boulder-strewn barrens. Deep weathering made necessary blasting to obtain fresh sample.

Description: The rock is megacrystic but much less so than the megacrystic monzogranite to the west. Megacrysts consist mostly of perthitic orthoclase although some plagioclase was observed. The groundmass consists of a hypidiomorphic granular mixture of quartz, plagioclase, biotite and muscovite. Plagioclase is subhedral, oscillatory zoned with clouded cores. Biotite forms subhedral flakes

which are commonly inclusion riddled with zircon and monazite. Apatite occurs as subhedral to euhedral grains spatially associated with the biotite. The rock is undeformed.

Sample No.: LR-5

Rock Type: Transitional monzogranite

Location: Located approximately 0.25 km south of Henry Lake in the central region of the pluton. The outcrop occurs within a small swampy barren ($200m^2$) surrounded by forest.

Outcrop Description:

The outcrop forms a ledge approximately 5 m by 20 m which is deeply weathered due to extremes of temperature. Blasting was required to obtain fresh sample.

Description: The rock is slightly megacrystic with subhedral to euhedral laths of clean, perthitic orthoclase. The groundmass consists of quartz, plagioclase (oligoclase), biotite and minor muscovite. The oligoclase is twinned, oscillatory zoned and somewhat clouded because of alteration to very fine-grained white mica. The lesser amount of biotite compared to that in the megacrystic monzogranite is of particular note. Apatite is associated with biotite and commonly displays resorbed boundaries.

Biotite contains abundant inclusions of monazite and zircon.

Sample No.: LR-6

Rock Type: Transitional monzogranite

Location: Located a short distance south and east of Henry Lake near the center of the pluton.

Outcrop Description:

The outcrop occurs as a small portion (5m long) of a large ledge which extends for a considerable distance toward the southwest. The outcrop is deeply weathered and required blasting to obtain a fresh sample.

Description: Slightly megacrystic with subhedral laths of microcline (cross-hatch twinning) in a groundmass of quartz, plagioclase, biotite and minor muscovite. Several megacrysts are mantled by oligoclase-albite. Biotite has monazite and zircon inclusions and is commonly associated with euhedral apatite. Subtle deformation textures present are sutured boundaries of quartz grains, minor sub-grain development, bent polysynthetic twins in plagioclase.

Sample No.: F6-G004

Rock Type: Biotite-muscovite monzogranite

Location: Collected from an outcrop along the northeast side of the highway joining Lundy and Larrys River. The outcrop is the only one of this rock type exposed along the highway and occurs immediately north of a sharp bend in the road east of Fougere Lake.

Outcrop Description:

Road building and blasting for a power pole has provided abundant fresh material for sampling.

Description: The rock is non-megacrystic with a hypidiomorphic granular texture. Major minerals consist of quartz, perthitic microcline, plagioclase (An_{24-28} optical identification), biotite and muscovite (ratio 60:40). Plagioclase is clear and normally zoned. Although the outcrop appears to be undeformed, definite deformational textures were observed in thin section. These include the microclinization of K-feldspar, sub-grain development, undulatory extinction and sutured boundaries in quartz and bent twin lamellae in plagioclase.

Sample No.: F6-G008

Rock Type: Biotite-muscovite monzogranite

Location: Collected from along a short, recently built, woods road leading south from the Lundy to Larrys River

highway. The woods road intersects the highway about 100m south from outcrop F6-G004. The outcrop is located about 100m from the intersection with the highway.

Outcrop Description:

This sample was collected from fresh material torn up from a small outcrop (<2m^2) during the recent road building.

Description: The rock is non-megacrystic, hypidiomorphic granular with a groundmass of quartz, perthitic microcline, oligoclase, biotite and muscovite. Plagioclase is clear and normally zoned. Biotite has zircon and monazite inclusions. Muscovite occurs both as replacement of biotite and as discrete grains. Muscovite and biotite are in roughly equal proportions. The sample has subtle deformation textures visible in thin section only. They include the microclinization of K-feldspar, sub-grain development, undulatory extinction and sutured boundaries in quartz and bent twin lamellae in plagioclase.

Sample No.: F6-G009

Rock Type: Biotite-muscovite monzogranite

Location: Collected from along a short, recently built, woods road leading south from the Lundy to Larrys River highway. The woods road intersects the highway about

100m south from outcrop F6-G004. The outcrop is located near the end of the woods road.

Outcrop Description:

This sample was collected from fresh material torn up from a small outcrop (<$1m^2$) during the recent road building.

Description: The rock has a non-megacrystic, hypidiomorphic granular texture. Major minerals are quartz, perthitic microcline, oligoclase, biotite and muscovite. Plagioclase is subhedral, clear, normally zoned and oligoclase in composition. Biotite is slightly more abundant than muscovite. The biotite has zircon and monazite inclusions and where chloritized, has associated rutile and Fe-oxide. Muscovite occurs both as replacement of biotite and as discrete grains. The sample has subtle deformation textures visible in thin section only. They include the microclinization of K-feldspar, sub-grain development, undulatory extinction and sutured boundaries in quartz and bent twin lamellae in plagioclase.

Sample No.: LR-7

Rock Type: Biotite-muscovite monzogranite

Location: The outcrop occurs along the west edge of a fire access road which leads to the central region of the

pluton. The entrance to the road is located along the Lundy to Larrys River highway, a short distance west of Fougere Lake. The outcrop is found about 200 m south of a stream joining two small unnamed lakes.

Outcrop Description:

The outcrop (<2m^2) forms a small rise in the road. Fresh material was obtained from rubble torn from the outcrop during road building.

Description: The rock is non-megacrystic with a hypidiomorphic granular texture. Major minerals include quartz, microcline, oligoclase (An_{24} optical identification), biotite and muscovite (ratio 65:35). Oligoclase is fresh and normally zoned. In outcrop the rock appears undeformed but in thin section subtle deformation textures occur. These include the microclinization of K-feldspar, subgrain development, undulatory extinction and sutured boundaries in quartz and bent twin lamellae in plagioclase.

Sample No.: F6-G005

Rock Type: Leucogranite

Location: The outcrop occurs in the gutter along the south side of the Lundy to Larrys River highway immediately north of Fougere Lake. Similar outcrops of this rock are exposed in the woods in the immediate area.

Outcrop Description:

The outcrop is exposed for about 30 m along the gutter and abundant fresh material is available from either the rubble blasted during road building or the from the fresh angular edges on the outcrop.

Description: The sample is fine-grained, sugary, light grey leucogranite. Major minerals consist of quartz, perthitic microcline, albite and muscovite. Muscovite occurs mostly as separate flakes although some fine-grained white mica occurs after albite. The sample contains very little biotite although some areas of the outcrop have a higher biotite content (≈0.5%). Accessory minerals include greenish apatite and garnet. The rock is undeformed.

I.2.4 **Sangster Lake Pluton**

Sample No.: F-G018

Rock Type: Average-response monzogranite

Location: Collected from a cliff face overlooking New Harbour River. The cliff is located a short distance upstream from where Eastern Fork Stream enters the New Harbour River.

Outcrop Description:

The outcrop forms a large, rounded knoll about 30 m high. The western face of the knoll is steep with abundant angular edges from one of which the sample was collected.

Description: The rock is non-megacrystic and hypidiomorphic granular. Major minerals consist of quartz, oligoclase, perthitic microcline, muscovite and biotite. Microcline is poikilitic with inclusions of quartz and muscovite. One example of an albite mantle on K-feldspar occurs. Muscovite is more abundant than biotite (ratio 60:40). Biotite has inclusions of zircon and monazite. Other accessories consist of apatite, associated with biotite and as separate grains, and garnet, as separate grains. Faint deformation indicated by quartz with undulatory extinction and presence of microcline.

Sample No.: SL-7

Rock Type: Average-response monzogranite

Location: This sample was collected from a large rounded knoll overlooking and immediately north of a sharp bend in Eastern Fork Stream. The outcrop is deeply weathered and drilling and blasting was required to obtain fresh material.

Outcrop Description:

The rounded knoll is barren and almost totally outcrop. The knoll is about 20 m high and has metasedimentary outcrops exposed along its low-lying perimeters in Eastern Fork Stream.

Description: The rock is non-megacrystic, coarse grained and allotriomorphic granular (except for subhedral plagioclase). Major minerals consist of quartz, perthitic microcline, normally zoned oligoclase (An_{22}), biotite and muscovite. Plagioclase has clouded, more calcic, cores. Muscovite is more abundant than biotite (ratio 2:1) and occurs as separate subhedral flakes and replacing biotite and plagioclase. Biotite has zircon and monazite inclusions and is chloritized. Accessories consist of monazite, zircon, apatite and rare garnet. Apatite occurs as separate grains, and as inclusions in biotite and muscovite.

Sample No.: F5-G001

Rock Type: Central monzogranite

Location: This sample site is located along the north edge of a wide expanse of barren which extends south to Sangster Lake. The outcrop occurs 0.8 km due north of Beans Lake.

Outcrop Description:

The outcrop forms an elongate ledge of strongly-foliated monzogranite. The sample was collected from the junction of two fracture surfaces.

Description: Highly deformed, muscovite-biotite monzogranite. Major minerals consist of quartz, microcline, albite, muscovite and biotite. Muscovite occurs as large flakes and as small flakes within albite. Muscovite is more abundant than biotite (ratio 65:35). Accessories consist of apatite, monazite and zircon. Apatite occurs as separate subhedral-euhedral grains and as minute grains within albite. The rock is strongly deformed with both 'c' and 's' fabrics present. The 's' fabric is defined by alignment of micas and shearing of major minerals. The 'c' fabric is defined by widely spaced shear planes. Albite has bent twin lamellae and muscovite has bent cleavage.

Sample No.: F5-G010

Rock Type: Central monzogranite

Location: This sample was collected from outcrops exposed along Patterson Brook at the extreme northeast corner of the pluton. These outcrops are the first encountered along Patterson Brook downstream from a small, unnamed lake south of Lundy.

Outcrop Description:

The outcrops are exposed in the brook and along the banks. Outcrops of monzogranite carry a well-developed foliation and are exposed within 0.5 m of a metasedimentary andalusite schist outcrop. This sample was collected from an angular joint face exposed beneath the root system of a fallen tree.

Description: Highly deformed, coarse-grained muscovite-biotite monzogranite. Major minerals consist of quartz, microcline, albite, muscovite and biotite. Muscovite occurs as large flakes and as small flakes within albite. Muscovite is more abundant than biotite (ratio 65:35). Accessories consist of apatite, monazite and zircon. Apatite occurs as separate subhedral-euhedral grains and as minute grains within albite. Both monazite and zircon occur as inclusions in biotite. The rock is intensely deformed with two preferred orientations. An 's' fabric is defined by alignment of micas and lensoid and subgrained quartz and feldspars. A 'c' fabric is defined by shear planes displacing the major minerals. Sutured grain boundaries are common.

Sample No.: SL-11

Rock Type: Central monzogranite

Location: This sample site is located at the top of a small granite cliff overlooking the Sangster Lake Au Prospect to the west.

Outcrop Description:

The outcrop forms a large, flat, glaciated surface which is deeply weathered. Drilling and blasting were required to obtain fresh sample.

Description: The rock is a massive, coarse-grained allotriomorphic granular, muscovite-biotite monzogranite. Major minerals are quartz, albite, microcline, muscovite and biotite. Microcline is perthitic. Albite is corroded with secondary fine-grained muscovite and apatite. Muscovite is more abundant than biotite (ratio 61:39). Biotite has monazite and zircon inclusions and is altering to chlorite. Apatite occurs associated with biotite and as inclusions in altered plagioclase. The rock has a very faint foliation defined by alignment of micas.

Sample No.: SL-12

Rock Type: Central monzogranite

Location: Collected along a prominent outcrop ridge located about 1 km southwest of Sangster Lake. The ridge is the westernmost outcrop in an area of abundant outcrop

extending west from Sangster Lake. Toward the west the outcrop exposure ends and the area is low-lying.

Outcrop Description:

The outcrop is a flat, glacial pavement with a small cliff about 4 m high. Deep weathering required drilling and blasting to obtain sample.

Description: The rock is a massive, coarse-grained allotriomorphic granular muscovite-biotite monzogranite. Major minerals are quartz, albite, microcline, muscovite and biotite. Microcline is slightly perthitic. Albite is highly corroded (altered to fine-grained muscovite). Muscovite is more abundant than biotite (ratio 75:25). Biotite has monazite and zircon inclusions. One grain of zircon was observed in the groundmass. Apatite occurs associated with biotite and as inclusions in altered plagioclase. The rock has a faint foliation defined by alignment of micas and rodding of quartz and feldspar.

Sample No.: SL-13

Rock Type: Central monzogranite

Location: The sample site is located near the center of the easternmost of three circular outcrop knolls which occur at the southwest end of Sangster Lake.

Outcrop Description:

The circular knoll forms one of the concentric structures recognized in air photo interpretation over the pluton. The structures are entirely of medium-grained monzogranite. Weathering required that drilling and blasting be used to obtain fresh material.

Description: The rock is a massive, coarse-grained, allotriomorphic granular, muscovite-biotite monzogranite. Major minerals are quartz, albite, K-feldspar, muscovite and biotite. Muscovite is more abundant than biotite (ratio 81:19). Muscovite occurs as large flakes and as a fine-grained alteration of albite. Biotite is chloritized with associated rutile and Fe-oxide. Accessories are monazite, apatite and rare garnet. The rock has a faint to moderate alignment of micas and lensoid quartz and feldspar.

Sample No.: SL-14

Rock Type: Central monzogranite

Location: The sample site is located in the center of a wide expanse of boulder-strewn barrens that extends from Sangster Lake to the north edge of the pluton. The outcrop occurs due north of Sangster Lake, approximately half way between the lake and the north edge of the pluton.

Outcrop Description:

The outcrop is elongate in shape and deeply weathered. Drilling and blasting were required to obtain fresh sample.

Description: The rock is a moderate- to highly deformed, massive, coarse-grained, allotriomorphic granular, muscovite-biotite monzogranite. Major minerals are quartz, albite, microcline, muscovite and biotite. Muscovite occurs as large flakes and as small flakes within albite. Muscovite is more abundant than biotite (ratio 85:15). Accessories include apatite, monazite and zircon. Apatite occurs as separate subhedral grains and as minute grains within albite. The rock is strongly deformed with both 'c' and 's' fabrics present. The 's' fabric is defined by alignment of micas and shearing of major minerals. The 'c' fabric is defined by widely spaced shear planes. Albite has bent polysynthetic twins and muscovite has bent cleavage.

Sample No.: SL-15

Rock Type: Central monzogranite

Location: The sample site is located due north of Sangster Lake near the contact with metasedimentary rocks south of Green Barrens Lake. The outcrop occurs in the transition from a boulder-strewn barrens into scrub softwood cover.

Outcrop Description:

The outcrop is a deeply weathered, glacial pavement. Drilling and blasting were required to obtain fresh material.

Description: Intensely deformed, coarse-grained, muscovite-biotite monzogranite. Major minerals are quartz, albite, microcline, muscovite and biotite. Muscovite occurs as large flakes and as small flakes within albite. Muscovite is more abundant than biotite (ratio 75:25). The amounts of muscovite and biotite are based on slab modal counts if the muscovite as alteration of plagioclase is included the proportion of muscovite increases greatly. Accessory minerals are apatite, Cl-bearing apatite, and very trace amounts of garnet, monazite and zircon. Apatite occurs as separate subhedral-euhedral grains and as minute grains within albite. Cl-bearing apatite occurs associated with a brown matted mineral. Both monazite and zircon occur as inclusions in biotite. The rock is intensely deformed with two preferred orientations. An 's' fabric is defined by alignment of micas and lensoid and sub-grained quartz and feldspars. A 'c' fabric is defined by shear planes displacing the major minerals. Sutured boundaries are common.

Sample No.: F-G001

Rock Type: High-response monzogranite

Location: Collected from an outcrop knoll overlooking a stillwater along Patterson Brook to the east. The knoll is located in the barrens immediately north of where a stream from Cranberry Lake enters Patterson Brook.

Outcrop Description:

The outcrop is the easternmost of a series of knolls which protrude from a boulder-strewn barrens. This knoll has the highest radiometric response in the pluton.

Description: The rock is a massive, coarse-grained, allotriomorphic granular, muscovite-biotite monzogranite. Major minerals are quartz, albite, K-feldspar, muscovite and biotite. K-feldspar is perthitic and is formed at the expense of albite. Albite is very highly corroded to secondary fine-grained muscovite and minute grains of apatite. Muscovite (15%) is much more abundant than biotite (0.9%). The amounts of muscovite and biotite are based on slab modal counts if the muscovite as alteration of plagioclase is included the proportion of muscovite increases greatly. Biotite has monazite and zircon inclusions and is chloritized. Accessory minerals are apatite, Cl-bearing apatite, garnet, and very rare monazite and zircon. Apatite occurs associated with biotite and as inclusions in corroded albite. Cl-bearing apatite is associated with a secondary brown matted

mineral (possibly an alteration of biotite). The rock has a faint foliation defined by alignment of micas and rodding of quartz and feldspar.

Sample No.: F-G003

Rock Type: High-response monzogranite

Location: Collected from an outcrop overlooking Cranberry Lake to the west. Located approximately 300 m west of sample F-G001.

Outcrop Description:

The outcrop is a glacial pavement with a small cliff face along its southern edge. The sample was collected from beneath an overhang.

Description: The rock is a massive, coarse-grained, allotriomorphic granular, muscovite-biotite monzogranite. Major minerals are quartz, albite, Orthoclase, muscovite and biotite. Orthoclase is secondary after albite and slightly perthitic. Albite is very highly corroded to secondary fine-grained muscovite and minute grains of apatite. Muscovite (14%) is much more abundant than biotite (2.5%). The amounts of muscovite and biotite are based on slab modal counts but if the muscovite as alteration of plagioclase is included the proportion of muscovite increases greatly. Biotite has monazite and zircon inclusions and is chloritized. Accessory minerals

are apatite, garnet, Cl-bearing apatite and very rare monazite and zircon. Apatite occurs associated with biotite and as inclusions in corroded albite. Cl-bearing apatite is associated with a secondary brown matted mineral (possibly an alteration of biotite). The rock has a faint foliation defined by alignment of micas.

Sample No.: F-G004

Rock Type: High-response monzogranite

Location: This sample was collected at the edge of the woods northeast of Cranberry Lake. The outcrop is about 300 m north of sample F-G003.

Outcrop Description:

The outcrop is a small, moss-covered, glacial pavement.

Description: The rock is a massive, coarse-grained, allotriomorphic granular, muscovite-biotite monzogranite. Major minerals are quartz, albite, K-feldspar, muscovite and biotite. K-feldspar is slightly perthitic and replacing albite. Albite is very highly corroded to secondary, fine-grained muscovite and minute grains of apatite. Muscovite (8.1%) is more abundant than biotite (2.3%). Biotite has monazite and zircon inclusions and most grains are chloritized yielding rutile and opaques. Accessory minerals are apatite, monazite and zircon.

Apatite occurs associated with biotite and as inclusions in corroded albite. The rock has a faint foliation defined by alignment of micas and rodding of quartz and feldspar.

Sample No.: F-G005

Rock Type: High-response monzogranite

Location: This sample was collected from a small knoll overlooking a stillwater on Patterson Brook. The area is a boulder-strewn barrens. Sample F-G001 was collected from a knoll 150 m to the south.

Outcrop Description:

The outcrop forms a small knoll protruding from a boulder-strewn barrens. Fresh material was collected with much difficulty.

Description: The rock is a massive, coarse-grained, allotriomorphic granular, muscovite-biotite monzogranite. Major minerals are quartz, albite, K-feldspar, muscovite and biotite. K-feldspar is slightly perthitic and replacing albite. Albite is very highly corroded to secondary, fine-grained muscovite and minute grains of apatite. Muscovite (8.1%) is much more abundant than biotite (4.7%). The amounts of muscovite and biotite are based on slab modal counts. If the muscovite as alteration of plagioclase is included in th mode the proportion of

muscovite increases greatly. Biotite has monazite and zircon inclusions and most grains are chloritized. Accessory minerals are apatite, Cl-bearing apatite, garnet, and very rare monazite and zircon. Apatite occurs associated with biotite and as inclusions in corroded albite. Cl-bearing apatite is associated with a secondary brown matted mineral (possibly an alteration of biotite). Garnets are separate, euhedral, inclusion free grains. The rock has a faint foliation defined by alignment of micas and rodding of quartz and feldspar.

Sample No.: F-G022

Rock Type: Leucomonzogranite

Location: This sample was collected from a prominent ridge in a barrens between Sangster and Beans Lakes. The outcrop is within the Beans Lake Leucomonzogranite but only a short distance from the contact with the monzogranite.

Outcrop Description:

The outcrop is a medium- to coarse-grained leucomonzogranite adjacent to a metasomatized contact zone developed along the contact with the monzogranite. The area hosts many quartz vein stockworks.

Description: The rock is a massive, medium- to coarse-grained, allotriomorphic granular, muscovite leucomonzogranite. Major minerals are quartz, orthoclase, albite and mus-

covite. Orthoclase is slightly perthitic. Albite is altered to fine-grained muscovite but this is less-developed than in the altered monzogranites. Muscovite also occurs as large books in the groundmass. Accessory minerals are apatite and garnet. The rock is undeformed.

Sample No.: F-G024

Rock Type: Leucomonzogranite

Location: The sample was collected from a large outcrop located at the southwest end of a stillwater along Patterson Brook a short distance south of Canter Lake.

Outcrop Description:

The sample was collected from a leucomonzogranite dyke intruding a large monzogranite outcrop. the monzo-granite has a faint foliation while the leucomonzogranite is undeformed. The metasediment contact occurs within 30 m. and likely follows the brook.

Description: The rock is a massive, fine-grained, sugary, mus-covite leucogranite-leucomonzogranite. Major minerals are quartz, orthoclase, albite and muscovite. Orthoclase is slightly perthitic. Albite is altered to fine-grained muscovite but this is less developed than in the altered monzogranites. Muscovite also occurs as large books in the groundmass. Accessory minerals are greenish apatite,

Cl-bearing apatite and garnet. The rock is undeformed while the enclosing monzogranite has a slight foliation.

Sample No.: F5-G004

Rock Type: Leucomonzogranite

Location: This sample was collected from an outcrop ledge located 200 m north of Beans Lake. This is the northernmost outcrop of the Beans Lake intrusion.

Outcrop Description:

The outcrop forms an elongate ledge with a 3 m high south face. The sample was collected from beneath an overhang.

Description: The rock is a massive, medium- to coarse-grained, allotriomorphic granular, muscovite leucomonzogranite. Major minerals are quartz, orthoclase, albite and muscovite. Orthoclase is slightly perthitic and is a secondary replacement of albite. Albite is also altered to fine-grained muscovite. Separate grains of muscovite are found in the groundmass. Accessory minerals are greenish apatite, Cl-bearing apatite and garnet. Apatite occurs as interstitial grains and as minute grains in albite. Cl-bearing apatite occurs as interstitial grains. Garnet forms rare small inclusion-free crystals. The rock is undeformed.

Sample No.: F5-G007

Rock Type: Leucomonzogranite

Location: The sample was collected from within the Beans Lake greisen zone. The outcrop is from the north end of the zone.

Outcrop Description:

The outcrop has sheeted quartz vein swarms with associated greisens but the sample was collected as far from the vein swarms as possible. The outcrop surface is intensely weathered but slightly weathered to fresh rock occur within 5 cm of surface.

Description: The rock is a medium- to coarse-grained, allotriomorphic granular, muscovite leucomonzogranite. It is inhomogeneous in texture with variable grain size and quartz-feldspar ratio. Major minerals are quartz, orthoclase, albite and muscovite. Orthoclase is slightly perthitic and together with quartz is replacing albite. Albite is also altered to fine-grained muscovite. Separate grains of muscovite are found in the groundmass. Accessory minerals are greenish apatite, Cl-bearing apatite, topaz, pyrite, garnet and rare amounts of wolframite, monazite and zircon. Apatite occurs as interstitial grains and as minute grains in albite. Cl-

bearing apatite, topaz and garnet occur as interstitial grains. The rock is undeformed.

Sample No.: F-G020

Rock Type: Greisen

Location: Collected from the central area of the Beans Lake greisen zone. The outcrop has sheeted quartz vein zones with associated greisenization.

Outcrop Description:

The south end of the outcrop is hydrothermally altered monzogranite while the north end is leucomonzogranite. This sample was collected from the gradational zone between these two end members. The outcrop surface is intensely weathered but slightly weathered to fresh rock occur within 5 cm of surface.

Description: The rock is a medium-grained, greisenized, muscovite leucomonzogranite. Major minerals are quartz, muscovite, albite, and garnet. Albite is much less abundant than in previous rocks and is altered to fine-grained muscovite. The rock is muscovite rich. Garnet occurs as abundant, small, euhedral-subhedral, inclusion-free grains throughout the sample. Accessory minerals are greenish apatite and rare amounts of wolframite and cassiterite. Apatite occurs as interstitial grains and as minute grains in

albite. Cl-bearing apatite, topaz and garnet occur as interstitial grains. The rock has a moderate to faint foliation.

APPENDIX II

ANALYTICAL METHODS

II.1 SAMPLE COLLECTION

Thirty one samples were collected for whole-rock chemical analyses, eighteen from the Sangster Lake Pluton and thirteen from the Larrys River Pluton (Appendix I). The barren physiography of the study area results in deep weathering, especially of coarse-grained rocks. This coupled with a lack of road cuts caused difficulty in finding fresh, unweathered samples. To eliminate the problem blasting of outcrops was required. A portable, gasoline-driven, Poinjar jackhammer drill was carried in a provincial government helicopter and used to drill 35 cm deep holes at pre-selected sample sites. The sites were then revisited and each was blasted with one stick of dynamite (40% Forsite). Samples were collected from the least weathered debris.

II.2 SAMPLE PREPARATION

Large samples were broken with a 6 lb hammer. The pieces were then reduced to approximately 3 cm in diameter with a hydraulic rock splitter. At this stage all weathered material was discarded. The fresh pieces were broken into small chips with a ceramic rock crusher. Between samples the plates of the crusher were cleaned with compressed air and acetone. A number of pieces from the next sample were then passed through the crusher and this material was discarded. The remaining portion of the sample was crushed and stored in sample bags.

The crushed samples were then passed through a sample splitter. One split (250-300 g) was crushed to -100 mesh in a W-carbide swing mill. A second split (100 g) was crushed (for W analysis) in a ceramic swing mill. Two samples were duplicated by sending one ceramic crushed powder and one W-carbide crushed powder for trace element analyses (samples F-G022 and F6-G004; Table II-4). This was done to check for contamination of trace elements other than W in the W-carbide crushed samples.

II.3 GEOCHEMICAL ANALYSES

II.3.1 Major Elements

II.3.1.1 Decomposition for Si, Al, Ti, Fe3+, Mn, Mg, K and Na

A portion of approximately 0.1000 g of each sample, duplicate and standard was weighed and transferred into teflon cups. A blank cup was also included. A slurry was made by addition of 0.5 ml distilled water and to this 2.5 ml of HNO_3 and 20 ml of a mixture of percloric acid and HF were added. The cups were capped and allowed to stand overnight on a steam bath. The caps were removed and the cups were heated for 5 hours. The cups were then placed in a sand bath and heated until percloric acid fumes were evolved and eventually driven off. After cooling, exactly 5 ml of distilled water was added to each. After capping they were placed on the waterbath and allowed to digest for 1 hour in boiling water. After cooling the contents were transferred to 250 ml volumetric flasks and topped with distilled water. the flasks

were shaken and the contents were transferred to polyethylene bottles. To each 20 ml of a solution of 5% La_2O_3 was added to counteract chemical interference. Standard solutions prepared from 1000 ppm standard rock solutions were provided by S. Parikh of the Geology Department, Dalhousie University.

International standards GSP-1 and JG-1 were used to determine accuracy and 3 samples were duplicated to access precision (Tables II-1 and II-2).

II.3.1.2 Decomposition for Ca, P and Li

The procedure for decomposition for Ca, P and Li is the same as above except that 1.0000 g of sample was used. Calcium was included in this decomposition as results for this element using the 0.1000 g decomposition were unacceptable. Five international standards (BCR-1, BM, SY-3, GSP-1 and JG-1) and two duplicated samples were also prepared.

II.3.1.3 Analytical Methods

1. Atomic Absorption

A Perkin Elmer (Model 503) atomic absorption spectrometer was used to analyze for Si, Ti, Al, Fe^{3+}, Mn, Mg, Ca, K, Na and Li. An air-acetylene flame was used for all of these elements except Si, Al and Ti in which case a nitrous oxide acetylene flame was used.

2. Colorimetry

Phosphorus was analysed colorimetrically. An accurately measured, 5 ml aliquot of the sample solution was pipetted into a 50 ml volumetric flask especially prepared for phosphorus analysis. A reagent solution of 3N H_2SO_4, ammonium molybdate, ascorbic acid and distilled water was added to the flasks. They were then topped to 50 ml. The solutions sat overnight after which measurements were made on a Bausch and Lomb Spectric 70 spectrophotometer at 827 nm using 4 cm cells. Reagent blank values were subtracted yielding the sample P concentration.

3. Titration

Ferrous iron was analysed for by titration. A accurately weighed portion of 0.2000 g of sample powder was transferred to a plastic flask. Exactly 5 ml of 0.1 N ammonium vanadate and 10 ml HF were added. The flasks were put on a shaker table overnight after which 10 ml of 1:2:2 solution of H_3PO_4:H_2SO_4:H_2O was added. The contents of the flasks were transferred to beakers containing 100 ml of 5% boric acid solution. To these, 10 ml of 0.05 N ferrous ammonium sulphate solution was added by pipette. Sixteen drops of 0.2% barium diphenylamine sulphonate indicator was added and the flasks were titrated to a grey end point with 0.05 N $K_2Cr_2O_7$ solution.

4. Penfield Tube

The penfield tube method was used to determine total water content (H_2O^++H_2O^-) in the samples. An accurately weighed portion of sample

TABLE II-1

MAJOR ELEMENT ERROR ANALYSES

Element (Method*)	(Standard)	Obtained Value	Accepted Value	Deviation (%)	Deviation (Mean %)
SiO_2	(JG-1)	73.39	72.36	1.42	1.56
(AA)	(GSP-1)	68.43	67.31	1.67	
TiO_2	(JG-1)	0.26	0.27	3.70	2.60
(AA)	(GSP-1)	0.65	0.66	1.52	
Al_2O_3	(JG-1)	13.84	14.20	2.54	3.48
(AA)	(GSP-1)	14.52	15.19	4.41	
FeO	(JG-1)	1.71	1.62	5.56	6.02
(Ttr.)	(GSP-1)	2.46	2.31	6.49	
Fe_2O_3	(JG-1)	2.023	2.16	6.30	5.75
(AA)	(GSP-1)	4.077	4.30	5.20	
MnO	(JG-1)	0.054	0.06	10.00	10.00
(AA)	(GSP-1)	0.034	0.04	10.00	
MgO	(JG-1)	0.74	0.76	2.63	2.88
(AA)	(GSP-1)	0.93	0.96	3.13	
CaO	(BCR-1	6.76	6.97	3.01	5.20
(AA)	(BM)	6.11	6.46	5.42	
	(SY-3)	7.83	8.26	5.21	
	(GSP-1)	1.89	2.03	6.90	
	(JG-1)	2.05	2.17	5.50	
Na_2O	(JG-1)	3.37	3.39	0.59	0.83
(AA)	(GSP-1)	2.83	2.80	1.07	
K_2O	(JG-1)	3.87	3.96	2.27	1.41
(AA)	(GSP-1)	5.56	5.53	0.54	
P_2O_5	(BCR-1)	0.36	0.33	9.10	4.19
(Col.)	(BM)	0.11	0.10	10.00	
	(SY-3)	0.53	0.54	1.85	
	(GSP-1)	0.28	0.28	0	
	(JG-1)	0.09	0.09	0	

* AA = Atomic Absorption
Ttr = Titration
Col = Colorimetric

TABLE II-2

MAJOR ELEMENT DUPLICATE ANALYSES

Sample No.	LR-G009		LR-G010		SL-12		F-G001		F-G004		F-G005		F5-G004		
Duplicate	I	II	I	II	I	II	I	II	I	II	I	II	I	II	III
SiO_2	-	-	71.80	72.84	72.21	72.99	74.67	72.62	-	-	-	-	-	-	-
TiO_2	-	-	0.40	0.40	0.23	0.23	0.12	0.11	-	-	-	-	-	-	-
Al_2O_3	-	-	15.35	15.17	15.34	15.34	15.39	15.05	-	-	-	-	-	-	-
Fe_2O_3TOT	-	-	2.40	2.38	1.86	1.85	1.22	1.23	-	-	-	-	-	-	-
FeO	-	-	2.03	1.90	1.46	1.32	1.03	1.01	-	-	-	-	-	-	-
MnO	-	-	0.05	0.05	0.07	0.07	0.05	0.05	-	-	-	-	-	-	-
MgO	-	-	0.72	0.73	0.41	0.40	0.25	0.24	-	-	-	-	-	-	-
CaO	1.08	1.09	-	-	-	-	-	-	0.47	0.46	-	-	-	-	-
K_2O	-	-	4.45	4.43	4.09	3.98	3.82	3.76	-	-	-	-	-	-	-
Na_2O	-	-	3.47	3.49	3.89	3.89	4.15	4.14	-	-	-	-	-	-	-
P_2O_5	0.26	0.26	-	-	-	-	-	-	0.47	0.47	-	-	-	-	-
CO_2	-	-	-	-	-	-	-	-	-	-	0.19	0.20	0.19	0.13	0.27

(0.5 g) was mixed with 2.5 g of dry flux (2:1:1 mixture of PbO_2:$PbCrO_4$:$NaWO_4$). Adsorbed water (H_2O^-) was determined by drying 0.5 g of sample powder at 110 °C for 2 hours. After cooling, the sample was reweighed with the decrease in weight being H_2O^-. Structural water (H_2O^+) was determined by subtracting the H_2O^- value from the total water (H_2O^++H_2O^-) value determined by the Penfield Tube method. Both these methods must be carried out on the same day to account for atmospheric changes resulting in variation in H_2O^- values.

5. Commercial Analysis for Carbon Dioxide

Carbon dioxide analyses was analyzed commercially at the Minerals Engineering Center, Technical University of Nova Scotia. The analyses were done with an induction furnace method. A sample, weighing 0.5 g is fused in a LECO carbon analyzer. The volume of evolved gas is measured in a gas burette to determine the total gas volume. The gas is then passed through a NaOH solution to absorb the CO_2. After this the gas is returned to the gas burette to determine the volume of gas lost to the NaOH. The amount lost is the volume of CO_2 from the sample.

II.3.2 Trace Elements

All trace elements except for Li (see previous section) were analysed commercially. The elements analysed at each laboratory and the methods used are given below.

II.3.2.1 Analyses for Ba, Rb, Sr, Zr, Pb and Zn.

The samples were analysed for Ba, Rb, Sr, Zr, Pb and Zn at the Saint Marys University X-Ray Fluorescence Laboratory. The analyses were determined in a Phillips PW-1400 sequential wavelength dispersive x-ray fluorescence spectrometer using a Rh-anode x-ray tube with 2.4 kilowatts of applied power. Accurately weighed, 10g samples were homogenized with 1.5 g of binding agent (phenolic resin). This mixture was pelletized and the pellets were analyzed on the spectrometer.

The accuracy was assessed with 5 international standards and precision with 4 duplicates (Tables II-3 and II-4).

II.3.2.2 Analyses for Mo, Ag, Be, B and Sn.

The samples were analyzed for Mo, Ag, Be, B and Sn at Bondar-Clegg and Company Limited, Ottawa, Ontario. Atomic absorption using HNO_3-HCL hot extraction was used for Mo and Ag, while the HF-H_2SO_4 (total metal digestion method) followed by HCL dissolution was used for Be.

Direct-current plasma emission spectrometry was used for B analysis. The powders were fused with KOH in a Ni-crucible. The residue is dissolved in HCL and the solution analysed on a direct-current emission spectrometer.

The samples were analyzed for Sn by x-ray fluorescence. The samples were first mixed with a binding agent and pelletized. The pellets were then analyzed on an x-ray spectrometer.

One internal standard (CG-1) and 6 duplicates were submitted with the samples to access accuracy and precision (Tables II-3 and II-4). Note that with two of the duplicated samples (F-G022 and F6-G004) one

run was on a powder crushed in a ceramic swing mill while the second run was on powder from a W-carbide swing mill, hence the highly anomalous W values.

II.3.2.3 Analyses for F and Cu

The samples were analyzed for F and Cu at the Minerals Engineering Center, Technical University of Nova Scotia, Halifax. Fluorine was determined by selective ion electrode. The samples (0.2-0.4 g) were fused with NaOH in a Ni-crucible. The solid is dissolved in an ammonium citrate buffer solution. The F level in the solution is determined by a fluoride-selective ion electrode by comparison with reference electrodes.

Copper was analyzed by atomic absorption spectrometry using 0.5 g samples.

The results of internal standard CG-1 and 3 duplicates are given in Tables II-3 and II-4.

II.3.2.4 Analyses for U, Th, W and Au

Analyses for U, Th, W and Au were by neutron activation analyses (NAA) at Nova Track Analysts Limited, Vancouver, British Columbia. The samples were irradiated in a high density neutron flux after which the resultant activation of the isotopes of interest was measured on a multi-channel gamma-spectrometer and extrapolated to elemental concentrations.

One internal standard and 4 duplicates were included and the results are given in Tables II-3 and II-4. Note that with two of the

TABLE II-3
TRACE ELEMENT ERROR ANALYSES

Element (Method*)	(Standard)	Obtained Value	Accepted Value**	Deviation (%)	Deviation (Mean %)
Li	(BCR-1)	14	13	7.7	6.4
(AA)	(BM)	75	70	7.1	
	(SY-3)	86	90	4.4	
Ba	(AGX)	1073	N/A	-	
(XRF)	(AGX)	1068	N/A	-	
	(JG-1)	433	460	5.9	8.2
	(SY-3)	347	440	21.1	
	(GSP-1)	1259	1300	3.2	
	(GSP-1)	1249	1300	3.9	
	(G-2)	1726	1850	6.7	
Rb	(AGX)	238	243	2.1	2.5
(XRF)	(AGX)	240	243	1.2	
	(JG-1)	175	185	5.4	
	(SY-3)	221	210	5.2	
	(GSP-1)	253	254.7	0.7	
	(GSP-1)	252	254.7	1.1	
	(G-2)	166	169.3	1.9	
Sr	(AGX)	172	175.2	1.8	2.1
(XRF)	(AGX)	172	175.2	1.8	
	(JG-1)	180	185	2.7	
	(SY-3)	306	300	2.0	
	(GSP-1)	229	233.1	1.8	
	(GSP-1)	231	233.1	0.9	
	(G-2)	460	476.3	3.4	
Zr	(AGX)	86	N/A	-	
(XRF)	(AGX)	86	N/A	-	
	(JG-1)	103	110?	6.4	3.5
	(SY-3)	308	340	9.4	
	(GSP-1)	503	500	0.6	
	(GSP-1)	503	500	0.6	
	(G-2)	302	300	0.7	
Pb	(AGX)	41	N/A	-	
(XRF)	(AGX)	37	N/A	-	
	(JG-1)	27	26?	26?	4.5
	(SY-3)	120	130	7.7	
	(GSP-1)	51	53	3.8	
	(GSP-1)	51	53	3.8	
	(G-2)	28	29	3.4	

TABLE II-3 (continued)
TRACE ELEMENT ERROR ANALYSES

Element (Method*)	(Standard)	Obtained Value	Accepted Value**	Deviation (%)	Deviation (Mean %)
Zn	(AGX)	27	N/A	-	
(XRF)	(AGX)	28	N/A	-	
	(JG-1)	43	40	7.5	3.8
	(SY-3)	250	250	0	
	(GSP-1)	101	98	3.1	
	(GSP-1)	103	98	5.1	
	(G-2)	82	85	3.5	
F	(CG-1)	900	660	36.3	20.4
(Ion)	(CG-1)	690	660	4.5	
Cu	(GSP-1)	33	35	5.7	5.7
(AA)					
Mo	(CG-1)	1	2	50.0	50.0
(AA)	(CG-1)	1	2	50.0	
Ag	(CG-1)	1.3	<1	-	
(AA)	(CG-1)	1.1	<1	-	
Be	(CG-1)	2.0	2?	0	12.5
(AA)	(CG-1)	1.5	2?	25.0	
B	(CG-1)	20	N/A	-	
(Plasma)	(CG-1)	25	N/A	-	
Sn	(CG-1)	7	N/A	-	
(XRF)	(CG-1)	6	N/A	-	
U	(CG-1)	2.9	2.5	16.0	8.0
(NAA)	(CG-1)	2.5	2.5	0	
Th	(CG-1)	13	N/A	-	
(NAA)	(CG-1)	13	N/A	-	
W	(CG-1)	4	<4	-	
(NAA)	(CG-1)	3	<4	-	
Au (ppb)	(CG-1)	16	N/A	-	
(NAA)	(CG-1)	14	N/A	-	

* AA = Atomic Absorption Plasma = Direct-Current Plasma
XRF = X-Ray Fluorescence NAA = Neutron Activation Analyses
Ion = Selective Ion Electrode

** International standards are from Abbey (1977) except AGX which is from Pankhurst and O'Nions (1973), and CG-1 which is unpublished.

TABLE II-4

TRACE ELEMENT DUPLICATE ANALYSES

Sample No.	AGX		GSP-1		CG-1		F-G001		F-G004		F-G005		
Duplicate	I	II	I	II	I	II	I	II	I	II	I	II	III
Li	-	-	-	-	-	-	-	-	256	248	-	-	-
Ba	1073	1068	1259	1249	-	-	-	-	-	-	19	21	23
Rb	238	240	253	252	-	-	-	-	-	-	374	375	377
Sr	172	172	229	231	-	-	-	-	-	-	29	30	29
Zr	86	86	503	503	-	-	-	-	-	-	48	47	48
Pb	41	37	51	51	-	-	-	-	-	-	17	16	18
Zn	27	28	101	103	-	-	-	-	-	-	56	57	58
F	-	-	-	-	900	690	-	-	-	-	660	640	-
Cu	-	-	33	35	-	-	-	-	-	-	2	2	-
Mo	-	-	-	-	1	1	1	2	-	-	-	-	-
Ag	-	-	-	-	1.3	1.1	0.2	<0.1	-	-	-	-	-
Be	-	-	-	-	2.0	1.5	13.0	26.0	-	-	-	-	-
B	-	-	-	-	20	25	20	30	-	-	-	-	-
Sn	-	-	-	-	7	6	23	19	-	-	-	-	-
U	-	-	-	-	2.9	2.5	15.9	16.0	-	-	-	-	-
Th	-	-	-	-	13	13	3	3	-	-	-	-	-
W	-	-	-	-	4	3	6	4	-	-	-	-	-
Au (ppb)	-	-	-	-	16	14	1	2	-	-	-	-	-

Sample No.	F-G022		F6-G004		F5-G004			SL-12		LR-5		LR-G009	
Duplicate	I[1]	II[2]	I[1]	II[2]	I	II	III	I	II	I	II	I	II
Li	-	-	-	-	-	-	-	-	-	-	-	130	130
Ba	-	-	-	-	12	15	15	-	-	-	-	-	-
Rb	-	-	-	-	423	421	424	-	-	-	-	-	-
Sr	-	-	-	-	93	96	95	-	-	-	-	-	-
Zr	-	-	-	-	20	20	19	-	-	-	-	-	-
Pb	-	-	-	-	12	14	13	-	-	-	-	-	-
Zn	-	-	-	-	16	15	17	-	-	-	-	-	-
F	-	-	-	-	240	210	240	-	-	-	-	-	-
Cu	-	-	-	-	8	8	7	-	-	-	-	-	-
Mo	1	2	1	1	-	-	-	<1	1	<1	1	-	-
Ag	0.1	0.1	0.1	0.4	-	-	-	<0.1	0.1	0.1	0.1	-	-
Be	5.0	5.5	4.5	5.0	-	-	-	4.5	5.0	5.0	5.5	-	-
B	20	20	25	25	-	-	-	30	25	35	30	-	-
Sn	24	30	4	7	-	-	-	20	14	3	6	-	-
U	10.1	9.7	4.5	4.2	-	-	-	17.8	17.3	3.3	3.5	-	-
Th	<1	<1	6	7	-	-	-	5	5	8	8	-	-
W	718	2	760	2	-	-	-	4	2	1	3	-	-
Au (ppb)	3	2	<1	1	-	-	-	4	2	5	6	-	-

1 = Tungsten-carbide crushed.
2 = Ceramic crushed.

duplicated samples (F-G022 and F6-G004) one run was on a powder crushed in a ceramic swing mill while the second run was on powder from a W-carbide swing mill, hence the highly anomalous W values.

II.3.2.5 Rare earth element analyses

Analyses of the rare earth elements La, Ce, Nd, Sm, Eu, Tb, Yb and Lu and the traces Cs, Hf, Sc and Ta were determined by multi-element instrumental neutron activation analysis (INNA) at Gamma Analysts, Guelph, Ontario (Table II-5). The method used is one first described by Gordon et al. (1968), that has been modified as described by Gibson and Jagam (1980). International standards BCR-1 and JG-1 were included with the samples.

TABLE II-5

RARE EARTH ELEMENT ERROR ANALYSES

Element	(Standard)	Obtained Value	Accepted Value*	Deviation (%)	Deviation (Mean %)
La	(BCR-1)	27.15	25	8.6	11.0
	(JG-1)	24.95	22?	13.4	
Ce	(BCR-1)	50.36	54	6.7	5.9
	(JG-1)	45.16	43?	5.0	
Nd	(BCR-1)	25.88	29	10.8	10.8
	(JG-1)	20.18	N/A	-	
Sm	(BCR-1)	6.71	6.6	1.7	4.0
	(JG-1)	4.89	4.6?	6.3	
Eu	(BCR-1)	1.73	1.9	8.9	5.9
	(JG-1)	0.68	0.7?	2.9	
Tb	(BCR-1)	0.78	1.0	22.0	22.0
	(JG-1)	0.78	N/A	-	
Yb	(BCR-1)	2.51	3.4	26.1	66.1
	(JG-1)	3.09	1.5?	106	
Lu	(BCR-1)	0.438	0.6?	27	80
	(JG-1)	0.468	0.2?	134	
Cs	(BCR-1)	0.91	0.95	4.2	3.6
	(JG-1)	10.3	10?	3.0	
Hf	(BCR-1)	4.33	4.5?	3.8	3.8
	(JG-1)	3.45	N/A	-	
Sc	(BCR-1)	30.5	34	10.3	5.2
	(JG-1)	6.5	6.5	0	
Ta	(BCR-1)	0.72	0.8?	10.0	10.0
	(JG-1)	1.6	N/A	-	

* Values for international standards obtained from Abbey (1977).

APPENDIX III

STATISTICAL METHODS

III.1 SPEARMAN RANK CORRELATION

Most statistical treatments require the assumption that the data are normally distributed about the sample mean. Geochemical data are often not normally distributed thus rendering most statistical approaches invalid. A Spearman's coefficient of rank correlation is one of several non-parametric statistical methods designed to accommodate non-normally distributed data (Ferguson, 1966). With this method the data variables are first rank-ordered from lowest to highest (i.e. lowest value = 1, second lowest = 2... highest value = Nth). Once ranked, the variable pairs are correlated against each other to produce rho (p), the Spearman's coefficient to rank correlation. For a perfect positive correlation rho = +1; a perfect negative correlation rho = -1; and a case of perfect independence rho = 0.

The level of significance of the value of rho can be defined for various sample sizes (N; Table III-1). For a small N the value of rho must be substantial before there are adequate grounds for rejecting the hypothesis that no association exists between the rankings. For example, for N=26 a rho of 0.465 or greater is required before we can argue that a significant association exists in a positive direction at the 5% level (i.e. 95% significant level).

III.2 DISCRIMINANT ANALYSIS

Discriminant analysis is a statistical treatment by which the

variation between 2 or more known groups of samples may be investigated and quantified (Klecka, 1975). This is done by computing a number of linear discriminant functions which are dependant on the number of defined groups. Once determined, the discriminant function may be applied to new data of unknown specimens allowing them to be allocated to one of the defined groups.

In the present study, discriminant analysis was selected to examine the within and between group variation of the primary and secondary muscovite geochemical analyses. The discriminant analysis produces a discriminant function formula which has the form $D = C_1 (Var_1) + C_2 (Var_2)...+ C_i (Var_i)$, where D = discriminant score; C_i = derived coefficient; Var_i = variable. The coefficients are derived in such a way so as to maximize the between group variation and minimize the within group variation.

There limitations and assumptions involved with discriminant analysis:

1. Geochemical data is affected by what is known as the constant sum or closure problem (Butler and Moronow, 1986). This occurs when the sum of all measured variables totals to a constant number (i.e 100%). In closed data, one variable cannot increase of decrease without causing one or more of the other variables to vary. In short then, individual components cannot vary independently. To minimize this problem one of the variables is used to normalize the others. This sacrifices the variable used for normalizing the data set. For this study, SiO_2 was used to normalized the data as: a) it is not a strong discriminator; and b)

TABLE III-1*

Critical values of rho (p), the Spearman rank correlation coefficient.

N	Significance level (one-tailed test)	
	0.05	0.01
4	1.000	
5	0.900	1.000
6	0.829	0.943
7	0.714	0.893
8	0.643	0.833
9	0.600	0.783
10	0.564	0.746
12	0.506	0.712
14	0.456	0.645
16	0.425	0.601
18	0.399	0.564
20	0.377	0.534
22	0.359	0.508
24	0.343	0.485
26	0.329	0.465
28	0.317	0.448
30	0.306	0.432

* From Ferguson (1966)

it is best to normalize using a variable with high values relative to the other variables.

2. Discriminant analysis assumes that all variables are normally distributed. To accommodate this requirement the normalized muscovite data was log transformed to better approximate normal distribution.

3. There is a problem of high dimensionality in discriminant analysis. If too few samples are used in an analysis relative to the number of variables, the discriminant function may over separate the groups (Foley, 1971). A suggested ratio of the number of cases (e.g. samples) to the number of variables is in the order of 10:1 (LeMaitre, 1982). The present study involves 44 samples, therefore, no more than 4 variables should be used. To select the best discriminating variables to use, the entire data set was subjected to discriminant analysis and the four best discriminators were chosen (TiO_2, Al_2O_3, FeO, MgO). The treatment was then repeated using only these variables.

In summary, with this study, the muscovite geochemical data were first normalized using SiO_2 after which the normalized values were log transformed. These values were then subjected to discriminant analysis and the four variables of highest discriminating value were chosen. The discriminant analysis was then repeated using these variables and the results of this treatment are presented in Chapter 5.

REFERENCES

Abbey, S.

1977: Studies in standard samples for use in the general analysis of silicate rocks and minerals; Geological Survey of Canada, Paper 77-34, 31 p.

Abbott, R. N.

1980: Pattern of K-spar foliation in granodiorites near Chedabucto Head; in Trip 21: The Igneous and Metamorphic Geology of Southern Nova Scotia; editors D. B. Clarke and G. K. Muecke; Geological Association of Canada, Field Trip Guidebook; Halifax, 1980, p.30.

Albuquerque, C. A. R. de

1977: Geochemistry of the tonalitic and granitic rocks of the Nova Scotia southern plutons; Geochemica et Cosmochemica Acta, v. 41, p. 1-13.

Alderton, D. M. H., Pearce, J. A. and Potts, P. J.

1980: Rare earth element mobility during granite alteration: evidence from southwest England; Earth and Planetary Science Letters, v. 49, p. 149-165.

Alisay, K. M.

1981: Zur geologie und geochemie des Sherbrooke-plutons, Nova Scotia; unpublished M.Sc. thesis, University Hamburg, Germany.

Allan, B. D. and Clarke, D. B.

1981: Occurrence and origin of garnets in the South Mountain Batholith, Nova Scotia; Canadian Mineralogist, v. 19, p. 19-24.

Baker, J. H.

1985: Rare earth and other trace element mobility accompanying albitization in a Proterozoic granite, W. Bergslagen, Sweden; Mineralogical Magazine, v. 49. p. 107-115.

Balashov, Y. A. and Krigman, L. D.

1975: The effects of alkalinity and volatiles on rare-earth separation in magmatic systems; Geochemistry.

Bell, W. A.

1929: Horton-Windsor district, Nova Scotia; Geological Survey of Canada, Memoir 155, 268 p.

Bell, K. and Blenkinsop, J.

1960: Mississippian Horton Group of type Windsor-Horton district, Nova Scotia; Geological Survey of Canada, Memoir 314, 112 p.

Benoit, W. R.

1971: Vertical zoning and differentiation in granitic rocks - central Flint Creek range, Montana; unpublished M.Sc. thesis, University of Montana, Missoula, Montana.

Beus, A. A.

1958: The role of complexes in transfers and accumulations of rare elements in endogenic solutions; Geochemistry, v. 4, p. 388-397.

Boehner, R. C.

1984: Stratigraphy and depositional history of marine evaporites in the Windsor Group, Shubenacadie and Musquodoboit structural basins, Nova Scotia, Canada; in Atlantic Coast Basins, ed. H. H. J. Geldsetzer; Neuvieme Congres International de Stratigraphie et de Geologie du Carbonifere, Compte Rendu 3, pt. 1. 163-178.

Bristow, Q.

1979: Gamma ray spestrometric methods in uranium exploration-airborne instrumentation; in Geophysics and Geochemistry in the Search for Metallic Ores, ed. Peter J. Hood, Geological Survey of Canada, Economic Geology Report 31, p. 135-146.

Burnham, C. W. and Ohomoto, H.

1980: Late-stage processes of felsic magmatism; Mining Geology Special Issue, editirs S. Ishihra and S. Takenouchi, v. 8, p. 1-11.

Butler, J. C. and Woronow, A.

1986: Discrimination among tectonic settings using trace element abundances of basalts; Journal of Geophysical Research, v. 91, p. 10289-10300.

Charbonneau, B. W., Killeen, P. G., Carson, J. M., Cameron, G. W. and Richardson, K. A.

1976: Significance of radioelement concentration measurements made by airborne gamma ray spectrometry over the Canadian Shield; IAEA Symposium on Exploration for Uranium Ore Deposits, Vienna, Austria, STl/PUB/434, p. 35-53, IAEA-SM 208/3.

Charest, M. H.

1976: Petrology, geochemistry and mineralization of the New Ross area, Lunenburg County, Nova Scotia; unpublished M.Sc. thesis, Dalhousie University, Halifax, Nova Scotia.

Charoy, B.

1986: The genesis of the Cornubian Batholith (south-west England): the example of the Carnmenellis Pluton; Journal of Petrology, v. 27, part 3, p. 571-604.

Chatterjee, A. K.

1983: Metallogenic Map of Nova Scotia; Nova Scotia Department of Mines and Energy, scale 1:500 000.

Chatterjee, A. K. and Muecke, G. K.

1982: Geochemistry and the distribution of uranium and thorium in the granitoid rocks of the South Mountain Batholith, Nova Scotia: some genetic and exploration implications; in Uranium in Granites, ed. Y. T. Maurice; Geological Survey of Canada, Paper 81-23, p. 11-17.

Chatterjee, A. K. and Strong, D. F.

1984: Rare-earth and other element variations in greisenized granites associated with the East Kemptville tin deposit, Nova Scotia, Canada; Transactions of the Institute of Mining and Metallurgy, Section B: Applied Earth Sciences, v. 93, p. B59-B70.

Chatterjee, A. K., Robertson, J. and Pollock, D.

1982: Asummary of the petrometallogenesis of the uranium mineralization at Millet Brook, South Mountain Batholith, Nova Scotia; in Mines and Minerals Branch Report of Activities 1981; Nova Scotia Department of Mines and Energy, Report 82-1, p. 57-66.

Chatterjee, A.K., Strong, D. F., Clarke, D. B., Robertson, J., Pollock, D. and Muecke, G. K.

1985: Geochemistry of the granodiorite hosting uranium mineralization at Millet Brook; in Guide to the Granites and Mineral Deposits of Southwestern Nova Scotia, eds. A. K. Chatterjee and D. B. Clarke; Nova Scotia Department of Mines and Energy, Preprint of Paper 85-3, p. 63-114.

Cerny, P., Meintzer, R. E. and Anderson, A. J.
1985: Extreme fractionation in rare-element granitic pegmatites: selected examples of data and mechanisms; Canadian Mineralogist, v. 23, p. 381-421.

Chevalier, B. A. M.
1983: Petrography and geochemistry of the Bull Ridge Pluton, Guysborough County, Nova Scotia; unpublished B.Sc. Honours thesis, Acadia University, Wolfville, Nova Scotia.

Chu, P.
1978: Metamorphism of the Muguma Group in the Shelburne area, Nova Scotia; unpublished M.Sc. thesis, Acadia University, Wolfville, Nova Scotia.

Clarke, D. B.
1981: The mineralogy of peraluminous granites: a review; Canadian Mineralogist, v. 19, p. 3-17.

Clarke, D.B., and Halliday, A. N.
1982: Strontium isotope geology of the South Mountain Batholith, Nova Scotia; Geochemica et Cosmochemica Acta, v. 44, p. 1045-1058.

Clarke, D.B., and Halliday, A. N.
1985: Sm/Nd isotope investigation of the age and origin of the Meguma Zone metasedimentary rocks; Canadian Journal of Earth Sciences, v. 22, p. 102-107.

Clarke, D. B. and Muecke, G. K.
1985: Review of the petrochemistry and origin of the South Mountain Batholith and associated plutons, Nova Scotia, Canada. in High Heat Production (HHP) Granites, Hydrothermal Circulation and Ore Genesis, Institution of

Mining and Metallurgy, St. Austell, Cornwall, England, 1985, p. 41-54.

Clarke, D. B., McKenzie, C. B., Muecke, G. K. and Richardson, S. W.
1976: Magmatic andalusite from the South Mountain batholith, Nova Scotia; Contributions to Mineralogy and Petrology, v. 56, p. 279-287.

Coolen, P.
1974: The geology of the Kinsac Pluton; unpublished B.Sc. Honours Thesis, Dalhousie University, Halifax, Nova Scotia.

Corey, M.C.
1986: Bedrock Geology of the South Mountain Batholith: NTS Map Sheet 11D/13; in Mines and Minerals Branch, Report of Activities, 1985, ed. J. L. Bates; Nova Scotia Department of Mines and Energy, Report 86-1, p. 137-147.

Cormier, R. F. and Smith, T. E.
1973: Radiometric ages of granitic rocks, southwestern Nova Scotia; Canadian Journal of Earth Sciences, v. 10, no. 8, p. 1201-1210.

Cullen, J. D.
1983: Metamorphic petrology and geochemistry of the Goldenville Formation metasediments, Yarmouth, Nova Scotia; unpublished M.Sc. thesis, Dalhousie University, Halifax, Nova Scotia.

Dallmeyer, R. D. and Keppie, J. D.
1987: Polyphase late Paleozoic tectonothermal evolution of the southwestern Meguma Terrane, Nova Scotia: evidence from $^{40}Ar/^{39}Ar$ mineral ages; Canadian Journal of Earth

Sciences, v. 24 p. 1242-1254.

Deer, W. A., Howie, R. A. and Zussman, J.
1962: The rock-forming minerals, (5 Volumes); Longmans, Green and Company Limited, London.

Deer, W. A., Howie, R. A. and Zussman, J.
1966: An introduction to the rock-forming minerals; Longman Group Limited, London.

El Bouseily, A. M. and El Sokkary, A. A.
1975: The relation between Rb, Ba and Sr in the granitic rocks; Chemical Geology, v. 16, p. 207-219.

Elias, P.
1986: Thermal history of the Meguma Terrane: a study based on $^{40}Ar/^{39}Ar$ and fission track dating; unpublished Ph.D. thesis, Dalhousie University, Halifax.

Fairbairn, H. W., Hurley, P. M., Pinson, W. H. and Cormier, R. F.
1960: Age of the granitic rocks of Nova Scotia; Geological Society of America Bulletin, v. 71, p. 399-414.

Fairbairn, H. W., Hurley, P. M., Pinson, W. H.
1964: Preliminary age study and initial $^{87}Sr/^{86}Sr$ of Nova Scotia granitic rocks by the Rb/Sr method; Geological Society of America Bulletin, v. 75, p. 253-258.

Farley, E. J.
1979: Mineralization at the Turner and the Walker deposits; South Mountain Batholith; unpublished M.Sc. thesis, Dalhousie University, Halifax, Nova Scotia.

Ferguson, G. A.

1966: Statistical Analysis in Psychology and Education (2nd edition); McGraw-Hill, London.

Fletcher, H. and Faribault, E. R.

1887: Geological map of the Chedabucto Bay area; Geological Survey of Canada, Old Series Geological Map, no. 25.

Flynn, R. T. and Burnham, C. W.

1978: An experimental determination of rare earth partition coefficients between a chloride containing vapour phase and silicate melts; Geochimica et Cosmochimica Acta, v. 42, p. 685-701.

Foley,

1971: The probability of error on the design set as a function of the sample size and dimensionality; Rome Air Development Centre Technical Report RADC-TR-71-171, 63 p.

Ford, K. L. and Ballantyne, S. B.

1983: Uranium and thorium distribution patterns and lithogeochemistry of Devonian granites in the Chedabucto Bay area, Nova Scotia; in Current Research, Part A; Geological Survey of Canada, Paper 83-1A, p. 109 119.

Ford, K. L. and O'Reilly, G. A.

1985: Airborne gamma ray spectrometric surveys as an indicator of granophile element specialization and associated mineral deposits in the granitic rocks of the Meguma Zone of Nova Scotia; in High heat production (HHP) granites, hydrothermal circulation and ore genesis; Institution of Mining and Metallurgy, St. Austell, Cornwall, England, 1985, p. 113-133.

Fyson, W. K.

1966: Structures in the Lower Paleozoic Meguma Group, Nova Scotia; Geological Society of America Bulletin, v. 77, p. 931-944.

Gibson, I. L. and Jagam, P.

1980: Instrumental neutron activation analysis of rocks and minerals; in editor G. K. Muecke, Neutron Activation Analysis in the Geosciences; Mineralogical Association of Canada, Short Course Handbook 5, p. 109-131.

Giles, P. S. and Boehner, R. C.

1979: Carboniferous stratigraphy of the Shubenacadie and Musquodoboit Basins, central Nova Scotia; Nova Scotia Department of Mines and Energy, Open File 410.

Gordon, G. E., Randle, K., Giles, G. G., Corliss, J. B., Beeson, M. H. and Oxley, S. S.

1968: Instrumental activation analysis of standard rocks with high-resolution gamma-ray detectors; Geochimica and Cocmochimica Acta, v. 32, p. 369-396.

Goudge, M.

1934: Gold, Sangster Lake, Guysborough County, Nova Scotia, miscellaneous memos and plans; Nova Scotia Department of Mines and Energy, Assessment File 11F/05A 21-G-42(00).

Grasty, R. L.

1979: Gamma-ray spectrometric methods in uranium exploration-theory and operational procedures. in Geophysics and Geochemistry in the Search for Metallic Ores. Edited by P. J. Hood, Geological Survey of Canada, Economic Geology Report 31, p. 147-161.

Gribble, C. D.

1969: Distribution of elements in igneous rocks of the normal calc-alkaline sequence; Scottish Journal of Geology, v. 5, p. 322-327.

Gromet, L. P. and Silver, L. T.

1983: Rare earth element distributions among minerals in a granodiorite and their petrogenetic implications; Geochimica and Cosmochimica Acta, v. 47, p. 925-939.

Ham, L. J., and Horne, R. J.

1986: Geology of the South Mountain Batholith on the eastern half of NTS Map Sheet 21A/16; in Mines and Minerals Branch, Report of Activities 1985, ed. J. L. Bates; Nova Scotia Department of Mines and Energy, Report 86-1, p. 149-159.

Ham, L. J. and Kontak, D. J.

1988: A textural and chemical study of white mica in the South Mountain Batholith, Nova Scotia: primary versus secondary origin; Maritime Sediments and Atlantic Geology, v. 24, issue no. 1.

Haskin, L. A., Haskin, M. A., Frey, F. A. and Wildeman, T. R.

1968: Relative and absolute terrestrial abundances of the rare earths; in editor L. H. Ahrens, Origin and Distribution of the Elements; Pergamon, Oxford, England.

Heier, K. S. and Billings, G. K.

1970: Rubidium; in editor K. H. Wedepohl Handbook of Geochemistry, v. 2, Springer-Verlag, Berlin.

Helgeson, H. C.

1985: Some thermodynamic aspects of geochemistry; Pure and Applied Chemistry, v. 57, no. 1, p. 31-44.

Higgins, N. C., Solomom, M. and Varne, R.
1985: The genesis of the Blue Tier Batholith, northeastern Tasmania, Australia; Lithos, v. 18, p. 129-149.

Howie, R. D.
1984: Carboniferous evaporites in Atlantic Canada; in Atlantic Coast Basins, ed. H. H. J. Geldsetzer; Neuvieme Congres International de Stratigraphie et de Geologie du Carbonifere, Compte Rendu, 3, pt. 1, p. 131-142.

Jefferies, N. L.
1983: The distribution of the rare earth elements within the Carnmenellis Pluton, Cornwall; Mineralogical Magazine, v. 49, p. 495-504.

Jegouzo, P.
1980: The South Armorican shear zone; Journal of Structural Geology, v. 2, no. 1/2, p. 39-47.

Kamineni, D. C.
1986: Distribution of uranium, thorium and rare earth elements in the Eye-Dashwa Lakes Pluton - a study of some analogue elements; Chemical Geology, v. 55, p. 361-373.

Keppie, J. D.
1977: Tectonics of southern Nova Scotia; Nova Scotia Department of Mines, Paper 77-1, 34 p.

Keppie, J. D. (compiler)
1979: Geological map of Nova Scotia; Nova Scotia Department of Mines and Energy, scale 1:500,000.

Keppie, J. D.
1982: Tectonic map of the province of Nova Scotia; Nova Scotia

Department of Mines and Energy, scale 1:500,000.

Keppie, J. D.
1983: Geological history of the Isaacs Harbour area, Guysborough County, Nova Scotia; in Mines and Minerals Branch, Report of Activities 1982; Nova Scotia Department of Mines and Energy, Report 83-1, p. 109-143.

Keppie, J. D.
1984: Geology of the easternmost Meguma Terrane of Nova Scotia, Canada; in Mines and Minerals Branch, Report of Activities 1983; Nova Scotia Department of Mines and Energy, Report 84-1, p. 193.

Keppie, J. D.
1985: Geology and tectonics of Nova Scotia; in Appalachians Geotraverse (Canadian Mainland); Geological and Mineralogical Associations of Canada Annual Meeting, Guidebook to Excursion 1, p. 23-108.

Keppie, J. D. and Dallmeyer, R. D.
1987: Dating transcurrent Terrane accretion: an example from the Meguma and Avalon composite Terranes in the northern Appalachians; Tectonics, v. 6, no. 6, p. 831-847.

Keppie, J. D. and Muecke, G. K. (compilers)
1979: Metamorphic map of Nova Scotia; Nova Scotia Department of Mines and Energy, scale 1:1,000,000.

Keppie, J. D. and Smith, P. K. (compilers)
1978: Compilation of isotopic age data of Nova Scotia;Nova Scotia Department of Mines, Report 78-4.

Keppie, J. D., Dallmeyer, R. D., Krogh, T. F., Cormier, R. F. and Halliday, A. N.

1985: Geochronological constraints for mineralization in the easternmost Meguma Terrane, Nova Scotia; in Information Series No. 9, Nova Scotia Department of Mines and Energy, p. 39-40.

Killeen, P. G.

1979: Gamma-ray spectrometric methods in uranium exploration-application and interpretation. In Geophysics and Geochemistry in the Search for Metallic Ores. Edited by P. J. Hood, Geological Survey of Canada, Economic Geology Report 31, p. 163-229.

Klecka, W. R.

1975: Discriminant analysis; in N. H. Nie, C. H. Hull, J. G. Jenkins, K. Steinbrenner and D. H. Bent, editors; SPSS-Statistical Package for the Social Sciences (2nd edition).

Kontak, D. J.

1987: East Kemptville tin deposit, Nova Scotia: structurally controlled lithophile-element mineralization associated with a shear-related/generated leucocratic topaz granite; Geological Association of Canada-Mineralogical Association of Canada, Program with Abstracts, v. 12, p. 63.

Kontak, D. J., Strong, D. F. and Kerrich, R.

1988: Crystal-meltþfluid phase equilibria versus late-stage fluid-rock interaction in granitoid rocks of the South Mountain Batholith, Nova Scotia: whole rock geochemistry and oxygen isotope evidence; Maritime Sediments and Atlantic Geology, v. 24, issue no. 1.

Kosterin, A. W.

1959: The possible modes of transport of the rare earths by hydrothermal solutions; Geochemistry, v. 4, p. 381-387.

Lane, T. E.

1975: Stratigraphy of the White Rock Formation; Maritime Sediments, v. 11, p. 87-106.

LeMaitre, R. W.

1982: Numerical petrology, statistical interpretation of geochemical data; Developments in Petrology Volume 8; Elsevier, New York, 281 p.

Liew, M. Y. C.

1979: Geochemical studies of the Goldenville Formation at Taylors Head, Nova Scotia; unpublished M.Sc. thesis, Dalhousie University, Halifax, Nova Scotia.

Logothetis, J.

1984: The mineralogy and geochemistry of metasomatized rocks from occurrences in the South Mountain Batholith: New Ross area, southwestern Nova Scotia; Unpublished M.Sc. thesis, Dalhousie University, Halifax, Nova Scotia, 359 p.

London, D.

1987: Internal differentiation of rare-element pegmatites: effects of boron, phosphorus and fluorine; Geochimica et Cosmochimica Acta, v. 51, p. 403-420.

Longstaffe, F. J., Smith, T. E. and Muehlenbachs, K.

1980: Oxygen isotope evidence for the genesis of Upper Paleozoic granitoids from southwestern Nova Scotia; Canadian Journal of Earth Sciences, v. 17, p. 132-141.

MacDonald, M. A.

1981: The mineralogy, petrology and geochemistry of the Musquodoboit Batholith; unpublished M.Sc. thesis, Dalhousie University, Halifax, Nova Scotia.

MacDonald, M. A. and Clarke, D. B.

1985: The petrology, geochemistry and economic potential of the Musquodoboit Batholith, Nova Scotia; Canadian Journal of Earth Sciences, v. 22, 1633-1642.

MacDonald, M. A., and Horne, R. J.

1986: The geology of the South Mountain Batholith: NTS sheets 11D/05 and 11D/12; in Mines and Minerals Branch, Report of Activities 1985, ed. J. L. Bates; Nova Scotia Department of Mines and Energy, Report 86-1, p. 119-135.

Maillet, L. A. and Clarke, D. B.

1985: Cordierite in the peraluminous granites of the Meguma Zone, Nova Scotia, Canada; Mineralogical Magazine, v. 49, p. 695-702.

Manning, D. A. C.

1981: The effect of fluorine on liquidus phase relationships in the system Qz-Ab-Or with excess water at 1kb; Contributions to Mineralogy and Petrology, v. 76, p. 206-215.

Manning, D. A. C. and Exley, C. S.

1984: The origins of late-stage fluids in the St. Austell granite - a re-interpretation; Journal of the Geological Society of London, v. 141, p. 581-591.

Martin, R. F., Whitley, J. E. and Woolley, A. R.

1978: An investigation of rare-earth mobility: fenitized

quartzites, Borralan Complex, N. W. Scotland; Contributions to Mineralogy and Petrology, v. 66, p. 69-73.

McKenzie, C. B.
1974: Petrology of the South Mountain Batholith, Nova Scotia; unpublished M.Sc. thesis, Dalhousie University, Halifax.

McKenzie, C. B. and Clarke, D. B.
1975: Petrology of the South Mountain Batholith, Nova Scotia; Canadian Journal of Earth Sciences, v. 12, p. 1209-1218.

McLennan, S. M. and Taylor, S. R.
1979: Rare-earth mobility associated with uranium mineralization; Nature, v. 282, p. 247-250.

Miller, C. F. and Mittlefehldt, D. H.
1982: Light rare earth element depletion in felsic magmas; Geology, v. 10, p. 129-133.

Miller, C. F., Stoddard, E. F., Bradfish, L. J. and Dollase, W. A.
1981: Composition of plutonic muscovite: genetic implications; Canadian Mineralogist, v. 19, p. 25-34.

Mittlefehldt, D. W. and Miller, C. F.
1983: Geochemistry of the Sweetwater Wash Pluton, California: implications for "anomalous" trace element behaviour during differentiation of felsic magmas; Geochimica et Cosmochimica Acta, v. 47, p. 109-124.

Montoto, M.
1973: Petrographic transformations in granitic rocks under tectonic stress; Special Publication Geological Society of South Africa, No. 3, p. 493-498.

Moore, R. G.

1967: Lithostratigraphic units in the upper part of the Windsor Group, Minas Sub-basin, Nova Scotia; Geological Association of Canada, Special Paper no. 4, p. 245-266.

Muecke, G. K. and Moller, P.

1988: The not so rare earths; Scientific American, v. 256, no. 1, p. 72-77.

Muecke, G. K., Elias, P. and Reynolds, P. H.

in press: Hercynian/Alleghanian overprinting of an Acadian Terrane: $^{40}Ar/^{39}Ar$ studies in the Meguma Zone, Nova Scotia; Isotope Geoscience.

Neiva, A. M. R.

1982: Geochemistry of muscovite and some physico-chemical conditions of the formation of some tin-tungsten deposits in portugal; in editor A. M. Evans, Metallization Associated with Acid Magmatism, v. 3, John Wiley and Sons, p. 243-259.

Nichols, D.

1976: Metamorphic and structural evolution of the metasediments and granites in the Whitehaven area, Guysborough County, Nova Scotia; unpublished B.Sc. thesis, Dalhousie University, Halifax.

Norton, D. and Knapp, R.

1977: Transport phenomena in hydrothermal systems: the nature of porosity; American Journal of Science, v. 277, p. 913-936.

Norton, D. and Knight, J.

1977: Transport phenomena in hydrothermal systems; cooling plutons; American Journal of Science, v. 277, p. 937-981.

O'Brien, B. H.

1983: The structures of the Meguma Group between Gegogan Harbour and Country Harbour, Guysborough County; in Mines and Minerals Branch, Report of Activities, 1982; Nova Scotia Department of Mines and Energy, Report 83-1, p. 145-181.

O'Brien, B. H.

1985a: Geological map of the Lahave area, Nova Scotia; Geological Survey of Canada, Open File 1158, scale 1;25,000.

O'Brien, B. H.

1985b: The formation of veins in greenschist facies rocks and the early deformation of the Meguma Group, Eastern Nova Scotia; Nova Scotia Department of Mines and Energy, Paper 85-2, 35p.

Ohmoto, M.

1986: Stable isotope geochemistry of ore deposits; in Stable Isotopes in High Temperature Geological Processes; Edited by J. W. Valley, H. P. Taylor, Jr., and J. R. O'Neil, Reviews in Mineralogy, v. 16. p. 491-559.

O'Reilly, G. A.

1976: The petrology of the Brenton Pluton, Yarmouth County, Nova Scotia; unpublished B.Sc. Honours thesis, Dalhousie University, Halifax, Nova Scotia.

O'Reilly, G. A., Farley, E. J. and Charest, M. H.

1982: Metasomatic-hydrothermal mineral deposits of the New Ross-Mahone Bay area, Nova Scotia; Nova Scotia Department of Mines and Energy, Paper 82-2, 96 p.

O'Reilly, G. A., Gauthier, G. and Brooks, C.

1985: Three Permo-Carboniferous Rb/Sr age determinations from the South Mountain Batholith, in Mines and Minerals Branch, Report of Activities 1984; Nova Scotia Department of Mines and Energy, Report 85-1.

Pankhurst, R. J. and O'Nions, R. K.

1973: Determination of Rb/Sr and $^{87}Sr/^{86}Sr$ ratios of some standard rocks and evaluation of x-ray fluorescence spectrometry in Rb-Sr geochemistry; Chemical Geology, v. 12, p. 127-136.

Parmentier, E. M. and Schedl, A.

1981: Thermal aureoles of igneous intrusions: some possible indications of hydrothermal convective cooling; Journal Geology, v. 89, p. 1-22.

Pichavant, M.

1981: An experimental study of the effect of boron on a water saturated haplogranite at 1 kbar pressure; Contributions to Mineralogy and Petrology, v. 76, p. 430-439.

Pichavant, M., Valencia Herrera, J., Boulmier, S., Briqueu, L., Joron, J. L., Juteau, M., Marin, L., Michard, A., Sheppard, S. M. F., Treuil, M. and Vernet, M.

1987: The Macusani glasses, SE Peru: evidence of chemical fractionation in peraluminous magmas; in editor B. O. Mysen, Magmatic Processes: Physiochemical Principles; The Geochemical Society Special Publication, no. 1.

Pollard, P. J.

1983: Magmatic and postmagmatic processes in the formation of rocks associated with rare-element deposits; Transactions, Institute of Mining and Metallurgy, Section B: (Applied Earth Science), v. 92.

Ponce de Leon, M. I. and Choukroune, P.

1980: Shear zones in the Iberian arc; Journal of Structural Geology, v. 2, no. 1/2, p. 63-68.

Reynolds, N. C.

1972: "Rubidium"; in The Encyclopedia of Geochemical and Environmental Sciences, v. 10A, Van Nostrand and Reinhold Co., New York, Volume IVA, p. 1050-1052.

Reynolds, P. H. and Muecke, G. K.

1978: Age studies on slates: applicability of the $^{40}Ar/^{39}Ar$ stepwise outgassing method; Earth and Planetary Science Letters, v. 40, p. 111-118.

Reynolds, P. H., Zentilli, M. and Muecke, G. K.

1981: K-Ar and $^{40}Ar/^{39}Ar$ geochronology of granitoid rocks from southern Nova Scotia: Its bearing on the geological evolution of the Meguma Zone of the Appalachians; Canadian Journal of Earth Sciences, v. 18, p. 386-394.

Reynolds, P. H., Elias, P., Muecke, G. K. and Grist, A. M.

1987: Thermal history of of the southwestern Meguma Zone, Nova Scotia, from a $^{40}Ar/^{39}Ar$ and fission track dating study of intrusive rocks. Canadian Journal of Earth Sciences, 24, p. 1952-1965.

Ribbe, P. H.

1983: Aluminum-silicon order in feldspars: domain textures and diffraction patterns; in editor P. H. Ribbe, Feldspar Mineralogy; Moneralogical Society of America, Reviews in Mineralogy, v. 2, p. 21-55.

Richardson, J. M. G., Spooner, E. T. C. and McAuslan, D. A.

1982: The East Kemptville tin deposit, Nova Scotia: an example

of a large tonnage, low grade greisen hosted deposit in the endocontact zone of a granite batholith; in Current Research, Part B, Geological Survey of Canada, Paper 82-1B, p. 27-32.

Ryerson, F. J. and Hess, P. C.

1980: The role of P_2O_5 in silicate melts; Geochimica et Cosmochimica Acta, v. 44, p. 611-624.

Saavedra, J.

1978: Geochemical and petrological characteristics of mineralized granites of the west center of Spain: in Metallization Associated with Acid Magmatism editors, M. Stemprok, L. Burnol, and G. Tischendorf; Geological Survey of v. 3, p. 279-291.

Sarkar, P.

1978: Petrology and geochemistry of White Rock metavolcanic suite, Yarmouth, Nova Scotia; unpublished Ph.D thesis, Dalhousie University, 368 p.

Sawka, W. N., Chappell, B. W. and Norrish, K.

1984: Light-rare-earth-element zoning in sphene and allanite during granitoid fractionation; Geology, v. 12, p. 131-134.

Schenk, P. E.

1971: Southeastern Atlantic Canada, northwestern Africa, and continental drift; Canadian Journal of Earth Sciences, v. 8, p. 1218-1252.

Schenk, P. E.

1983: The Meguma terrane of Nova Scotia, Canada - an aid in trans-Atlantic correlation; in P. E. Schenk editor, Regional Trends in the Geology of the Appalachian -

Caledonian - Hercynian - Mauritanide Orogen; NATO ASI Series, D, Reidel Publishing Co., p. 121-130.

Schenk, P. E.

1984: Carbonate-sulphate relations in the Windsor Group, central Nova Scotia, Canada; Atlantic Coast Basins, ed. H. H. J. Geldsetser, Neuvieme Congres International de Stratigraphie et de Geologie du Carbonifere, Compte Rendu, 3, pt. 1, p. 143-162.

Schenk, P. E. and Lane, T. E.

1982: Pre-Acadian sedimentary rock of the Meguma Zone, Nova Scotia - a passive continental margin juxtaposed against a volcanic island arc; International Association of Sedimentolgists, Excursion 5B Guidebook, 85p.

Schiller, E. A.

1959: Petrography and petrology of the andalusite schists in the Port Felix area, Nova Scotia, Canada; unpublished M.Sc. thesis, Michigan State University, 50 p.

Schiller, E. A.

1961: Geology, Guysborough, Nova Scotia; Geological Survey of Canada, Map 27-1961, scale 1:63,360.

Schiller, E. A.

1963: Mineralogy and geology of the Guysborough area, Nova Scotia, Canada; unpublished Phd. thesis, University of Utah, 162 p.

Sheppard, S. M. F.

1986: Igneous Rocks: III Isotopic case studies of magmatism in Africa, Eurasia and Oceanic Islands; in Edited by J. W. Valley, H. P. Taylor, Jr., and J. R. O'Neil, Reviews in Mineralogy, v. 16. p. 319-371.

Smith, J. V.

1983: Some chemical properties of feldspars; in editor P. H. Ribbe, Feldspar Mineralogy, Reviews in Mineralogy; Mineralalogical Society of America, v. 2, p. 281-296.

Smith, T. E.

1974: The geochemistry of the granitic rocks of Halifax County, Nova Scotia; Canadian Journal of Earth Sciences, v. 11, p. 650-657.

Smith, T. E. and Turek, A.

1976: Tin-bearing potential of some Devonian granitic rocks in southwest Nova Scotia; Mineralum Deposita, v. 11, p. 234-245.

Smitheringale, W. G.

1973: Geology of parts of Digby, Bridgetown and Gaspereau Lake map-areas; Geological Survey of Canada, Memoir 375, 78 p.

Steiger, R. H. and JÊger, E.

1977: Subcommission on geochronology: Convention on the use of decay constants in geo- and cosmo-chronology; Earth and Planetary Science, v.36, p. 359-362.

Stemprok, M.

1979: Mineralized granites and their origin; Episodes, v. 1979, no. 3, p. 20-24.

Stevenson, I. M.

1964: Geology, Chedabucto Bay, Nova Scotia; Geological Survey of Canada, Map 1156A, scale 1:63,360.

Streckeisen, A.

1976: To each plutonic rock its proper name. Earth Science Review, 12, pp. 1-33.

Strong, D. F.

1981: Ore deposit models-5, A model for granophile mineral deposits; Geosceince Canada, v. 8, no. 4, p. 155-161.

Taylor, F. C.

1967: Reconnaissance geology of the Shelburne map-area,Nova Scotia; Geological Survey of Canada, Memoir 349, 83 p.

Taylor, F. C.

1969: Geology of the Annapolis-St. Marys Bay map area, Nova Scotia (21A, 21B, east half); Geological Survey of Canada, Memoir 358, 65 p.

Taylor, H. P., Jr.

1977: Water/rock interactions and the origin of H_2O in granitic batholiths; Journal of the Geological Society of London, v. 133, p. 509-558.

Taylor, R. G.

1979: Geology of tin deposits; Developments in Economic Geology, 11, Elsevier Scientific Publishing Co.

Taylor, R. P. and Fryer, B. J.

1983: Rare earth element lithogeochemistry of granitoid mineral deposits; Canadian Institute of Mining and Metallurgy Bulletin, v. 76, p. 74-84.

Taylor, F. C. and Schiller, E. A.

1966: Metamorphism of the Meguma Group of Nova Scotia; Canadian Journal of Earth Sciences, v. 3, p. 959-974.

Tischendorf, G.

1977: Geochemical and petrographic characteristics of silicic magmatic rocks associated with rare element mineralizati-

on; in Metallization Associated With Acid Magmatism, eds. M. Stemprok, L. Burnol, and G. Tischendorf; Geological Survey Prague, v. 2, p. 41-96.

Van de Pijpekamp, B.

1982: Petrological criteria for establishing the tin potential in granitoid complexes; in A. M. Evans editor, Metallization Associated With Acid Magmatism, v. 6, p. 273-278.

Vernon, R. H., Williams, V. A. and D'Arcy, W. F.

1982: Grain-size reduction and foliation development in a deformed granitoid batholith; Tectonophysics, v. 92, p. 123-145.

Wark, J. M. and Clarke, D. B.

1980: Geochemical discriminators and the palaeotectonic environment of the North Mountain basalts, Nova Scotia; Canadian Journal of Earth Sciences, v. 12, p. 1740-1745.

Wendlandt, R. F. and Harrison, W. J.

1979: Rare earth psrtitioning between immiscible carbonate and silicate liquids and CO_2 vapor: results and implications for the formation of light rare earth-enriched rocks; Contributions to Mineralogy and Petrology, v. 69, p. 409-419.

Williams, H.

1978: Tectonic lithofacies map of the Appalachian Orogen; Memorial University of Newfoundland, Map 1, scale 1:1,000,000.

Wright, W. J.

1931: Data on the method of granitic intrusion in Nova Scotia; Transactions of the Royal Society of Canada, 3rd series,

v. 25, sec. 4, p. 309-327.

Yeates, A. N., Wyatt, B. W. and Tucker, D. H.

1982: Application of gamma-ray spectrometry to prospecting for tin and tungsten granites, particularly within the Lachlin Fold Belt, New South Wales; Economic Geology, v. 77, p. 1725-1738.